Molecular and functional characterization of MICAL proteins

Yeping Zhou

Rudolf Magnus Institute of Neuroscience

2011

ISBN: 978-90-8891-319-8

Cover design: Yeping Zhou, 天离地何等的高, 2011
Printed by: Proefschriftmaken.nl || Printyourthesis.com
Published by: Uitgeverij BOXPress, Oisterwijk

Molecular and functional characterization of MICAL proteins

Moleculaire en cellulaire karakterisering van MICAL eiwitten

(met een samenvatting in het Nederlands)

PROEFSCHRIFT

ter verkrijging van de graad van doctor aan de Universiteit Utrecht

op gezag van de rector magnificus, prof.dr. G.J. van der Zwaan,

ingevolge het besluit van het college voor promoties

in het openbaar te verdedigen op

maandag 19 september 2011 des middags te 4.15 uur

door

Yeping Zhou

geboren op 7 november 1977 te China

Promotor: Prof. dr. J.P.H. Burbach

Co-promotor: Dr. R.J. Pasterkamp

Contents

Chapter 1

Introduction

Yeping Zhou and R. Jeroen Pasterkamp

Submitted as an invited review to *Cellular and Molecular Life Sciences*.

Preface

The translation of extracellular signals into a specific cellular response critically depends on the activation of intracellular signal transduction pathways. These pathways become activated upon stimulation by signaling proteins such as membrane receptors and can have various downstream effects. MICALs form a relatively novel and unusual family of intracellular signaling proteins that operate in various cellular processes in different species. The aim of this thesis is to unravel the function, mechanism-of-action and regulation of MICAL proteins, focusing on the founding member of the MICAL family, MICAL-1. In this thesis, we define different aspects of the MICAL-1 protein including the activity and function of its flavoprotein monooxygenase domain, novel binding partners and new cellular functions. This thesis provides novel insight into the regulation and function of MICAL proteins and forms an important basis for future studies into the role and actions of these unique intracellular proteins.

The MICAL gene family

In 2002, the founding member of the MICAL family, human MICAL-1, was identified in a screen for CasL-interacting proteins (hence the name MICAL for Molecule interacting with CasL) (Suzuki et al., 2002). Since then, two more MICAL proteins (MICAL-2 and MICAL-3) have been identified in vertebrate species on the basis of amino acid sequence and structural similarities (Fig. 1A) (Suzuki et al., 2002; Terman et al., 2002; Pasterkamp et al., 2006; Xue et al., 2010). MICALs are now known to comprise an evolutionary conserved family of signaling proteins which also includes members in invertebrate species. For example, *Drosophila melanogaster* has one MICAL (Mical) protein which exists in three different splice forms (Terman et al., 2002). In addition to MICALs, a group of MICAL-like (MICAL-L) proteins has been described. MICAL-Ls have an overall domain organization which is similar to MICALs but lack the conserved N-terminal region (Fig. 1B) (Terman et al., 2002). Two MICAL-L proteins are found in vertebrates, MICAL-L1 and MICAL-L2. The properties and functions of MICAL-Ls will be discussed in more detail in a subsequent section.

MICALs are unusual multidomain proteins as they contain an N-terminal flavoprotein monooxygenase (MO) domain in addition to a Calponin Homology (CH) domain, a LIM domain and coiled-coil (CC) motifs linked by non-conserved variable regions (Fig. 1A) (Suzuki et al., 2002; Terman et al., 2002). The combination of an MO domain with several different protein-protein interaction domains in one protein is unique and invites the speculation that MICALs may interact with multiple different proteins and control their activity through redox modifications (Terman et al., 2002). Interestingly, MICALs function in several different cellular and physiological processes. In *Drosophila,* Mical is required for motor axon pathfinding, synaptic bouton distribution, and dendritic pruning during neural development (Terman et al., 2002; Beuchle et al., 2007; Kirilly et al., 2009). Furthermore, *Drosophila* Mical influences myofilament patterning and bristle formation (Hung et al., 2010; Beuchle et al., 2007). Vertebrate MICALs have been implicated in axon guidance, the positioning of neuronal cell bodies, and axon outgrowth in the developing nervous system and in prostate cancer progression (Schmidt et al., 2008; Bron et al., 2007; Pasterkamp et al., 2006; Ashida et al., 2006). In contrast to invertebrate Mical, *in vivo* evidence for these functional roles of vertebrate MICALs is lacking and the molecular pathways employed by MICAL proteins to exert their diverse cellular effects remain largely uncharacterized. This thesis aims at beginning to fill this void by investigating the biochemical properties, function and regulation of MICAL-1, a best-characterized vertebrate MICAL family member to date (Suzuki et al., 2002; Weide et al., 2003; Pasterkamp et al., 2006; Schmidt et al., 2008). The following sections briefly summarize our current knowledge of the structural organization, regulatory mechanism, expression and function of MICAL-1, supplemented by knowledge of other MICALs.

Structure and domain organization of MICAL-1

MICAL proteins have a unique structure as they combine an N-terminal enzymatic part with several protein-protein interaction modules that are known to interact with cytoskeletal and signaling cues when

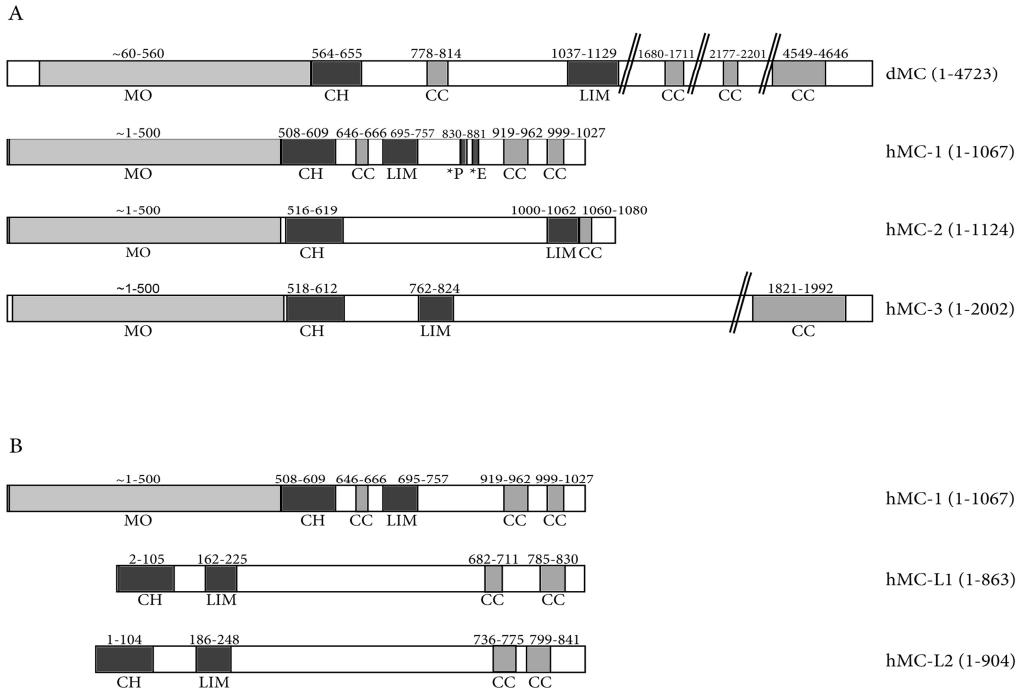

Figure 1. MICALs form an evolutionary conserved family of signaling proteins.

(A) Domain alignment of Drosophila Mical (dMC, UniProtKB Q86BA1) and human MICAL 1, 2 and 3 (hMC-1, 2 and 3 (UniProtKBQ8TDZ2, O94851, and Q7RTP6)). MICALs contain a highly conserved N-terminal flavoprotein monooxygenase (MO) domain, followed by a Calponin Homology (CH) domain, LIM domain and Coiled-coil motifs (CC). These domains are linked by variable regions (white regions). In the hMC-1 protein, a PPKPP motif (*P) and a glutamic acid-rich motif (*E) are depicted. These motifs are not presnt in other MICALs. The numbers indicate amino acid positions.

(B) MICAL-Like1 and 2 (hMC-L1 and 2 (UniProtKB Q8N3F8 and Q8IY33)) proteins are aligned with hMC-1, showing a similar arrangement of the CH, LIM and CC domains but lacking the N-terminal MO domain.

present in other proteins. Below we discuss the different protein domains that have been identified in MICALs.

Flavoprotein monooxygenase domain

The MICAL MO domain is located at the most N-terminal part of MICAL proteins and covers about 500 amino acids (Fig. 1A). It is conserved among family members, but clearly distinct from MO domains described previously (Terman et al., 2002; Siebold et al., 2005; Nadella et al., 2005). Within the MICAL MO domain, three conserved motifs can be discerned that define the flavin adenine dinucleotide (FAD) binding domain (FBD) present in flavoprotein monooxygenases. The sequence and spacing of these three motifs are highly similar to those found in other monooxygenases (Terman et al., 2002; Siebold et al., 2005; Nadella et al., 2005). Together with studies on the tertiary structure of the MICAL-1 MO domain (Nadella et al., 2005; Siebold et al., 2005), these features support the idea that MICALs are true flavoprotein monooxygenases.

The overall topology of the MICAL MO domain closely resembles PHBH (*p*-hydroxybenzoate hydroxylase), an NADPH-dependent flavoenzyme (Entsch et al., 2005; Cole et al., 2005; Siebold et al., 2005; Nadella et al., 2005). Not surprisingly, activity of the MICAL-1 MO domain is also NADPH-dependent (Siebold et al., 2005; Nadella et al., 2005; Schmidt et al., 2008; Hung et al., 2010). PHBH catalyzes oxidization of small molecules such as *p*-hydroxygenzoate and steroids. In contrast, it has been suggested that the MO domain of MICAL-1 has much larger substrates, such as proteins, because of the enlarged active-site cavity present in the MICAL-1 MO domain (Siebold et al., 2005; Nadella et al., 2005). In line with this observation, enzymatic experiments suggest that CRMPs (collapsin response mediator proteins) and actin filaments may be substrates for the MICAL MO domain (Schmidt et al., 2008; Hung et al., 2010). However, further studies on the identification and characterization of potential MICAL-1 MO substrates are needed to firmly establish that MICAL-1 modifies protein substrates through redox signaling.

In cells, the isolated MO domain of MICALs can induce morphological changes in various cellular structures (Schmidt et al., 2008; Hung et al., 2010). For example, in *Drosophila* overexpressed MO domain increases the number of filopodia on growth cones at the tip of the axon and induces bristle branching (Hung et al., 2010). After transfection in cultured mammalian cells, cells undergo a contraction response, showing a decreased surface area and an increase in filopodia like processes (Schmidt et al., 2008). Several physiological functions of MICALs have been found to rely on the intact MICAL MO domain. *Drosophila* Mical, for example, mediates semaphorin1A-plexinA induced repulsive axon guidance with a requirement for the MICAL MO domain. In *Mical* loss-of-function flies, motor axons are severely misguided. This phenotype can be rescued by reintroducing a wild type Mical construct. In contrast, a Mical mutant with an inactive MO domain fails to rescue the motor phenotype, supporting the requirement for MO activity in this process (Terman et al., 2002). Similar dependencies on the MO domain have been observed in cultured vertebrate neurons. Addition of semaphorin3A (Sema3A), one of the repulsive axon guidance cues of semaphorin family, to axons reduces their outgrowth. Several lines of evidence indicate that this effect of Sema3A is dependent on the proper functioning of the MICAL MO domain. First, a MICAL-1 mutant lacking the N-terminal MO domain serves as dominant negative mutant inhibiting Sema3A induced axonal repulsion when overexpressed in cultured neurons (Schmidt et al., 2008). Second, the repellent effect of Sema3A can be blocked by treatment with EGCG (epigallocatechin gallate), a green tea extract known to inhibit flavin monooxygenases (Abe et al., 2000a, b; Terman et al., 2002). Thus, these results support the idea that the MO domain of MICAL is required for axon guidance mediated by semaphorins.

Monooxygenases can mediate redox reactions and for example introduce a single atom of molecular oxygen into their substrates (Joosten and van Berkel, 2007). As flavoprotein monooxygenases, MICALs may also function to modify substrates through redox reactions thereby regulating axon guidance and other cellular functions. Further studies are needed to identify MICAL substrates and to reveal whether these substrates are modified through redox reactions.

Calponin Homology domain

The MO domain of MICALs is followed by a Calponin Homology (CH) domain (Fig. 1A). The CH domain was first described in calponin, an actin-binding protein which plays a regulatory role in muscle contractility and non-muscle cell motility (Wu and Jin, 2008). Three main types of CH domains have been described. A combination of type 1 and 2 CH domains forms the actin binding domain of a large number of F-actin interacting proteins. Type 1 CH domains have the intrinsic ability to bind to F-actin. Type 2 domains, however, lack this binding ability but are required to facilitate high-affinity binding (Gimona et al., 2002). Type 3 CH domains can be found as a single CH domains in several cytoskeletal and signaling proteins (Korenbaum and Rivero, 2002; Gimona et al., 2002).

Structural work has shown that MICALs contain a type 2 CH domain (Sun et al., 2006). Interestingly, purified CH domain of human MICAL-1 does not bind F-actin (Sun et al., 2006). Similarly, the CH domain of *Drosophila* Mical is not required for F-actin interactions (Hung et al., 2010). This is in line with the fact

that type 2 CH domains normally assist actin binding but do not mediate the interaction itself (Gimona et al., 2002). It has been proposed that the MICAL CH domain facilitates F-actin binding to the MO domain (Hung et al., 2010). Alternatively, the CH domain may function as a protein-protein interaction module for proteins other than actin (Korenbaum and Rivero, 2002; Gimona et al., 2002). Interestingly, the tertiary structure of the MICAL-1 CH domain shows hydrophobic residues on its surface, which have the potential to form hydrophobic interactions with other proteins (Sun et al., 2006).

LIM domain

The LIM (Lin11, Isl-1 and Mec-3) domain is another domain shared by all MICAL proteins. It is connected to the CH domain by a variable region, which is not conserved among family members and variable in length (Fig. 1A). Many LIM domain containing proteins are expressed in the nervous system and mediate various functions during neuronal development (Bach, 2000). However, how the LIM domain facilitates the functions of these proteins remains largely unknown.

The LIM domain is a cysteine-histidine rich, zinc-coordinating domain. Unlike zinc fingers for DNA binding, (for example GATA-type domains), LIM domains do not bind DNA. Rather, LIM domains have been implicated in mediating specific protein-protein interactions (Dawid et al., 1998; Bach, 2000). The MICAL LIM domain also seems to be a docking site for other protein(s). For example, in chapter 5 the LIM domain of MICAL-1 is shown to be involved in binding to NDR kinase. Interestingly, the MICAL-1 LIM domain also mediates an intramolecular interaction with the C-terminal region. This intramolecular interaction results in an autoinhibited protein conformation that blocks the enzymatic activity of the MO domain (Schmidt et al., 2008). This intriguing role of the LIM domain will be discussed further in a subsequent section.

Proline-rich regions

Proline-rich regions are not only important for proper protein folding, but also have a potential to interact with other proteins (Williamson, 1994; Kay et al., 2000). MICAL-1 contains a proline-rich region close to its C-terminal coiled-coil motifs. Within this region, a PPKPP (Pro-Pro-Lys-Pro-Pro) motif has been identified that specifically interacts with the SH3 domain of Cas family members, Cas and CasL (Fig. 1A) (Suzuki et al., 2002). The PPKPP motif is conserved between mouse and human MICAL-1, but absent from MICAL-2 and 3 (Pasterkamp et al., 2006). However, in all vertebrate and invertebrate MICALs, proline-rich regions can be found scattered throughout the protein sequence. It is therefore possible that all MICALs utilize proline-rich regions for interacting with other proteins.

Glutamic acid-repeat

Human and mouse MICAL-1, but not other MICAL proteins, contain a glutamic acid-repeat region in the vicinity of the C-terminal coiled-coil motifs (Fig. 1A) (Weide et al., 2003; Pasterkamp et al., 2006). The function of this stretch is unknown, but several glutamic acid-rich proteins have been shown to interact with histones via their glutamic acid-rich regions (Rayala et al., 2006; Woodcock and Dimitrov 2001; Vadlamudi et al., 2001). Whether MICAL-1 can engage in similar interactions remains to be addressed.

Coiled-coil motifs

The coiled-coil motif is a ubiquitous protein folding and assembly motif. Predictions based on analysis of primary sequences suggest that approximately 2-3% of all proteins form coiled-coils (Wolf et al., 1997; Burkhard et al., 2001). By 2002, already more than 200 proteins containing coiled-coil motifs had been identified (Yu, 2002). These proteins exhibit a broad range of different functions related to their specific coiled-coil motifs (Burkhard et al., 2001).

All MICAL proteins have several coiled-coil motifs distributed in their linear structures (Fig. 1). In case of MICAL-1, coiled-coil motifs are present in the C-terminal region (Fig. 1A). This region is involved in

interactions with several different proteins including plexinA, vimentin, Rab1 and NDR1 (Terman et al., 2002; Suzuki et al., 2002; Weide et al., 2003; Schmidt et al., 2008; chapter 5). Furthermore, in MICAL-1 this region binds to the LIM domain containing part of the protein, thereby inducing an intramolecular interaction that autoinhibits MO domain activity (Schmidt et al., 2008). It remains to be shown, however, whether the coiled-coil motifs themselves or other sequences in the C-terminal region are required for mediating these inter- and intramolecular interactions. Nevertheless, coiled-coil motifs are potential protein interacting modules that may mediate the recruitment of other proteins or mediate MICAL intramolecular interactions.

In conclusion, MICAL proteins contain a number of well known protein-protein interaction modules with the potential to recruit other structural or signaling proteins. Although several proteins have been identified as interactors of the C-terminal region of MICALs, binding partners for other domains in MICALs remain unknown.

Intramolecular autoinhibitory regulation of MICAL-1

Our own work and that of Schmidt et al. shows that deletion of the C-terminal region (about 290 amino acids) of mouse MICAL-1 leads to a large increase in hydrogen peroxide (H_2O_2) production by the MICAL-1 MO domain and in cell contraction (chapter 3; Schmidt et al., 2008). Interestingly, these effects can be inhibited by addition of purified C-terminal region to cell lysates (for H_2O_2 production) or by expression of the C-terminal part of MICAL-1 in cells (for cell contraction). The C-terminal region of MICAL-1 can physically interact with the N-terminal part of MICAL-1 containing the LIM domain. These results support a model in which a physical interaction between the N- and C-terminal regions of MICAL-1 induces an autoinhibitory conformation of MICAL-1 to restrict MO activity (see Schmidt et al., 2008 for more details). It has therefore been suggested that proteins interacting with the C-terminal region of MICALs may release the autoinhibitory state and induce enzymatic activity (Schmidt et al., 2008). However, which proteins function to regulate the autoinhibitory state of MICALs is currently unknown.

Expression and distribution of MICALs

In HeLa, HEK293, COS-7 and L cells, endogenous or exogenous MICAL-1 mainly localizes to the cytosol and occasionally in filopodia or lamellipodia, but is absent from the nuclear compartment (Schmidt et al., 2008; Suzuki et al., 2002; chapter 5). This is supported by cell fractionation studies showing that endogenous MICAL-1 is present in the cytoplasmic fraction and marginally in membrane fractions (Weide et al., 2003). MICAL-3 has also been found in the cytosol and may attach to the membrane via interactions with small GTPases (Fischer et al., 2005). Interestingly, one study has suggested that MICAL-1 and 3 interact with the microtubule cytoskeleton in cells (Fischer et al., 2005). The cellular distribution of MICAL-2 is currently unknown.

MICAL proteins are widely expressed in different tissues. In mouse, MICAL-1 and 3 proteins are detected in brain, lung, spleen and kidney (Suzuki et al., 2002; Fischer et al., 2005). The distribution of MICALs in the brain has been studied in detail using Northern blot analysis and *in situ* hybridization (Pasterkamp et al., 2006). *MICAL-1* and *MICAL-3* transcripts are expressed at comparable levels from E15 (Embryonic day 15) to adulthood in the brain (Pasterkamp et al., 2006). *MICAL-2* transcripts can only be detected starting from E18 and levels increase towards adulthood (Pasterkamp et al., 2006). The spatiotemporal distribution patterns of different the MICALs in brain tissue are highly similar with a few exceptions. For example, MICAL-2 expression is delayed and is absent from the striatum and hypothalamus where MICAL-1 and 3 are found (Pasterkamp et al., 2006). These expression patterns indicate overlapping and distinct functions for the three vertebrate MICALs during brain development and homeostasis (Pasterkamp et al., 2006).

Cellular functions of MICAL proteins

MICALs exert different cellular effects via interactions with a variety of membrane-associated or cytoplasmic proteins. The proteins currently known to interact with MICALs are discussed here in light of their cellular functions. The role of MICALs during neural development is discussed in a separate section.

Cytoskeletal regulation

MICALs have been shown to bind cytoskeletal proteins and to regulate their organization (Suzuki et al., 2002; Fischer et al., 2005; Beuchle, 2007; Hung et al., 2010). The most compelling piece of evidence for a role for MICALs in cytoskeletal regulation was obtained recently from work on bristle formation in *Drosophila*. It was shown that purified Mical MO domain directly binds F-actin and is able to disassemble both individual and bundled actin filaments (in the presence of NADPH) (Hung et al., 2010). In agreement with a role in F-actin regulation, Mical is required for the development of bristles in the fruit fly. The bristle structure is maintained by actin filaments within the chitin-cuticle. Manipulation of Mical expression, by decreasing or increasing its levels, causes abnormal bristle branching and accompanying defects in actin filaments (Hung et al., 2010). In addition, Mical deficient larva show disorganized and accumulated actin and myosin filaments instead of a regular sarcomeric pattern in somatic muscles (Beuchle, 2007). Actin regulation by Mical has also been implicated in dendritic pruning, a process that selectively removes redundant neurites without causing neuronal death (Kirilly et al., 2009). During this process, Mical has been suggested to either affect actin filament bundling directly or to bind other actin-regulators to rearrange dendritic actin and consequently remodel neurites (Kirilly et al., 2009).

Several lines of evidences suggest that vertebrate MICALs affect the cytoskeleton either directly or indirectly through interacting proteins. First, the MO domain of MICAL-1 induces dramatic cell contraction which is accompanied by rearrangements of the cytoskeleton (Schmidt et al., 2008). Second, MICAL-1 may indirectly regulate the cytoskeleton via binding to CasL (Suzuki et al., 2002). CasL belongs to the p130Cas (Cas) family and has been indicated in the regulation of actin dynamics (Suzuki et al., 2002). Third, MICALs have been found to associate with other cytoskeletal components, such as vimentin intermediate filaments or tubulin-containing microtubules. MICAL-1 colocalizes with vimentin in human cell lines and binds to vimentin via its C-terminal region (Suzuki et al., 2002). MICAL-1 and 3 both have been suggested to associate with microtubules. Fischer et al. showed a filamentous distribution of MICAL-1 and 3 in HeLa cells, and these specific distribution patterns were disrupted when the microtubule network was destroyed by nocodazole treatment (Fischer et al., 2005). In all, these studies suggest that MICALs regulate cytoskeletal elements in invertebrates and vertebrates both directly though their MO domains and indirectly via interacting proteins.

Vesicle transport

All three MICALs (MICAL-1, 2 and 3) interact with the small GTPase Rab1, a protein involved in vesicle trafficking between the endoplasmic reticulum (ER) and the Golgi complex (Weide et al., 2003; Fischer et al., 2005). Interestingly, MICAL-Like proteins (MICAL-L1 and 2) also interact with Rab proteins and have been implicated in vesicle transport events. As mentioned before, MICAL-Like proteins have a similar domain organization as MICALs but lack the N-terminal MO domain. Endogenous MICAL-L1 is essential for the recycling of several receptors including transferrin and integrins. Depletion of MICAL-L1 impairs the transport of these receptors from endocytic recycling compartments back to the plasma membrane (Sharma et al., 2009, 2010). During this process, MICAL-L1 recruits Rab8 and EHD1 (an endocytosis regulator) to tubular recycling endosomes to exert their regulatory functions on these structures (Sharma et al., 2009; Grosshans et al., 2006; Rapaport et al., 2006).

MICAL-L2 also binds Rab8. This interaction mediates the transport of cell junction proteins to the plasma membrane (Yamamura et al., 2008). In addition, MICAL-L2 recruits Rab13 to function in the endocytic recycling of occludin, an integral tight junction protein mediating cell-cell adhesion (Furuse et al.,

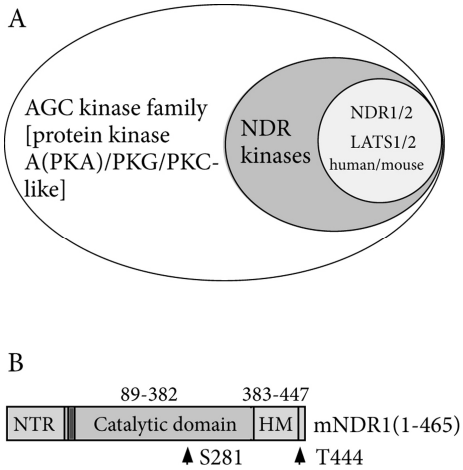

Figure 2. NDR kinases belong to the AGC kinase family.
(A) NDR kinases are members of the AGC kinase family. Currently, four NDR kinases are known in human and mouse, i.e. NDR 1 and 2, and LATS 1 and 2.
(B) Schematic representation of mouse NDR1 (mNDR1). The domain structure shows an N-terminal region (NTR), followed by a catalytic domain and a hydrophobic motif (HM). Two highly conserved phosphorylation sites which regulate NDR1 kinase activity are depicted as S281 and T444. The numbers on each domain indicate amino acid positions.

1993). Terai et al. observed that a MICAL-L2 mutant lacking the Rab13-binding domain (the C-terminal coiled-coil containing region) specifically inhibited occludin endocytic recycling (Terai et al., 2006). A more recent report from the same group noticed that depletion of MICAL-L2 inhibits the transportation of several other cell junction proteins including claudin-1 and E-cadherin (Yamamura et al., 2008). These results suggest that MICAL-Like (and probably also MICAL) proteins recruit Rab small GTPase to facilitate the transport of receptors and/or cell junction proteins.

NDR kinases mediated apoptosis

In this thesis, a novel function for MICAL-1 in the regulation of apoptosis is described. In chapter 4 and 5, we identify NDR1 kinase as a MICAL-1 interacting protein and show a functional relationship between MICAL-1 and NDR kinases during apoptosis. Our current knowledge of the function and mechanism-of-action of NDR kinases is summarized in the following section.

Structure and regulation of NDR kinases

NDR kinases belong to serine/threonine AGC (protein kinase A (PKA) /PKG /PKC-like) kinase family (Hergovich and Hemmings, 2009). They are named Nuclear Dbf2-related kinases after Dbf2 kinase, a NDR homolog in budding yeast, which shares about 80% similarity with human NDRs (Millward et al., 1995). Human and rodents express 4 NDR kinases, NDR1, NDR2 (also known as serine threonine kinase 38 (STK38) and STK38-like) and LATS-1, LATS-2 (large tumor suppressor-1 and 2) (Hergovich and Hemmings, 2009) (Fig. 2A).

NDR 1 and 2 (NDR1/2) are highly similar proteins (~86% amino acid identical), but their distribution at the cellular level is different (Stegert et al., 2004; Devroe et al., 2004). Northern blot analysis indicates that NDR1 is transcribed in brain, thymus, muscle, testis, spleen, lung, fat tissue, placenta, ovary and leukocyte, whereas NDR2 is mainly transcribed in brain, thymus, muscle, testis, heart, liver, kidney, stomach and intestine (Millward et al., 1995; Stegert et al., 2004; Devroe et al., 2004; Stork et al., 2004).

NDR1/2 contain an N-terminal regulatory region, followed by a catalytic region and a C-terminal hydrophobic region (Fig. 2B). These two proteins have similar intra- and inter-molecular regulatory mechanisms.

The N-terminal region of NDRs is conserved among NDR family members and has been suggested to regulate NDR kinase activity via interactions with S100B or MOB1 proteins. S100B, a calcium binding protein, and MOB1 regulate several different cellular processes such as morphology, differentiation,

migration and growth (Donato et al., 2009; Devroe et al., 2004). S100B and MOB1 regulate NDR kinase activity in a similar manner; they both induce a conformational change in the NDR protein upon binding (Bichsel et al., 2004).

The most interesting feature of NDRs is in their catalytic domain. NDR kinases contain 12 subdomains in their catalytic domain (Tamaskovic et al., 2003a, b). Unlike other AGC family members, an insertion of about 30 amino acids is present in between subdomains VII and VIII. This peptide is highly basic and has been suggested to inhibit NDR kinase activity (Bichsel et al., 2004). Indeed, the activation induced by MOB1 is mediated by relieving this autoinhibited structure (Bichsel et al., 2004). Serine 281/282 (S281/282 in NDR1/2, respectively) within the catalytic domain contributes to the regulation NDR1/2 activity. S281/282 can be autophosphorylated by NDR kinases and this phosphorylation is enhanced by S100B or MOB1 binding. S281/282 phosphorylation augments NDR kinase activity (Bichsel et al., 2004; Tamaskovic et al., 2003b).

Like other AGC protein kinases, NDRs have a regulatory C-terminal hydrophobic motif (Tamaskovic et al., 2003a). PKA and PKB, two AGC kinases, are activated by phosphorylation of their hydrophobic motif, which promotes a topological transition to generate a kinase-active conformation (Tamaskovic et al., 2003a). This mechanism may function in NDR kinases as well. A conserved phosphorylation site, threonine 444/442 (T444/442 in NDR1/2, respectively), has been found within hydrophobic motif of NDR1/2 and phosphorylation of T444/442 is required for full NDR kinase activity. An upstream kinase of NDR1/2, MST kinase (Mammalian Ste20-Like) has been found to phosphorylate NDR1/2 at T444/442 and consequently to activate these kinases (Stegert et al., 2005).

Function of NDR kinases

MST and MOB1 work together to activate NDR kinases in different biological processes (Hirabayashi et al., 2008; Ponchon et al., 2004). During the cell cycle, the MST-MOB-NDR complex is required for duplication of centrosomes and for alignment of chromosomes on the metaphase plate (Hergovich, et al., 2009; Chiba et al., 2009). These events are important for ensuring the equal segregation of genetic material between the two daughter cells.

MST, MOB and NDR also work together during apoptosis. A Fas receptor mediated apoptotic pathway was identified that contained the MOB-MST-NDR complex (Vichalkovski et al., 2008). In this pathway, the tumor suppressor RASSF1A (Ras association domain family 1 isoform A) receives signals from Fas receptor and exerts its proapoptotic effects on MST kinase. MST, accompanied by MOB, activates NDR kinases and consequently induces apoptosis (Vichalkovski et al., 2008). In addition, indirect evidence shows that $NDR1^{-/-}$ and $NDR1^{+/-}$ mice become more sensitive to the development of T cell lymphomas as compared to wild-type mice (Cornils et al., 2010). This is most likely due to defective apoptosis by a decrease in NDR levels (Cornils et al., 2010). These findings define NDRs as proapoptotic kinases (Vichalkovski et al., 2008).

Functions of MICALs during neural development

Thus far, MICAL proteins have been best characterized for their role during neural circuit development, especially in axon guidance, as intracellular binding partners of plexin receptors. These and other neuronal functions of MICALs are described in this section.

Axon guidance

The process of axon guidance

During neural development, neurons extend axons along predefined routes within the developing embryo. Chemotactic molecules in extracellular environment, known as guidance cues, instruct axons to grow into the proper direction. These guidance cues can either be diffusible or membrane-bound. Furthermore, some guidance cues prevent axons from growing into specific territories and are defined as

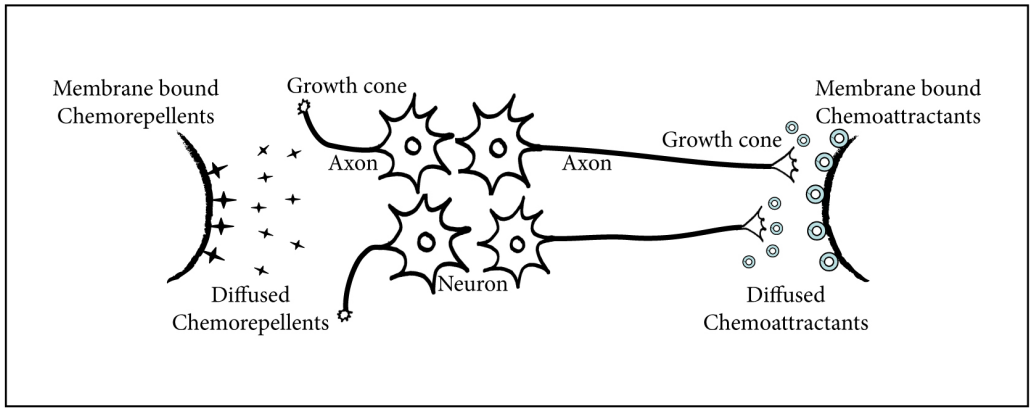

Figure 3. The schematic representation of axon guidance.

During development, neurons send out axons along molecularly predefined routes towards distant targets. The growth cone at the tip of each axon senses environmental signals (guidance cues) that determine the direction of growth. Diffusible or membrane-bound guidance cues can either prevent axons from growing into specific territories (repellents) or attract them into specific directions (attractants).

repellents; while others permit or stimulate axon growth into a specific direction and are called attractants (Fig. 3) (Van den Heuvel and Pasterkamp, 2008; Bashaw and Klein, 2010).

Axon guidance cues are detected by the growth cone, a highly motile structure at the tip of each growing axon. Growth cones express different receptors to interact with extracellular signals such as guidance cues. Interactions between growth cone receptors and guidance cues triggers intracellular signaling events, which ultimately lead to a modification of the cytoskeleton and changes in growth cone morphology and axon steering.

Semaphorin and MICALs

Semaphorins form one of the five large families of axon guidance cues (Van den Heuvel and Pasterkamp, 2008; Pasterkamp and Giger, 2009). Various growth cone receptors and intracellular effectors are involved in detecting and mediating the effects of semaphorins on growth cones and cells. Semaphorins and their receptors are described in detail in chapter 2.

In *Drosophila*, Mical is required for semaphorin1A-plexinA-mediated repulsive axon guidance. Mical physically interacts with the plexinA cytosolic region. Depletion of Mical disturbs the proper patterning of (inter)segmental nerves preventing normal muscle innervation. This (mis)guidance phenotype is identical to phenotypes observed in *semaphorin 1A* and *plexinA* deficient flies (Terman et al., 2002). Taking into account the effect of Mical on actin dynamics it has been proposed that Mical forms a bridge between plexinA receptors and the cytoskeleton and induces cytoskeletal modification upon semaphorin ligand binding.

Vertebrate MICAL-1 has been implicated in semaphorin3A (Sema3A) signaling. Sema3A can be sensed by a receptor complex composed of neuropilins and plexinAs. In this complex, plexinAs function as the signal transducing co-receptor. MICAL-1 has been considered to be an effector that binds to the plexinA1 cytosolic region and modulates the cytoskeleton via its MO domain, as has been postulated for *Drosophila* Mical (Fig. 4) (Schmidt et al., 2008). Although *in vivo* evidence for a role of MICALs in vertebrate axon guidance is still lacking, several *in vitro* observations support a role for MICAL-1 in the Sema3A pathway. First, MICAL-1 physically interacts with plexinA1 and this interaction is enhanced by Sema3A stimulation

Figure 4. Simplified schematic representation of the role of MICAL in semaphorin signaling.
Class 3 semaphorins (Sema) bind a receptor complex composed of neuropilin and plexin proteins at the surface of growth cones to regulate axon guidance through the modification of the cytoskeleton. MICALs bind plexins and may serve as a direct regulatory link to the actin cytoskeleton (for more details on semaphorin signaling, see chapter 2).

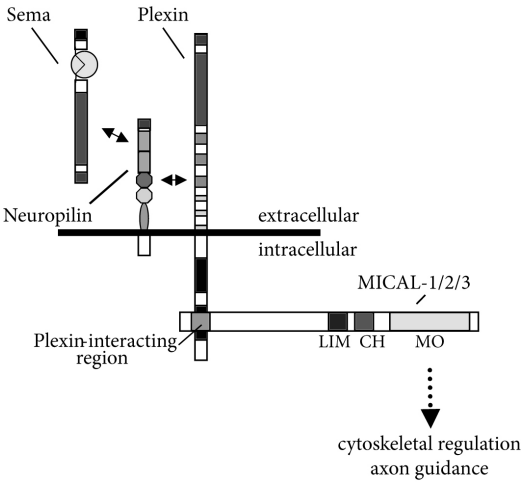

(Schmidt et al., 2008). Second, overexpression of MO truncated MICAL-1 mutants in neurons abolishes their reaction to Sema3A (Schmidt et al., 2008). Third, in agreement with point two, when MO activity is blocked by monooxygenase inhibitors, neurons become unresponsive to Sema3A stimulation (Terman et al., 2002). Fourth, MICAL-1 can bind to other effectors of Sema3A pathway including CRMP and RanBPM (Ran small GTPase binding protein) (Schmidt et al., 2008; Togashi et al., 2006). The interaction of MICAL-1 with CRMP induces cell contraction, a phenomenon resembling growth cone collapse induced by Sema3A treatment (Schmidt et al., 2008). MICAL-1 has been suggested to regulate the interaction between RanBPM and plexinA1, which has been shown to be involved in Sema3A induced axon repulsion (Togashi et al., 2006).

Synaptic structure

In Drosophila, Mical is a critical regulator of synaptic structure during postembryonic development (Beuchle et al., 2007). First, synaptic bouton distribution at neuromuscular junctions is largely influenced by Mical. In Mical mutants, synaptic boutons have the tendency to cluster around initial nerve-muscle contact sites and along synaptic branches and therefore fail to spread properly along the muscle fiber (Beuchle, 2007). Second, Mical is important for the highly structured postsynaptic domain. Postsynaptic sites are normally wrapped by an insulating layer of subsynaptic reticulum. In Mical mutants, however, the subsynaptic reticulum can hardly be discerned from myofilaments, which are normally absent from this region (Beuchle, 2007).

Other neuronal functions

In addition to axon guidance and synapse development, Mical also plays an important role during dendritic pruning in *Drosophila* (Kirilly et al., 2009). Dendritic pruning is a refinement process during nervous system development, which functions to selectively remove unsuitable or inaccurate neurites for building precise neural circuits (Kirilly et al., 2009). In *Drosophila*, larval-born neurons undergo extensive remodeling at the early metamorphosis stage to construct the adult nervous system (Kirilly et al., 2009). During this stage, Mical expression is upregulated. Mical depletion in fruit flies results in a failure to severe inappropriate dendrites from the neuronal soma. Although the precise mechanism by which Mical regulates dendritic pruning is unknown, it may involve regulation of the cytoskeleton (Kirilly et al., 2009).

In the chick spinal cord, MICAL-3 has been found to be involved in the proper positioning of motor neuron somata (Bron et al., 2007). During development of nervous system, neurons migrate from sites of neurogenesis to their final destination. MICAL-3 is required for determining the final position of motor neurons in the spinal cord. Knockdown of MICAL-3 by shRNA in chick motor neurons leads to their ectopic positioning in the PNS (peripheral nervous system). This is consistent with phenotypes observed following depletion or knockdown of Sema3B, neuropilin-2 or plexinA2, indicating a functional interaction between these proteins (Bron et al., 2007). Most likely, motor neurons sense Sema3B via a receptor complex composed of neuropilin-2 and plexinA2 that regulates MICAL-3 and consequently triggers a reorganization of the cytoskeleton (Bron et al., 2007).

Aim and outline of this thesis

The translation of extracellular signals into a specific cellular response critically depends on the activation of intracellular signal transduction pathways. These pathways become activated upon stimulation of upstream factors such as membrane receptors and can have various downstream effects. MICALs form a relatively novel and unusual family of intracellular signaling proteins that operate in various cellular processes in different species. The aim of this thesis is to further our understanding of the function, mechanism-of-action and regulation of MICAL proteins, focusing on the founding member of the MICAL family, MICAL-1.

The functions of MICALs have been studied extensively in the signal transduction cascades that operate downstream of semaphorins and their plexin receptors. In chapter 2, we therefore provide an overview of our current knowledge of semaphorin signaling. Semaphorins can be divided in several different classes and this chapter summarizes the receptors and signaling complexes utilized by semaphorins to exert their biological effects.

MICALs have an unusual domain organization as they contain an enzymatic domain in addition to several protein-protein interaction motifs. In chapter 3, we show that the MICAL-1 MO domain is catalytically active and required for inducing cell contraction responses. Interestingly, preliminary results suggest that MICAL-1 functions as a homo-oligomer and that it may be regulated by upstream kinases, since specific phosphorylation sites were identified in MICAL-1.

Since it is largely unknown how the MO activity of MICALs is regulated or which other signaling proteins function in conjunction with MICALs, we applied different methods to obtain MICAL-1-containing protein complexes and characterized these complexes by mass spectrometry in chapter 4. Several novel MICAL-1 interacting proteins were identified and one of these interactors, NDR1 kinase, is studied in detail in chapter 5. Chapter 5 shows that MICAL-1 and NDR1 cooperate in the control of apoptosis and that MICAL-1 serves as a competitive inhibitor for MST, an upstream kinase that normally activates NDR kinases. MICAL-1 negatively regulates MST-mediated NDR activation and thereby blocks apoptosis.

Interestingly, both MICAL-1 and NDR kinases have been implicated in the control of axon growth and guidance. In chapter 6, we examine whether like MICAL-1, NDR kinases function in axon guidance downstream of semaphorins and their plexin receptors. Although we do not provide data for a cooperation of MICAL-1 and NDR kinases in semaphorin-plexin mediated signaling, NDR1 is reported to bind plexin receptors suggesting a role in this signaling pathway.

Finally, in chapter 7, we discuss the results of the work outlined in this thesis in light of what is known about MICAL function and signaling with a particular emphasis on the upstream and downstream factors involved in MICAL signaling. The studies described in this thesis improve our understanding function and mechanism-of-action of MICAL proteins and provide a valuable framework for future studies on the role of MICALs in physiological and pathological processes.

Reference

Abe, I., K. Kashiwagi, and H. Noguchi. (2000a). Antioxidative galloyl esters as enzyme inhibitors of p-hydroxybenzoate hydroxylase. FEBS Lett 483:131–134.

Abe, I., T. Seki, K. Umehara, T. Miyase, H. Noguchi, J. Sakakibara, and T. Ono. (2000b). Green tea polyphenols: novel and potent inhibitors of squalene epoxidase. Biochem Biophys Res Commun 268:767–771.

Ashida S, Furihata M, Katagiri T, Tamura K, Anazawa Y, Yoshioka H, Miki T, Fujioka T, Shuin T, Nakamura Y, Nakagawa H. (2006). Expression of novel molecules, MICAL2-PV (MICAL2 prostate cancer variants), increases with high Gleason score and prostate cancer progression. Clin Cancer Res. 2006 May 1;12(9):2767-73.

Bach I. (2000). The LIM domain: regulation by association. Mech Dev. 2000 Mar 1;91(1-2):5-17.

Bashaw GJ, Klein R. (2010). Signaling from axon guidance receptors. Cold Spring Harb Perspect Biol. 2010 May 1;2(5):a001941.

Beuchle D, Schwarz H, Langegger M, Koch I, Aberle H. (2007). Drosophila MICAL regulates myofilament organization and synaptic structure. Mech Dev. 2007 May;124(5):390-406.

Bichsel SJ, Tamaskovic R, Stegert MR, Hemmings BA. (2004). Mechanism of activation of NDR (nuclear Dbf2-related) protein kinase by the hMOB1 protein. J Biol Chem. 2004 Aug 20;279(34):35228-35.

Bron R, Vermeren M, Kokot N, Andrews W, Little GE, Mitchell KJ, Cohen J. (2007). Boundary cap cells constrain spinal motor neuron somal migration at motor exit points by a semaphorin-plexin mechanism. Neural Dev. 2007 Oct 30;2:21.

Burkhard P, Stetefeld J, Strelkov SV. (2001). Coiled coils: a highly versatile protein folding motif. Trends Cell Biol. 2001 Feb;11(2):82-8.

Chiba S, Ikeda M, Katsunuma K, Ohashi K, Mizuno K. (2009). MST2- and Furry-mediated activation of NDR1 kinase is critical for precise alignment of mitotic chromosomes. Curr Biol. 2009 Apr 28;19(8):675-81.

Cole LJ, Entsch B, Ortiz-Maldonado M, Ballou DP. (2005). Properties of p-hydroxybenzoate hydroxylase when stabilized in its open conformation. Biochemistry. 2005 Nov 15;44(45):14807-17.

Cornils H, Stegert MR, Hergovich A, Hynx D, Schmitz D, Dirnhofer S, Hemmings BA. (2010). Ablation of the kinase NDR1 predisposes mice to the development of T cell lymphoma. Sci Signal. 2010 Jun 15;3(126):ra47.

Dawid IB, Breen JJ, Toyama R. (1998). LIM domains: multiple roles as adapters and functional modifiers in protein interactions.Trends Genet. 1998 Apr;14(4):156-62.

Devroe E, Erdjument-Bromage H, Tempst P, Silver PA. (2004). Human Mob proteins regulate the NDR1 and NDR2 serine-threonine kinases. J Biol Chem. 2004 Jun 4;279(23):24444-51.

Donato R, Sorci G, Riuzzi F, Arcuri C, Bianchi R, Brozzi F, Tubaro C, Giambanco I. (2009). S100B's double life: intracellular regulator and extracellular signal. Biochim Biophys Acta. 2009 Jun;1793(6):1008-22.

Entsch B, Cole LJ, Ballou DP. (2005). Protein dynamics and electrostatics in the function of p-hydroxybenzoate hydroxylase. Arch Biochem Biophys. 2005 Jan 1;433(1):297-311.

Fischer J, Weide T, Barnekow A. (2005). The MICAL proteins and rab1: a possible link to the cytoskeleton? Biochem Biophys Res Commun. 2005 Mar 11;328(2):415-23.

Furuse, M., Hirase, T., Itoh, M., Nagafuchi, A., Yonemura, S., and Tsukita, S. (1993). Occludin: a novel integral membrane protein localizing at tight junctions. J. Cell Biol. 123, 1777-1788.

Gimona M, Djinovic-Carugo K, Kranewitter WJ, Winder SJ. (2002). Functional plasticity of CH domains.FEBS Lett. 2002 Feb 20;513(1):98-106.

Grosshans, B. L., Ortiz, D., and Novick, P. (2006). Rabs and their effectors: achieving specificity in membrane traffic. Proc. Natl. Acad. Sci. USA 103, 11821–11827.

Hergovich A, Hemmings BA. (2009). Mammalian NDR/LATS protein kinases in hippo tumor suppressor signaling. Biofactors. 2009 Jul-Aug;35(4):338-45.

Hergovich A, Kohler RS, Schmitz D, Vichalkovski A, Cornils H, Hemmings BA. (2009). The MST1 and hMOB1 tumor suppressors control human centrosome duplication by regulating NDR kinase phosphorylation. Curr Biol. 2009 Nov 3;19(20):1692-702.

Hirabayashi S, Nakagawa K, Sumita K, Hidaka S, Kawai T, Ikeda M, Kawata A, Ohno K, Hata Y. (2008). Threonine 74 of MOB1 is a putative key phosphorylation site by MST2 to form the scaffold to activate nuclear Dbf2-related kinase 1. Oncogene. 2008 Jul 17;27(31):4281-92.

Hung RJ, Yazdani U, Yoon J, Wu H, Yang T, Gupta N, Huang Z, van Berkel WJ, Terman JR. (2010). Mical links semaphorins to F-actin disassembly. Nature. 2010 Feb 11;463(7282):823-7.

Joosten V, van Berkel WJ. (2007). Flavoenzymes. Curr Opin Chem Biol. 2007 Apr;11(2):195-202.

Kay BK, Williamson MP, Sudol M. (2000). The importance of being proline: the interaction of proline-rich motifs in signaling proteins with their cognate domains. FASEB J. 2000 Feb;14(2):231-41.

Kirilly D, Gu Y, Huang Y, Wu Z, Bashirullah A, Low BC, Kolodkin AL, Wang H, Yu F. (2009). A genetic pathway composed of Sox14 and Mical governs severing of dendrites during pruning. Nat Neurosci. 2009 Dec;12(12):1497-505.

Korenbaum E, Rivero F. (2002). Calponin homology domains at a glance.J Cell Sci. 2002 Sep 15;115(Pt 18):3543-5.

Millward T, Cron P, Hemmings BA. (1995). Molecular cloning and characterization of a conserved nuclear serine(threonine) protein kinase. Proc Natl Acad Sci U S A. 1995 May 23;92(11):5022-6.

Nadella M, Bianchet MA, Gabelli SB, Barrila J, Amzel LM. (2005). Structure and activity of the axon guidance protein MICAL. Proc Natl Acad Sci U S A. 2005 Nov 15;102(46):16830-5.

Pasterkamp RJ, Dai HN, Terman JR, Wahlin KJ, Kim B, Bregman BS, Popovich PG, Kolodkin AL. (2006). MICAL flavoprotein monooxygenases: expression during neural development and following spinal cord injuries in the rat. Mol Cell Neurosci. 2006 Jan;31(1):52-69.

Pasterkamp RJ, Giger RJ. (2009). Semaphorin function in neural plasticity and disease. Curr Opin Neurobiol. 2009 Jun;19(3):263-74.

Ponchon L, Dumas C, Kajava AV, Fesquet D, Padilla A. (2004). NMR solution structure of Mob1, a mitotic exit network protein and its interaction with an NDR kinase peptide. J Mol Biol. 2004 Mar 12;337(1):167-82.

Rapaport, D., Auerbach, W., Naslavsky, N., Pasmanik-Chor, M., Galperin, E., Fein, A., Caplan, S., Joyner, A. L., and Horowitz, M. (2006). Recycling to the plasma membrane is delayed in EHD1 knockout mice. Traffic 7, 52–60.

Rayala SK, den Hollander P, Manavathi B, Talukder AH, Song C, Peng S, Barnekow A, Kremerskothen J, Kumar R. (2006). Essential role of KIBRA in co-activator function of dynein light chain 1 in mammalian cells. J Biol Chem. 2006 Jul 14;281(28):19092-9.

Schmidt EF, Shim SO, Strittmatter SM. (2008). Release of MICAL autoinhibition by semaphorin-plexin signaling promotes interaction with collapsin response mediator protein. J Neurosci. 2008 Feb 27;28(9):2287-97.

Sharma M, Giridharan SS, Rahajeng J, Caplan S, Naslavsky N. (2010). MICAL-L1: An unusual Rab effector that links EHD1 to tubular recycling endosomes. Commun Integr Biol. 2010 Mar;3(2):181-3.

Sharma M, Giridharan SS, Rahajeng J, Naslavsky N, Caplan S. (2009). MICAL-L1 links EHD1 to tubular recycling endosomes and regulates receptor recycling. Mol Biol Cell. 2009 Dec;20(24):5181-94.

Siebold C, Berrow N, Walter TS, Harlos K, Owens RJ, Stuart DI, Terman JR, Kolodkin AL, Pasterkamp RJ, Jones EY. (2005). High-resolution structure of the catalytic region of MICAL (molecule interacting with CasL), a multidomain flavoenzyme-signaling molecule. Proc Natl Acad Sci U S A. 2005 Nov 15;102(46):16836-41.

Stegert MR, Hergovich A, Tamaskovic R, Bichsel SJ, Hemmings BA. (2005). Regulation of NDR protein kinase by hydrophobic motif phosphorylation mediated by the mammalian Ste20-like kinase MST3. Mol Cell Biol. 2005 Dec;25(24):11019-29.

Stegert MR, Tamaskovic R, Bichsel SJ, Hergovich A, Hemmings BA. (2004). Regulation of NDR2 protein kinase by multi-site phosphorylation and the S100B calcium-binding protein. J Biol Chem. 2004 May 28;279(22):23806-12.

Stork O, Zhdanov A, Kudersky A, Yoshikawa T, Obata K, Pape HC. (2004). Neuronal functions of the novel serine/threonine kinase Ndr2. J Biol Chem. 2004 Oct 29;279(44):45773-81.

Sun H, Dai H, Zhang J, Jin X, Xiong S, Xu J, Wu J, Shi Y. (2006). Solution structure of calponin homology domain of Human MICAL-1. J Biomol NMR. 2006 Dec;36(4):295-300.

Suzuki T, Nakamoto T, Ogawa S, Seo S, Matsumura T, Tachibana K, Morimoto C, Hirai H. (2002). MICAL, a novel CasL interacting molecule, associates with vimentin. J Biol Chem. 2002 Apr 26;277(17):14933-41.

Tamaskovic R, Bichsel SJ, Hemmings BA. (2003a). NDR family of AGC kinases--essential regulators of the cell cycle and morphogenesis. FEBS Lett. 2003 Jul 3;546(1):73-80.

Tamaskovic R, Bichsel SJ, Rogniaux H, Stegert MR, Hemmings BA. (2003b). Mechanism of Ca2+-mediated regulation of NDR protein kinase through autophosphorylation and phosphorylation by an upstream kinase. J Biol Chem. 2003 Feb 28;278(9):6710-8.

Terai T, Nishimura N, Kanda I, Yasui N, Sasaki T. (2006). JRAB/MICAL-L2 is a junctional Rab13-binding protein mediating the endocytic recycling of occludin. Mol Biol Cell. 2006 May;17(5):2465-75.

Terman JR, Mao T, Pasterkamp RJ, Yu HH, Kolodkin AL. (2002). MICALs, a family of conserved flavoprotein oxidoreductases, function in plexin-mediated axonal repulsion. Cell. 2002 Jun 28;109(7):887-900.

Togashi H, Schmidt EF, Strittmatter SM. (2006). RanBPM Contributes to Semaphorin3A Signaling through plexin-A Receptors. J Neurosci. 2006 May 3; 26(18): 4961–4969.

Vadlamudi R.K., Wang R.-A., Mazumdar A., Kim Y.-S., Shin J., Sahin A., Kumar R. (2001). Molecular cloning and characterization of PELP1, a novel human coregulator of estrogen receptor alpha. J. Biol. Chem. 276:38272-38279(2001)

Van den Heuvel DM, Pasterkamp RJ. (2008). Getting connected in the dopamine system. Prog Neurobiol. 2008 May;85(1):75-93.

Vichalkovski A, Gresko E, Cornils H, Hergovich A, Schmitz D, Hemmings BA. (2008). NDR kinase is activated by RASSF1A/MST1 in response to Fas receptor stimulation and promotes apoptosis. Curr Biol. 2008 Dec 9;18(23):1889-95.

Weide T, Teuber J, Bayer M, Barnekow A. (2003). MICAL-1 isoforms, novel rab1 interacting proteins. Biochem Biophys Res Commun. 2003 Jun 20;306(1):79-86.

Williamson MP. (1994). The structure and function of proline-rich regions in proteins.Biochem J. 1994 Jan 15;297 (Pt 2):249-60.

Wolf E, Kim PS, Berger B. (1997). MultiCoil: a program for predicting two- and three-stranded coiled coils. Protein Sci. 1997 Jun;6(6):1179-89.

Woodcock CL, Dimitrov S. (2001). Higher-order structure of chromatin and chromosomes. Curr Opin Genet Dev. 2001 Apr;11(2):130-5.

Wu KC, Jin JP. (2008). Calponin in non-muscle cells. Cell Biochem Biophys. 2008;52(3):139-48.

Xue Y, Kuok C, Xiao A, Zhu Z, Lin S, Zhang B. (2010). Identification and expression analysis of mical family genes in zebrafish. J Genet Genomics. 2010 Oct;37(10):685-93.

Yamamura R, Nishimura N, Nakatsuji H, Arase S, Sasaki T. (2008). The interaction of JRAB/MICAL-L2 with Rab8 and Rab13 coordinates the assembly of tight junctions and adherens junctions. Mol Biol Cell. 2008 Mar;19(3):971-83.

Yu YB. (2002). Coiled-coils: stability, specificity, and drug delivery potential. Adv Drug Deliv Rev. 2002 Oct 18;54(8):1113-29.

Chapter 2

Semaphorin signaling: progress made and promises ahead

Yeping Zhou, Rou-Afza F. Gunput, R. Jeroen Pasterkamp

Semaphorin signaling: progress made and promises ahead.

Zhou Y, Gunput RF, Pasterkamp RJ.

Trends Biochem Sci. 2008 Apr;33(4):161-70. Review.

Review

Cell PRESS

Semaphorin signaling: progress made and promises ahead

Yeping Zhou, Rou-Afza F. Gunput and R. Jeroen Pasterkamp

Department of Neuroscience and Pharmacology, Rudolf Magnus Institute of Neuroscience, University Medical Center Utrecht, Universiteitsweg 100, 3584 CG, Utrecht, The Netherlands

Semaphorins were initially characterized according to their role in repulsive axon guidance but are now recognized as crucial regulators of morphogenesis and homeostasis over a wide range of organ systems. The pleiotropic nature of semaphorin signaling and its implication in human disease has triggered an enormous interest in the receptor and intracellular signaling mechanisms that direct the cell-type-specific and diverse biological effects of semaphorins. Recent breakthroughs in our understanding of semaphorin signaling link integrin and semaphorin signaling pathways, identify novel ligand–receptor interactions and provide insight into the cellular and molecular bases of bifunctional and reverse signaling events. These discoveries could lead to therapeutic advances in axonal regeneration, cancer and other diseases.

Semaphorins: pleiotropic mediators of development and disease

A limited number of molecular cues control a wide range of biological processes across several organ systems. It is, therefore, not surprising that molecules originally thought to be specific for one particular biological process or for the development and function of individual organ systems are now recognized as simultaneously performing crucial functions in several different cellular processes and systems. A compelling example of a group of pleiotropic signaling molecules is the semaphorin family [1]. Semaphorins initially were characterized according to their role in repulsive axon guidance but now are known as crucial regulators of morphogenesis and homeostasis over a wide range of organ systems [2]. Within these systems, semaphorins influence a variety of biological processes ranging from cell migration to cytokine release. In addition, human genetic analyses implicate semaphorins and their associated receptors and cytosolic signaling molecules as susceptibility and/or causal genes in several diseases, including schizophrenia, cancer and neurodegenerative disease [3,4].

Semaphorin proteins are defined by their semaphorin domains and PSI (plexins, semaphorins and integrins) domains and are further distinguished by distinct protein domains, including immunoglobulin-like (Ig), thrombospondin and basic C-terminal domains. Semaphorins are categorized into eight classes: invertebrate semaphorins are grouped in classes 1, 2 and 5 (five semaphorins in total); classes 3–7 are vertebrate semaphorins (20 semaphorins); and class V contains virally encoded semaphorins (two semaphorins). Class 1, 4, 5, 6 and 7 semaphorins are membrane associated [transmembrane or glycosylphosphatidylinositol (GPI) linked], and semaphorins in classes 2, 3 and V are secreted [1]. Some membrane-associated semaphorins are proteolytically cleaved to generate soluble proteins, generating further diversity [5,6].

The pleiotropic nature of semaphorin signaling and its implication in human disease has triggered an enormous interest in semaphorin function. Work over the past several years has greatly advanced our understanding of semaphorin biology and also has provided insight into the underlying intracellular signaling mechanisms that direct the semaphorins' diverse biological effects. For example, recent findings show that different semaphorin subfamilies bind and signal through the same plexin receptors to elicit varying cellular effects. Furthermore, individual semaphorin proteins can be bifunctional, exerting both repulsive and attractive effects. Additionally,

Corresponding author: Pasterkamp, R.J. (r.j.pasterkamp@umcutrecht.nl).

Glossary

Axon guidance: the process during which extending axons are attracted or repelled by soluble or membrane-associated axon guidance cues in their environment during neural development, thereby instructing them to grow in a specific direction.
Cas: a member of the 130^{Cas} family that serve as docking molecules to assemble and transduce intracellular signals. Cas, localizing at focal adhesions, plays an important role in integrin-induced signaling.
Cofilin: a member of the ADF/cofilin family that binds actin monomers and filaments, causing actin filament depolymerization and preventing their reassembly.
DAP12: an ITAM (immuno-receptor tyrosine-based activation motif)-bearing adaptor protein that is expressed by natural killer and myeloid cells. DAP12 mediates signaling for numerous cell-surface receptors including TREMs.
FAK: a focal adhesion-associated protein kinase involved in cell adhesion and spreading. FAK, localizing at focal adhesions, plays an important role in integrin-induced signaling.
Fyn: a membrane-associated tyrosine kinase and member of the protein-tyrosine kinase oncogene family.
Growth cone: a hand-like structure at the tip of extending axons that senses the outside environment for molecular signals.
Growth-cone collapse: the abrupt retraction of extending growth cones. Observed *in vitro* when neuronal cells are exposed to repulsive axon-guidance molecules such as semaphorins.
Intersegmental nerve (ISN): nerve bundles located between the body segments and carrying information from the ventral cord to the muscle field.
LIMK1: an actin-binding kinase that phosphorylates members of the ADF/cofilin family of actin-binding and filament-severing proteins.
PAK: a serine/threonine kinase that is targeted by Cdc42 and Rac1 and that phosphorylates LIMK.
PDZ domain: a protein–protein interaction module that is found in a wide variety of cytoplasmic molecules associated with cell-surface proteins.
Trabeculation: the process of making myocardial ridges, caused by the perpendicular migration of myocardial cells.
Trem2: A member of a family of cell-surface receptors (TREMs) that participate in diverse cellular processes, including inflammation and bone homeostasis.

certain transmembrane semaphorins can function both as ligands and as receptors. In this article, we discuss these recent developments to create a comprehensive understanding of semaphorin signaling throughout many cellular processes.

Semaphorin signaling

The most prominent semaphorin receptors are the plexin proteins. Plexins can be divided into four classes and include two members in invertebrate species (PlexA and PlexB) and nine members in vertebrates (plexinA1–plexinA4, plexinB1–plexinB3, plexinC1 and plexinD1). In addition to plexins, semaphorin holoreceptor complexes contain numerous coreceptors. These coreceptors can serve as ligand-binding modules (for example, the neuropilins, or Npns) or modulatory subunits (for example, Ig superfamily cell adhesion molecules, or IgCAMs). Non-plexin receptors, such as CD72 and Tim-2 (T cell immunoglobulin and mucin-domain-containing 2), provide further diversity to semaphorin function. The best characterized intracellular semaphorin signaling pathways are those used for repulsive axon guidance and cell migration. A common downstream target of semaphorin signaling pathways in all cells, however, is the cytoskeleton [4,7,8]. We now describe recent advances in our understanding of the receptor and intracellular signaling mechanisms utilized by different subfamily classes of semaphorins.

Invertebrate class 1 and 2 semaphorins

The molecular basis of invertebrate semaphorin signaling has been best characterized in *Drosophila melanogaster*. *D. melanogaster* PlexA is a receptor for the transmembrane semaphorins, Sema-1a and Sema-1b, whereas PlexB binds the secreted semaphorin Sema-2a [9,10] (Figure 1). Sema-1a and Sema-2a bind PlexA and PlexB, respectively, to promote repulsive axon guidance, dendritic targeting and synapse formation [9–12]. In addition to PlexA, the Sema-1a receptor complex contains Off-track (OTK) (Figure 1). OTK, a putative receptor tyrosine kinase (RTK), associates with PlexA *in vitro* and modulates Sema-1a–PlexA-mediated axon repulsion *in vivo* through unidentified mechanisms [13]. Another transmembrane protein that functions in Sema-1a–PlexA signaling is the receptor type guanylyl cyclase Gyc76C (Figure 1). Although currently it is unclear whether Gyc76C associates directly with PlexA, site-directed mutagenesis of the Gyc76C catalytic cyclase domain suggests that cGMP production by Gyc76C is essential for its function in repulsive Sema-1a–PlexA signaling [14]. Gyc76C might provide an *in vivo* link between the semaphorin and cGMP signaling pathways that were previously characterized *in vitro* [15] (Box 1).

Only a few downstream effectors of PlexA and PlexB receptors have been identified. The PlexA, but not PlexB, cytoplasmic domain binds Nervy, an A-kinase anchoring protein (AKAP), and the flavoprotein monooxygenase protein MICAL (molecule interacting with CasL) [16,17]. Nervy couples PlexA to type II protein kinase A (PKA RII), suggesting the potential for spatiotemporally regulated, cAMP-dependent target-protein phosphorylation. MICAL activation could trigger redox modifications of downstream signaling components or affect integrin signaling by antagonizing Cas function. PlexB, but not PlexA, associates with the small GTPases Rac and Rho [18,19] (Figure 1).

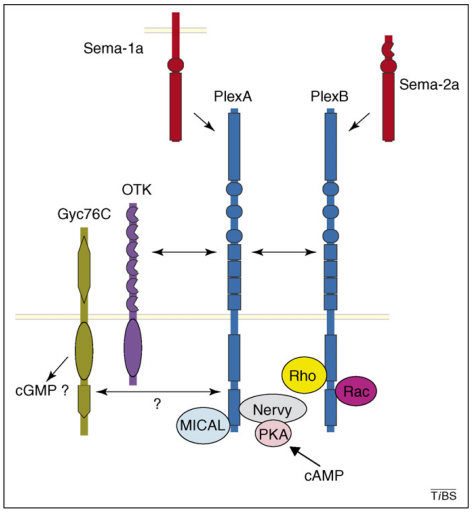

Figure 1. Invertebrate semaphorins signal through PlexA and PlexB. The molecular basis of invertebrate semaphorin signaling has been best characterized in *D. melanogaster*. Two *D. melanogaster* plexins have been described, PlexA and PlexB (blue). PlexA functions as a receptor for the transmembrane semaphorins Sema-1a (red) and Sema-1b (not shown), whereas PlexB binds the secreted semaphorin Sema-2a (red). *D. melanogaster* Sema-1a binds PlexA to influence neuronal and non-neuronal processes. The putative receptor tyrosine kinase OTK (purple) binds PlexA (indicated by arrow) and is required for Sema-1a-mediated axon repulsion. The receptor-type guanylyl cyclase Gyc76C (olive) also functions with Sema-1a and PlexA and might be part of the PlexA receptor complex. The intracellular signaling cascades downstream of Sema-1a and PlexA are poorly understood but include at least two PlexA-binding proteins, Nervy (silver) and MICAL (light blue). The function and mechanism of action of these signaling cues are largely unknown but support a role for cAMP-dependent PKA (protein kinase A; light pink) signaling (through Nervy) and redox signaling (through MICAL) in Sema-1a function. *D. melanogaster* PlexB is a functional Sema-2a receptor and interacts directly with both Rac (magenta) and Rho (yellow). Interestingly, PlexA and PlexB might form heteromultimeric receptor complexes (indicated by an arrow) to promote cooperative guidance effects by granting PlexA access to PlexB-dependent signaling pathways (e.g. those involving Rac) and vice versa (e.g. those involving MICAL).

Interestingly, PlexA and PlexB might perform both distinct and shared functions. For example, defects in the intersegmental nerve (ISN)b are strikingly similar in *plexA*- and *plexB*-deficient flies, whereas defects in longitudinal projections are clearly distinct. The cooperative actions of PlexA and PlexB might be explained by their ability to form heteromultimeric receptor complexes *in vivo* [9] (Figure 1). This association could enable PlexA to access signaling molecules that only bind PlexB (e.g. small GTPases) and vice versa (Figure 1). Although heterophilic interactions also can occur between vertebrate plexins [20], further work is needed to establish the role of heteromultimeric–plexin-receptor associations in semaphorin signaling.

Class 3 semaphorins

Class 3 semaphorins (Sema3A–Sema3G) act as axon repellents and, in a few cases, axon attractants that control the formation of neuronal connections *in vivo*. Sema3s also are

Box 1. The two faces of semaphorins: attraction versus repulsion

Individual semaphorins are bifunctional and can exert repulsive or attractive effects depending on the biological context in which they are encountered. Both extrinsic and intrinsic modulatory signals can facilitate repulsive or attractive semaphorin responses. Extracellular cues (e.g. IgCAMs, proteoglycans and RTKs) generally influence semaphorin function by serving as modulatory receptor subunits [32,42,49,51,54,64]. It is tempting to speculate that these extrinsic factors trigger unique signaling events, either directly or via signal-transducing receptors, such as plexins, that dictate semaphorin repulsion or attraction. This hypothesis is supported by recent work on Sema3B signaling in neurons. Sema3B-mediated attraction, but not repulsion, of cortical axons is accompanied by increased FAK activity [49]. Thus, FAK-associated signaling might be required only for Sema3B-mediated attraction. Although the extrinsic factors that dictate the differential response of neurons to Sema3B remain incompletely defined, other semaphorins require specific extracellular cues for attractive or repulsive effects. By example, HSPGs are required for Sema5A-mediated attraction and might serve as components of axonal Sema5A receptors (Figure 3e). In midbrain axons, CSPGs convert Sema5A from being an attractant to a repellent, presumably by inducing conformational changes that facilitate interactions with a repulsive receptor other than plexinB3 [51] (Figure 3e). Similarly, the differential association of plexinA1 with OTK and VEGFR2 enables Sema6D to exert distinct chemotropic activities in adjacent regions of the developing heart [54] (Figure 2d). Furthermore, in zebrafish distinct neuropilins might underlie Sema3D axon attraction and repulsion, whereas in mouse neurons Npn-1 converts Sema3E–plexinD1 repulsion into attraction [32,65]. Additionally, Sema4D–plexinB1-mediated signaling can be regulated through the differential association of plexinB1 with ErbB2 or Met [42].

Extensive work indicates that the activation state and availability of intracellular signaling cues also critically contribute to the functional outcome of semaphorin ligand–receptor interactions. By example, the application of cyclic nucleotides to cultured neurons converts Sema3A repulsive activity into attraction, whereas lowering *Caenorhabditis elegans* Rac expression (encoded by *mig-2* and *ced-10*) switches responses from attractive to repulsive [15,66]. The physiological relevance of the modulatory effects of cyclic nucleotides is further supported by the recent implication of Nervy and Gyc76C in Sema-1a signaling (see invertebrate class 1 and 2 semaphorins) [14,16] and the role of soluble guanylate cyclase in the differential chemotropic effects of Sema3A on cortical axons and dendrites. The asymmetric localization of soluble guanylate cyclase to the developing apical dendrites of cortical neurons might allow Sema3A to act as a dendrite attractant, whereas cortical axons are repelled by Sema3A [67].

expressed in non-neuronal tissues and regulate cardiac morphogenesis, angiogenesis, organogenesis and cancer through their effects on cell growth, survival, migration and proliferation [2]. Plexins belonging to classes A and D serve as receptors for Sema3s in both neurons and non-neuronal cells.

PlexinAs

Sema3s do not interact directly with plexinA receptors but, instead, bind Npn-1 or Npn-2 to assemble and activate Npn–plexinA holoreceptor complexes. In this complex, plexinAs serve as signal-transducing subunits. In addition, Npn–plexinA receptor complexes can require the IgCAMs L1 or NrCAM for specific repulsive or attractive axon guidance events [21] (Figure 2a and Box 1). The current view is that *in vivo* in neurons, Npn-1–plexinA4 complexes are principal Sema3A receptors, whereas Npn-2–plexinA3 complexes mediate responses to Sema3F [22,23].

One of the best characterized intracellular signaling events downstream of repulsive semaphorins is ligand-binding-induced R-Ras inactivation mediated by the plexin RasGAP (GTPase-activating protein) domain [24]. PlexinA GAP activity is regulated by FARP2-mediated Rac1 activation [FARP2 (or FERM, RhoGEF and pleckstrin domain protein 2) is a RacGEF (guanine nucleotide exchange factor)]. After Sema3A exposure, FARP2 dissociates from plexinA1 and activates Rac1 in neuronal growth cones. Active Rac1 facilitates the association of Rnd1, a small GTPase, with plexinA1 and might modulate actin dynamics through the sequential activation of p21-activated kinase (PAK), LIM kinase 1 (LIMK1) and cofilin [8,25] (Figure 2a). Rnd1–plexinA1 interactions stimulate plexinA1 GAP activity toward R-Ras by releasing inhibitory interactions within the plexin cytoplasmic region [26,27] (Figure 2a). The subsequent decrease in the amount of active R-Ras triggers the inactivation of phosphatidylinositol-3-OH kinase (PI3K) to inhibit β1 integrin signaling. This is probably not the sole mechanism by which semaphorins regulate integrin function because after its release from plexinA1, FARP2 can inhibit type 1 phosphatidylinositol phosphate kinase (PIPKIγ661) and consequently suppress integrin activation [25] (Figure 2a).

Another consequence of neuronal plexin-induced PI3K inactivation is the inactivation of Akt (v-akt murine thymoma viral oncogene homolog). Interestingly, plexins employ different strategies to suppress PI3K–Akt signaling; Sema3A repulsive signaling in neurons also requires the downregulation of PTEN (phosphatase and tensin homolog deleted on chromosome 10), a PIP3 phosphatase and a negative regulator of the PI3K–Akt pathway [28]. Plexin-induced inhibition of PI3K–Akt signaling prevents the inactivation of the serine/threonine kinase glycogen synthase kinase-3β (GSK-3β), thus promoting the phosphorylation and inactivation of Collapsin response mediator protein 2 (CRMP2) [29] (Figure 2a).

CRMPs comprise a small family of plexinA-interacting phosphoproteins that contribute to Sema3A-induced growth-cone collapse [30]. GSK-3β-mediated CRMP2 phosphorylation is dependent on a Cyclin-dependent kinase 5 (Cdk5)-mediated CRMP2-priming phosphorylation event. Sema3A-dependent Cdk5 activation relies on the recruitment of a Fyn–Cdk5 complex to the plexinA cytoplasmic domain and subsequent Fyn-mediated Cdk5 tyrosine phosphorylation [31] (Figure 2a). Other CRMP-associated proteins that have been implicated in Sema3 signaling include the tyrosine kinase Fes (also called Fps), α2-chimaerin and phospholipase D2 [8]. Further work is necessary to determine how these different cues cooperate to regulate CRMP function.

In addition to the aforementioned proteins, several other intracellular proteins have been implicated in Sema3 signaling, including cell division cycle 42 (Cdc42), the Ras family members RhoD and RhoA, 12/15 lipoxygenase, Ran-binding protein (RanBPM) and mitogen-activated protein kinases (MAPKs) [7,8]. If or how these signaling molecules function in the pathways detailed above should be a focus of much future research.

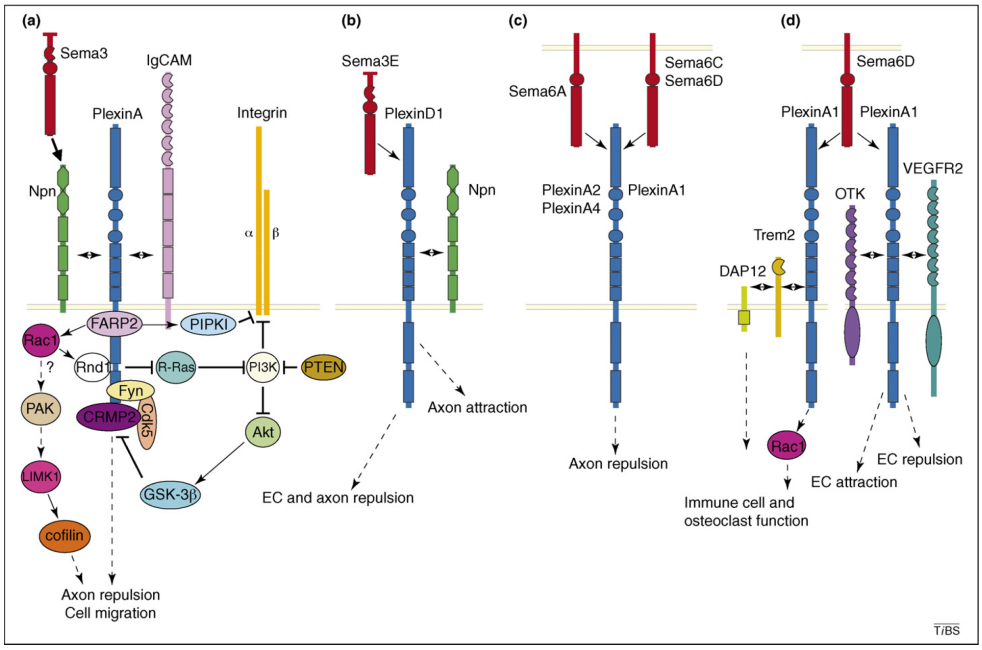

Figure 2. PlexinAs are receptors for Sema3s and Sema6s. Sema3s and Sema6s (red) mediate diverse biological functions including axon guidance, cardiovascular development and immune function. PlexinAs (blue) are receptors for Sema3s and Sema6s. In contrast to Sema3s, Sema6s do not require neuropilins (green) to direct plexinA binding. **(a)** Sema3s bind neuropilins (Npn-1 or Npn-2) with high affinity to assemble a Npn–plexinA receptor complex. This receptor complex requires IgCAMs (light purple) for specific repulsive or attractive axon guidance events. Sema3 binding to the Npn–plexinA complex promotes FARP2 (plum) dissociation from plexinA. Dissociated FARP2 activates Rac1 (magenta), which facilitates the Rnd1 (white)–plexinA association and drives PIPKIγ661 (light sky blue)-mediated integrin (orange) inhibition. Active Rac1 also might facilitate the sequential activation of PAK (tan), LIMK1 (deep pink) and cofilin (orange) to control actin dynamics. Rnd1–plexinA interactions stimulate plexinA RasGAP activity, which suppresses R-Ras (turquoise) and inactivates PI3K (bisque) signaling. Sema3s can also inhibit PI3K through PTEN (dark golden). PI3K inactivation inhibits integrin-mediated adhesion signaling and induces the sequential inhibition of Akt (light green), activation of GSK-3β (cyan) and inactivation of CRMP2 (purple). Phosphorylation of CRMP2 by GSK-3β relies on a Cdk5 (light salmon)- and Fyn (yellow)-dependent priming phopshorylation. CRMP2 has been proposed to regulate microtubule dynamics and endocytosis. **(b)** Unlike other Sema3s, Sema3E directly binds plexinD1 to induce endothelial cell (EC) repulsion and controls intersomitic vessel patterning through unidentified cytosolic mechanisms. Sema3E also acts as an axon repellent or attractant through plexinD1. Sema3E–plexinD1-mediated attraction, but not repulsion, requires Npn-1. **(c)** During neural development, Sema6s bind plexinAs to regulate lamina-specific axon projections. Sema6A binds plexinA2 and plexinA4, whereas Sema6C and Sema6D bind plexinA1 to elicit axon repulsion. **(d)** Sema6D can cause endothelial cell repulsion or attraction by interacting with OTK (purple)–plexinA1 or VEGFR2 (dark cyan)–plexinA1 receptor complexes, respectively (Box 1). The intracellular signaling pathways that operate downstream of plexinA1 in endothelial cell repulsion or attraction are currently unknown. Sema6D binding to a plexinA1–Trem2 (gold)–DAP12 (green-yellow) receptor complex on immune cells and osteoclasts promotes Rac activation and DAP12 phosphorylation.

PlexinD1

Sema3E, in contrast to the other Sema3s, directly binds a plexin (plexinD1), providing guidance for growing axons and migrating endothelial cells. In the embryonic nervous system, Sema3E attracts or repels specific subsets of axons by using plexinD1 and controls the formation of select forebrain projections [32]. During vascular patterning, Sema3E–plexinD1 signaling repels endothelial cells, restraining intersomitic blood-vessel extension and branching [33–35] (Figure 2b). Although Sema3E does not bind Npns, Sema3E attraction, but not repulsion, requires Npn-1 in addition to plexinD1 [32,34]. How Npn-1 converts Sema3E–plexinD1 repulsion into attraction is unknown. Npn-1 and plexinD1 associate in the absence of ligand binding [32,33]; this suggests that the regulated assembly of receptor complexes might determine the functional outcome of Sema3E signaling. Npns physically interact with plexinD1; however, they do not affect Sema3E–plexinD1 binding [32,33]. In addition, the Npn-1 extracellular domain is sufficient to convert Sema3E-mediated axon repulsion to attraction [32], suggesting that this switch reflects changes that are currently unknown in intracellular signaling events downstream of plexinD1. Interestingly, Sema3E and Sema4A (see class 4 semaphorins) bind, with different affinities, to overlapping sites on plexinD1 [36] (Figure 3c). It is, therefore, tempting to speculate that these structurally distinct semaphorins activate similar downstream signaling cascades. In addition to neuronal and vascular phenotypes, *plexinD1* – but not *Sema3E* – knockout mice display cardiac outflow tract patterning deficiencies [33,34]. This aspect of cardiac development is proposed to require Sema3A and Sema3C signaling through plexinD1 complexes containing Npn-1 and Npn-2, respectively [33]. Thus, in addition to its role in Sema3E and Sema4A signaling [32,34,36], plexinD1 might have other receptor functions. It will be interesting to

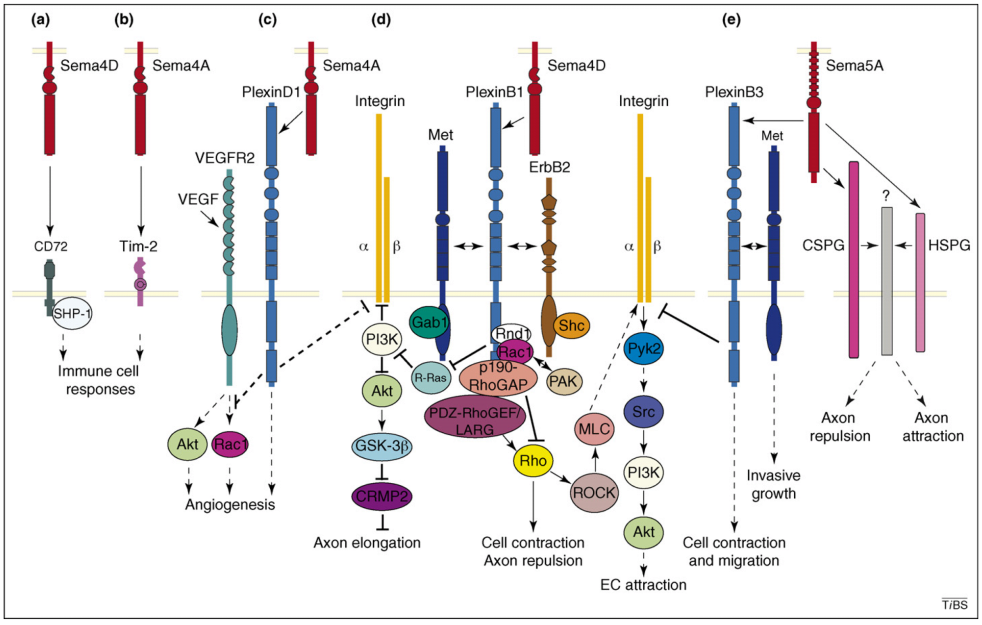

Figure 3. Sema4s and Sema5s signal through shared and separate receptors. Sema4s mediate immune responses, angiogenesis, axon guidance and invasive growth. The biological functions of Sema5s are less well understood but include the regulation of invasive growth, vascular patterning and axon guidance. Interestingly, Sema4s and Sema5s (red) bind shared (plexinBs) and separate receptors (Sema4s; Tim-2, CD72 and plexinD1, Sema5s; proteoglycans). **(a,b)** CD72 (dark gray) and Tim-2 (purple) are low-affinity receptors for Sema4D and Sema4A, respectively, and are located on immune cells. Sema4D–CD72 binding directs the dissociation of SHP-1 (light cyan) from the CD72 cytoplasmic domain and enhances B-cell activation. **(c)** Sema4A binds plexinD1 to inhibit angiogenesis. Sema4A–plexinD1 interactions modulate VEGF-mediated EC migration and proliferation at the intracellular level by suppressing VEGF–VEGFR2 (dark cyan)-induced activation of Rac1 (magenta), Akt (light green) and integrins (orange yellow). **(d)** Sema4D binds plexinB1 to induce repulsive or attractive effects in neuronal and non-neuronal cells. PlexinB1 associates with the receptor tyrosine kinases Met (dark blue), ErbB2 (brown) and OTK (not shown). Sema4D–plexinB1 interactions promote phosphorylation of plexinB1, Met and ErbB2 and the downstream effectors Gab1 (green) and Shc (orange). Met signaling is required for Sema4D–plexinB1-mediated cell migration and invasive growth, whereas ErbB2 functions in Sema4D-induced cell migration and growth-cone collapse. Repulsive Sema4D–plexinB signaling involves four GTPases; Rnd1 (white), R-Ras (turquoise), Rho (yellow) and Rac1. Sema4D–plexinB1 binding promotes Rnd1-dependent activation of the plexinB1 GAP domain and transient suppression of R-Ras activity. R-Ras inactivation promotes PI3K (bisque) and Akt inactivation followed by GSK-3β (cyan) activation and CRMP2 (purple) inactivation. In addition, plexinB1 associates with the RhoGEFs PDZ-RhoGEF and LARG (bordeaux) and with p190RhoGAP (salmon) to regulate Rho activity and to influence cytoskeletal dynamics. Rac1–plexinB1 binding might sequester Rac1 away from PAK (tan). Sema4D-mediated attraction of ECs requires Rho, but not R-Ras, signaling. Sema4D-mediated plexinB1 activation activates Rho and its downstream effector ROCK (brown). ROCK then phosphorylates MLC (light coral) to induce actomyosin stress fiber contraction and to direct the assembly of focal adhesion complexes and integrin-mediated adhesion. Integrin activation triggers Pyk2 (purple blue) phosphorylation, an event that is required for the sequential activation of Src (indigo), PI3K and Akt. Phospho-Pyk2 is recruited, along with PI3K and Src, to the plexinB1 cytoplasmic domain. **(e)** Sema5A binds plexinB3 to inhibit integrin-mediated adhesion and to influence cell migration through repulsive mechanisms. Sema5A–plexinB3-mediated Met activation regulates invasive growth. During neural development, Sema5A can act as an attractant or repellent for midbrain axons. HSPGs (light pink) are required for Sema5A-mediated attraction and might be components of axonal Sema5A receptors. CSPGs (pink) switch Sema5A from an attractant to a repellent, presumably by facilitating interactions with a repulsive receptor other than plexinB3 (Box 1).

determine whether the distinct modes of plexinD1 activation triggered by these different ligands and coreceptors lead to unique intracellular signaling events.

Class 4 semaphorins

Transmembrane class 4 semaphorins (Sema4A– Sema4D, Sema4F and Sema4G) regulate various phases of the immune response. Sema4D (originally named CD100) binds CD72 to mediate B-cell–B-cell and B-cell–T-cell interactions and thereby regulates B-cell activation. Conversely, Sema4A binds the transmembrane receptor Tim-2 to facilitate T-cell-mediated immune responses [37]. Sema4s not only influence the activation state of cells but also modulate their migration and survival [2,4]. The effects of Sema4s on nonlymphoid cells are mediated by plexinD1 and plexinBs (Figure 3a–d).

CD72 and Tim-2

CD72 and Tim-2 are low-affinity immune receptors for Sema4D and Sema4A, respectively. Our understanding of the intracellular events that occur downstream of Tim-2 and CD72 upon Sema4 ligand engagement is limited. Sema4A induces Tim-2 tyrosine phosphorylation, whereas Sema4D stimulates CD72 tyrosine dephosphorylation. CD72 dephosphorylation is caused by the dissociation of CD72 from the B-cell receptor (BCR) complex upon Sema4D ligation and triggers the dissociation of Src homology 2 domain-containing tyrosine phosphatase 1 (SHP-1) from CD72. This mechanism contributes to the regulation of B-cell homeostasis and B-cell-mediated immunity, presumably by controlling the strength of BCR signaling [37] (Figure 3a,b).

PlexinD1

In contrast to CD72 and Tim-2, plexins are high-affinity Sema4 receptors. PlexinD1 mediates Sema4A's inhibitory effects on vascular endothelial growth factor (VEGF)-mediated endothelial cell migration and proliferation *in vitro* and angiogenesis *in vivo* [36]. These effects rely on the ability of Sema4A to suppress VEGF–VEGFR2-mediated Rac-GTP-dependent cytoskeletal rearrangements, Akt activation and integrin-mediated adhesion via plexinD1 [36] (Figure 3c). In addition to negatively regulating angiogenesis, Sema4A induces growth-cone collapse in a Rho Kinase (ROCK)-dependent fashion [38]. It is, however, unknown whether plexinD1 mediates these neuronal Sema4A functions.

PlexinBs

PlexinBs mediate a wide range of Sema4 functions, including axon guidance, dendritic cell migration and angiogenesis [4,5,39]. PlexinBs associate with the RTKs Met, ErbB2 and OTK, and Sema4D–plexinB1 binding stimulates the tyrosine kinase activity of Met or ErbB2. This increase in kinase activity leads to the phosphorylation of plexinB1, Met or ErbB2 and of downstream effectors including Gab1 (GRB2-associated binding protein 1) and Shc [Src-homology-2 (SH2)-containing]. Met signaling is required for Sema4D–plexinB1-mediated cell migration and invasive growth, whereas ErbB2 functions in Sema4D-induced cell migration and growth-cone collapse [39–42] (Figure 3d).

The signal transduction cascades triggered by Sema4D–plexinB1 interactions have been studied intensely (Figure 3d). Like Sema3A and plexinA1 (see class 3 semaphorins), Sema4D–plexinB1 binding promotes Rnd1-dependent activation of the plexinB1 GAP domain and transient R-Ras inactivation [24]. Decreased neuronal R-Ras signaling promotes the sequential inhibition of PI3K and Akt, activation of GSK3β and CRMP2 inactivation (Figure 3d). Sema4D-induced CRMP2 inactivation is thought to inhibit microtubule assembly and axon elongation [29]. In contrast to the acute effects of semaphorin signaling (e.g. growth-cone collapse), which are mediated by a redistribution of actin, CRMP-dependent regulation of microtubules might mediate longer term responses (e.g. growth-cone turning). Unlike plexinA1, plexinB1 does not bind FARP2. Although Rac1 associates with plexinB1, it is unknown whether, similar to plexinA1, Rac1 activation is required for Rnd-dependent R-Ras inactivation. Alternatively, plexinB1 might sequester Rac1 from PAK and thereby inhibit PAK signaling [8] (Figure 3d).

Regulation of Rho activity also is required for Sema4D-induced cell migration and growth-cone collapse. PlexinB1 constitutively associates with PDZ (PSD-95, Discs large, zona occludens-1)-RhoGEF and leukaemia-associated RhoGEF (LARG) through a C-terminal PDZ-domain-binding motif. Rho activation through PDZ-RhoGEF and LARG is required for Sema4D-induced endothelial and breast carcinoma cell migration and growth-cone collapse [8,27]. Interestingly, other work shows that plexinB1 also transiently associates with and activates p190RhoGAP, triggering a transient decrease in activated Rho. p190RhoGAP is required for Sema4D-mediated inhibitory effects on the migration of epithelial and primary endothelial cells [43]. Although much remains to be learned about the roles of p190RhoGAP, PDZ-RhoGEF and LARG during Sema4D signaling, a series of recent studies support the idea that Rho signaling in Sema4D–plexinB1 function might be cell-type or context dependent. In addition to its repulsive or inhibitory effects on axons and migrating cells, Sema4D, acting through plexinB1, is a strong chemoattractant for endothelial cells [40,44]. Several lines of evidence suggest that in endothelial cells, Sema4-induced Rho activation promotes the formation of focal adhesion complexes and increased integrin-mediated adhesion [45] (Figure 3d). A model has been proposed in which Sema4D–plexinB1 binding activates Rho and its downstream effector, ROCK. ROCK then phosphorylates myosin light chain (MLC) to induce actomyosin stress fiber contraction. The isometric tension produced by stress fiber contraction directs focal adhesion complex assembly and promotes integrin-mediated adhesion. Integrin activation then promotes the phosphorylation of Pyk2 (proline-rich tyrosine kinase 2), Erk1 and Erk2. Pyk2 is required for the sequential activation of the proto-oncoprotein Src, PI3K and Akt and is recruited, along with PI3K and Src, to the plexinB1 cytoplasmic domain. A requirement for Rho activation in Sema4D promigratory effects also has been reported for breast carcinoma cells that express ErbB2 (but not Met). By contrast, breast carcinoma cells expressing Met, but not ErbB2, display a reduction in activated Rho and antimigratory responses upon Sema4D exposure [42]. The promigratory effects of Sema4D reported by Basile *et al.* and Swiercz *et al.* are independent of Met activation [42,45], in contrast to previous work that demonstrated a requirement for Met in Sema4D–plexinB1-mediated endothelial and epithelial cell attraction [40]. A plausible explanation for these seemingly contradictory results is that Sema4D can employ different mechanisms (e.g. involving either Rho or Met) to elicit promigratory responses. The observation that Met might not be required for Sema4D promigratory effects in all cell types underscores the cell-type-dependent nature of Sema4D signaling. Further work, therefore, is needed to delineate and compare Sema4D signaling cascades in different cell types and tissues.

The finding that Sema4D–plexinB1 interactions not only suppress (through R-Ras for repulsive responses) but also increase (through Rho for attraction) integrin function [45,46] seemingly contradicts the idea that reduced integrin adhesion is required for semaphorin-mediated axon guidance and cell migration [47,48]. The molecular basis for these differential effects of Sema4D–plexinB1 signaling on integrin function remains unclear, but the activation of focal adhesion kinase (FAK), a downstream effector of integrins, during Sema3B-mediated axon attraction [49] suggests that integrin activation might be central to chemoattractive semaphorin signaling. Alternatively, mechanisms to inhibit and increase integrin activity might function in parallel, thereby allowing Sema4D to induce cyclic adhesion and de-adhesion events, which are required for cell migration [4].

Class 5 semaphorins

Our understanding of the biological functions and signaling of class 5 semaphorins (Sema5A and Sema5B) is rudimentary. Sema5s have been implicated in invasive growth, vascular patterning and axon guidance [2]. Sema5A induces the collapse of NIH-3T3 fibroblasts through plexinB3 and elicits chemoattractive reponses of epithelial and primary endothelial cells via a plexinB3–Met receptor complex. Sema5A-induced cell migration requires Met signaling [50] (Figure 3e). Studies in the developing nervous system show that Sema5A can act as an attractant or repellent for midbrain axons. Heparan sulfate proteoglycans (HSPGs) are required for Sema5A-mediated axon attraction, and chondroitin sulfate proteoglycans (CSPGs) switch Sema5A from being an axon attractant to being a repellent. The effects of Sema5A on growing axons are likely to be independent of plexinB3 [51] (Figure 3e and Box 1).

Class 6 semaphorins

PlexinAs are receptors for Sema3s and Sema6s (Sema6A–6D). In contrast to Sema3s, Sema6s directly bind plexinAs in an Npn-independent fashion. In addition, Sema6s, as well as other membrane-associated semaphorins, can themselves function as receptors (Box 2). Recent observations reveal an important role for Sema6–plexinA forward signaling in the formation of lamina-specific axon projections. Sema6A binds plexinA2 and plexinA4 to establish lamina-restricted axon projections in the hippocampus, and interactions between Sema6C, Sema6D and plexinA1 shape the stereotypic trajectories of sensory axons in the spinal cord [52,53] (Figure 2c). In addition to axon targeting, Sema6D–plexinA1 interactions influence a wide range of other biological processes. During cardiac development, Sema6D attracts or repels endothelial cells in the cardiac tube depending on the expression patterns of specific coreceptors in addition to plexinA1 [54] (Figure 2d and Box 1). Furthermore, Sema6D binds a receptor complex comprising plexinA1, Trem2 (triggering receptor expressed on myeloid cells 2) and DAP12 on dendritic cells and osteoclasts to mediate T-cell–DC interactions and to control bone development, respectively [55] (Figure 2d).

The intracellular signaling events triggered by the various Sema6–plexinA interactions outlined above remain elusive. However, the available data suggest that Sema6-mediated activation of the plexinA1-Trem2-DAP12 receptor activates Rac1, presumably through plexinA1, and promotes DAP12 phosphorylation through unidentified mechanisms [55] (Figure 2d). As plexinAs are shared between Sema3s and Sema6s, it is tempting to speculate that these structurally distinct semaphorins activate (partly) overlapping intracellular signaling pathways. One must keep in mind, however, that the plexinA mechanism of activation is critically different for Sema3s and Sema6s (i.e. Npn dependent versus Npn independent). Although the Npn cytoplasmic domain is not required for repulsive signaling in Sema3s, the precise effect of Npns on intracellular signaling is largely unknown (but see [25]). Furthermore, it will be interesting to determine whether structurally distinct semaphorins (and their coreceptors) induce comparable conformational changes in plexins and, if not, whether this differential activation is responsible for the recruitment and activation of distinct cytosolic signaling molecules.

Box 2. Semaphorin signaling in reverse: bidirectional signaling

Accumulating evidence indicates that transmembrane semaphorins serve not only as ligands but also as receptors, a process termed bidirectional signaling. Bidirectional signaling is likely to be a general property of Sema6s. For example, the class 6 semaphorin, Sema6D, is both a plexinA1 ligand (i.e. forward signaling) and a receptor (i.e. reverse signaling) during chick cardiac development; myocardial cell migration relies on Sema6D functioning as a plexinA1 receptor, whereas Sema6D–plexinA1 forward signaling controls ventricular expansion [68]. Sema6D–plexinA1 binding triggers the recruitment of activated Abl to the large, proline-rich Sema6D cytoplasmic domain. Abl binds Sema6D through its Src-homology-3 (SH3) domain and phosphorylates the Ena/Vasp family member, mammalian Enabled (Mena), which triggers its release from the Sema6D cytoplasmic region. This signaling event regulates the expansion of the outer myocardial layer and trabeculation in the myocardium of the developing cardiac ventricle [68]. The Sema6A cytoplasmic domain binds Ena/Vasp-like protein (EVL) through its zyxin-like motif and Sema6B binds Src through its SH3 domain [69,70]. The physiological significance of these biochemical interactions remains unclear. In addition, Sema-1a, the invertebrate semaphorin most closely related to the Sema6s, is required for cell-autonomous synapse formation and for targeting axons and dendrites in *D. melanogaster* [71–73]. Genetic studies support a role for Enabled (Ena) in repulsive Sema-1a reverse signaling [72].

In addition to the Sema6s, several Sema4s associate with cytoplasmic signaling molecules. Sema4B, Sema4C and Sema4F interact with the postsynaptic density protein of 95 kDa (PSD-95) through their C-terminal PDZ domain interaction motifs. In addition, Sema4C binds the PDZ protein SEMCAP-1 (also called GIPC, GLUT1CBP, TIP-2, synectin and NIP-1) and Norbin. Sema4D interacts with CD45, a protein tyrosine phosphatase, and immunoprecipates with a serine/threonine kinase activity in immune cells [2,7].

Thus far, to our knowledge, the only intracellular binding partners identified for Sema5s are SEMCAP-1 and SEMCAP-2. SEMCAP-1 binds the Sema5A C-terminal PDZ domain interaction motif and regulates Sema5A subcellular distribution in neurons [74]. Furthermore, the GPI-linked semaphorin Sema7A might participate in reverse signaling events through the (indirect) association with unidentified protein kinase(s) [75]. Thus, most (if not all) membrane-associated semaphorins probably are capable of mediating reverse signaling events. Future work undoubtedly will continue to reveal upstream and downstream components in semaphorin reverse signaling.

Sema7A and viral semaphorins

Two viral semaphorins have been described: SemaVA (originally named A39R) in vaccinia virus and SemaVB in alcelaphine herpesvirus. Presumably, viral semaphorins are secreted by infected cells to frustrate the host immune response [2]. Viral semaphorins and their vertebrate homolog Sema7A (originally named Cdw108) bind plexinC1 to influence immune cell functions, including cytokine production. Similar to other plexin–semaphorin interactions, plexinC1 activation by SemaVA or Sema7A decreases integrin-mediated cell attachment and spreading [56,57]. Although the signal-transduction pathways that transduce semaphorin–plexinC1 functions remain largely unknown, FAK and the actin-severing protein cofilin have been implicated in the inhibition of DC adhesion by SemaVA–plexinC1 [57] (Figure 4). In

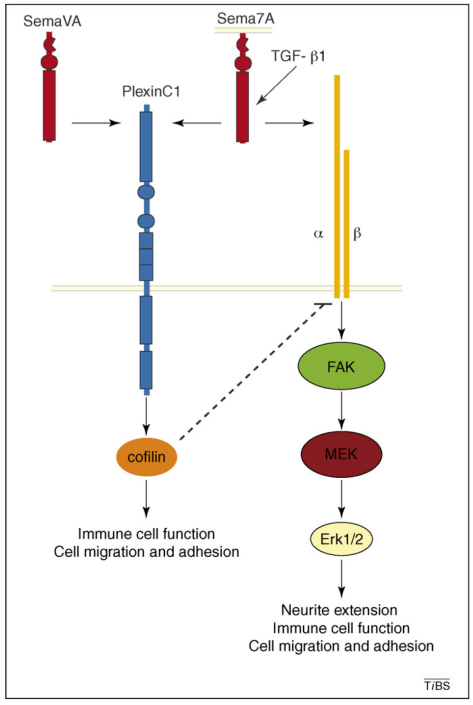

Figure 4. Sema7A signals through plexinC1 and β1 integrins. The viral semaphorin SemaVA (red) and the GPI-linked semaphorin Sema7A (red) both bind plexinC1 (blue) to influence the function and migration of immune, neuronal, bone and/or skin cells. Activation of plexinC1 by SemaVA or Sema7A reduces integrin (orange)-mediated cell attachment and spreading through unidentified mechanisms. The actin-severing protein cofilin (orange red) and FAK (not shown) have been implicated in SemaVA–plexinC1 signaling. In addition to plexinC1, Sema7A binds β1-integrins to stimulate process extension and cell adhesion in various organ systems including the immune and nervous systems. Sema7A-mediated α1β1-integrin activation induces integrin clustering and the activation of FAK (lime), MAPK (MEK; dark red, Erk1/Erk2; light yellow) and Abl kinase (not shown) signaling pathways. Interestingly, by binding different receptors Sema7A appears to both negatively (via plexinC1) and positively (via integrins) regulate cell morphology and adhesion. Sema7A also plays a critical role in TGF-β1-induced pulmonary fibrosis. TGF-β1 induces fibrosis and other tissue responses, PI3K–Akt signaling and gene expression changes through Sema7A-dependent mechanisms in the murine lung.

addition to plexinC1, Sema7A binds β1-integrins to induce integrin clustering and activation of Abelson (Abl) kinase, FAK and MAPK signaling pathways [58–60]. Sema7A–integrin interactions regulate diverse biological processes. In the immune system, Sema7A expressed on activated T cells triggers inflammatory processes by stimulating macrophages to produce proinflammatory cytokines through β1-integrins. *Sema7A* knockout mice are defective in T-cell-mediated immune responses such as contact hypersensitivity (CHS) and experimental autoimmune encephalomyelitis (EAE) [60]. During neural development, Sema7A enhances peripheral and central axon growth through β1-integrins and is required for proper axon tract formation *in vivo* [59]. Furthermore, Sema7A–β1-integrin interactions promote melanocyte adhesion [56]. Thus, by binding different receptors, Sema7A appears to both negatively (via plexinC1) and positively (via integrins) regulate cell morphology and adhesion.

In addition to CHS and EAE, Sema7A also plays a critical role in transforming growth factor (TGF)-β1-induced pulmonary fibrosis. Through Sema7A-dependent mechanisms, TGF-β1 induces fibrosis, PI3K–Akt signaling and gene expression (including the enhanced expression of Sema7A, plexinC1 and β1-integrins) in the murine lung [61] (Figure 4). It is unknown whether these effects rely on plexinC1 and/or β1-integrins.

Concluding remarks and future perspectives

Our knowledge of the cellular actions of semaphorins has advanced significantly over the past several years, and the receptors and intracellular signal transduction events that underlie these effects are being unveiled at a rapid pace. A unifying feature of semaphorin receptors is their multimeric nature. It is now clear that receptor composition not only determines ligand specificity but also modulates the functional outcome of ligand–receptor interactions. It is likely that these coreceptors trigger unique signaling events that dictate specific semaphorin responses. The identity of these intracellular signaling events and molecules remains a main focus for many future experiments.

A major breakthrough in defining semaphorin signaling pathways is the demonstration that plexins, after ligand binding, function as RasGAPs [26]. Although intrinsic RasGAP activity remains to be shown for most plexins, downregulation of R-Ras activity is considered to be a common feature of plexin signaling. However, in addition to suppressing R-Ras, plexins might employ other strategies to positively or negatively influence integrin activity (e.g. involving FARP2 or Rho) [25,45]. It will be interesting to determine if and how these different mechanisms cooperate to regulate intregin-mediated adhesion.

Recent studies have not only highlighted the common features of semaphorin signaling pathways but also supported the notion that semaphorin signaling events are cell-type specific. Therefore, it is crucial to carefully assess whether semaphorin signaling events observed in one particular cell type or tissue hold for other cells and tissues. Nevertheless, several intriguing questions remain within the field of semaphorin signaling. In particular: which are the upstream and downstream transducers of transmembrane semaphorin reverse signaling events? Do plexins within the same subfamily class trigger identical or distinct signaling events after ligand binding? Similarly, does binding of structurally distinct semaphorins to the same plexin receptor induce the recruitment and activation of similar or different cytosolic signaling molecules?

Human genetic analyses and mouse models implicate semaphorins and their associated receptor and cytosolic signaling molecules in neurodegenerative and neurodevelopmental disorders (e.g. Parkinson's disease and schizophrenia), cancer, immune disease and various other disorders [3,4,37]. Thus far, however, the role of semaphorins in the development and progression of cancer has been best characterized. Semaphorins mediate neovascularization, tumor growth and metastasis and are actively

exploited as therapeutic targets for cancer. Semaphorins also act as molecular inhibitors of axonal regeneration. Human neural scar tissue contains repulsive semaphorins that inhibit the regrowth of severed axons [62]. An elegant study by Kaneko *et al.* [63] confirms the potential use of semaphorins as therapeutic targets for promoting axonal regeneration. The application of SM-216289, a fungus-derived Sema3A inhibitor, to the injured rat spinal cord promotes anatomical and functional regeneration of nerve tracts in the spinal cord [63]. Therefore, we can expect that experiments over the next few years will not only enhance our understanding of semaphorin signaling but also will lead to therapeutic advances in cancer and axonal regeneration.

Acknowledgements

We apologize to our colleagues for not being able to cite many additional relevant publications owing to space restrictions. We thank Alex Kolodkin, Atsushi Kumanogoh and Luca Tamagnone for critically reading the manuscript and members of Pasterkamp laboratory for continuous discussion and support. Work in the authors' laboratory is supported by grants from the Netherlands Organization of Scientific Research, the Dutch Brain Foundation, the International Parkinson Foundation, the Human Frontier Science Program and the ABC Genomics Center Utrecht (to R.J.P.). R.J.P. is a NARSAD Henry and William Test Investigator.

References

1 (1999) Unified nomenclature for the semaphorins/collapsins. Semaphorin Nomenclature Committee. *Cell* 97, 551–552
2 Yazdani, U. and Terman, J.R. (2006) The semaphorins. *Genome Biol.* 7, 211
3 Mann, F. *et al.* (2007) Semaphorins in development and adult brain: implication for neurological diseases. *Prog. Neurobiol.* 82, 57–79
4 Tamagnone, L. and Comoglio, P.M. (2004) To move or not to move? Semaphorin signalling in cell migration. *EMBO Rep.* 5, 356–361
5 Chabbert-de Ponnat, I. *et al.* (2005) Soluble CD100 functions on human monocytes and immature dendritic cells require plexin C1 and plexin B1, respectively. *Int. Immunol.* 17, 439–447
6 Zhu, L. *et al.* (2007) Regulated surface expression and shedding support a dual role for semaphorin 4D in platelet responses to vascular injury. *Proc. Natl. Acad. Sci. U. S. A.* 104, 1621–1626
7 Kruger, R.P. *et al.* (2005) Semaphorins command cells to move. *Nat. Rev. Mol. Cell Biol.* 6, 789–800
8 Pasterkamp, R.J. and Kolodkin, A.L. (2003) Semaphorin junction: making tracks toward neural connectivity. *Curr. Opin. Neurobiol.* 13, 79–89
9 Ayoob, J.C. *et al.* (2006) Drosophila Plexin B is a Sema-2a receptor required for axon guidance. *Development* 133, 2125–2135
10 Winberg, M.L. *et al.* (1998) Plexin A is a neuronal semaphorin receptor that controls axon guidance. *Cell* 95, 903–916
11 Lattemann, M. *et al.* (2007) Semaphorin-1a controls receptor neuron-specific axonal convergence in the primary olfactory center of Drosophila. *Neuron* 53, 169–184
12 Sweeney, L.B. *et al.* (2007) Temporal target restriction of olfactory receptor neurons by Semaphorin-1a/PlexinA-mediated axon-axon interactions. *Neuron* 53, 185–200
13 Winberg, M.L. *et al.* (2001) The transmembrane protein Off-track associates with Plexins and functions downstream of Semaphorin signaling during axon guidance. *Neuron* 32, 53–62
14 Ayoob, J.C. *et al.* (2004) The Drosophila receptor guanylyl cyclase Gyc76C is required for semaphorin-1a-plexin A-mediated axonal repulsion. *J. Neurosci.* 24, 6639–6649
15 Song, H. *et al.* (1998) Conversion of neuronal growth cone responses from repulsion to attraction by cyclic nucleotides. *Science* 281, 1515–1518
16 Terman, J.R. and Kolodkin, A.L. (2004) Nervy links protein kinase a to plexin-mediated semaphorin repulsion. *Science* 303, 1204–1207
17 Terman, J.R. *et al.* (2002) MICALs, a family of conserved flavoprotein oxidoreductases, function in plexin-mediated axonal repulsion. *Cell* 109, 887–900
18 Driessens, M.H. *et al.* (2001) Plexin-B semaphorin receptors interact directly with active Rac and regulate the actin cytoskeleton by activating Rho. *Curr. Biol.* 11, 339–344
19 Hu, H. *et al.* (2001) Plexin B mediates axon guidance in Drosophila by simultaneously inhibiting active Rac and enhancing RhoA signaling. *Neuron* 32, 39–51
20 Usui, H. *et al.* (2003) Plexin-A1 and plexin-B1 specifically interact at their cytoplasmic domains. *Biochem. Biophys. Res. Commun.* 300, 927–931
21 Tran, T.S. *et al.* (2007) Semaphorin regulation of cellular morphology. *Annu. Rev. Cell Dev. Biol.* 23, 263–292
22 Suto, F. *et al.* (2005) Plexin-a4 mediates axon-repulsive activities of both secreted and transmembrane semaphorins and plays roles in nerve fiber guidance. *J. Neurosci.* 25, 3628–3637
23 Yaron, A. *et al.* (2005) Differential requirement for Plexin-A3 and -A4 in mediating responses of sensory and sympathetic neurons to distinct class 3 Semaphorins. *Neuron* 45, 513–523
24 Pasterkamp, R.J. (2005) R-Ras fills another GAP in semaphorin signalling. *Trends Cell Biol.* 15, 61–64
25 Toyofuku, T. *et al.* (2005) FARP2 triggers signals for Sema3A-mediated axonal repulsion. *Nat. Neurosci.* 8, 1712–1719
26 Oinuma, I. *et al.* (2004) The Semaphorin 4D receptor Plexin-B1 is a GTPase activating protein for R-Ras. *Science* 305, 862–865
27 Puschel, A.W. (2007) GTPases in semaphorin signaling. *Adv. Exp. Med. Biol.* 600, 12–23
28 Chadborn, N.H. *et al.* (2006) PTEN couples Sema3A signalling to growth cone collapse. *J. Cell Sci.* 119, 951–957
29 Ito, Y. *et al.* (2006) Sema4D/plexin-B1 activates GSK-3β through R-Ras GAP activity, inducing growth cone collapse. *EMBO Rep.* 7, 704–709
30 Schmidt, E.F. and Strittmatter, S.M. (2007) The CRMP family of proteins and their role in Sema3A signaling. *Adv. Exp. Med. Biol.* 600, 1–11
31 Ahmed, A. and Eickholt, B.J. (2007) Intracellular kinases in semaphorin signaling. *Adv. Exp. Med. Biol.* 600, 24–37
32 Chauvet, S. *et al.* (2007) Gating of Sema3E/PlexinD1 signaling by neuropilin-1 switches axonal repulsion to attraction during brain development. *Neuron* 56, 807–822
33 Gitler, A.D. *et al.* (2004) PlexinD1 and semaphorin signaling are required in endothelial cells for cardiovascular development. *Dev. Cell* 7, 107–116
34 Gu, C. *et al.* (2005) Semaphorin 3E and plexin-D1 control vascular pattern independently of neuropilins. *Science* 307, 265–268
35 Torres-Vazquez, J. *et al.* (2004) Semaphorin-plexin signaling guides patterning of the developing vasculature. *Dev. Cell* 7, 117–123
36 Toyofuku, T. *et al.* (2007) Semaphorin-4A, an activator for T-cell-mediated immunity, suppresses angiogenesis via Plexin-D1. *EMBO J.* 26, 1373–1384
37 Suzuki, K. *et al.* (2008) Semaphorins and their receptors in immune cell interactions. *Nat. Immunol.* 9, 17–23
38 Yukawa, K. *et al.* (2005) Semaphorin 4A induces growth cone collapse of hippocampal neurons in a Rho/Rho-kinase-dependent manner. *Int. J. Mol. Med.* 16, 115–118
39 Swiercz, J.M. *et al.* (2004) Plexin-B1/RhoGEF-mediated RhoA activation involves the receptor tyrosine kinase ErbB-2. *J. Cell Biol.* 165, 869–880
40 Conrotto, P. *et al.* (2005) Sema4D induces angiogenesis through Met recruitment by Plexin B1. *Blood* 105, 4321–4329
41 Giordano, S. *et al.* (2002) The Semaphorin 4D receptor controls invasive growth by coupling with Met. *Nat. Cell Biol.* 4, 720–724
42 Swiercz, J.M. *et al.* (2007) ERBB-2 and met reciprocally regulate cellular signaling via plexin-B1. *J. Biol. Chem.* 283, 1893–1901
43 Barberis, D. *et al.* (2005) p190 Rho-GTPase activating protein associates with plexins and it is required for semaphorin signalling. *J. Cell Sci.* 118, 4689–4700
44 Basile, J.R. *et al.* (2004) Class IV semaphorins promote angiogenesis by stimulating Rho-initiated pathways through plexin-B. *Cancer Res.* 64, 5212–5224
45 Basile, J.R. *et al.* (2007) Plexin-B1 utilizes RHOA and ROK to promote the integrin-dependent activation of AKT and ERK, and endothelial cell motility. *J. Biol. Chem.* 282, 34888–34895

46 Oinuma, I. *et al.* (2006) Semaphorin 4D/Plexin-B1-mediated R-Ras GAP activity inhibits cell migration by regulating β(1) integrin activity. *J. Cell Biol.* 173, 601–613
47 Barberis, D. *et al.* (2004) Plexin signaling hampers integrin-based adhesion, leading to Rho-kinase independent cell rounding, and inhibiting lamellipodia extension and cell motility. *FASEB J.* 18, 592–594
48 Serini, G. *et al.* (2003) Class 3 semaphorins control vascular morphogenesis by inhibiting integrin function. *Nature* 424, 391–397
49 Falk, J. *et al.* (2005) Dual functional activity of semaphorin 3B is required for positioning the anterior commissure. *Neuron* 48, 63–75
50 Artigiani, S. *et al.* (2004) Plexin-B3 is a functional receptor for semaphorin 5A. *EMBO Rep.* 5, 710–714
51 Kantor, D.B. *et al.* (2004) Semaphorin 5A is a bifunctional axon guidance cue regulated by heparan and chondroitin sulfate proteoglycans. *Neuron* 44, 961–975
52 Suto, F. *et al.* (2007) Interactions between Plexin-A2, Plexin-A4, and semaphorin 6A control lamina-restricted projection of hippocampal mossy fibers. *Neuron* 53, 535–547
53 Yoshida, Y. *et al.* (2006) PlexinA1 signaling directs the segregation of proprioceptive sensory axons in the developing spinal cord. *Neuron* 52, 775–788
54 Toyofuku, T. *et al.* (2004) Dual roles of Sema6D in cardiac morphogenesis through region-specific association of its receptor, Plexin-A1, with off-track and vascular endothelial growth factor receptor type 2. *Genes Dev.* 18, 435–447
55 Takegahara, N. *et al.* (2006) Plexin-A1 and its interaction with DAP12 in immune responses and bone homeostasis. *Nat. Cell Biol.* 8, 615–622
56 Scott, G.A. *et al.* (2007) Semaphorin 7a promotes spreading and dendricity in human melanocytes through β1-integrins. *J. Invest. Dermatol.* 128, 151–161
57 Walzer, T. *et al.* (2005) Plexin C1 engagement on mouse dendritic cells by viral semaphorin A39R induces actin cytoskeleton rearrangement and inhibits integrin-mediated adhesion and chemokine-induced migration. *J. Immunol.* 174, 51–59
58 Moresco, E.M. *et al.* (2005) Integrin-mediated dendrite branch maintenance requires Abelson (Abl) family kinases. *J. Neurosci.* 25, 6105–6118
59 Pasterkamp, R.J. *et al.* (2003) Semaphorin 7A promotes axon outgrowth through integrins and MAPKs. *Nature* 424, 398–405
60 Suzuki, K. *et al.* (2007) Semaphorin 7A initiates T-cell-mediated inflammatory responses through α1β1 integrin. *Nature* 446, 680–684
61 Kang, H.R. *et al.* (2007) Semaphorin 7A plays a critical role in TGF-β1-induced pulmonary fibrosis. *J. Exp. Med.* 204, 1083–1093
62 Tannemaat, M.R. *et al.* (2007) Human neuroma contains increased levels of semaphorin 3A, which surrounds nerve fibers and reduces neurite extension *in vitro*. *J. Neurosci.* 27, 14260–14264
63 Kaneko, S. *et al.* (2006) A selective Sema3A inhibitor enhances regenerative responses and functional recovery of the injured spinal cord. *Nat. Med.* 12, 1380–1389
64 Ben-Zvi, A. *et al.* (2007) Modulation of semaphorin3A activity by p75 neurotrophin receptor influences peripheral axon patterning. *J. Neurosci.* 27, 13000–13011
65 Wolman, M.A. *et al.* (2004) Repulsion and attraction of axons by semaphorin3D are mediated by different neuropilins *in vivo*. *J. Neurosci.* 24, 8428–8435
66 Dalpe, G. *et al.* (2004) Conversion of cell movement responses to Semaphorin-1 and Plexin-1 from attraction to repulsion by lowered levels of specific RAC GTPases in *C. elegans*. *Development* 131, 2073–2088
67 Polleux, F. *et al.* (2000) Semaphorin 3A is a chemoattractant for cortical apical dendrites. *Nature* 404, 567–573
68 Toyofuku, T. *et al.* (2004) Guidance of myocardial patterning in cardiac development by Sema6D reverse signalling. *Nat. Cell Biol.* 6, 1204–1211
69 Eckhardt, F. *et al.* (1997) A novel transmembrane semaphorin can bind c-src. *Mol. Cell. Neurosci.* 9, 409–419
70 Klostermann, A. *et al.* (2000) The orthologous human and murine semaphorin 6A-1 proteins (SEMA6A-1/Sema6A-1) bind to the enabled/vasodilator-stimulated phosphoprotein-like protein (EVL) via a novel carboxyl-terminal zyxin-like domain. *J. Biol. Chem.* 275, 39647–39653
71 Cafferty, P. *et al.* (2006) Semaphorin-1a functions as a guidance receptor in the Drosophila visual system. *J. Neurosci.* 26, 3999–4003
72 Godenschwege, T.A. *et al.* (2002) Bi-directional signaling by Semaphorin 1a during central synapse formation in Drosophila. *Nat. Neurosci.* 5, 1294–1301
73 Komiyama, T. *et al.* (2007) Graded expression of semaphorin-1a cell-autonomously directs dendritic targeting of olfactory projection neurons. *Cell* 128, 399–410
74 Wang, L.H. *et al.* (1999) A PDZ protein regulates the distribution of the transmembrane semaphorin, M-SemF. *J. Biol. Chem.* 274, 14137–14146
75 Angelisova, P. *et al.* (1999) Characterization of the human leukocyte GPI-anchored glycoprotein CDw108 and its relation to other similar molecules. *Immunobiology* 200, 234–245

Chapter 3

Molecular and functional characterization of the signaling protein MICAL-1

Yeping Zhou[1], Youri Adolfs[1],
Jeroen Demmers[2], R. Jeroen Pasterkamp[1]

[1]Department of Neuroscience and Pharmacology, Rudolf Magnus Institute of Neuroscience, University Medical Center Utrecht, Universiteitsweg 100, 3584 CG, Utrecht, The Netherlands
[2]Proteomics Center, Erasmus University Medical Center, Dr Molewaterplein 50, 3015 GE, Rotterdam, The Netherlands

Abstract
MICAL proteins are atypical multi-domain flavoproteins with reported functions in cellular processes such as cytoskeletal regulation and vesicle trafficking. Moreover, MICAL proteins contribute to the regulation of nervous system development and have been implicated in neuronal regeneration after injury and progression of prostate cancer. All MICALs contain an N-terminal flavoprotein monooxygenase (MO) domain, followed by a Calponin Homology (CH) domain, a LIM domain, and coiled-coil motifs. The molecular mechanisms by which MICALs exert their diverse cellular effects remain, however, largely unknown. Defining the function of these individual domains will significantly further understanding of the role and mechanism-of-action of MICALs. Here, we show that the MO domain of MICAL-1 is able to catalyze hydrogen peroxide (H_2O_2) production in the absence of the C-terminal region of MICAL-1. This is interesting since it has been suggested previously that similar to C-terminally truncated MICAL-1, H_2O_2 may directly induce cell contraction responses. Our results unveil that the MO domain, but not H_2O_2 production, is required for cell contraction. This suggests that direct redox modification of potential substrates may mediate the effect of MICAL-1 on cell morphology. We also report two novel properties of MICAL-1. First, co-immunoprecipitation experiments show that MICAL-1 can form homo-dimers (oligomers). This self-association is mediated by the CH domain which is generally implicated in protein-protein interactions. Second, by using mass spectrometry, we identified MICAL-1 as a phosphoprotein modified at serine 777 located in the linker region between the LIM domain and coiled-coil motifs. Together, these results contribute to our understanding of organization and potential regulation of MICAL-1 and provide important avenues for future studies on MICAL proteins.

Introduction

Mouse MICAL-1 belongs to the recently identified MICAL family of evolutionary conserved flavoenzymes (Suzuki et al., 2002; Terman et al., 2002; Kolk and Pasterkamp, 2007). To date, MICALs have been best-characterized for their roles during neural development. During this process, MICALs contribute to the regulation of axon guidance, neurite outgrowth, synapse formation, dendritic pruning, and the positioning of neuronal cell bodies (Terman et al., 2002, Schmidt et al., 2008; Beuchle et al., 2007; Kirilly et al., 2009; Bron et al., 2007). Almost all of these functions have been proposed to rely on the ability of MICALs to modify actin and regulate actin dynamics (Terman et al., 2002, Schmidt et al., 2008; Beuchle et al., 2007; Hung et al., 2010). This function of MICALs is closely related to their unique structure, which is markedly distinct from other known proteins. The most interesting feature of MICALs is their N-terminal NADPH-dependent flavoprotein monooxygenase domain, which makes MICALs flavoenzymes. Moreover, MICALs combine their flavoprotein monooxygenase domain with several other protein interaction domains, namely a Calponin Homology (CH) domain, a LIM domain and coiled-coil (CC) motifs (Fig. 1A) (Terman et al., 2002; Suzuki et al., 2002; Kolk and Pasterkamp, 2007). The function(s) of these domains as well as their specific binding partners remain poorly understood.

The N-terminal monooxygenase (MO) domain of mouse MICAL-1 has been analyzed by X-ray crystallography (Fig. 1C) (Siebold et al., 2005; Nadella et al., 2005). This analysis revealed that a FAD cofactor is embedded in a pocked-like FAD binding domain within the MO domain (Fig. 1C). Three conserved FAD binding motifs contact different portions of the FAD molecule. The GxGxxG motif defines FAD binding domain fingerprint 1 and binds to the ADP moiety of FAD. The DG and GD motifs bind to the pyrophosphate and ribose moieties of FAD, respectively (Fig. 1B, 1C) (Terman et al., 2002; Siebold et al., 2005; Nadella et al., 2005). The structure of the MICAL-1 MO domain closely resembles that of the bacterial flavoprotein monooxygenase p-hydroxybenzoate hydroxylase (PHBH) (Siebold et al., 2005; Nadella et al., 2005). Monooxygenases classically catalyze insertion of one molecule oxygen into small molecule substrates such as *p*-hydroxygenzoate, steroids and amino acids (Entsch et al., 2005; Cole et al., 2005; Siebold et al., 2005; Nadella et al., 2005). The substrates of the MO domain of MICALs, however, have been suggested to be larger molecules, such as proteins, on basis of the enlarged active-site cavity present in MICAL-1 (Siebold et al., 2005; Nadella et al., 2005). Enzymatic experiments suggest that CRMPs (collapsin response mediator proteins) and actin filaments may be substrates for the MICAL MO domain (Schmidt et al., 2008; Hung et al., 2010).

The integrity of the MO domain is essential for several of the physiological roles of MICALs reported to date. For example, in *Drosophila* the MO domain of Mical is required for mediating axon guidance events. Mical loss-of-function larva exhibit specific motor axon guidance defects, which can be rescued by re-introducing wild type but not MO mutated Mical into the nervous system (Terman et al., 2002). When a constitutively activate Mical MO domain is overexpressed in *Drosophila* neurons, growth cones show an expanded surface area and increased filopodia number (Hung et al., 2010). Moreover, bristle-specific exogenous expression of constitutively active MO domain increases bristle branching (Hung et al., 2010). Together, these findings support a requirement for MO enzymatic activity during Mical functioning *in vivo*.

Several lines of evidence also implicate the MO domain of vertebrate MICALs in the regulation of cell morphology. First, in cultured neurons MICAL MO activity is required for transducing the effect of semaphorin3A (Sema3A), a chemorepulsive axon guidance molecule that can prevent neurite outgrowth (Terman et al., 2002; Schmidt et al., 2008). Second, the green tea extract EGCG (epigallocatechin gallate), which is known to inhibit flavin monooxygenases (Abe et al., 2000a, b), neutralizes responses of axons to Sema3A most likely via inhibiting the function of the MO domain of MICALs (Terman et al., 2002; Pasterkamp et al., 2006). Third, an N-terminal truncation mutant of MICAL-1, which lacks the MO domain, can serve as a dominant negative mutant inhibiting Sema3A-induced axon repulsion (Schmidt et al., 2008). Fourth, constitutively active MICAL-1 MO domain induces COS-7 contraction (Schmidt et al., 2008). Thus, an intact MO domain is required for the effects of vertebrate MICALs on cell morphology *in vitro*.

The goal of this study was to obtain more insight into enzymatic activity of the MO domain and the potential regulatory roles of the other domains by characterization of MICAL-1 as a representative member of the MICAL family. By using biochemical, molecular and cellular approaches, we confirmed the monooxygenase enzymatic activity of the MO domain and demonstrated two novel properties of MICAL-1, homo-oligomerization via the CH domain and phosphorylation.

Materials and methods

Plasmids

Mouse MICAL-1 cDNA was amplified from embryonic whole brain cDNA using standard molecular techniques. Full length MICAL-1 and deletion constructs were cloned between the *SalI* and *NotI* sites of the pRK5-myc and pRK5-HA vectors (chapter 5). Full length MICAL-1 was also cloned into the pEF-His/V5 vector using the Gateway cloning system (Invitrogen). MICAL-1 $N1^{G3/W3}$ and $N2^{G3/W3}$ mutants were generated on the backbone of MICAL-1 N1 and N2, respectively, by site-directed Quickchange mutagenesis (Stratagene) using the following primers: "GTGTCTCG-TGGTATGGGCCTGGCCTTGCTGGCTTCGGGCTGCTGTG" and "CACAGCAGCCCGAAGCCAGCAAG-GCCAGGCCCATACCACGAGACAC". MICAL-1 S777A (full length) was also generated by site-directed mutagenesis using the following primers: "CTCCTGTGACGAGGGTCGCCCCTGTCCCAAGCCCCAG" and "CTGGGGCTTGGGACAGGGGCGACCCTCG TCACAGGAG".

Antibodies and reagents

We used the following commercially available antibodies: anti-Flag (M2; Stratagene), anti-HA (3F10; Roche), anti-cleaved caspase3 (cell signaling), anti-myc (Roche), anti-V5 (Invitrogen), anti-tubulin (Sigma), and anti-VSV (Sigma). Generation of rabbit anti-mouse MICAL-1 antibodies was as described (chapter 6). 4NQO and catalase were purchased from Sigma.

Cell culture, transfection and treatments

COS-7, Neuro2A and HEK293 cells were maintained in high glucose Dulbecco's modified Eagle's medium (DMEM; GIBCO) supplemented with 10% FBS (Lonza), penicillin/ streptomycin, and L-glutamine (PAA) at 37°C with 5% CO_2. For cell contraction experiments, COS-7 cells were transfected with FuGene (Roche) according to the manufacturer's instructions. In brief, $0.5\text{-}1\times10^4$ cells/cm^2 were plated on glass coverslips and transfected after 24 hrs with a mixture of DNA : FuGene (1:3) in DMEM. After overnight culture, cells were fixed and analyzed by assessing GFP fluorescence or by immunocytochemistry. For protein analysis, 4×10^4 cells/cm^2 cells (HEK293 or Neuro2A) were seeded in a 10 cm cell culture plate. After 24 hrs, a mixture containing 8 µg cDNA, 20 µl Lipofectamine (Invitrogen) and 1 ml DMEM was added to the cells. After 24 hrs in culture, cells were harvested by pipetting. For catalase, H_2O_2 and 4NQO treatments, COS-7 cells were seeded at 10^4 cells/cm^2. After 24 hrs in culture, culture media containing different concentrations of the stimuli were applied to the cells. Catalase and H_2O_2 treated cells were fixed with 4% paraformaldehyde (PFA) in PBS and visualized by immunofluorescent staining. 4NQO treated cells were harvested for protein analysis.

Immunoprecipitation (IP) and Western blotting

HEK293 cells from one 10 cm dish were resuspended by pipetting and centrifuged at 1000 rpm for 5 min. After one wash with cold PBS, 1000 µl ice cold lysis buffer (Tris-HCl, pH 8.0, 150 mM KCl, 0.1% Triton-X100 and complete protein inhibitors (Roche)) was added to the cell pellet. The lysate was left on ice for 15 min and then centrifuged at 14,000 rpm at 4°C for 30 min. The supernatant was collected in another eppendorf tube and the corresponding antibody was added to the lysate and incubated overnight at 4°C. Protein G agarose beads (30 µl suspension from the original vial) (Roche) were washed 3 times, and then the lysate-antibody mixture was transferred to the pre-washed beads. After 2 hrs incubation at 4°C, beads were washed 4 times with lysis buffer. Then proteins were eluted with 30 µl 1× Sample Buffer (60 mM Tris-HCl, pH 6.8, 5% glycerol, 2% SDS and 50 mM DTT).

For the analysis of MICAL-1 proteins, 7% SDS-PAGE or NuPAGE (Invitrogen) precast gel were used, for cleaved caspase-3 a 15% SDS-PAGE gel was used. After separating proteins in gel, proteins were transferred onto nitrocellulose membrane (Hybond-C Extra, Amersham). After 1 hr blocking in 5% milk in PBS-T (137 mM NaCl, 2.7 mM KCl, 10 mM Na_2HPO_4, 1.8 mM KH_2PO_4, pH 7.4 and 0.01% Tween20), corresponding antibodies were diluted

in PBS-T and applied to the membrane to detect the protein(s) of interest. Chemiluminescence (Supersignal, from Thermo Scientific) was detected by CL-XPosure Film (Thermo Scientific).

Immunofluorescent staining

COS-7 cells on coverslips were fixed in 4% PFA in PBS (137 mM NaCl, 2.7 mM KCl, 10 mM Na_2HPO_4, 1.8 mM KH_2PO_4, pH 7.4), washed once with PBS and permeabilized with 0.2% Triton-X100 in PBS for 5 min. After two washes with PBS, cells were blocked for 10 min in 2% bovine serum albumin (BSA) in PBS, followed by PBS washes and primary myc-antibody (Roche) incubation for 1 hr at room temperature (RT). After 3 washes in PBS, secondary anti-mouse Alexa 594 antibody (Invitrogen) was added to the cells for 45 min at RT. After subsequent washes in PBS, cells on coverslips were embedded in Mowiol-PPD and analyzed with an Axiovert 405M Fluorescent microscope (Zeiss).

ProQ and Colloidal blue staining

Phosphoproteins in NuPAGE Bis-Tris gel (Invitrogen) were stained with "Pro-Q Diamond Phosphoprotein gel stain (Invitrogen)" according to the instructions of the manufacturer. Briefly, the gel was fixed in 50% methanol and 10% acedic acid for 30 min followed by incubation in the same fix solution overnight at RT. Then the gel was washed 3 times with ultrapure water, stained in ProQ stain for 90 min in the dark, and destained 3 times in a solution containing 20% acetonitrile and 50 mM sodium acetate, pH 4.0. After a brief wash in ultra-pure water, the gel was imaged on a FLA-5000 analyzer (Fuji Photo Film Co, Ltd.) using excitation at 532 nm and LPG filter. The colloidal blue staining Kit (Invitrogen) was used according to manufacturer's instructions to visualize total protein in NuPAGE (Invitrogen) gel.

Alkaline Phosphatase (AP) treatment

AP treatment experiments were performed according to the methods described by Kishida et al. (2001). Phosphorylated Dvl (Dishevelled) was used as a positive control for the AP treatment (Kishida et al., 2001). Lysates expressing HA-tagged proteins were immunoprecipitated with anti-HA antibody 3F10 (Roche), and immunoprecipitates were incubated with 6 U of alkaline phosphatase (Roche) in 20 µl reaction buffer containing 50 mM Tris-HCl, pH 8.0, 10 mM $MgCl_2$, and 0.1 mg/ml BSA for 30 min at 37°C. Negative controls were treated with reaction buffer with or without Na_3VO_4, respectively. After incubation, the reaction was stopped by adding 7 µl 4× NuPAGE sample buffer (Invitrogen) and incubation at 70°C for 10 min.

Phosphoproteomics sample preparation

Postnatal day 7 mouse brain was grinded in ice-cold lysis buffer (50 mM Tris-HCl, pH 8.0, 100 mM KCl, 1% NP40, 1 mM DTT and protease inhibitors (Roche) and phosphatase inhibitors (Sigma)). After ultracentrifugation at 50,000 rpm at 4°C for 1 hr, supernatant was collected and mixed with anti-mouse MICAL-1 antibody and pre-washed protein G agarose. After 2 hrs incubation at 4°C, beads were washed once with lysis buffer, once in 300 mM KCl buffer (50 mM Tris-HCl, pH 8.0, 300 mM KCl, 1% NP40, 1 mM DTT and protease inhibitor cocktail (Roche) and phosphatase inhibitors (Sigma)), twice in 800 mM KCl buffer (50 mM Tris-HCl, pH 8.0, 800 mM KCl, 1% NP40, 1 mM DTT and protease inhibitor cocktail (Roche) and phosphatase inhibitors (Sigma)), twice in 300 mM KCl buffer and twice in ABC buffer. ABC buffer refers to Ammonium bicarbonate buffer containing 50 mM ammonium bicarbonate, pH>7.9. Overexpressed HA-MICAL-1 was purified from Neuro2A cells using the same protocol except for the immunoprecipitation antibody, which was anti-HA 3F10 (Roche).

Nanoflow LC-MS/MS analysis

Proteins on bead were digested with trypsin (Promega, sequencing grade), as described by Wilm et al. (1996). Nanoflow LC-MS/MS was performed on a 1100 series capillary LC system (Agilent Technologies) coupled to an LTQ-Orbitrap mass spectrometer (Thermo) both operating in positive mode and equipped with a nanospray source. Peptide mixtures were trapped on a ReproSil C18 reversed phase column (Dr Maisch GmbH; column dimensions 1.5 cm × 100 µm, packed in-house) at a flow rate of 8 µl/min. Peptide separation was performed on ReproSil C18 reversed phase column (Dr Maisch GmbH; column dimensions 15 cm × 50 µm, packed in-house) using a linear gradient from 0 to 80% B (A = 0.1 % formic acid; B = 80% (v/v) acetonitrile, 0.1 % formic acid) in 70 min and at a constant flow rate of 200 nl/min using a splitter. The column eluent was directly sprayed into the ESI source of the

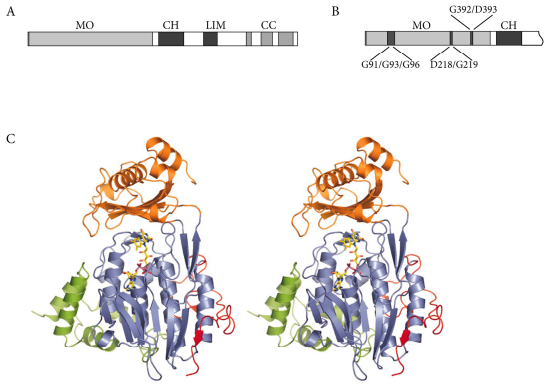

Figure 1. Structure of the MICAL-1 protein.
(A) A schematic representation of the mouse MICAL-1 domain structure showing at the N terminus the flavoprotein monooxygenase (MO) domain, followed by a calponin homology (CH) domain, a LIM domain and coiled-coil (CC) motifs.
(B) Schematic representation of the MO domain of mouse MICAL-1. Conserved FAD binding motifs are marked. GxGxxG (where x denotes any amino acid) defines FAD binding domain fingerprint 1; GD defines FAD binding domain fingerprint 2, and DG is a conserved FAD binding motif. The exact positions of these residues are shown. The GxGxxG represents G91/G93/G96 of mouse MICAL-1, and the DG and GD motifs represent D218/G219 and G392/D393, respectively.
(C) Ribbon diagram of the tertiary structure of the MICAL-1 MO domain revealed by X-ray crystallography (the figure is adapted with permission from Siebold et al., 2005). The first 85 amino acids at the N-terminus of the protein form a four-helix bundle domain which is depicted in green. The FAD binding domain is in slate, the monooxygenase enzymatic domain is in orange and the linker region (to the CH domain) is in red. The FAD molecule is depicted as sticks.

mass spectrometer. Mass spectra were acquired in continuum mode; fragmentation of the peptides was performed in data-dependent mode. Peak lists were automatically created from raw data files using the Mascot Distiller software (version 2.3; MatrixScience). The Mascot search algorithm (version 2.2, MatrixScience) was used for searching against the IPI database (IPI_human_20100507.fasta). The peptide tolerance was typically set to 10 ppm and the fragment ion tolerance was set to 0.8 Da. A maximum number of 2 missed cleavages by trypsin were allowed and carbamidomethylated cysteine and oxidized methionine were set as fixed and variable modifications, respectively. The Mascot score cut-off value for a positive protein hit was set to 60. Individual peptide MS/MS spectra with Mascot scores below 40 were checked manually and either interpreted as valid identifications or discarded. Typical contaminants, also present in immunopurifications using beads coated with pre-immune serum or antibodies directed against irrelevant proteins, were omitted from the table.

H_2O_2 measurement
The Amplex Red Hydrogen Peroxide Assay Kit (Invitrogen) was used for H_2O_2 detection. Cells in one well of a 6 well plate were transfected with various constructs and lysed by sonication in 120 µl lysis buffer containing 20 mM HEPEs, pH 7.4, 100 mM NaCl and 1×EDTA-free protease inhibitor mixture (Roche) (Schmidt et al., 2008). A reaction mixture containing 50 µM Amplex Red reagent, 0.1 U/ml HRP, 200 µM NADPH and 50 µl cell lysate filled up to 100 µl with reaction buffer was incubated for 30 min in dark at RT. Absorbance at 560 was measured by using Wallac Victor 1420 Multilabel counter.

Results

Regulation of the MICAL-1 monooxygenase domain
Determination of the crystal structure of the MICAL-1 monooxygenase (MO) domain revealed that this part of MICAL-1 resembles *p*-hydroxybenzoate hydroxylase (PHBH), an NADPH-dependent flavoenzyme (Siebold et al., 2005; Nadella et al., 2005). PHBH is an intracellular bacterial flavoenzyme that catalyzes the hydroxylation of aromatic compounds, e.g. *p*-hydroxygenzoic acid, to form oxygenated products (Entsch and van Berkel, 1995; Entsch et al., 2005; Cole et al., 2005). Similar to PHBH, the isolated MO domain of

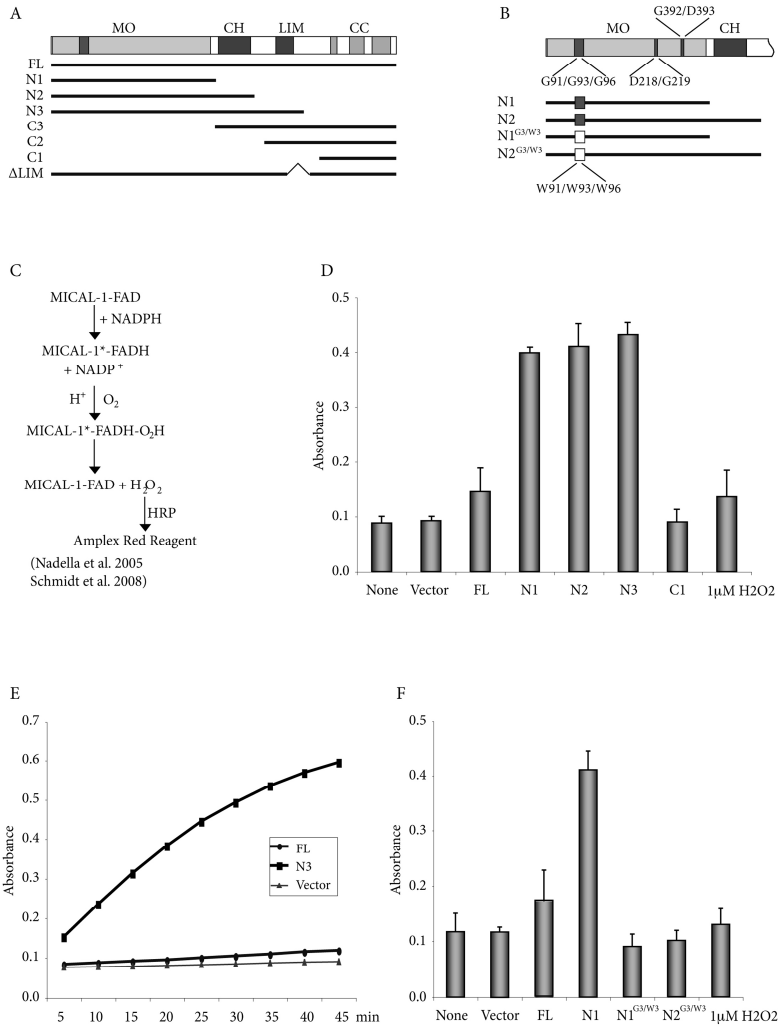

Figure 2. Mouse MICAL-1 mediates H_2O_2 production *in vitro*.

(A) Mouse MICAL-1 truncation mutants were generated lacking specific domains at the N- or C- terminus of MICAL-1. ΔLIM indicates a LIM domain-deletion mutant. CC, coiled-coil; CH, calponin homology; FL, full length; MO, monooxygenase.

(B) Schematic representation of the MO domain of mouse MICAL-1. Conserved FAD binding motifs are marked as G91/G93/G96, D218/G219 and G392/D393. Three mutation sites (GGG to WWW) were induced in FAD binding finger print 1 (GxGxxG) in the N1 and N2 MICAL-1 constructs and named $N1^{G3/W3}$ and $N2^{G3/W3}$, respectively.

(C) Overview of the enzyme-linked assay used to determine H_2O_2 levels produced by MICAL-1 or its truncation mutations. Addition of NADPH to MICAL-1 protein leads to the reduction of FAD. The intermediate hydroperoxide form of MICAL-1 is unstable in the absence of substrate and therefore decomposes when exposed to molecular oxygen to form oxidized FAD and H_2O_2, the latter of which can be measured by the Amplex Red Peroxidase assay (adapted from Nadella et al., 2005 and Schmidt et al., 2008).

(D) Measurement of H_2O_2 production from lysates of HEK293 cells transfected with FL MICAL-1 or MICAL-1 truncation mutants in the presence of 200 μM NADPH. Cell lysates from non-transfected cells (None), or vector transfected cells (Vector) were used as negative controls. 1μM H_2O_2 in PBS was used as positive control for H_2O_2 measurement.
(E) The lysates of HEK293 cells transfected with FL, N3 MICAL-1 or a control vector were mixed with Amplex Red reaction reagent in the presence of 200 μM NADPH. H_2O_2 levels were recorded every 5 minutes for 45 minutes in total. The reaction speed of N3 was much higher than of FL MICAL-1.
(F) When mutation sites were introduced into FAD binding fingerprint 1 of the N1 and N2 MICAL-1 mutants, the corresponding mutants, $N1^{G3/W3}$ and $N2^{G3/W3}$, failed to produce H_2O_2. Panels D and F show means ±SEM from 3 independent experiments.

MICAL-1 is hyperactive in the presence of NADPH and able to produce hydrogen peroxide (H_2O_2) in the absence of substrate (Nadella et al., 2005; Schmidt et al., 2008). NADPH reduces the FAD molecule within the MO domain and transfers the MO domain to an unstable intermediate form, which catalyzes molecular oxygen to form oxidized FAD and H_2O_2 (Fig. 2C) (Nadella et al., 2005; Schmidt et al., 2008). In addition to the MO domain, MICAL-1 contains multiple protein-protein interaction domains (Fig. 1A, 2A). To examine whether these domains can influence the function and enzymatic properties of the MICAL-1 MO domain, a series of MICAL-1 truncation mutants were generated (Fig. 2A).

To evaluate the enzymatic activity of the MO domain of MICAL-1, we adopted an enzyme-linked H_2O_2 detection assay based on the "Amplex Red reagent kit" (Nadella et al., 2005). Truncated and full-length (FL) MICAL-1 constructs were expressed in HEK293 cells and H_2O_2 levels were assessed in cell lysates. The cell lysates were mixed with the Amplex Red reaction mixture in the presence of 200 μM NADPH, a concentration close to the affinity constant of NADPH (Km=222 μM) (Nadella et al., 2005). Lysates from non-transfected cells and from cells transfected with empty vector were used as negative controls. No MO enzymatic activity was detected in lysates from control cells or from cells transfected with the truncation mutant composed of the C-terminal domain (C1). Cells transfected with FL MICAL-1 only produced moderate levels of H_2O_2 (Fig. 2D). In contrast, truncation mutants containing the MO domain (N1, N2 and N3) were all able to generate high levels of H_2O_2 (Fig. 2D). To further estimate the difference in reaction velocity between FL and N3 MICAL-1, kinetic curves were calculated based on the production of H_2O_2 in real time. The Amplex Red reactions of lysates from FL MICAL-1, N3 truncation mutant or control vector expressing cells were monitored for 45 minutes. As shown in Fig. 2E, both FL and N3 proteins catalyzed H_2O_2 production in a nearly linear manner within the time scale of the measurements. H_2O_2 production by FL MICAL-1 was low but steadily increased compared to the negative control. N3, however, showed a fast increase in catalytic activity (Fig. 2E). From these experiments, we can conclude that the MO domain of MICAL-1 is highly active when the C-terminal region is absent, which functions to inhibit the MO domain, and that the flanking CH and LIM domains do not significantly influence MO enzymatic activity. Interestingly, FL MICAL-1 is inhibited with respect to its enzymatic activity.

The MICAL-1 crystal structure indicates that MICAL-1 is a FAD-binding monooxygenase (Siebold et al., 2005; Nadella et al., 2005) and our own structure-function experiments show that truncation mutants containing the N-terminal MO domain are constitutively active with respect to H_2O_2 production. Three conserved motifs within the MO domain bind the FAD molecule in the FAD binding domain (Fig. 1B, 2B). The GxGxxG motif binds the ADP moiety of FAD, and the DG and GD motifs bind the pyrophosphate and ribose of FAD, respectively (Terman et al., 2002; Nadella et al., 2005; Siebold et al., 2005). To confirm the necessity of FAD binding for MICAL-1 enzymatic activity, mutation sites were introduced into the MO domain of the N1 and N2 constructs by site-directed mutagenesis. In the two mutants, $N1^{G3/W3}$ and $N2^{G3/W3}$, glycines within the FAD binding finger print 1 (GxGxxG) were mutated to tryptophans (WxWxxW, Fig. 2B), abolishing the ability of FAD binding but leaving the overall structure intact (Terman et al., 2002). The

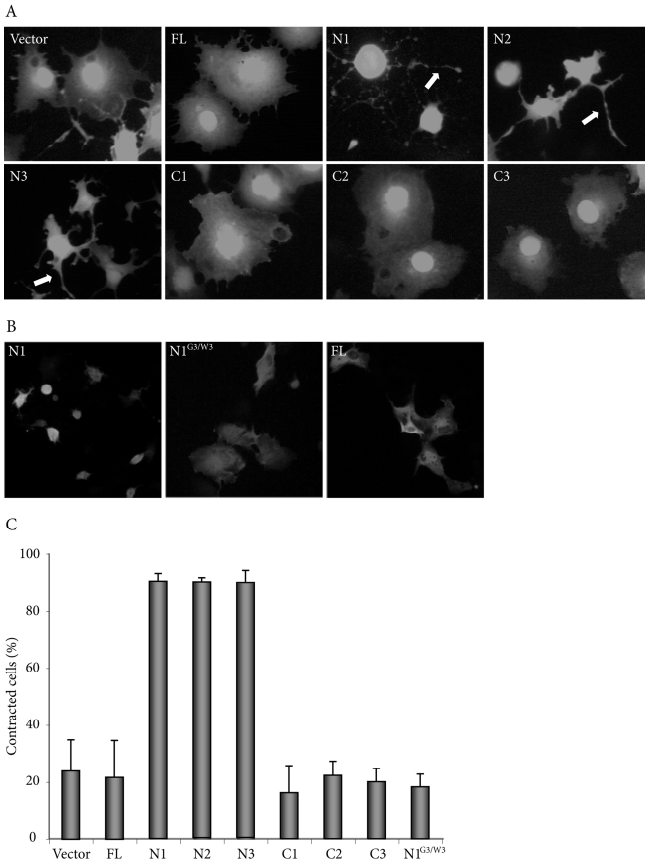

Figure 3. The monooxygenase domain of MICAL-1 mediates cell contraction responses.
(A) COS-7 cells were transfected with vector, FL MICAL-1 or the indicated truncation mutants, together with eGFP to visualize cell morphology. FL MICAL-1 and the C1-C3 truncation mutants did not change cell morphology compared to vector transfected cells. In contrast, N1-N3 MICAL-1 induced cell contraction characterized by a smaller surface area and long and thin processes (white arrows).
(B) Myc-tagged N1, $N1^{G3/W3}$ and FL MICAL-1 were transfected in COS-7 cells and visualized by fluorescent immunocytochemistry using anti-myc antibody. Cells transfected with N1 MICAL-1 were contracted. In contrast, transfection of mutant $N1^{G3/W3}$ and FL MICAL-1 did not result in cell contraction.
(C) Quantification of the percentage of contracted cells in the experiments shown in A and B. Contraction is defined by a cell surface area of less than 1600 μm^2 (Takahashi and Strittmatter, 2001; Schmidt et al., 2008). Graph shows means ±SEM from 3-5 independent experiments.

MICAL-1 mutants were expressed in HEK293 cells and H_2O_2 levels were assessed in cell lysates. H_2O_2 levels in cells transfected with $N1^{G3/W3}$ and $N2^{G3/W3}$ were comparable to control (Fig. 2F). These results indicate that binding of the coenzyme FAD is required for the enzymatic activity of the MICAL-1 MO domain in the presence of NADPH.

These data suggest that MICAL-1 can exist in an enzymatically quiescent state and point to the possibility that modification of its structure may elevate the MO activity.

The MICAL-1 monooxygenase domain mediates cell morphological changes

To begin to understand the physiological role of the MICAL-1 MO domain in mammalian cells, FL MICAL-1 and MICAL-1 truncation mutants (Fig. 2A) were transfected in COS-7 cells together with eGFP to visualize cell morphology. Cells expressing the N1, N2 or N3 constructs, which are able to produce H_2O_2, showed a dramatic contraction of COS-7 cells with a decreased cell surface and characteristic thin processes (Fig. 3A, C). In contrast, expression of FL MICAL-1 or of the C1 to C3 mutants did not influence cell morphology. This is consistent with findings of Schmidt et al. (2008) showing robust cell contraction following transfection of MO domain-containing MICAL-1 truncation mutants. We also tested the effect of

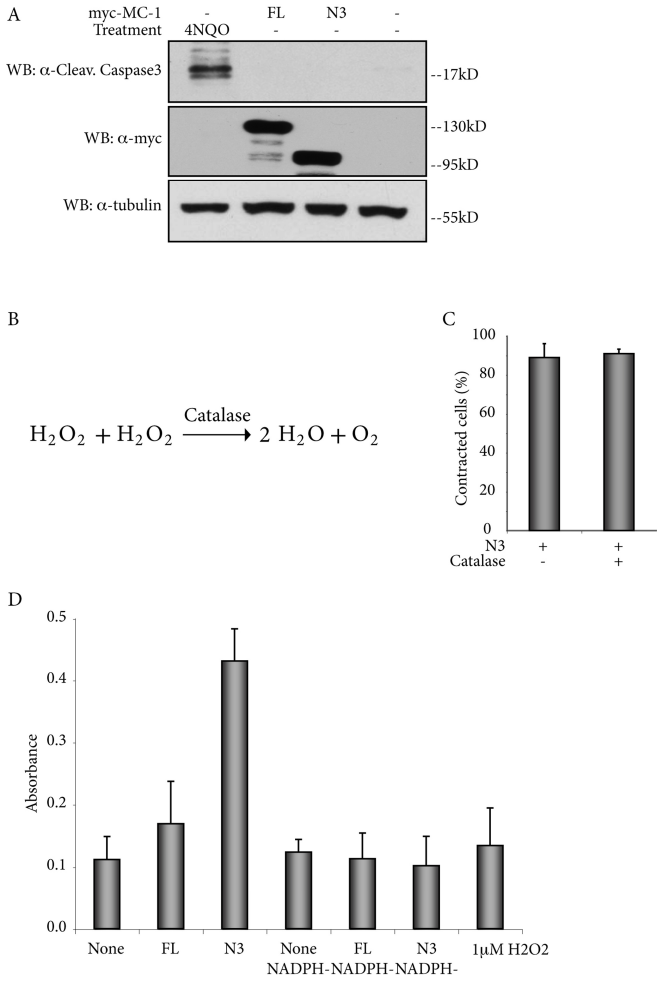

Figure 4. Cell contraction induced by N1-N3 MICAL-1 is not due to apoptosis nor directly mediated by H_2O_2.

(A) COS-7 cells were transfected with N3 or FL MICAL-1. The level of cleaved caspase3 (Cleav. Caspase3) was examined in cell lysates. 4NQO-treated or non-treated COS-7 cell lysates were used as positive or negative controls for cleaved caspase3, respectively. Western blotting showed that N3 or FL MICAL-1 do not induce caspase3 processing. MC-1, MICAL-1.

(B) Catalase is a H_2O_2 scavenger that degrades H_2O_2 into water and oxygen.

(C) N3 MICAL-1 expressing COS-7 cells were treated with vehicle or catalase. The percentage of contracted cells is shown. Catalase treatment did not alter the extent of cell contraction induced by N3 MICAL-1.

(D) H_2O_2 levels in COS-7 cell lysates expressing the indicated proteins were measured in the presence or absence of NADPH (NADPH-). In the absence of NADPH, H_2O_2 levels in N3 or FL MICAL-1 transfected cells were comparable to those observed in non-transfected cells (None). Graphs in C and D show means ±SEM from 3 independent experiments.

N1, N2 and N3 in other cell lines, including L cells, Neuro2A cells and HEK293 cells, and found similar contraction effects (chapter 5 and data not shown). Thus, the constitutively active MO domain of MICAL-1 can alter cell morphology in several types of mammalian cells in culture.

To confirm the requirement of FAD binding and monooxygenase activity for the cell contraction that was induced by N1 to N3, MICAL-1 FL, N1 and $N1^{G3/W3}$ constructs were transfected into COS-7 cells. In contrast to N1, FL MICAL-1 and $N1^{G3/W3}$ were ineffective in inducing cell contraction indicating that FAD-dependent monooxygenase activity is required for cell contraction mediated by MICAL-1 (Fig. 3B, C).

Being a monooxygenase, the *in vivo* role of MICAL-1 is assumed to be production of H_2O_2 or durect modification of its substrates via a redox reaction. Redox modifications have not only been implicated in the regulation of the cytoskeleton but also in the initiation of apoptosis in cells (Haddad, 2004). To exclude the possibility that the observed cell contraction was due to apoptosis, we examined cleaved caspase3 levels in

Figure 5. MICAL-1 forms oligomers via its CH domain.

(A) HEK293 cells were transfected with myc-MICAL-1 or vector together with MICAL-1-V5. Cell lysates were subjected to immunoprecipitation with anti-myc antibody followed by Western blotting with anti-V5 or anti-myc antibody. Note that MICAL-1-V5 co-immunoprecipitated with myc-MICAL-1.

(B) HA-MICAL-1 FL and truncation mutants (N1-N3 and C1-C3) were co-expressed with MICAL-1-V5 in HEK293 cells. HA-tagged proteins were immunoprecipitated with anti-HA antibody to examine binding of MICAL-1-V5 as visualized with anti-V5 antibody. MICAL-1-V5 co-immunoprecipitated with HA-tagged FL, N2, N3 and C3 MICAL-1.

(C) Myc-tagged ΔLIM or FL MICAL-1 were co-transfected with MICAL-1-V5 in HEK293 cells. After immunoprecipitation using anti-myc antibody, proteins were detected with anti-V5 and anti-myc antibodies. Both myc-tagged ΔLIM and FL MICAL-1 co-immunoprecipitated with MICAL-1-V5.

(D) Schematic indicating the self-association of individual MICAL-1 molecules (Schmidt et al., 2008) and oligomerization of MICAL-1 via the CH domain. The MICAL-1 C-terminal region interacts with a more N-terminal part of the protein to inhibit the MO domain activity. In addition, the CH domains of different MICAL-1 molecules interact to form oligomers.

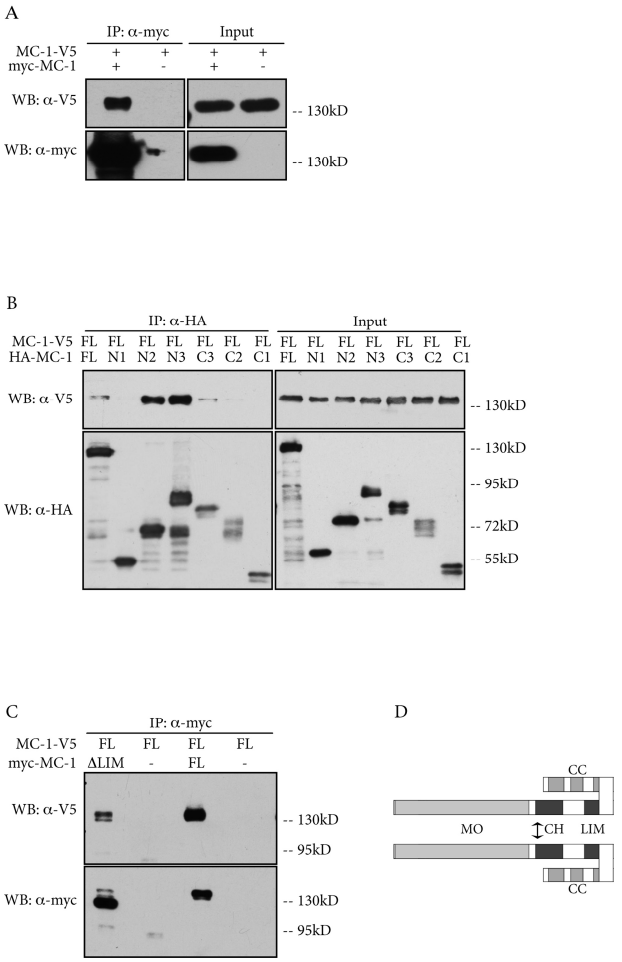

COS-7 cells expressing MICAL-1 FL or N3. During apoptosis, caspase3 undergoes proteolytic processing to produce two subunits (Cohen, 1997). Cleaved caspase3 is commonly used to identify apoptotic cells. 4NQO (4-Nitroquinoline 1-oxide, an apoptotic stimulus)-treated cells showed high levels of cleaved caspase-3 and were used as positive control (Fig. 4A; Han et al., 2007). In contrast, no cleaved caspase3 was found in lysates from FL, N3 or untransfected cells (Fig. 4A), suggesting that cell contraction induced by N3 is not the result of apoptosis.

Our work and that of others shows that the MICAL-1 MO domain can produce H_2O_2. As a reactive oxygen intermediate, H_2O_2 has been reported to induce contraction in several different cell types (Valen et al., 1999; Gloy et al., 1999; Yang et al., 1999). We therefore examined whether H_2O_2 directly mediated the MICAL-1-induced cell contraction. Several different manipulations and measurements of cellular H_2O_2 levels were performed, as outlined below.

First, H_2O_2 was depleted from COS-7 cells expressing the N3 construct. COS-7 cells were transfected with N3 and treated with vehicle or 500 U/ml catalase for 12 hours starting 4 hours following transfection. Catalase degrades H_2O_2 to water and oxygen (Fig. 4B). COS-7 growth was impaired following catalase treatment with a decrease in cell number as compared to vehicle treated cells (data not shown). This is consistent with previous findings showing that catalase inhibits fibroblast cell growth (Preston et al., 2000). However, catalase did not affect the ability of N3 to induce cell contraction (Fig. 4C).

As a second approach to examine the potential role of H_2O_2 in MICAL-1-induced cell contraction, H_2O_2 was added to untransfected COS-7 cells. H_2O_2 has been reported to induce cell contraction in several cell types (Valen et al., 1999; Gloy et al., 1999; Yang et al., 1999). However, 4 hours of treatment with 10-200 μM H_2O_2 (to mimic the amount of H_2O_2 produced by N3) did not induce contraction of COS-7 cells in comparison to non-treated control cells (data not shown).

Finally, MICAL-1 FL and N3 enzymatic activity was measured in the absence of exogenous NADPH. NADPH aids MO activity by donating an electron to the FAD co-enzyme (Schmidt et al., 2008; Siebold et al., 2005), and in the absence of additional NADPH H_2O_2 measurements will reveal endogenous H_2O_2 levels in the cell. As shown in Fig. 4D, in the absence of exogenous NADPH, N3-containing cell lysates displayed H_2O_2 levels comparable to those observed in lysates of non-transfected cells, indicating that H_2O_2 levels in cells that contract in response to a constitutively active MICAL-1 MO domain (N3) are not changed.

Together, these results strongly argue against a direct role for H_2O_2 in the cell contraction effects of MICAL-1 N1-N3, and suggest that protein substrates of MICAL-1 exist that mediate this cellular response.

MICAL-1 molecules exist as oligomers

In addition to a MO domain, MICAL-1 contains a CH domain, a LIM domain and coiled-coil motifs (Fig. 1A). A common feature of these modules is their docking potential for other domains/motifs. Furthermore, all of these modules have been suggested to mediate homo-oligomer formation by interacting with an identical domain or with other domains in another copy of the same protein. We therefore examined whether MICAL-1 exists as an oligomer.

Myc-MICAL-1 and MICAL-1-V5 were co-expressed in HEK293 cells and subjected to co-immunoprecipitation. Myc-MICAL-1 was immunoprecipitated from cell lysates using an anti-myc antibody followed by Western blotting using anti-myc and anti-V5 antibodies. Interestingly, MICAL-1-V5 co-immunoprecipitated with myc-MICAL-1 (Fig. 5A). Vice versa, myc-MICAL-1 could be detected following immunoprecipitation of MICAL-1-V5 (data not shown). This suggests that MICAL-1 is able to form homo-dimers or oligomers. A native gel was then used to estimate the number of MICAL-1 copies in the MICAL-1 oligomer complex. However, due to the high molecular weight of a single MICAL-1 (116.7 kD), we failed to determine the precise copy number of MICAL-1 in the oligomer complex (data not shown).

Then, we mapped the domain(s) involved in the oligomerization of MICAL-1. HA-tagged constructs of N1-3, C1-3 and FL MICAL-1 were co-transfected with MICAL-1-V5 in HEK 293 cells. After immunoprecipitation with anti-HA antibody, MICAL-1-V5 was detected by Western blotting. As shown in Fig. 5B, N2 and N3 bound to full length MICAL-1 protein efficiently. C3 was also able to interact, but with lower affinity. In some experiments, the C2 fragment was able to precipitate small amounts of MICAL-1 (data not shown). The inability of N1 and C1 to bind MICAL-1-V5 indicated that the MO domain and the coiled-coil motifs are not involved in MICAL-1-MICAL-1 interactions (Fig. 5B). The marginal binding of C2 to full length MICAL-1 suggests that the LIM domain may be involved in oligomerization (data not shown). The LIM domain has been found to mediate protein dimerization in many different proteins (Feuerstein et al., 1994; Gill, 1995). Therefore, we further assessed the requirement of the LIM domain for MICAL-1-MICAL-1 association by using a deletion mutant in which the LIM domain was deleted (ΔLIM, Fig. 1A). Myc tagged ΔLIM or FL MICAL-1 were transfected into HEK293 cells together with MICAL-1-V5 and immunoprecipitated using anti-myc antibody. As shown in Fig. 5C, both ΔLIM and FL were able to pull down MICAL-1-V5, indicating that the LIM domain is not essential for oligomerization. Thus, the

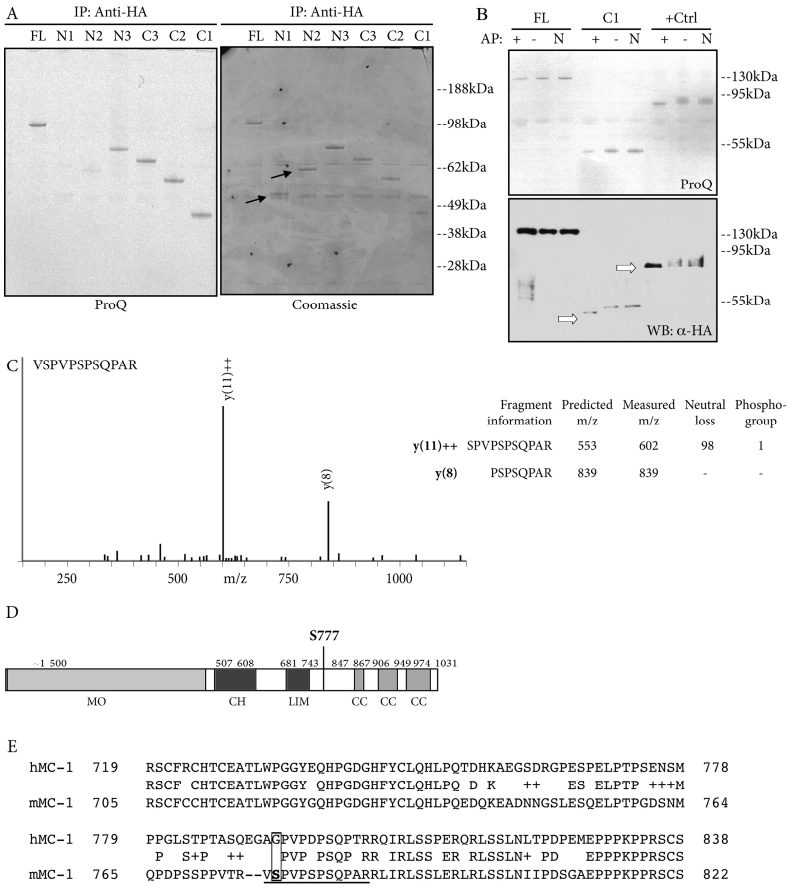

Figure 6. MICAL-1 is a phosphoprotein.
(A) HA-tagged MICAL-1 FL and truncation mutants were expressed in HEK293 cells, immunoprecipitated by anti-HA antibody, separated on gel and subjected to ProQ staining followed by coomassie staining. ProQ staining revealed that FL, N3, C3, C2 and C1 MICAL-1 contain phosphorylated residue(s).
(B) Anti-HA purified FL or C1 MICAL-1 were divided into three aliquots and treated with alkaline phosphatase (+), Na3VO4 (-) or reaction buffer (N, see material and methods). After treatment, proteins were analyzed by SDS-PAGE coupled in-gel ProQ staining or blotted with anti-HA antibody. A known phosphoprotein, Dvl (disheveled) was used as positive control for AP treatment. AP treatment decreased the ProQ intensity of FL, C1 and Dvl. Band shifts of C1 and Dvl after AP treatment could be discerned on western blot.
(C) Mass spectrometry identified one phosphorylated peptide in endogenous and overexpressed MICAL-1: "VSPVPSPSQPAR". The peptide fragment spectrum is obtained after peptide collision and analysis by tandem MALDI MS/MS. More than 30 peaks are depicted and the most abundant fragments of y(11)++ and y(8) are labeled. Y(11)++ showed a m/z shift, which equals to a neutral loss of 98 (H_3PO_4 group), while the Y(8) fragment matched the predicted m/z value. Therefore, the MICAL-1 phosphorylation site is mapped to the first serine of the peptide "VSPVPSPSQPAR".
(D) The location of identified phosphorylated serine corresponds to serine777 (S777) in mouse MICAL-1.
(E) Alignment of the mouse and human MICAL-1 sequence shows the position of the identified peptide (underlined). The box indicates the S777 phosphorylation site in mouse MICAL-1 and the corresponding amino acid in human MICAL-1.

domain required for MICAL-1 oligomerization is the CH domain, the only common region of the N2, N3 and C3 truncation mutants. Taken together, our data show that MICAL-1 exists as an homo-oligomer and that this self-association is mediated by the CH domain. At present, studies are ongoing to establish the role of the CH domain and MICAL-1 oligomerization.

MICAL-1 is a phosphoprotein

During a search for MICAL-1 interacting proteins, several kinases were identified as potential binding partners of MICAL-1 (chapter 4 and 5). These results suggested that MICAL-1 is a potential phosphoprotein and may be regulated by upstream kinases. Therefore, we examined the phosphorylation status of MICAL-1.

To analyze MICAL-1 phosphorylation by ProQ staining, which only labels phosphorylated proteins, FL MICAL-1 was transfected in HEK 293 cells, immunoprecipitated, separated in gel and subjected to ProQ staining. Full length MICAL-1 was robustly labeled using ProQ staining indicating the presence of phosphorylated residues in its protein sequence (Fig. 6A).

To map the location of the phosphorylated residue(s) within the MICAL-1 protein sequence, MICAL-1 truncation mutants were transfected in HEK 293 cells, isolated by immunoprecipitation and subjected to ProQ staining. N3 and C1-C3, but not N1 or N2 were detected by ProQ in-gel staining, indicating the presence of phosphorylation site(s) in the C-terminal region of MICAL-1 encompassing the LIM domain and coiled-coil motifs (Fig. 6A). To further confirm the presence of phosphorylation sites in MICAL-1, immuno-purified FL and C1 MICAL-1 were treated with AP (alkaline phosphatase) to remove potential phospho groups. Following AP treatment, ProQ staining of FL and C1 MICAL-1 was reduced as compared to control (Fig. 6B). Detection of FL and C1 MICAL-1 protein by Western blotting of the same sample as used for AP treatment revealed a characteristic band shift for the C1 mutant to a smaller size after AP treatment. Due to technical limitations of the gel used no band shift for FL MICAL-1 was detected (Fig. 6B). Together, these experiments indicate that the LIM domain and C-terminal region (C1) of MICAL-1 contain potential phosphorylation sites.

To determine the residues in mouse MICAL-1 that can be phosphorylated, mass spectrometry analysis was performed. MICAL-1 protein was obtained by immunoprecipitation of HA-tagged MICAL-1 from transfected Neuro2A cells or of endogenous MICAL-1 from mouse postnatal day 7 brain tissue using anti-HA and anti-MICAL-1 antibodies, respectively. Before mass spectrometry analysis, purified proteins were examined using ProQ staining to confirm their phosphorylated status (data not shown). Proteins were subjected to on-bead tryptic digestion and peptides were analyzed by tandem MALDI MS/MS. In both HA-MICAL-1 and endogenous MICAL-1 one phosphorylated peptide was identified, VSPVPSPSQPAR (residues 776-787). Upon peptide collision, the peptide fragment spectrum of "VSPVPSPSQPAR" was determined (Fig. 6C). The "SPVPSPSQPAR" (y(11)++) fragment showed a neutral loss of 98 Da (H_3PO_4), indicating the presence of a phospho group within this fragment. The observation that the "PSPSQPAR" (y(8)) fragment does not show a neutral loss indicates that the first serine residue of the peptide "V<u>S</u>PVPSPSQPAR" is the only phosphorylated residue. This serine residue corresponds to serine777 (S777) of mouse MICAL-1 (Fig. 6D).

S777 is located in the variable region of mouse MICAL-1 between the LIM domain and coiled-coil motifs (Fig. 6D). This region is not conserved among family members, varies in length and is not found in other proteins (Terman et al., 2002; Pasterkamp et al., 2006). Alignment of human and mouse MICAL-1 indicated that S777 is not conserved between human and mouse (Fig. 6E). Nevertheless, we analyzed the functional significance of S777. By site-directed mutagenesis, a MICAL-1 mutant was generated in which serine 777 was replaced by an alanine (S777A). We then asked whether the S777A mutant could alter MICAL-1 functions. Overexpressed MICAL-1-S777A did not influence cell morphology and showed a distribution similar to intact FL MICAL-1 (Fig. 7A). In addition, the ability of S777A and FL MICAL-1 to produce H_2O_2 was similar (Fig. 7B). We further examined whether this mutant affected binding to known

Figure 7. Mutagenesis of S777 has no effect on MICAL-1 function.
(A) Myc-tagged MICAL-1 mutant S777A or FL MICAL-1 were transfected into COS-7 cells and visualized by immunofluorescent staining with anti-myc antibody. S777A and FL MICAL-1 have no effect on cell morphology and show a similar distribution in cells.
(B) COS-7 cells were transfected with vector or FL, S777A, N1 MICAL-1 and cell lysates were subjected to H_2O_2 detection in the presence of 200 μM NADPH. S777A has no effect the level of H_2O_2 produced by MICAL-1. Panel B shows means ±SEM from 3 experiments.

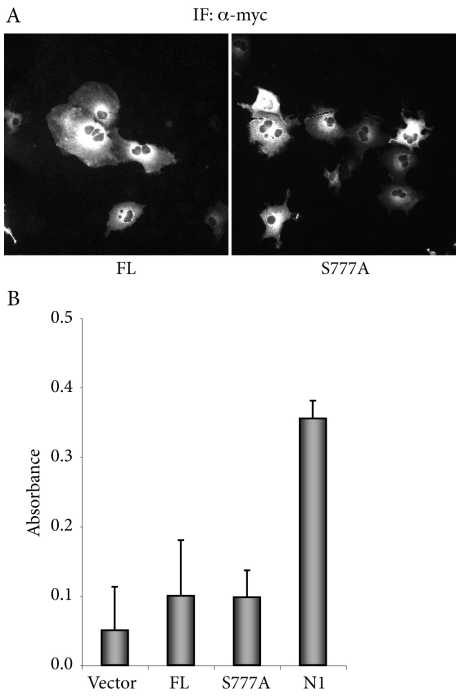

MICAL-1 interacting proteins such as plexinA1, CRMP1 and NDR1 (Schmidt et al., 2008; chapter 5), but no differences were found (data not shown). Overall, these results suggest that phosphorylation of S777 does not contribute to the currently reported functions of MICAL-1.

Discussion

MICAL proteins have been implicated in several physiological and pathological processes including in axon guidance, dendritic pruning, synapse formation, bristle development, spinal cord injury and cancer progression (Terman et al., 2002; Beuchle, 2007; Kirilly et al., 2009; Pasterkamp et al., 2006; Ashida et al., 2006, Hung et al., 2010; Schmidt et al., 2008). Many of these functions have been suggested to rely on the ability of MICALs to bind and regulate cytoskeletal components. However, how MICALs themselves are regulated and which other cellular processes they may control is largely unknown. The present study aimed at characterizing the regulation and mechanism-of-action of vertebrate members of the MICAL family. We focused on MICAL-1 which is the founding member of this family and has been best-characterized at the functional level. Here, we show that the MICAL-1 MO domain is enzymatically active, i.e. able to produce H_2O_2, and mediates cell contraction responses in the absence of the MICAL-1 most C-terminal region. In addition, we report that MICAL-1 exists as a homo-oligomer and contains phoshorylated residues hinting at the regulation of this protein through protein phosphorylation.

Several lines of evidence support the idea that MICAL-1 contains a flavoenzyme capable of mediating redox signaling. First, MICAL-1 and other family members contain three conserved FAD binding motifs within their MO domain (Terman et al., 2002). The sequence and spacing of these motifs is identical to the FAD binding motifs present in other monooxygenases (Terman et al., 2002). Second, X-ray crystallography studies reveal that the MO domain of MICAL-1 contains a FAD cofactor and has a "monooxygenase-like"

topology, which is most similar to that of the NADPH-dependent monooxygenase PHBH (Nadella et al., 2005; Siebold et al., 2005). Indeed, similar to PHBH MICAL-1 MO activity is NADPH-dependent (Nadella et al., 2005; Siebold et al., 2005; Schmidt et al., 2008). Third, our data and a study by Schmidt et al. (2008) show that the MO domain can produce H_2O_2 (Fig. 2D, E). This effect depends on FAD binding as mutagenesis of one of the FAD-binding motifs within the MICAL-1 MO domain abolished H_2O_2 production (Fig. 2F). In contrast to MICAL-1 truncation mutants lacking the C-terminal region (N1-N3), full length MICAL-1 protein only produces moderate levels of H_2O_2. This is in line with the observation that the native MICAL-1 protein exists in an autoinhibited conformation due to intramolecular interactions between the C-terminal and the LIM domain containing N-terminal regions within this protein (Schmidt et al., 2008). The factors that control this autoinhibited conformation and as a result MICAL-1 MO activity remain unknown.

MICAL-1 truncation mutants lacking the C-terminal region not only constitutively produce H_2O_2 but also induce extensive cell contraction and neurite growth inhibition (Fig. 3A; Schmidt et al., 2008). This effect relies on an enzymatically active MO domain since interfering with the FAD binding capacity of this domain abolished the cell contraction effects of MICAL-1. Interestingly, H_2O_2 has been reported to induce cell contraction (Valen et al., 1999; Gloy et al., 1999; Yang et al., 1999; Rhee, 2006). Our experiments, however, argue against a direct role for H_2O_2 in cell contraction mediated by MICAL-1. First, exogenous application of H_2O_2 did not induce cell contraction in COS-7 cells while catalase treatment failed to prevent MICAL-1 induced contraction. Second, H_2O_2 levels in control cells and cells expressing constitutively active MICAL-1 mutants were similar. Together these observations support a model in which MICAL-1 triggers the redox modification of a specific protein substrate(s) to induce cell morphological changes rather than using H_2O_2 as a second messenger.

Thus far, two possible substrates for the MICAL-1 MO domain have been described, CRMP-1 and actin (Schmidt et al., 2008; Hung et al., 2010). CRMP-1 physically interacts with MICAL-1 and co-transfection of MICAL-1 and CRMP-1 induces cell contraction. In the presence of CRMP-1, H_2O_2 production by the MICAL-1 MO domain is reduced which may indicate that CRMP is a substrate of the MO domain, i.e. the MICAL-1 MO domain may target CRMP-1 rather then producing H_2O_2 (Schmidt et al., 2008). However, further work is needed to establish that CRMP-1 is a true MICAL-1 substrate and that this protein is subjected to redox modifications. Another potential substrate is actin. Recombinant *Drosophila* Mical MO domain binds F-actin and disassembles actin filaments and bundles in the presence of exogenous NADPH *in vitro* (Hung et al., 2010). This has been suggested to be the consequence of the direct oxidation of actin filaments. It is known that oxidation of actin leads to the disassembly of actin filaments, reduced ability of actin to interact with actin crosslinking proteins, and a decrease in the ability of actin monomers to form polymers (Dalle-Donne et al., 2001a,b; Mizani et al., 1997). It remains to be established, however, whether MICALs can directly oxidize actin. In addition to actin, MICALs interact with vimentin and tubulin, two other components of the cytoskeleton (Suzuki et al., 2002; Weide et al., 2003). It will be interesting to determine whether these cytoskeletal proteins are substrates for the MICAL MO domain and whether their dynamics can be regulated through MICAL-mediated redox signaling.

In contrast to the MO domain, the function of the other domains present in MICAL proteins is largely unknown. Our present work suggests that the CH domain facilitates oligomerization of MICAL-1 by mediating an intermolecular interaction between individual MICAL-1 molecules. However, it is interesting to note that isolated CH domains exist as monomers in solution (Sun et al., 2006). This hints at the involvement of an additional domain in MICAL oligomerization. The most likely candidate is the MO domain. Our data show that MO-CH domain containing truncation mutants (N2 and N3) bind far more efficiently to full length MICAL-1 molecules as compared to mutant that contains the CH domain but lacks the MO domain (C3). This idea gains support from the observation that PHBH, which closely resembles MICAL, can homo-dimerize via its monooxygenase domain (Westphal et al., 2006). Although the purified MO domain of MICAL-1 exists as monomer (Siebold et al., 2005; Nadella et al., 2005), it may facilitate

oligomer formation in presence of the CH domain. Further studies are needed to fine map the region(s) in MICALs required for oligomerization and to establish the functional role of this process (Marianayagam et al., 2004).

Protein interaction experiments (chapter 4 and 5) have identified several kinases as potential binding partners of MICAL-1. This suggests that MICAL-1 may be phosphorylated and targeted by upstream kinases. Indeed, the present study shows that both exogenous as well as endogenous, brain-derived MICAL-1 are phosphorylated on serine 777. The functional significance of this phosphorylation event is unclear as S777 is neither conserved among species nor required for the current reported functions of MICAL-1. For example, mutating S777 into an alanine did not change the distribution or the enzymatic and cell contraction activity of MICAL-1. The sequence around S777 does not correspond to any known protein kinase recognition motifs. Prediction programs (e.g. Phosida) hint at the presence of multiple phosphorylation sites in MICAL-1 while our work also points at at least one more phosphorylated residue in the LIM domain-containing region (Fig. 6). Although future work is needed to identify these phosphorylation sites and establish their role in MICAL-1 function, the presence of phosphorylated residues in MICAL-1 suggests that the localization and/or function of this protein may be regulated through phosphorylation.

Since the identification of the MICAL family in 2002 (Suzuki et al., 2002; Terman et al., 2002), MICAL proteins have been implicated in several physiological processes and in disease, including in spinal cord injury and prostate cancer progression (Terman et al., 2002; Beuchle, 2007; Kirilly et al., 2009; Pasterkamp et al., 2006; Ashida et al., 2006). Our results provide important insight into the function and regulation of MICAL proteins and provide new avenues for interfering with MICAL function. For example, following spinal cord injury cells in the lesion site increase their expression of secreted semaphorins which is thought to contribute to the neurite growth inhibitory properties of the injured CNS and prevent successful regeneration (Pasterkamp et al., 2006). Since MICALs are thought to provide direct links between semaphorin receptors (plexins) and the actin cytoskeleton these proteins may constitute excellent targets for blocking inhibitory semaphorin-plexin signaling following injury. Strategies targeting the enzymatic activity of MICAL, its oligomerization or phosphorylation may be used to impair MICAL signaling and promote regeneration. Although much further work is needed to unravel the precise function and regulation of MICAL proteins, they may represent powerful therapeutic targets in and outside the nervous system.

Acknowledgements

We thank Katsumi Fumoto for help with the alkaline phosphatase treatment. This work was supported by the Netherlands Organization for Health Research and Development (ZonMW-VIDI and ZonMW-TOP), the Human Frontier Science Program (HFSP-CDA), and the Genomics Center Utrecht (to R.J.P.).

References

Abe, I., K. Kashiwagi, and H. Noguchi. 2000a. Antioxidative galloyl esters as enzyme inhibitors of p-hydroxybenzoate hydroxylase. FEBS Lett 483:131–134.

Abe, I., T. Seki, K. Umehara, T. Miyase, H. Noguchi, J. Sakakibara, and T. Ono. 2000b. Green tea polyphenols: novel and potent inhibitors of squalene epoxidase. Biochem Biophys Res Commun 268:767–771.

Ashida, S., M. Furihata, T. Katagiri, K. Tamura, Y. Anazawa, H. Yoshioka, T. Miki, T. Fujioka, T. Shuin, Y. Nakamura, and H. Nakagawa. 2006. Expression of novel molecules, MICAL2-PV (MICAL2 prostate cancer variants), increases with high Gleason score and prostate cancer progression. Clin Cancer Res. 2006 May 1;12(9):2767-73.

Beuchle, D., H. Schwarz, M. Langegger, I. Koch, and H. Aberle. 2007. Drosophila MICAL regulates myofilament organization and synaptic structure. Mech Dev 124(5):390-406.

Bron, R., M. Vermeren, N. Kokot, W. Andrews, G.E. Little, K.J. Mitchell, and J. Cohen. 2007. Boundary cap cells constrain spinal motor neuron somal migration at motor exit points by a semaphorin-plexin mechanism. Neural Dev. 2007 Oct 30;2:21.

Cohen, G. M. 1997. Caspases: the executioners of apoptosis. Biochem J.326 (Pt 1):1-16.

Cole, L. J., B. Entsch, M. Ortiz-Maldonado, D. P. Ballou. 2005. Properties of p-hydroxybenzoate hydroxylase when stabilized in its open conformation. Biochemist 44(45):14807-17.

Dalle-Donne, I., R. Rossi, D. Giustarini, N. Gagliano, L. Lusini, A. Milzani, P. Di Simplicio, and R. Colombo. 2001a. Actin carbonylation: from a simple marker of protein oxidation to relevant signs of severe functional impairment, Free Radic. Biol. Med. 31 (2001), pp. 1075–1083 a.

Dalle-Donne, I, R. Rossi, A. Milzani, P. Di Simplicio, and R. Colombo. 2001b. The actin cytoskeleton response to oxidants: from small heat shock protein phosphorylation to changes in the redox state of actin itself, Free Radic.Biol. Med. 31(2001), pp.1624–1632 b.
Entsch, B., and W. J. van Berkel. 1995. Structure and mechanism of para-hydroxybenzoate hydroxylase. FASEB J. 9(7):476-83.
Entsch, B., L. J. Cole, and D. P. Ballou. 2005. Protein dy-namics and electrostatics in the function of p-hydroxybenzoate hydroxylase. Arch Biochem Biophys 433(1):297-311.
Feuerstein, R., X. Wang, D. C. Song, N. E. Cooke, and S. A. Liebhaber. 1994. The LIM/double zinc-finger motif func-tions as a protein fimerization domain. Proc. Natl. Acad. Sci. 91:10655-10659.
Gill, G. N. 1995.The enigma of LIM domains.Structure. 3(12):1285-9.
Gloy, J., K. G. Fischer, T. N. Meyer, P. Schollmeyer, R. Greger, and H. Pavenstädt. 1999. Hydrogen peroxide activates ion currents in rat mesangial cells. Kidney International 56:181–189.
Haddad, J. J. 2004. Redox and oxidant-mediated regulation of apoptosis signaling pathways: immuno-pharmaco-redox conception of oxidative siege versus cell death commitment. Int Immunopharmacol.4(4):475-93.
Han, H., Q. Pan, B. Zhang, J. Li, X. Deng, Z. Lian, and N. Li. 2007. 4-NQO induces apoptosis via p53-dependent mitochondrial signaling pathway. Toxicology 230(2-3):151-63.
Hung, R. J., U. Yazdani, J. Yoon, H. Wu, T. Yang, N. Gupta, Z. Huang, W. J. van Berkel, and J. R. Terman. 2010. Mical links semaphorins to F-actin disassembly. Nature 463(7282):823-7.
Kirilly, D., Y. Gu, Y. Huang, Z. Wu, A. Bashirullah, B. C. Low, A. L. Kolodkin, H. Wang, and F. Yu. 2009. A genetic pathway composed of Sox14 and Mical governs severing of dendrites during pruning. Nat Neurosci 12(12):1497-505.
Kishida, M., S. Hino, T. Michiue, H. Yamamoto, S. Kishida, A. Fukui, M. Asashima, and A. Kikuchi. 2001. Synergistic activation of the Wnt signaling pathway by Dvl and casein kinase Iepsilon. J Biol Chem 276(35):33147-55.
Kolk, S.M, and R.J. Pasterkamp. 2007. MICAL flavoprotein monooxygenases: structure, function and role in semaphorin signaling. Adv Exp Med Biol. 2007;600:38-51.
Letourneau, P. C. 2009. Actin in axons: stable scaffolds and dynamic filaments. Results Probl Cell Differ. 2009;48:65-90.
Marianayagam, N. J., M. Sunde, and J. M. Matthews. 2004. The power of two: protein dimerization in biology. Trends Biochem Sci 29(11):618-25.
Milzani, A, I. Dalle-Donne, and R. Colombo. 1997. Prolonged oxidative stress on actin, *Arch. Biochem. Biophys.* 339 (1997), pp. 267–274.
Nadella, M., M. A. Bianchet, S. B. Gabelli, J. Barrila, and L. M. Amzel. 2005.Structure and activity of the axon gui-dance protein MICAL. Proc Natl Acad Sci 102(46):16830-5.
Pasterkamp, R. J., H. N. Dai, J. R. Terman, K. J. Wahlin, B. Kim, B. S. Bregman, P. G. Popovich, and A. L. Kolodkin. 2006. MICAL flavoprotein monooxygenases: expression during neural development and following spinal cord injuries in the rat. Mol Cell Neurosci 31(1):52-69.
Preston, T. J., W. J. Muller, and G. Singh. 2001. Scavenging of extracellular H2O2 by catalase inhibits the proliferation of HER-2/Neu-transformed rat-1 fibroblasts through the induction of a stress response. J Biol Chem 276(12):9558-64.
Rhee, S. G. 2006. H2O2, a Necessary Evil for Cell Signaling. Science 312:1882-1883.
Schmidt, E. F., S. O. Shim, and S. M. Strittmatter. 2008. Release of MICAL autoinhibition by semaphorin-plexin signaling promotes interaction with collapsin response mediator protein. J Neurosci 28(9):2287-97.
Siebold, C., N. Berrow, T. S. Walter, K. Harlos, R. J. Owens, D. I. Stuart, J. R. Terman, A. L. Kolodkin, R. J. Pasterkamp, and E. Y. Jones. 2005. High-resolution structure of the catalytic region of MICAL (molecule interacting with CasL), a multidomain flavoenzyme-signaling molecule. Proc Natl Acad Sci 102(46):16836-41.
Sun, H., H. Dai, J. Zhang, X. Jin, S. Xiong, J. Xu, J. Wu, and Y. Shi. 2006. Solution structure of calponin homology domain of Human MICAL-1. J Biomol NMR 36(4):295-300.
Suzuki, T., T. Nakamoto, S. Ogawa, S. Seo, T. Matsumura, K. Tachibana, C. Morimoto, and H. Hirai. 2002. MICAL, a novel CasL interacting molecule, associates with vimentin. J Biol Chem 277(17):14933-41.
Takahashi, T., and S. M. Strittmatter. 2001. Plexina1 autoinhibition by the plexin sema domain. Neuron. 2001 Feb;29(2):429-39.
Terman, J. R., T. Mao, R. J. Pasterkamp, H. H. Yu, and A. L. Kolodkin. 2002. MICALs, a family of conserved flavoprotein oxidoreductases, function in plexin-mediated axonal repulsion. Cell 109(7):887-900.
Valen, G., A. Sondén, J. Vaage, E. Malm, and B.T. Kjellström. 1999. Hydrogen peroxide induces endothelial cell atypia and cytoskeleton depolymerization. Free Radic Biol Med 26(11-12):1480-8.
Weide, T., J. Teuber, M. Bayer, and A. Barnekow. 2003. MICAL-1 isoforms, novel rab1 interacting proteins. Biochem Biophys Res Commun. 2003 Jun 20;306(1):79-86.
Westphal, A. H., A. Matorin, M. A. Hink, J. W. Borst, W. J. van Berkel, and A. J. Visser. 2006. Real-time enzyme dynamics illustrated with fluorescence spectroscopy of p-hydroxybenzoate hydroxylase. J Biol Chem 281(16):11074-81.
Wilm, M., A. Shevchenko, T. Houthaeve, S. Breit, L. Schweigerer, T. Fotsis, and M. Mann. 1996. Femtomole sequencing of proteins from polyacrylamide gels by nano-electrospray mass spectrometry. Nature 379: 466-9.
Yang, Z. W., T. Zheng, J. Wang, A. Zhang, B. T. Altura, and B. M. Altura. 1999. Hydrogen peroxide induces contraction and raises [Ca2+]i in canine cerebral arterial smooth muscle: participation of cellular signaling pathways. Naunyn Schmiedebergs Arch Pharmacol 360(6):646-53.

Chapter 4

Identification of novel MICAL-1 interacting proteins by mass spectrometry

Yeping Zhou[1], Youri Adolfs[1], Jeroen Demmers[2], Vanessa R. Marques Donegá[1], W.W.M. Pim Pijnappel[3], Ka Wan Li[4], Roel C. Van der Schors[4], August B. Smit[4], Casper C. Hoogenraad[5], R. Jeroen Pasterkamp[1]

[1]Department of Neuroscience and Pharmacology, Rudolf Magnus Institute of Neuroscience, University Medical Center Utrecht, Universiteitsweg 100, 3584 CG, Utrecht, The Netherlands
[2]Proteomics Center, Erasmus University Medical Center, Dr Molewaterplein 50, 3015 GE, Rotterdam, The Netherlands
[3]Netherlands Proteomics Center, Department of Physiological Chemistry, University Medical Center Utrecht, Universiteitsweg 100, 3584 CG, Utrecht, The Netherlands
[4]Department of Molecular and Cellular Neurobiology, CNCR, Neuroscience Campus Amsterdam, VU University, De Boelelaan 1085, 1081 HV Amsterdam, The Netherlands
[5]Department of Neuroscience, Erasmus Medical Center, Dr. Molewaterplein 50, 3015GE, Rotterdam, The Netherlands

Abstract:
The multidomain protein MICAL-1 is considered to be a scaffold protein with the potential to recruit multiple distinct signaling and structural proteins into signaling complexes that mediate various cellular processes. Although several proteins have been found to bind to MICAL-1, binding partners for the majority of MICAL-1 protein domains and motifs remain unknown. Identification of the binding partners of MICAL-1 may help to further understand how MICAL-1 is regulated, in which cellular processes it participates and which other proteins it needs to exert these cellular functions. In this study we used different approaches to purify MICAL-1-containing signaling complexes from mammalian cells followed by mass spectrometry to identify potential MICAL-1 binding proteins. The binding partners of full-length MICAL-1 identified in this study could be divided into two groups: proteins that are involved in regulation of cytoskeleton dynamics or in tight-junction formation. In contrast, in pull down assays using the C-terminal region of MICAL-1, MAPK signaling proteins and apoptosis related proteins were enriched, while N-terminal MICAL-1 was found to bind a multitude of proteins ranging from proteins involved in DNA transcription to cytoskeleton regulation. In a preliminary analysis, NDR1, DOCK7 and staufen were confirmed as novel MICAL-1 binding partners. Together, our results identify a plethora of potential novel MICAL-1-interacting proteins and reveal marked differences in the protein binding profiles of the isolated N- and C- terminal parts of MICAL-1. These findings provide important new leads for future studies on the physiological roles of MICAL proteins.

Introduction:

Since their identification (Suzuki et al., 2002; Terman et al., 2002), more and more interesting properties about the structure, activity, regulation and functions of MICAL proteins have been revealed. The structural organization of MICALs is characterized by a unique flavoprotein monooxygenase (MO) domain at the N-terminus, followed by a Calponin Homology (CH) domain, a LIM domain and coiled-coil (CC) motifs. The MO domain is highly conserved among family members and efficiently catalyzes redox reactions (Schmidt et al., 2008; Siebold et al., 2005; Nadella et al., 2005). The other domains are common components of a large number of proteins. The CH domain mainly serves as an actin binding domain, but can also mediate other protein-protein interactions. The MICAL-1-CH domain shows hydrophobic residues on the surface of its tertiary structure, indicating the potential for hydrophobic interactions with other proteins or domains (Sun et al., 2006; Gimona et al., 2002). The LIM domain is also a protein binding module most likely providing a structural scaffold for protein docking (Kadrmas and Beckerle, 2004). LIM domain-containing proteins show highly variable binding preferences as they are known to bind to structural proteins, kinases, other LIM domain proteins, transcription factors and cytoskeletal proteins (Bach, 2000). Coiled-coil motifs also mediate protein-protein interactions (Burkhard et al., 2001). Several MICAL binding proteins were found to interact with MICAL through this region (Suzuki et al., 2002; Schmidt et al., 2008; Weide et al., 2003). In addition to these domains, MICAL-1, the founding member of vertebrate MICAL, has several proline-rich regions and a glutamic acid-rich stretch (Suzuki et al., 2002; Terman et al., 2002; Weide et al., 2003). Both motifs can potentially mediate protein-protein interactions (Kay et al., 2000; Rayala et al., 2006). Considering the combination of protein interaction domains and motifs in their structure, MICALs are considered to be scaffold proteins which organize signaling proteins into functional complexes.

The first MICAL-1-interacting protein to be identified, CasL, binds to MICAL-1 via one of its proline-rich regions (Suzuki et al., 2002). Subsequently, more MICAL interacting proteins were identified namely, vimentin, CRMP (collapsin response mediator protein), plexinA and Rab1 small GTPase. These proteins all bind to the MICAL C-terminal region containing coiled-coil motifs, except CRMP which binds to N-terminal region encompassing the LIM domain. Another interacting protein, actin, seems to bind directly to the MO domain (Hung et al., 2010). MICALs have been implicated in various biological processes via interaction with these previously identified interactors.

Several studies have revealed or indicated roles for MICALs in various cellular processes. For example, via their interaction with plexin, MICALs mediate semaphorin signaling during axon guidance in both *Drosophila* and mammalian cells (Terman et al., 2002; Hung et al., 2010; Pasterkamp et al., 2006; Schmidt et al., 2008; chapter 2). Moreover, CRMP has been reported to form a complex with plexinA and MICAL-1 in vertebrates and serves as an activator and/or substrate of MICAL-1 (Schmidt et al., 2008). MICALs also function in other processes in nervous system including in synapse formation, dendritic pruning and the positioning of somata in the spinal cord (Beuchle et al., 2007; Kirilly et al., 2009; Bron et al., 2007). How these processes are regulated by MICALs remains elusive. Further insight into the binding partners of MICALs will help to unveil their functional role and mechanism-of-action.

The cytoskeleton is an important target of MICAL proteins. *Drosophila* Mical is essential for proper myofilament organization and controls actin filament dynamics in bristles (Beuchle et al., 2007; Hung et al., 2010). The association of MICAL-1 with vimentin, and perhaps tubulin, has been implicated in the regulation of these proteins (Suzuki et al., 2002; Fischer et al., 2005). CasL belongs to the Cas protein family, a group of cytoskeletal regulators (Suzuki et al., 2002). Therefore, CasL binding to MICALs further supports a role of MICALs in cytoskeleton regulation (Suzuki et al., 2002).

Despite the recent identification of several MICAL-interacting proteins, the binding partners of most structural domains in MICALs remain unknown. Further identification of MICAL interacting proteins will help to understand how MICALs are regulated; in which processes they participate and which other proteins they need to exert these cellular functions.

We chose mouse MICAL-1 for the identification of new MICAL binding partners since it is the best-characterized vertebrate MICAL to date. To identify the full complement of MICAL-1 interacting proteins, we performed mass spectrometry based proteomics studies on immunoprecipitated (IP) protein complexes. Since it is notoriously difficult to obtain naïve and intact protein complexes from cells by IP, two protein complex purification methods were performed and compared with respect to their efficiency and specificity. This approach led to the identification of numerous known and novel MICAL-1 interacting proteins. We used full-length MICAL-1 protein to identify interacting proteins as well as MICAL-1 truncation mutants, MICAL-1-N3 and C1, which contain the N-terminal three domains and C-terminal coiled-coil containing regions, respectively, for detection of the proteins specifically binding to these two regions. MICAL-1 N3 represents a constitutively active form of the MO domain of MICAL-1, while MICAL-1-C1 represents a regulatory region (Schmidt et al., 2008). Various proteins were identified and clustered into functional groups, providing a profile of MICAL-1 interactors and indicating potential physiological roles in different cellular processes.

Material and methods

Plasmids

Mouse *MICAL-1* was subcloned into a pBABE-FLAG-HA destination vector using the GATEWAY cloning system (for the generation of stable L cell lines) (Invitrogen). *MICAL-1* cDNA was subcloned into the pRK5-myc vector as described in chapter 5. To generate bio-eGFP-MICAL-1-N3 and C1, respectively, the N-terminal 2238 base pairs or C-terminal 447 base pairs of the mouse *MICAL-1* coding region were subcloned in between the *EcoRI* and *SalI* sites of the bio-eGFP, which contains a latent biotinylation peptide N-terminally flanked by eGFP on a pEGFP backbone (Lansbergen et al., 2006). Full-length *MICAL-1* was also subcloned into this vector using the *EcoRV* site. The expression vector expressing the biotin ligase BirA was as described previously (Lansbergen et al., 2006). Mouse *NDR1, EFHD2* and *CasL* cDNAs were amplified from embryonic whole brain cDNA using standard molecular techniques. These cDNAs were subcloned into the pFLAG-CMV4 vector (Sigma). The FLAG-DOCK7 construct was a kind gift from Dr. M. M. Maurice (UMC Utrecht, Utrecht, The Netherlands).

Cell culture

HEK293 and stable L cell lines (see chapter 5 for more detail) were maintained in high glucose Dulbecco's modified Eagle's medium (DMEM; GIBCO) supplemented with 10% FBS (Lonza), penicillin/streptomycin, and L-glutamine (PAA) at 37°C with 5% CO_2. For HEK293 cell transfection, exponentially growing cells were plated at 3.5×10^4cells/cm^2 and transfected the following day using Lipofectamine 2000 (Invitrogen) as described by the manufacturer.

Protein purification buffers and procedures

Immunoprecipitation from stable L cells: Mouse MICAL-1-FLAG/HA expressing (D1) and control (C0) L cells were cultured in 500 cm^2 plates (Corning) to 90% confluency. Ten plates from each cell line were harvested by scraping after 2 washes with cold PBS. The following procedures were performed at 4°C unless stated otherwise. Cells were centrifuged at 1000 rpm for 15 min and lysed by douncing in 3 ml hypotonic lysis buffer containing 10 mM HEPES, pH 8.0, 1.5 mM $MgCl_2$, 10 mM KCl, 0.5 mM PMSF, 0.5 mM DTT and protease inhibitor cocktail (Sigma). After centrifugation at 14,000 rpm for 15 min, supernatant was transferred to a clean Falcon tube and an equal volume of 2 × salt buffer containing 30 mM HEPES, pH 8.0, 190 mM KCl, 30 mM NaCl, 40% glycerol, 0.4 mM EDTA, 0.5 mM PMSF, 0.5 mM DTT and protease inhibitor cocktail (Sigma) was added. After measuring protein concentration, 100 mg protein from each cell line was added to 100 µl pre-washed M2 affinity resin (Sigma) and incubated for 3 hrs. Then, the resin was washed 4 times with washing buffer (BC-150) containing 20 mM HEPES, pH 8.0, 150 mM NaCl and 0.5 mM PMSF. Between the third and last wash, the sample was washed once in washing buffer (BC-300) containing 20 mM HEPES, pH 8.0, 300 mM NaCl and 0.5 mM PMSF for 10 min. The proteins were eluted with FLAG peptide (Sigma) at 16 µg/µl in BC-150 buffer. The eluted proteins were precipitated as described previously (Wessel and Flugge, 1984) and dissolved in 1 × NuPAGE LDS Sample buffer (Invitrogen).

For tandem affinity purification (TAP), anti-HA coupled Dynabeads (Invitrogen) were prepared. Pre-washed protein A Dynabeads were mixed with anti-HA 12CA5 (produced in house) at a ratio of 1 ml : 2 mg ($V_{original\ suspension}$: $W_{antibody}$) in Tris-glycine buffer, pH 8-8.5. After 1 hr incubation at room temperature (RT), the Dynabeads were washed 2 times in PBS followed by 2 washes in 0.2 M triethanolamine, pH 8.2, which served as cross-linking buffer. Subsequently 20 mM DMP (dimethyl pimelimidate dihydrochloride) (Pierce) in cross-linking buffer was applied to antibody-coupled Dynabeads and incubated for 30 min at RT. After removal of the cross-linking reagent, the reaction was stopped by adding 50 mM Tris, pH 7.5 at 1 : 2 ratio ($V_{original\ suspension}$: $V_{Tris\ buffer}$). Following 15 min of incubation, Dynabeads were collected by placing the tube on the magnet, and the supernatant was discarded. The anti-HA coupled Dynabeads were 3 × washed in PBS and stored in PBS in presence of 0.02% NaN_3 at 4°C.

FLAG peptide-eluted proteins from the anti-FLAG immunoprecipitation were incubated with 100 µl anti-HA (12CA5) pre-coupled Dynabeads overnight at 4°C (the volume of Dynabead equals the volume of the original suspension). After 3 washes with BC300, 100 µl elution buffer (2 mg/ml HA peptide (KKKRILKMYPYDVPD-YARIL) in BC300) was applied at 4°C to remove contaminants, followed by elution with the same buffer at RT. The eluted proteins were precipitated and dissolved in 1× NuPAGE LDS Sample buffer.

Biotin pull down: Two days after co-transfection of the biotin ligase BirA with different bio-eGFP constructs in HEK293 cells in 10 cm plates, cells were harvested by pipetting. After centrifugation (1000 rpm, 5 min, 4°C) and washes with PBS, cells were lysed in 150 µl lysis buffer (per 10 cm dish) containing 20 mM Tris-HCl pH 8.0, 150 mM KCl, 1% TritonX-100 and protease inhibitors (Roche). After 10 min incubation on ice, the supernatants were collected by centrifugation at 13,000 rpm for 10 min at 4°C. The lysates were mixed with 25 µl streptavidin beads (volume of original suspension) (Invitrogen), which had been pre-washed and blocked by 125 µl blocking buffer (20 mM Tris-HCl pH 8.0, 150 mM KCl, 0.2 µg/ml albumin from Sigma and 20% glycerol). After 1 hr incubation at 4°C, beads were washed 4 times with washing buffer (20 mM Tris-HCl pH 8.0, 150 mM KCl, 0.1% TritonX-100 and protease inhibitors). The proteins were eluted by 1× NuPAGE LDS Sample buffer at 70°C for 10 min.

In-Gel analysis

Protein samples from the purification procedures were separated on a NuPAGE Novex 4-12% Bis-Tris gradient gel following the manufacturer's description (Invitrogen). Proteins were stained using the colloidal blue staining kit (Invitrogen) and the lanes were excised to several pieces for analysis by mass spectrometry. In addition, 1/20 of each sample was loaded on another NuPAGE gel and processed for silver staining. Briefly, the gel was soaked twice in 50% methanol for 15 min and soaked in 5% methanol for 10 min. After 3 rinses in water, the gel was incubated in 10 µM DTT for 20 min, followed by 0.1% $AgNO_3$ for 20 min. Then the gel was washed once in water and twice in developer containing 3% sodium carbonate and 0.02% formaldehyde. The gel was incubated in developer until protein bands appeared. The reaction was stopped with solid citric acid (about 5% w/v). The gel was washed with water and scanned.

Gel digestion and NanoLC and MALDI TOF/TOF analysis of full-length MICAL-1 complexes

Separated proteins stained by colloidal blue were in-gel digested according to methods previously described (Shevchenko et al., 1996). Samples were analyzed by MALDI-TOF/TOF mass spectrometry as described (Li et al., 2007) with minor modification. In brief, peptides were separated on a nanocapillary LC system (LC Packings/Dionex, Sunnyvale, CA) using an analytical capillary C18 column (150 mm x 100 µm ID) at 400 nl/min, with a linear increase in concentration of acetonitrile from 5 to 50% (v/v) in 90 min and to 90% in 10 min. The eluted gradient was mixed with matrix solution (7 mg of re-crystallized α-cyano-hydroxycinnaminic acid in 1 ml 50% (v/v) acetonitrile, 0.1%(v/v) trifluoroacetic acid, 10 mM ammonium dicitrate) and spotted offline to a stainless steel MALDI plate (Applied Biosystems) to form a predefined 16 x 24 array (384 spots) using a ProbotTM system (LC Packings/Dionex). The mass spectrometric analysis was carried out using a MALDI-TOF/TOF instrument (4800 Proteomics Analyzer, Applied Biosystems) with reflector positive ion mode. For MS analysis, 800–3000 m/z mass range was used with 1250 shots per spectrum. A maximum of 20 precursors per spot with minimum signal/noise ratio of 50 were selected for data-dependent MS/MS analysis. A 1-kV collision energy was used for CID, and 2500 acquisitions were accumulated for each MS/MS spectrum. All analyses were performed using default calibration, and the mass accuracy was calibrated to within 100 ppm using calibration standards (Applied Biosystems) before each run.

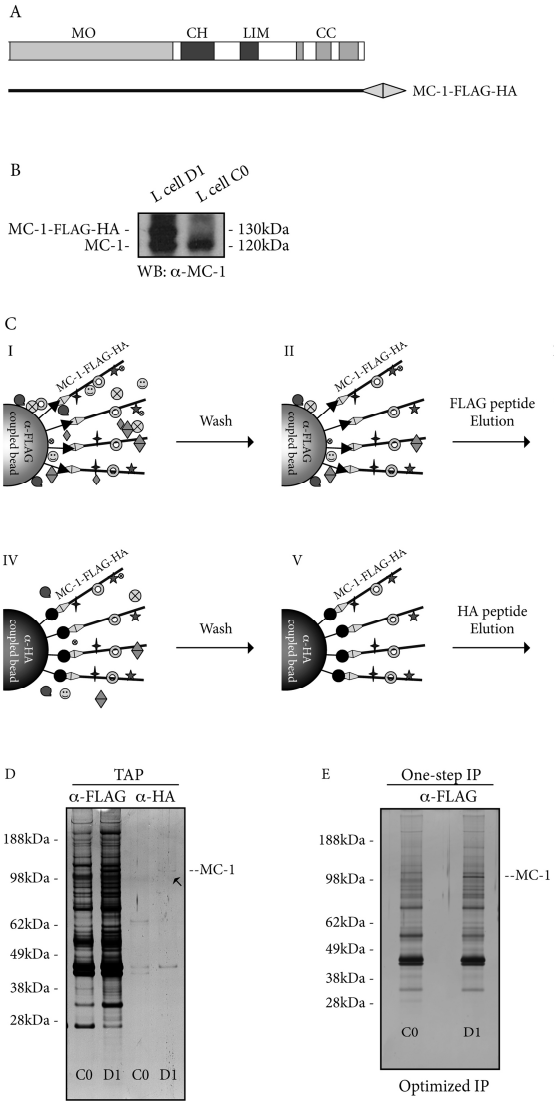

Figure 1. Immunoprecipitation and tandem affinity purification (TAP)

(A) To purify MICAL-1 protein complexes, a FLAG-HA-tagged MICAL-1 construct was generated and stably expressed in L cells.

(B) Western blotting was used to detect the expression of endogenous (~120 kD) and overexpressed (~130 kD) MICAL-1 in D1 and C0 (control) L cell lines. MC-1, MICAL-1.

(C) Schematic representation of the TAP method used to isolate MICAL-1 complexes. First, L cell lysates were incubated with anti-FLAG coupled agarose beads to isolate MICAL-1 (MC-1) protein complexes (I-III). The eluted proteins were then purified using anti-HA coupled Dynabeads to reduce non-specific binding (IV-VI). After two purification steps, the number of non-specific binding proteins was greatly reduced.

(D) TAP purification. Samples from D1 and C0 cell lines were first purified with anti-FLAG antibody, followed by a second purification with anti-HA antibody. The eluted proteins from each step were separated on a NuPAGE gel and protein bands were visualized by silver staining. The MICAL-1-FLAG-HA band is indicated (MC-1; arrow). After anti-HA purification, most of the background bands observed following anti-FLAG IP were gone, unfortunately, the yield of MICAL-1-FLAG-HA was much lower as compared to a single anti-FLAG IP.
(E) After optimizing of the washing conditions, anti-FLAG-IP samples from D1 and C0 cell lines were separated on NuPAGE gel and protein bands were visualized by silver staining. The MICAL-1-FLAG-HA band is indicated (MC-1). Although background bands were still detected in both D1 and C0 lanes, the background was significantly reduced as compared to the anti-FLAG purification shown in (D).

Gel digestion and Nanoflow LC-MS/MS analysis of MICAL-1 N3 or C1 protein complexes

1D SDS-PAGE gel lanes were cut into 2-mm slices using an automatic gel slicer and subjected to in-gel reduction with DTT, alkylation with iodoacetamide and digestion with trypsin (Promega, sequencing grade), as described by Wilm et al. (1996). Nanoflow LC-MS/MS was performed on a CapLC system (Waters, Manchester, UK) coupled to a Q-TOF Ultima mass spectrometer (Waters, Manchester, UK) operating in positive mode and equipped with a Z-spray source. Peptide mixtures were trapped on a Jupiter™ C18 reversed phase column (Phenomenex; column dimensions 1.5 cm × 50 μm, packed in-house) using a linear gradient from 0 to 80% B (A = 0.1 M acetic acid; B = 80% (v/v) acetonitrile, 0.1 M acetic acid) in 70 min and at a constant flow rate of 200 nl/min using a splitter. The column eluent was directly sprayed into the ESI source of the mass spectrometer. Mass spectra were acquired in continuum mode; fragmentation of the peptides was performed in data-dependent mode. Peak lists were automatically created from raw data files using the ProteinLynx Global Server software (version 2.0). The background subtraction threshold for noise reduction was set to 35% (background polynomial 5). Smoothing (Savitzky-Golay) was performed (number of interactions: 1, smoothing window: 2 channels). Deisotoping and centroiding settings were: minimum peak width: 4 channels, centroid top: 80%, TOF resolution: 5000, NP multiplier: 1. Mascot search algorithm (version 2.0, MatrixScience) was used for searching against the NCBInr database that was available on the MatrixScience server. The peptide tolerance was typically set to 150 ppm and the fragment ion tolerance was set to 0.2 Da. A maximum number of 1 missed cleavage by trypsin was allowed and carbamidomethylated cysteine and oxidized methionine were set as fixed and variable modifications, respectively. The Mascot score cut-off value for a positive protein hit was set to 60.

In silico data analysis

For functional clustering of proteins identified by mass spectrometry, the DAVID database was used (http://david.abcc.ncifcrf.gov/home.jsp) (Dennis et al., 2003 and Huang et al., 2009). All the standard protein names were adopted from UniprotKB (http://www.uniprot.org).

Immunoprecipitation and Western blotting

Protein-protein interactions were detected by standard immunoprecipitation and western blotting protocols as described in chapter 5. Briefly, cells were collected, washed in cold PBS and lysed in lysis buffer (20 mM Tris-HCl, pH 8.0, 150 mM KCl, 0.1% TritonX-100 and protease inhibitor cocktail (Roche)). After centrifugation at 14,000 rpm for 10 min at 4°C, the lysate was transferred to a clean eppendorf tube and boiled with sample buffer. For IP, corresponding antibodies were added to each cell lysate and incubated overnight at 4°C. Then pre-washed protein A or G agarose (Roche) was added to the lysate and incubated for at least 2 hrs at 4°C. After 4 washes with lysis buffer, proteins were eluted with sample buffer and boiled at 90°C. To analyze proteins from IP samples or cell lysates, we used SDS-PAGE and transfered proteins to nitrocellulose (Hybond-C Extra, Amersham). Chemiluminescence (Supersignal, Thermo Scientific) was detected by CL-XPosure Film (Thermo Scientific). The antibodies used for IP and western blot were anti-mouse MICAL-1 (chapter 6), anti-human MICAL-1 (a kind gift from Takahiro Suzuki, see Suzuki et al., 2002), anti-FLAG M2 (Stratagene), anti-HA(3F10) (Roche), anti-tubulin (Sigma), anti-GFP (Invitrogen), and anti-STAU (Abcam).

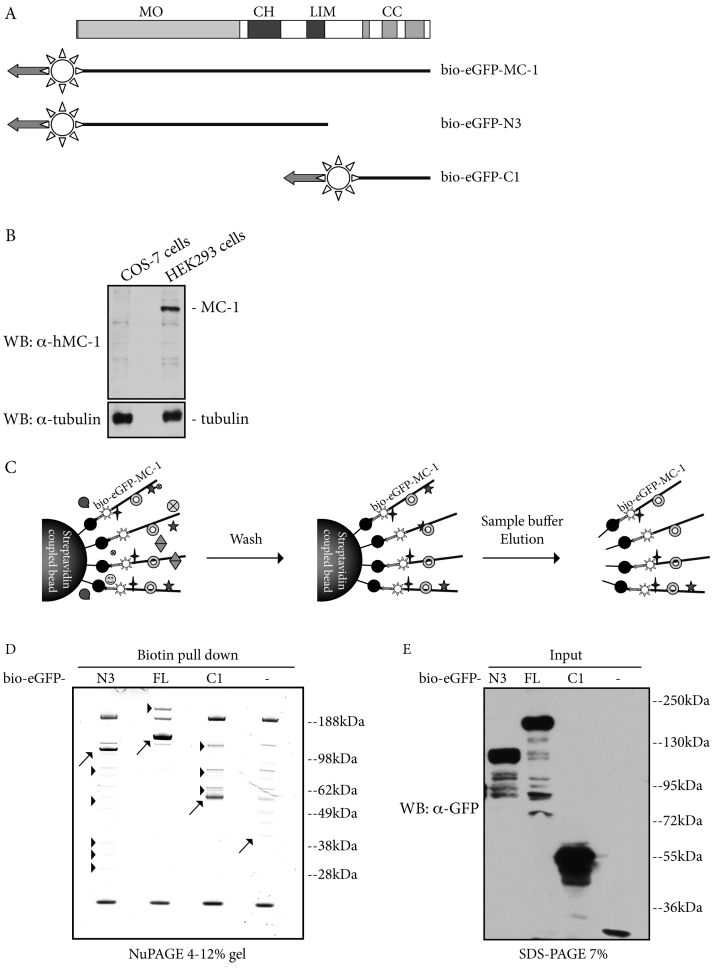

Figure 2. Biotin-streptavidin based protein complex purification

(A) To purify MICAL-1 protein complexes from mammalian cells via the biotin-streptavidin based pull down system, a biotinylation peptide was added to the N-terminus of eGFP-MICAL-1 (full-length), eGFP-MICAL-1-N3 and eGFP-MICAL-1-C1. N3 and C1 represent MICAL-1 truncation mutants containing specific N-terminal domains (MO, CH and LIM) or a C-terminal region (Coiled-coil motifs), respectively. eGFP, enhanced green fluorescent protein; MC-1, MICAL-1.

(B) COS-7 and HEK293 cell lysates were subjected to Western blotting using anti-human MICAL-1 (hMC-1) antibody. HEK293 cells, but not COS7 cells, expressed endogenous human MICAL-1.

(C) Schematic representation of the biotin pull-down assay. The biotinylation peptide of the fusion protein (in this case MICAL-1) is biotinylated by co-transfected BirA biotin ligase. The fusion protein is then isolated by streptavidin beads. After washing to remove aspecific binding proteins, biotinylated protein is eluted from streptavidin beads by boiling in sample buffer.

(D) Coomassie staining showing biotinylated proteins isolated from HEK293 cells following biotin-streptavidin purification. The bait proteins, bio-eGFP-MICAL-1-N3, FL and C1 and bio-eGFP are indicated by arrows; while unique protein bands in each sample are indicated by arrow-heads. Bio-eGFP was used as control for detection of non-specific binding.
(E) Analysis of cell lysates (Input) from the experiment shown in (D). Western blot shows expression of bio-eGFP and bio-eGFP-tagged MICAL-1 N3, FL and C1 proteins using an anti-GFP antibody.

Results

MICAL-1 is a multidomain protein with the potential to bind several other proteins. To identify novel MICAL-1 interacting proteins, two methods were used to isolate mouse MICAL-1-containing protein complexes from cells. The first method was based on immunoprecipitation (IP) of FLAG and HA-tagged MICAL-1 and the second was based on streptavidin-mediated pull-down of biotinylated MICAL-1.

MICAL-1 protein complexes isolated using IP and Tandem affinity purification (TAP)

Advantages of purifying MICAL-1 from vertebrate cells, as compared to for example yeast-2-hybrid, are 1) the ability to purify the entire MICAL-1 protein (~120 kD), and 2) the potential to isolate naïve protein complexes with physiologically relevant functions. To isolate MICAL-1 complexes, a stable L cell line was generated exogenously expressing MICAL-1-FLAG-HA (D1; Fig. 1A). L cells are murine fibroblasts that endogenously express mouse MICAL-1 (Fig. 1B). Constitutively active MICAL-1 expression can induce morphological changes in L cells (data not shown), suggesting that these cells contain signaling proteins that are crucial for MICAL-1 function. L cells expressing an empty expression vector served as a control (C0; Fig. 1B) (for more details on the stable L cell lines, see chapter 5).

To isolate MICAL-1 complexes and to evaluate the specificity of the IP system, anti-FLAG antibody coupled agarose beads were applied to cell lysates of D1 and C0 cells. The immunoprecipitated proteins were eluted from agarose beads with FLAG peptide to obtain intact MICAL-1 complex without antibodies. The isolated protein complexes from both cell lines were separated on a NuPAGE gradient gel. Silver staining revealed a specific MICAL-1 band in the D1 lane (Fig. 1C I-III, D α-FLAG). However, the vast amount of protein bands in the C0 lane indicated the pull down of numerous background proteins. Therefore, we examined a tandem affinity purification (TAP) method to obtain MICAL-1 complexes.

TAP was performed by sequential IPs with anti-FLAG and anti-HA antibodies. Briefly, cell lysates from D1 or C0 cells were first subjected to IP with FLAG antibody as described above. Then, the protein complexes were eluted with FLAG peptide to keep the MICAL-1 complex intact. To reduce non-specific binding, a second purification step with HA antibody coupled Dynabeads was applied. This IP system has an alternative antibody and a magnetic Dynabead-based isolation approach, which further reduces non-specific protein binding (Fig. 1C IV-VI). Indeed, after the second purification, background bands were largely reduced (Fig. 1D α-HA).

The TAP procedure yielded highly purified protein complexes with a low amount of background proteins. However, during the TAP procedure large amounts of bait protein complexes were lost (Fig. 1D). Due to the limitation of our cell culture system for adherent L cells, the TAP method did not yield enough protein complexes for mass spectrometry analysis. Therefore, we further optimized the one step FLAG-IP to prepare protein complexes. By optimizing the washing conditions we reduced background protein levels (Fig. 1E). Proteins from D1 or C0 cells were separated on a NuPAGE gel and visualized by Coomassie staining. Lanes with protein bands were cut into several pieces, in-gel digested with trypsin and analyzed by MALDI TOF/TOF mass spectrometry. The analysis and validation of the identified proteins is reported in the following sections.

MICAL-1 complexes purified using streptavidin-biotin pull down

As an alternative approach to the anti-FLAG IP described above, a biotin-streptavidin based purification method was used to purify MICAL-1 complexes from HEK293 cells, which endogenously express human MICAL-1 (Fig. 2B). Human and mouse MICAL-1 are conserved orthologs sharing more than 80% identity at the protein level (Terman et al., 2002). Our previous studies showed that mouse MICAL-1 exerts its functions, such as H_2O_2 production and cell contraction, in both HEK293 and murine cell lines. This indicates that the protein complexes that mediate MICAL-1 function also exist in HEK293 cells. Therefore, HEK293 cells were used for the isolation of MICAL-1 protein complexes by biotin-streptavidin-based pull down assays. The interaction between biotin and streptavidin has a high specificity and affinity (dissociation constant, $K_d \approx 10^{-14}$-10^{-16} M) (Laitinen et al., 2006), allowing highly specific pull downs and tolerating stringent washing conditions.

To adapt MICAL-1 to the biotin-streptavidin system, the mouse MICAL-1 cDNA was inserted into the pBio-eGFP vector thereby linking MICAL-1 to a biotinylation peptide and an eGFP sequence (Lansbergen et al., 2006). The biotinylation peptide can be biotinylated by the biotin ligase BirA (Lansbergen et al., 2006). We generated a full-length MICAL-1 construct (bio-eGFP-MICAL-1) to purify MICAL-1 interacting proteins (Fig. 2A). In addition, to elucidate potential substrates regulated by the MO domain of MICAL-1, we generated a bio-eGFP-N3 construct containing the MO, CH and LIM domains (Fig. 2A). The N3 truncation mutant is considered to be a constitutively active form of MICAL-1 showing hyperactive H_2O_2 production in presence of NADPH and cell contraction when overexpressed in mammalian cells (Schmidt et al., 2008; chapter 3). We confirmed that bio-eGFP-N3 had similar effects on H_2O_2 production and cell contraction (data not shown). To get a comprehensive understanding of MICAL-1 binding proteins, the C-terminal region of MICAL-1 was also subcloned into the pBio-eGFP vector (bio-eGFP-C1) (Fig. 2A). This fragment contains the most C-terminal coiled-coil motifs, facilitating interactions with several identified MICAL-1 interactors such as CasL, vimentin, plexinAs and Rab1 (Suzuki et al., 2002; Schmidt et al., 2008; Weide et al., 2003). Moreover, the C-terminal region engages in intramolecular interactions with a more N-terminal region in MICAL-1 containing the LIM domain. This association results in autoinhibition of MICAL-1 preventing MO activity. Identification of binding proteins for this region may provide insight into the regulatory mechanisms that control the auto-inhibitory state of MICAL-1.

After cotransfection of the bio-eGFP constructs with BirA in HEK293 cells, cell lysates were prepared and incubated with streptavidin-coupled Dynabeads to isolate biotinylated proteins (Fig. 2C, D). To preserve protein-protein interactions within the potential MICAL-1 complex, beads were washed with Tris buffer containing KCl up to 150 mM followed by elution in sample buffer. After separation of the protein complex in a NuPAGE gradient gel, proteins were visualized by Coomassie staining. Bait proteins were visible in addition to differential bands as compared to control (bio-eGFP pull down) (Fig. 2D). Thus, this method clearly led to the isolation of specific proteins in addition to MICAL-1 with a relatively low background.

Lanes in the NuPAGE gel were excised and trypsin-digested. Full-length protein complexes and N3 or C1 complexes were analyzed by different mass spectrometry methods. Consistent with full-length MICAL-1 from L cells (Fig. 1), bio-eGFP-MICAL-1 was also analyzed by MALDI TOF/TOF, whereas the N3 and C1 protein complexes were analyzed by LC MS/MS due to our previous experience with biotin-streptavidin purified protein complexes (Lansbergen et al., 2006). In the following paragraphs, the processing and interpretation of both the anti-FLAG IP and biotin pull down datasets will be presented.

In silico analysis of potential MICAL-1 binding proteins

Potential MICAL-1 binding proteins cluster into functional groups of cytoskeletal regulation and tight junction formation

The first purpose of our screen was to find full-length MICAL-1 binding proteins in L cells. The purified protein complexes from the D1 or C0 cell lines (sample and control) were analyzed using MALDI TOF/TOF mass spectrometry. Common proteins identified in both the sample and control were discarded and only proteins exclusively identified from the D1 cell line were considered. Further, proteins with a total ion score confidence interval % (TIS C.I. %, Table 1, Page 68) of higher than 95% were selected. After omission of keratins, antibodies, ribosomal proteins and chaperons, a list of putative MICAL-1 interactors was obtained (Table 1). Surprisingly, we did not find known MICAL-1 interactors in this list. This can be due to several reasons. First, specific protein-protein interactions can be cell line dependent (L cells were not used in studying of MICAL-1 interacting proteins in previously published reports). Second, our protein purification procedure may be more stringent as compared to previously reported MICAL-1 (co-)IP experiments (Suzuki et al., 2002; Schmidt et al., 2008), possibly excluding weakly interacting proteins.

To survey the functional role(s) of the candidate MICAL-1 interactors, a database-supported functional analysis (DAVID) was performed to cluster proteins by their known functions (http://david.abcc.ncifcrf.gov) (Dennis et al., 2003; Huang et al., 2009). Using DAVID, two clusters were identified, one cluster of proteins involved in the regulation of the cytoskeleton (Fig. 3A) and the other with functions in tight junction formation (Fig. 3B). Interestingly, MICAL proteins have previously been suggested to function in both cellular pathways (Fischer et al., 2005; Hung et al., 2010; Nakatsuji et al., 2008; Suzuki et al., 2002; Terman et al., 2002; Yamamura et al., 2008). To assess the potential relevance of these proteins for MICAL function, we searched literature and briefly describe the current knowledge of these proteins in the following section.

Proteins grouped in the regulation of the actin cytoskeleton are shown in Fig. 3A. Among them, Asef and APC are involved in signaling of the Rac small GTPase, a key regulator of actin dynamics (Kawasaki et al., 2000). mDia and LIMK are both regulators of actin dynamics functioning in different regulating pathways (Takahashi et al., 2003; Wen et al., 2004). Integrin (ITG) and focal adhesion kinase (FAK) promote cell migration by altering actin filaments (Hildebrand et al., 1993; Sieg et al., 2000). Interestingly, ITG and FAK also interact with Cas proteins, which have been identified as MICAL-1-interacting proteins in a previous study (Schlaepfer et al., 1999; Suzuki et al., 2002) (Fig. 4A). In this cluster, we also found myosin. Interaction of myosin and actin is responsible for muscle contraction or nonmuscle cell movements (Adelstein and Eisenberg, 1980).

The proteins that grouped in the tight-junction cluster are shown in Fig. 3B. ZO-1 is a scaffolding protein anchoring membrane proteins to the cytoskeleton and tethering signaling proteins to tight junctions (González-Mariscal et al., 2008). Several of these proteins emerged in our screen such as Par3, myosin, G protein (guanine nucleotide binding protein; Gα) and PP2A protein phosphatase, which positively or negatively regulates tight junction formation (Ebnet et al., 2001; González-Mariscal et al., 2008; Seth et al., 2007; Popoff and Geny, 2009). Although these proteins are scattered on the map, they indicate a potential role(s) of MICAL-1 in tight junctions.

In the pull down of full-length MICAL-1 protein complexes from HEK293 cells using the biotin-streptavidin system, only 7 unique proteins were identified (data not shown). Among these proteins, interesting candidates were desmoplakin and desmocollin, both of which are involved in the formation of desmosomes, the intercellular junctions that tether intermediate filaments to the plasma membrane (Delva et al., 2009).

Potential MICAL-1-N3 binding proteins belong to various functional groups.

Different from the analysis of full-length MICAL-1 protein complexes, LC-MS/MS was performed to identify proteins from bio-eGFP-MICAL-1-N3 protein complexes due to our previous experience with biotin based protein complex purification (Lansbergen et al., 2006). The Mascot score cut-off value for a positive protein hit was set of 60 (Lansbergen et al., 2006). From the sample list, we first omitted proteins

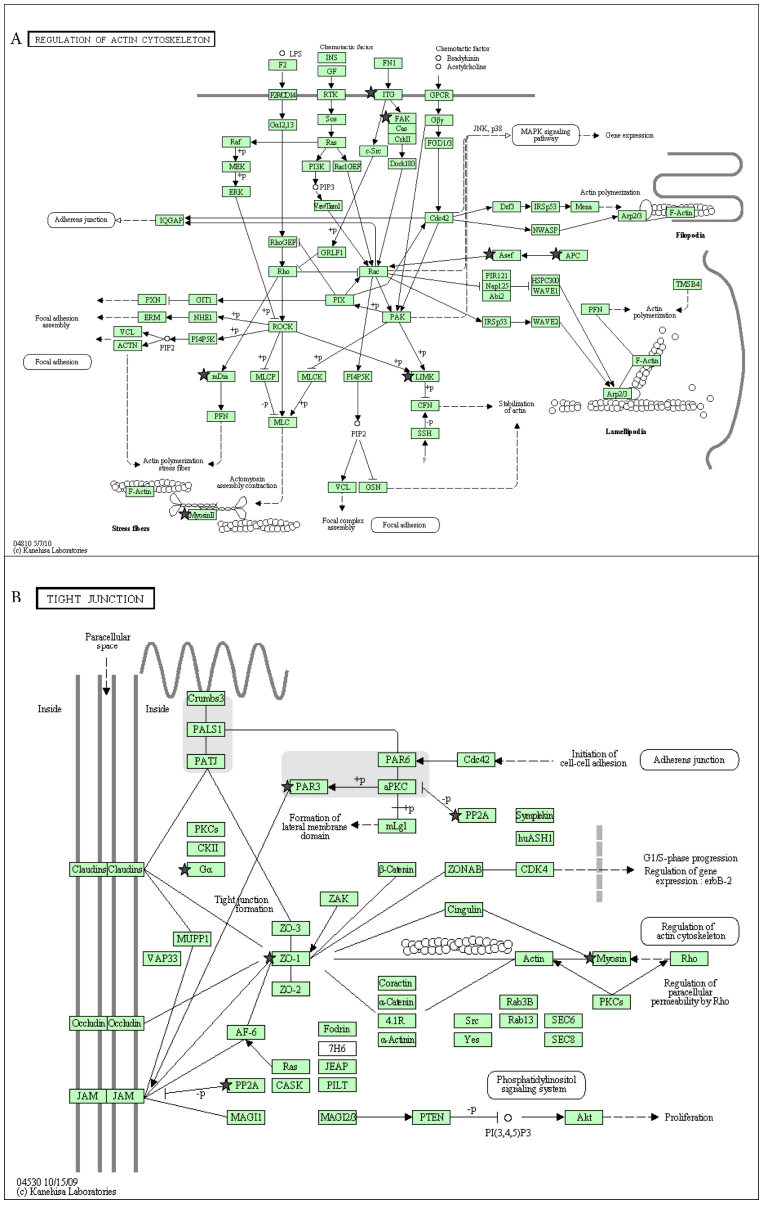

Figure 3. ***In silico*** **analysis of potential MICAL-1 binding proteins identified from full-length MICAL-1 protein complexes**

The DAVID database was used to cluster proteins by their reported functions. Proteins identified in the pull down from D1 cells were found to cluster in two signaling pathways, one in the regulation of the actin cytoskeleton (A) and the other in tight junction formation (B). The stars indicate proteins that were identified in MICAL-1 pull downs.

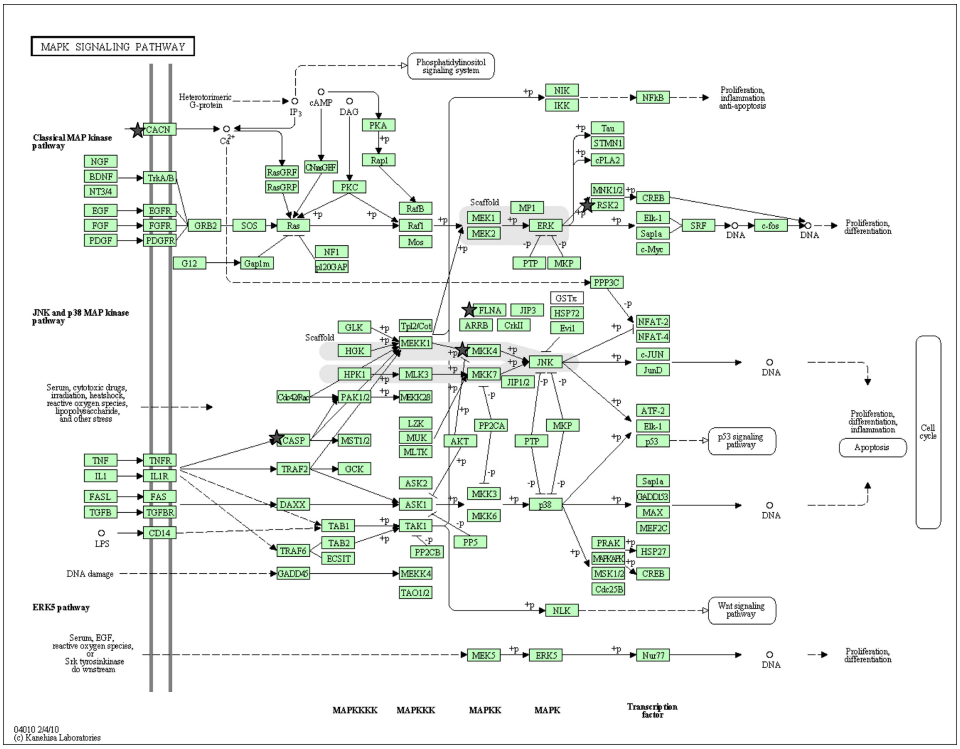

Figure 4. *In silico* analysis of the potential MICAL-1 binding proteins identified from C1 (MICAL-1) protein complexes

The DAVID database was used to cluster proteins by their reported functions. The proteins identified following pull down of the MICAL-1-C1 region from HEK293 cells were found to be enriched in the MAPK signaling pathway. The stars indicate proteins that were isolated in our experiment.

identified both in sample and control purifications, and further excluded keratin, antibodies, ribosomal proteins and chaperons. The identified putative MICAL-1-N3 interacting proteins are listed in Table 2 (Page 72). In this list, vimentin, which has been shown to interact with MICAL-1, was present (Suzuki et al., 2002).

We analyzed the data set by DAVID analysis. Although the proteins did not cluster into functional groups, N3 binding proteins contribute to various biological processes including transcription and translation, biosynthesis, energy transduction, cytoskeleton regulation, membrane organization, protein transport and apoptosis.

Potential MICAL-1-C1 binding proteins are mainly involved in MAPK signaling or apoptosis.

Bio-eGFP-MICAL-1-C1 protein complexes were analyzed as described for MICAL-1-N3 (Table 3, Page 74). Interestingly, several known MICAL-1 interacting proteins were identified. For example, Rab proteins, which function in vesicle trafficking, were found (Table 3). Among them, Rab1a and 1b have been shown to interact with the C-terminal part of MICAL-1 (Weide et al., 2003). Vimentin was also identified in C1

protein complexes (Suzuki et al., 2002). It is interesting to note that vimentin has been identified in both MICAL-1-N3 and C1 pull down experiments (Table 2, 3). N3 and C1 do not contain overlapping sequences, and therefore it is possible that different regions of MICAL-1 mediate the interaction with vimentin.

DAVID analysis of potential MICAL-1-C1 binding proteins revealed two functional groups: MAPK signaling and apoptosis (Fig. 4, Table 3). MAPK signaling pathways are well studied signal transduction cascades targeting transcription and translation. We identified calcium channel (CACN), caspase3 (CASP), filaminA (FLNA), MKK4 and RSK2 proteins, which occupy different positions of the MAPK signaling pathway (Fig. 4).

Several proteins (Dual-specificity tyrosine-(Y)-phosphorylation regulated kinase 2, Alpha1A-voltage-dependent calcium channel, Spatacsin, Caspase 3 and MTCH1 protein) have been shown to have a role in apoptosis (Table 3). However, they could not be grouped into apoptosis signaling pathways. Nevertheless, these proteins indicate that the C-terminal region of MICAL-1 may be involved in apoptosis-related functions.

The protein complex isolation experiments described in this study identified a wide variety of potential new MICAL-1 interactors and implicate MICAL-1 in various known and novel biological processes. To confirm our purification approaches, we selected several candidates based on both their significance (total ion scores/Mascot scores and unique peptide number) and reported functions and performed co-IPs.

Novel MICAL-1 interacting proteins

NDR1 and DOCK7, but not EFHD2, bind to full-length MICAL-1

Among the proteins listed in Table 1, NDR1 and EFHD2 (Swiprosin-1) were considered interesting protein candidates because of their high total ion scores and unique peptide number, and interesting reported functions in relation to the known functions of MICAL-1. EFHD2 (Swiprosin-1) binds F-actin and has been suggested to regulate actin dynamics (Ramesh et al., 2009). NDR1 belongs to the conserved NDR kinase family with functions in cell division, apoptosis and neurite growth (Hergovich et al., 2009; Stork et al., 2004; Vichalkovski et al., 2008). The interaction of these two proteins with MICAL-1 was further examined using biochemical approaches (see below).

We also noted DOCK7 among the list of identified proteins. Nine unique peptides were identified in the pull down from D1 cells, whereas two peptides were found in the control cell line (C0) (data not shown). However, the difference between the total ion scores (D1 238 vs. C0 38) suggested binding to MICAL-1. Interestingly, knock down of DOCK7 prevents axon formation, whereas overexpression induces multiple axons (Watabe-Uchida et al., 2006). Since DOCK7 might collaborate with MICALs in axon regulation, the interaction of DOCK7 and MICAL-1 was also evaluated (see below).

As shown in Fig. 5A, myc-MICAL-1 was co-expressed with FLAG-tagged EFHD2 or FLAG-tagged NDR1 in HEK293 cells. FLAG-CasL was used as a positive control (Suzuki et al., 2002). Co-IPs confirmed the interaction of MICAL-1 with CasL and NDR1 (Fig. 5A). However, EFHD2 failed to interact with MICAL-1 following overexpression of both proteins (Fig. 5A).

A biotin pull down assay was applied to study the interaction of MICAL-1 and DOCK7. Here NDR1 was used as a positive control. Bio-eGFP-MICAL-1 or control bio-eGFP vector (both with BirA enzyme) were co-transfected with FLAG-tagged DOCK7 or NDR1. Following pull down with streptavidin Dynabeads, the protein complexes were analyzed with anti-FLAG antibody. Both DOCK7 and NDR1 were detected following bio-eGFP-MICAL-1 pull down, confirming the interaction between DOCK7 and MICAL-1 (Fig. 5B).

Staufen interacts with MICAL-1 via its N-terminal domain

Staufen was selected from the bio-eGFP-MICAL-N3 pull down because of its high Mascot scores and interesting functions. Staufen binds double-stranded RNA (regardless of the sequence) and tubulin, and may

play a role in the specific positioning of mRNAs by cross-linking cytoskeletal and RNA components (Wickham et al., 1999). Considering the reported role of MICALs in cytoskeletal regulation, we examined the interaction of staufen with different MICAL-1 truncation mutants.

HEK293 cells were transfected with bio-eGFP-MICAL-1 full-length, N3 and C1 constructs or bio-eGFP vector together with BirA. After pull down, endogenous staufen from HEK293 cells was detected using specific antibodies (Todd et al., 2010). As shown in Fig. 5C, staufen co-IPed with N3 and full-length MICAL-1, indicating that the N-terminal three domains of MICAL-1 mediate the interaction with staufen.

Discussion

Using different protein complex purification approaches and mass spectrometry we were able to identify a large number of novel, putative MICAL-1 interacting proteins. Pathway analyses of these newly identified MICAL-1 interactors indicated enrichment in pathways controlling the cytoskeleton, tight junction formation and MAPK signaling. In addition, the interaction of NDR1, DOCK7 and staufen with MICAL-1, all identified by mass spectrometry, was confirmed by co-IP, expanding our current knowledge of MICAL-binding proteins (Table 4, Page 79). These results implicate MICAL-1 in several known and new biological pathways and will help to direct future studies on the function and mechanism-of-action of MICAL proteins.

Isolation and characterization of MICAL-1 protein complexes

In this study, different purification methods were used to isolate MICAL-1-containing protein complexes: anti-FLAG IP, TAP (combination of anti-FLAG and anti-HA IP), and biotin-streptavidin-based pull down. Our results indicate that each of these methods has advantages and disadvantages. For example, the purity of protein complexes obtained using these methods varied significantly. TAP yielded protein complexes without a lot of background proteins due to the two-step IP procedures with different antibodies and bead systems. One-step purifications such as anti-FLAG IP and biotin pull down were less efficient in eliminating background proteins. However, in comparison to anti-FLAG IP, biotin-streptavidin pull down yielded protein complexes with fewer contaminants. When considering protein yield, one step purifications led to the isolation of much more bait protein as compared to TAP. To obtain equal amount of protein complexes for mass spectrometry analysis, TAP requires a large quantity of input proteins as compared to one-step purifications, especially when the bait protein is expressed at low levels. Since we used adherent cells in our studies (HEK293 and L cells), we were unable to obtain enough cell material to successfully apply the TAP procedure. Non-adherent cells grown in a bioreactor format may be more suitable for using TAP. TAP purification is also more labor intensive because of the two subsequent purifications with different pull down systems. After having tested different purification methods, we favor the biotin-streptavidin system because it is simple, leads to large yields of bait protein and allows stringent washing conditions. Intriguingly, the purification of full-length MICAL-1 from HEK293 or L cells resulted in the isolation of different putative interactors. In addition, purification from L cells resulted in the identification of significantly more potential binding partners. These differences may be explained as follows. First, HEK 293 cells are human embryonic kidney cells, while L cells are mouse fibroblasts and it is possible that MICAL-1 functions in different tissues through the association with different binding partners. Second, the expression levels of exogenous MICAL-1 were very different in the two cell lines. HEK293 cells transiently over-expressed high levels of MICAL-1 protein, while the D1 cell line is a stable cell line with near endogenous MICAL-1 expression. Third, the purification procedure used for HEK293 or L cells was different which may for example influence the ability to co-purify interactors. However, despite these differences, identification of MICAL-1 binding proteins from both HEK293 and L cells provided insights into the roles of MICAL proteins. Proteins with functions in two related processes cytoskeletal regulation and tight junction formation were clearly enriched. These findings both support and extend previous studies implicating MICAL-1 in the regulation of cytoskeletal dynamics (Terman et al., 2002; Schmidt et al., 2008;

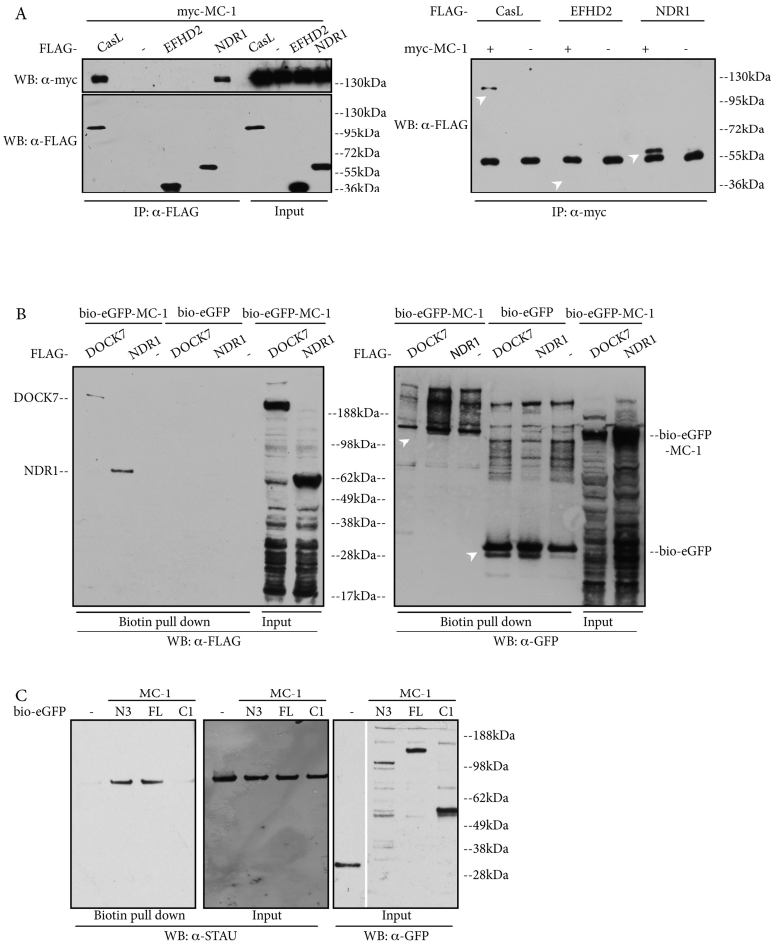

Figure 5. NDR1, DOCK7 and staufen bind MICAL-1

(A) Protein candidates identified in MICAL-1 pull down experiments were evaluated by co-IP. FLAG-tagged CasL, EFHD2 or NDR1 were co-expressed with myc-MICAL-1 in HEK293 cells. Following IP with anti-FLAG antibody of CasL and NDR1 expressing cell lysates, myc-MICAL-1 could be detected. Reciprocally, following IP with anti-myc antibody, CasL and NDR1 were found, indicating that CasL and NDR1 interact with MICAL-1. EFHD2, EF hand domain containing 2; NDR1, Nuclear Dbf-2-related (NDR) kinase 1.

(B) FLAG-tagged DOCK7 and NDR1 were co-expressed with bio-eGFP-MICAL-1 or bio-eGFP vector in the presence of the biotin ligase, BirA, in HEK293 cells. Biotinylated proteins were pulled down using streptavidin beads. Western blotting with anti-FLAG antibody detected both DOCK7 and NDR1 following bio-eGFP-MICAL-1 pull down. Anti-GFP staining shows purified bio-eGFP-MICAL-1 and bio-eGFP proteins (white arrow heads). DOCK7, Dedicator of cytokinesis 7.

(C) After pull down of the indicated biotinylated proteins, protein complexes were analyzed by western blotting with the indicated antibodies. Staufen binds MICAL-1 FL and N3 but not C1. α-STAU, anti-staufen antibody.

Hung et al., 2010).

In addition to full-length protein, the binding partners of two MICAL-1 truncation mutants were studied. The N3 truncation mutant represents a constitutively active form of MICAL-1. Following removal of the C-terminal region, the MO domain becomes hyperactive and mediates the production of hydrogen peroxide (H_2O_2) in presence of NADPH (Schmidt et al., 2008; chapter 3). In other monooxygenases, this reaction is thought to only occur in the absence of a substrate for the MO domain. Analysis of the tertiary structure of MICAL-1 indicates that large molecules such as proteins may serve as substrates for the MICAL-1 MO domain (Nadella et al., 2005; Siebold et al., 2005). Thus far, actin filaments and CRMPs have been suggested as substrates (Terman et al., 2002; Schmidt et al., 2008; Hung et al., 2010). However, it remains unknown if or how these proteins are modified by the MICAL MO domain. By searching for proteins that bind the N3 mutant we were aiming at the identification of MICAL-1 substrates. Interestingly, putative N3 interacting proteins with roles in various biological processes including energy transduction, biosynthesis and cytoskeleton regulation were identified (Table 2). It is tempting to speculate that some of these proteins may be substrates for MICAL-1 and that by binding these proteins, the MICAL-1 MO domain contributes to the regulation of for example energy metabolism or cytoskeletal regulation. Further studies are required to confirm the identified interactions and to examine whether they represent substrates for the MICAL-1 MO domain.

The C-terminal region of MICAL-1 was also used as bait because of the protein binding abilities of the coiled-coil motifs and proline-rich stretch within this region and because of its regulatory effect on MICAL-1 enzyme activity (Schmidt et al., 2008; Suzuki et al., 2002; Weide et al., 2003). Most of the currently identified MICAL-1 interactors, such as CasL, vimentin, plexinA1 and Rab1 bind this region (Schmidt et al., 2008; Suzuki et al., 2002; Weide et al., 2003). Binding of proteins to the C-terminal region may induce conformational changes that release the autoinhibited state of the MICAL-1 protein thereby allowing it to regulate downstream signaling pathways (Schmidt et al., 2008). Thus, identification of proteins that bind to the C-terminal region of MICAL-1 may help us to understand how MICAL-1 MO activity is regulated. Several known interactors such as vimentin and Rab proteins were identified in the pull down of MICAL-1 C1 (Table 3). Potential novel interactors can be clustered into MAPK signaling and apoptosis related protein groups (Fig.4; Table 3). It is interesting to find MICAL in the MAPK signaling pathway, since MICAL-1 has been shown to be a phosphoprotein (see chapter 3 and 5). MICAL-1 may be phosphorylated or regulated by kinases in MAPK singling pathway. It is also possible that MICAL-1 regulates these proteins via the redox potential of the MO domain. In addition, as a suggested scaffold protein (Terman et al., 2002), MICAL-1 may serve as docking site for signaling proteins. Identification of apoptosis related proteins supports our observation that MICAL-1 has a function during apoptosis. MICAL-1 can inhibit apoptosis stimulated by etoposide or TNF (Tumor Necrosis Factor), and the binding capacity of the C-terminal region is most likely to be the key regulatory mechanism during these processes (chapter 5). Further analysis of these binding proteins is necessary to elucidate their functional relevance to MICAL-1 regulation and function.

Surprisingly, almost no overlap was found between the binding proteins of MICAL-1 full-length and N3 or C1. This may due to several reasons. First, the identification of full-length MICAL-1 was performed in L cells, a mouse fibroblast cell line, while the N3 and C1 binding proteins were identified from HEK293 cells, a cell line originating from the human kidney. Second, removal of specific regions from the MICAL-1 protein (such as in the N3 or C1 truncation mutants) may induce conformational changes which favor an interaction with specific proteins. On the other hand five proteins were identified that bound both the N3 and C1 fragments, although these fragments do not share any overlapping sequences (vimentin, MLLT6 protein, dual-specificity tyrosine-(Y)-phosphorylation regulated kinase 2, nebulin, and trinucleotide repeat containing 6A) (Table 2 and 3). It is possible that these proteins simultaneously bind different regions of the MICAL-1 protein.

NDR1, DOCK7 and staufen are novel MICAL-1 interactors

In this report, several of the protein candidates were tested using co-IP to confirm their interaction with MICAL-1 (NDR1, DOCK7, staufen). NDR1 is a highly conserved serine threonine kinase with reported functions in cell division, apoptosis and neurite growth (Hergovich et al., 2009; Vichalkovski et al., 2008; Stork et al., 2004). In our follow-up study described in chapter 5, NDR1 kinase activity was found to be inhibited by MICAL-1 during apoptosis. DOCK7 plays important roles in axon formation. Considering the role of MICAL-1 in axon guidance, the interaction of DOCK7 and MICAL-1 supports the idea that these two proteins collaborate in axon outgrowth and guidance. Staufen can bind both double-strand RNA and tubulin and contributes to the specific positioning of mRNAs in the cell (Wichham et al., 1999). Interestingly, MICAL-1 has been shown to bind microtubles (Fischer et al., 2005) and it is therefore possible that MICAL-1 and staufen cooperate in the localization of mRNAs. A possible collaboration of these three proteins may be deduced that DOCK7 promotes axon outgrowth, while MICAL-1, besides regulation of cytoskeletal dynamics, localizes mRNAs into growth cone on the tip of axon in collaboration with staufen. mRNA transport to growth cone is important for the local translation of proteins, which is required for axon growth and guidance (Lin and Holt, 2008).

Taken together, by using different protein complex purification methods followed by mass spectrometry this study has led to the identification of a myriad of novel, putative interactors of MICAL-1, and potentially of other MICALs as well. Although most of these interactors await further analysis, to for example confirm their interaction with MICAL-1 in relevant cells or tissues, the identification of NDR1, DOCK7 and staufen as MICAL-1 interactors expands the list of known MICAL-interacting proteins (Table 4). The results of this study provide new directions for further research on the role, regulation and mechanism-of-action of MICAL proteins in different biological pathways and in pathological conditions such as cancer or brain injury (Pasterkamp et al., 2006; Ashida et al., 2006).

Tables

Table 1. Unique proteins identified in pull downs from the MICAL-1-FLAG-HA stable L cell line (D1)

Protein Name	Uniprot Entry Name	Unique peptide number	Total ion score	TIS C.I.%	Mw	Biology process
MICAL-1*	MICA1	124	2400.9	100.0	117875	cytoskeleton organization; oxidation-reduction process; signal transduction
Septin-9	SEPT9	12	553.5	100.0	65534	Cell cycle; cell division
Serine/threonine-protein kinase 38 (NDR1 protein kinase)	STK38	8	345.9	100.0	54139	Intracellular protein kinase cascade negative regulation of MAP kinase activity; protein phosphorylation
Protein disulfide-isomerase A4	PDIA4	7	343.8	100.0	71929	Cell redox homeostasis
Filamin-B (FLN-B)	FLNB	8	317.8	100.0	277579	Skeletal muscle tissue development
ATP synthase subunit alpha	ATPA	6	239.7	100.0	59716	ATP synthesis; hydrogen ion transport; ion transport; transport
Dolichyl-diphosphooligosaccharide--protein glycosyltransferase 67 kDa subunit	RIB1	5	238.1	100.0	68486	Cleavage of RNA
Fascin	FSCN1	4	159.1	100.0	54371	Actin filament bundle assembly; cell migration
Cation-independent mannose-6-phosphate receptor	MPRI	5	154.3	100.0	273639	Transport
Neutral alpha-glucosidase AB	GANAB	4	140.5	100.0	106844	N-glycan processing
NADPH--cytochrome P450 reductase	NCPR	4	125.2	100.0	76995	Oxidation-reduction process
EF-hand domain-containing protein 2 (Swiprosin-1)	EFHD2	3	114.0	100.0	26775	Involved in spontaneous apoptosis
Annexin A5 (Annexin V)	ANXA5	2	107.9	100.0	35730	Blood coagulation
RING finger protein C13orf7 homolog	CM007	2	95.1	100.0	79908	Protein binding; zinc ion binding

Protein Name	Uniprot Entry Name	Unique peptide number	Total ion score	TIS C.I.%	Mw	Biology process
LIM domain and actin-binding protein 1	LIMA1	2	94.9	100.0	84038	Actin filament bundle assembly; negative regulation of actin filament depolymerization; ruffle organization
Spectrin alpha chain	SPTA2	2	94.6	100.0	284422	Actin filament capping
Alpha-internexin	AINX	1	89.0	100.0	55708	Differentiation; neurogenesis
Glucosidase 2 subunit beta	GLU2B	2	81.5	100.0	58756	N-glycan processing
Lamin-A/C	LMNA	3	78.1	100.0	74193	Nuclear envelope organization; positive regulation of cell aging; sterol regulatory element binding protein import into nucleus; ventricular cardiac muscle cell development
Myosin-Va	MYO5A	2	66.5	100.0	215459	Locomotion involved in locomotory behavior
Translocon-associated protein subunit alpha	SSRA	1	64.9	100.0	32045	Retention of ER resident proteins
Lysosome-associated membrane glycoprotein 2	LAMP2	1	64.5	100.0	45618	Implicated in tumor cell metastasis
Kinesin family member 21B	KI21B	3	62.1	100.0	186048	Microtubule-based movement
Integrin beta-2	ITB2	1	62.1	100.0	84970	Cell adhesion
Serotransferrin	TRFE	2	59.3	100.0	76674	Ion transport; iron transport; transport
Major facilitator superfamily domain-containing protein 1	MFSD1	2	59.1	100.0	51362	Transport
Serine-protein kinase ATM	ATM	1	57.4	100.0	349264	Cell cycle; DNA damage; DNA repair
26S proteasome non-ATPase regulatory subunit 1	PSMD1	1	55.4	100.0	105663	Regulation of protein catabolic process
Polypeptide N-acetylgalactosaminyltransferase 2	GALT2	1	52.0	100.0	64473	Catalyzes the initial reaction in O-linked oligosaccharide biosynthesis
Telomerase protein component 1	TEP1	1	51.9	100.0	291275	Component of the telomerase ribonucleoprotein complex
Dystrophin	DMD	2	50.5	100.0	425552	Muscle cell homeostasis; neurotransmitter receptor metabolic process; olfactory nerve structural organization; regulation of transcription
Plastin-3 (T-plastin)	PLST	1	47.5	100.0	70322	Actin binding and bundling
N-acetylglucosamine-6-sulfatase	GNS	2	46.9	99.9	61136	Hydrolysis of the 6-sulfate groups of the N-acetyl-D-glucosamine 6-sulfate units of heparan sulfate and keratan sulfate.
Breast cancer type 2 susceptibility protein homolog	BRCA2	2	46.6	99.9	370432	Cell cycle; DNA damage; DNA recombination; DNA repair
Macrophage mannose receptor 2	MRC2	1	45.3	99.9	166988	Endocytosis
Toll-interacting protein	TOLIP	1	45.3	99.9	30325	Immunity; inflammatory response; innate immunity
Focal adhesion kinase 1	FAK1	3	45.3	99.9	123432	Actin regulation; cell motility, proliferation and apoptosis
Myosin-14	MYH14	2	44.6	99.9	228446	Actin regulation; actin binding
SLIT-ROBO Rho GTPase-activating protein 3	SRGP2	1	44.2	99.9	124341	GTPase-activating protein
Dipeptidase 3	DPEP3	1	43.5	99.9	54213	Meiosis
Hydroxyacyl-coenzyme A dehydrogenase, mitochondrial	HCDH	1	42.7	99.9	34442	Fatty acid metabolism; lipid metabolism
Uncharacterized protein C14orf44 homolog	CN044	7	42.3	99.9	66927	
Hypoxia-inducible factor 1 alpha	HIF1A	2	42.3	99.8	93457	Transcription; transcription regulation
Ankyrin repeat domain-containing protein 26	ANR26	1	41.5	99.8	180535	Negative regulation of multicellular organism growth; negative regulation of organ growth; regulation of fatty acid metabolic process; regulation of feeding behavior

Protein Name	Uniprot Entry Name	Unique peptide number	Total ion score	TIS C.I.%	Mw	Biology process
Succinate dehydrogenase [ubiquinone] flavoprotein subunit	DHSA	1	41.2	99.8	72539	Electron transport; transport; tricarboxylic acid cycle
Zinc finger protein HRX	HRX	2	40.9	99.8	429382	Transcription; transcription regulation
Calmodulin-regulated spectrin-associated protein 3	CAMP3	1	40.8	99.8	135091	Epithelial cell-cell adhesion; microtubule anchoring; regulation of microtubule cytoskeleton organization; zonula adherens maintenance
Rho-related BTB domain-containing protein 2	RHBT2	1	40.5	99.8	82609	
Lysyl-tRNA synthetase	SYK	1	40.4	99.8	67796	Protein biosynthesis
ATP-dependent Clp protease ATP-binding subunit ClpX-like	CLPX	1	40.4	99.8	69271	Protein folding
Elongation factor 1-alpha 1	EF1A1	2	40.4	99.8	50082	Protein biosynthesis
Heterogeneous nuclear ribonucleoprotein A/B	ROAA	1	39.8	99.7	30812	Transcription; transcription regulation
Myosin-9	MYH9	2	39.8	99.7	226217	Cell shape
Calcium-binding mitochondrial carrier protein Aralar2	CMC2	1	39.6	99.7	74420	Transport
ERO1-like protein alpha	ERO1A	1	39.5	99.7	54004	Electron transport; transport
Reticulocalbin-1	RCN1	1	39.0	99.7	38090	May regulate calcium-dependent activities in the endoplasmic reticulum lumen or post-ER compartment.
Heterogeneous nuclear ribonucleoproteins A2/B1	ROA2	1	39.0	99.7	37380	mRNA processing; mRNA splicing
Ran-binding protein 3	RANB3	1	38.9	99.7	52541	Protein transport; transport
Mucosa-associated lymphoid tissue lymphoma translocation protein 1 homolog	MALT1	2	38.6	99.6	93156	Ubl conjugation pathway
Probable ATP-dependent RNA helicase DDX17	DDX17	1	38.6	99.6	72354	RNA-dependent ATPase activity
Guanylate cyclase soluble subunit beta-1	GCYB1	1	38.5	99.6	70553	cGMP biosynthesis
WAS/WASL interacting protein family member 2	WIPF2	2	38.0	99.6	46269	Cytoplasm; cytoskeleton
Protein PTHB1	PTHB1	2	37.8	99.6	98995	Fat cell differentiation
Reticulocalbin-3 precursor	RCN3	1	37.4	99.5	37978	Calcium ion binding
T-complex protein 1 subunit epsilon	TCPE	3	37.1	99.5	59586	Protein folding
Protein COQ10 B	CQ10B	2	36.8	99.5	27251	Required for the function of coenzyme Q in the respiratory chain
Phosphoinositide 3-kinase regulatory subunit 6	PI3R6	3	36.7	99.4	84610	Regulatory subunit of the PI3K gamma complex
Ubiquitin carboxyl-terminal hydrolase 47	UBP47	1	36.5	99.4	157356	Ubl conjugation pathway
Vacuolar ATP synthase subunit C	VATC	2	36.4	99.4	43833	Hydrogen ion transport; ion transport; transport
Protein FAM5C	FAM5C	2	36.1	99.4	88426	
Catenin delta	CTND2	2	35.7	99.3	134916	Cell adhesion; transcription; transcription regulation
Dual specificity mitogen-activated protein kinase kinase 7	MP2K7	1	35.7	99.3	59274	Protein phosphorylation; stress-activated MAPK cascade
Putative GTP-binding protein Parf	PARF	1	35.3	99.2	79782	Small GTPase mediated signal transduction
Cytospin-A	CYTSA	2	35.1	99.2	124412	Cell cycle; cell division
Microtubule-actin cross-linking factor 1	MACF1	1	34.9	99.2	607600	Wnt receptor signaling pathway; cell cycle arrest
Axin-1	AXN1	2	34.9	99.2	96254	Apoptosis; Wnt signaling pathway

Protein Name	Uniprot Entry Name	Unique peptide number	Total ion score	TIS C.I.%	Mw	Biology process
Pleckstrin homology-like domain family B member 1	PHLB1	3	34.8	99.2	149978	
Leucine-rich repeat-containing protein 40	LRC40	1	34.8	99.2	68033	
Abnormal spindle-like microcephaly-associated protein homolog	ASPM	1	34.8	99.2	363891	Cell cycle; cell division; mitosis
Alpha-2-macroglobulin receptor-associated protein precursor	AMRP	1	34.3	99.1	42189	Interacts with LRP1/alpha-2-macroglobulin receptor and glycoprotein 330
P2X purinoceptor 3	P2RX3	4	33.9	99.0	44408	Ion transport; transport
PAR-3	PARD3	2	33.8	98.9	148969	Cell cycle; cell division
G2/mitotic-specific cyclin-B3	CCNB3	1	33.6	98.9	158870	Cell cycle; cell division; meiosis
StAR-related lipid transfer protein 5	STAR5	1	33.1	98.7	23907	Lipid transport; transport
Periplakin	PEPL	2	33.0	98.7	203880	Keratinization
E3 ubiquitin-protein ligase UHRF1	UHRF1	2	32.9	98.7	88248	Cell cycle; DNA damage; DNA repair; transcription; transcription regulation; Ubl conjugation pathway
Chondroitin sulfate synthase 1	CHSS1	1	32.7	98.6	91325	Has both beta-1,3-glucuronic acid and beta-1,4-N-acetylgalactosamine transferase activity
Bifunctional methylenetetrahydrofolate dehydrogenase/cyclohydrolase	MTDC	1	32.5	98.6	37839	One-carbon metabolism
Probable ATP-dependent RNA helicase DDX10	DDX10	2	32.1	98.4	100676	Putative ATP-dependent RNA helicase
PP2A-beta	PP2AB	2	31.9	98.3	35552	Negative regulation of apoptosis; proteasomal ubiquitin-dependent protein catabolic process; regulation of gene expression; response to antibiotic; response to hydrogen peroxide
tRNA (cytosine-5-)-methyltransferase	TRDMT	1	31.8	98.3	46764	tRNA processing
Guanine nucleotide-binding protein G(k) subunit alpha (G(i) alpha-3)	GNAI3	1	31.7	98.3	40512	G-protein coupled receptor protein signaling pathway
Syntaxin-7	STX7	1	31.6	98.2	29802	Intracellular protein transport
Rho guanine nucleotide exchange factor 4 (Asef)	ARHG4	1	31.6	98.2	56644	Regulation of Rho protein signal transduction
Leucine-rich repeat and calponin homology domain-containing protein 4	LRCH4	1	31.6	98.2	73118	
Centrosomal protein Cep290	CE290	2	31.4	98.1	288899	Cell division and chromosome partitioning
Mitogen-activated protein kinase 15	MK15	1	31.1	98.0	60641	Protein autophosphorylation
Neurocan core protein	CSPG3	1	30.5	97.7	137114	Cell adhesion
Relaxin receptor 2	RXFP2	2	30.2	97.6	82890	Activation of adenylate cyclase activity by G-protein signaling pathway
Tight junction protein ZO-1	ZO1	1	30	97.2	194711	Blastocyst formation
Ran-binding protein 8	IPO8	1	29.6	97.2	116975	Protein transport; transport
Nogo-B receptor	NGBR	1	29.5	97.2	33464	Angiogenesis; differentiation
Sacsin	SACS	2	29.3	97.0	520353	May be involved in the processing of other ataxia-linked proteins
Usherin	USH2A	1	29.3	97.0	569352	Hearing; sensory transduction; vision
Transcription initiation factor IIE subunit beta	T2EB	1	29.2	96.9	33026	Transcription; transcription regulation
LIM domain kinase 1	LIMK1	1	29.1	96.8	72746	Positive regulation of axon extension; protein phosphorylation

Protein Name	Uniprot Entry Name	Unique peptide number	Total ion score	TIS C.I.%	Mw	Biology process
Structural maintenance of chromosomes protein 6	SMC6	1	29.0	96.8	127118	DNA damage; DNA recombination DNA repair
ADP/ATP translocase 2	ADT2	1	28.9	96.7	32910	Chromosome partition; transport
Protein SERAC1	SRAC1	2	28.7	96.5	73940	Extracellular matrix organization
Scavenger receptor class B member 1	SCRB1	1	28.2	96.1	56717	Blood vessel endothelial cell migration; cell adhesion; cholesterol catabolic process
Syntaxin-binding protein 3	STXB3	1	27.6	95.5	67899	Protein transport; transport
Rho GTPase-activating protein 18	RHG18	4	27.6	95.5	74884	Signal transduction
Vacuolar ATP synthase subunit B	VATB2	1	27.3	95.2	56515	Hydrogen ion transport; ion transport; transport

* MICAL-1 is the bait protein. Mw, molecular weight. TIS C.I.%, Total Ion Score Confidence Interval.

Table 2. Unique proteins identified in the bio-eGFP-MICAL-1-N3 pull down experiment

Protein Name	Uniprot Entry Name	Unique peptide number	Cover %	Mascot score	Mw	Biological process
MICAL1*	MICA1	45	50.5	3883	117875	cytoskeleton organization; oxidation-reduction process; signal transduction
Acetyl-CoA carboxylase 2	ACACB	25	14	1506	276541	Fatty acid biosynthesis; lipid synthesis
Vimentin	VIME	18	47	1160	53653	Intermediate filament
Treacher Collins syndrome	TCOF	15	15.6	1106	152106	Transport
Branched chain acyltransferase	ODB2	13	33.8	799	53487	Branched chain family amino acid catabolic process; fatty-acyl-CoA biosynthetic process
E1B-55kDa-associated protein	HNRL1	11	17.5	746	95739	Transcription regulation
Programmed cell death 8	AIFM1	9	20.1	639	66901	Apoptosis
Nucleolin	NUCL	9	14.1	614	76614	Cytoplasm; nucleus
Propionyl Coenzyme A carboxylase, beta polypeptide variant	PCCB	10	26.4	542	58216	Fatty acid beta-oxidation
CSDA protein	DBPA	5	21	405	40090	Transcription; transcription regulation
Tubulin, beta polypeptide	TBB5	5	16.7	400	49671	G2/M transition of mitotic cell cycle; microtubule-based movement; natural killer cell mediated cytotoxicity; protein polymerization
ADP/ATP translocase 3	ADT3	5	18.1	372	32866	Apoptosis; host-virus interaction; transport
Autoantigen La	LA	6	23.3	368	46837	Histone mRNA metabolic process; tRNA modification
CLLL7 protein	RCBT1	5	13.6	334	58252	Cell cycle; transcription; transcription regulation
Cytoskeleton-associated protein 4	CKAP4	7	15.9	334	66022	
Staufen protein	STAU1	5	14.3	334	63182	Specific positioning of mRNAs
Nucleophosmin	NPM	4	16.4	310	32575	Host-virus interaction
Alpha 1 actin	ACTS	6	21.9	286	42051	Muscle filament sliding skeletal muscle fiber development
Translation elongation factor 1 alpha 1-like 14	EF1A1	5	19.3	276	50141	Protein biosynthesis
Collagen binding protein 2	SERPH	3	12.4	210	46441	Stress response
IGF-II mRNA-binding protein 2	IF2B2	3	9.4	204	66121	Translation regulation
Lactate dehydrogenase B	LDHB	3	11.7	197	36638	Glycolysis

Protein Name	Uniprot Entry Name	Unique peptide number	Cover %	Mascot score	Mw	Biological process
Insulin receptor substrate 4	IRS4	5	6.3	194	133768	SH3/SH2 adaptor activity
HBxAg transactivated protein 2	BA2L2	4	2.2	156	317008	Protein C-terminus binding
Creatine kinase	KCRB	2	9.7	149	42644	Creatine metabolic process
Interleukin enhancer binding factor 2	ILF2	3	10.3	143	43062	Transcription; transcription regulation
WD repeats and SOF1 domain containing	DCA13	4	9.5	141	51402	Ribosome biogenesis; Ubl conjugation pathway; rRNA processing
Filamin A	FLNA	3	1.8	140	280739	Actin crosslink formation; actin cytoskeleton; reorganization
Transformation up-regulated nuclear protein	HNRPK	2	7.8	140	50976	Host-virus interaction; mRNA processing; mRNA splicing
Cell division protein kinase 1	CDK1	3	12.8	118	34081	Cell cycle; cell division; mitosis
NY-REN-2 antigen	YTHD2	2	4	113	62334	Humoral immune response
U4/U6 snRNP 60 kDa protein	PRP4	2	5	106	58449	mRNA processing; mRNA splicing
PDZ domain-containing 2	PDZD2	6	4.7	102	301641	Cell adhesion
DDX6 protein	DDX6	1	12.8	101	54417	Exonucleolytic nuclear-transcribed mRNA catabolic process involved in deadenylation-dependent decay
Kinesin family member 1B	KIF1B	5	4.5	97	204476	Apoptosis
ATP-binding cassette, sub-family F, member 1	ABCF1	1	1.9	96	95926	Inflammatory response
Regulating synaptic membrane exocytosis 1	RIMS1	5	4.7	94	189073	Exocytosis; neurotransmitter transport; sensory transduction; transport; vision
Dual-specificity tyrosine-(Y)-phosphorylation regulated kinase 2	DYRK2	3	8.1	92	66652	Apoptosis
PSD-95/SAP90-associated protein-2	DLGP2	5	7.2	92	117620	Cell junction; cell membrane; postsynaptic cell membrane; synapse
Cofilin 1	COF1	1	8.4	89	18502	Rho protein signal transduction; anti-apoptosis; axon guidance
Mitochondrial malate dehydrogenase	MDHM	2	10.7	89	35503	Tricarboxylic acid cycle
MLLT6 protein	AF17	3	10.5	87	112076	Regulation of transcription, DNA-dependent
Stress-induced-phosphoprotein 1 (Hsp70/Hsp90-organizing protein)	STIP1	2	4.6	85	62639	Axon guidance; response to stress
Solute carrier family 25 member 3	MPCP	2	6.1	84	40095	Symport; transport
Fragile X mental retardation-related protein 1	FXR1	1	2.4	83	69721	Differentiation; myogenesis
Phosphoglucomutase 2	PGM2	3	5.9	79	68283	Carbohydrate metabolism; glucose metabolism
ATPase family, AAA domain containing 5	ATAD5	4	3.4	77	207570	DNA damage
Nebulin	NEBU	6	1.3	77	772927	Cytoplasm; cytoskeleton
Centrosomal protein 170kDa	CE170	4	3.6	76	175293	Microtubule organization
Nucleostemin	GNL3	2	6.7	76	61993	Regulation of cell proliferation
Tau-tubulin kinase	TTBK2	2	1.6	75	137412	Cell death; protein phosphorylation
Methionyl-tRNA synthetase	SYMC	1	1.1	72	101116	Protein biosynthesis
Exosome component 10	EXOSX	1	1.9	69	100831	Nonsense-mediated mRNA decay; rRNA processing
Piwi-like 3	PIWL3	3	4	69	101089	Differentiation; meiosis; RNA-mediated gene silencing; spermatogenesis; translation regulation
Calcium-dependent activator protein for secretion 1	CAPS1	2	4	68	152786	Exocytosis; protein transport; transport

Protein Name	Uniprot Entry Name	Unique peptide number	Cover %	Mascot score	Mw	Biological process
Pleckstrin homology domain containing, family A member 5	PKHA5	3	7.2	68	127464	Phosphatidylinositol binding
Slit and trk like 3 protein	SLIK3	2	3.3	68	108934	Suppresses neurite outgrowth
80K-L protein	MARCS	1	5.7	67	31555	Energy reserve metabolic process
ATPase, Class I, type 8B, member 2	AT8B2	3	4	67	137440	ATP biosynthetic process
Disabled homolog 2-interacting protein	DAB2P	3	4.4	67	131625	Activation of JUN kinase activity
6-phosphofructo-2-kinase	F262	2	6.7	65	58477	Fructose 2,6-bisphosphate metabolic process
ALL1 fused gene from 5q31	AFF4	3	4.9	65	127459	Transcription; transcription regulation
FASTKD1 protein	FAKD1	2	3.4	65	97411	Apoptosis; cellular respiration
Growth factor receptor-bound protein 7	GRB7	2	6.8	65	59681	Blood coagulation; epidermal growth factor receptor; signaling pathway; leukocyte migration
KIAA0317	K0317	2	3.4	65	94223	Ubl conjugation pathway
KIAA0589	PI51C	2	5.2	65	73260	Axon guidance
Trinucleotide repeat containing 6A	TNR6A	2	3.3	65	210297	RNA-mediated gene silencing; translation regulation
MAPRE1 protein	MARE1	1	10.4	65	29999	Cell cycle; cell division; mitosis
Centrosomal protein of 290 kDa	CE290	4	2.4	64	290386	Cilium biogenesis/degradation; protein transport; transport
Splicing coactivator subunit SRm300	SRRM2	3	1.7	64	299615	mRNA processing; mRNA splicing
T-cell lymphoma invasion and metastasis 1	TIAM1	3	3.7	62	177508	Apoptosis; small GTPase mediated signal transduction
Guanine monophosphate synthetase	GUAA	2	3.6	61	76715	GMP biosynthesis; purine biosynthesis
FAM21A protein	FA21A	2	1.9	60	147184	Transport
Glucose phosphate isomerase	G6PI	2	8.8	60	63147	Angiogenesis; gluconeogenesis; glycolysis
Glycoprotein, synaptic 2	TECR	1	3.9	60	36034	Fatty acid biosynthesis; lipid synthesis

* The bait protein is a mouse MICAL-1 N3 fragment; proteins identified from human HEK293 cells. Mw, molecular weight.

Table 3. Unique proteins identified in the bio-eGFP-MICAL-1-C1 pull down experiment

Protein Name	Uniprot Entry Name	Unique peptide number	Cover%	Mascot score	Mw	Biological process
MICAL1	MICA1	17	11.7	1252	117875	cytoskeleton organization; oxidation-reduction process; signal transduction
Ras-related GTP-binding protein RAB10	RAB10	13	52.5	935	22541	Protein transport; transport
Protein kinase PKNbeta	PKN3	10	18.1	682	99421	Protein phosphorylation signal transduction
Mel transforming oncogene	RAB8A	10	45.4	673	23668	Protein transport; transport
Ras-related protein Rab-15	RAB15	7	46.2	593	24391	Protein transport; transport
RAB8B, member RAS oncogene family	RAB8B	8	42.5	560	23584	Protein transport; transport
RAB1A, member RAS oncogene family	RAB1A	6	29.2	444	22678	ER-Golgi transport; protein transport; transport
RAB1B, member RAS oncogene family	RAB1B	6	34.3	370	22171	Protein transport
RAB-R protein	AGFG2	12	6.4	345	48963	Regulation of ARF GTPase activity
Prohibitin	PHB	4	15.8	309	29804	DNA synthesis

Protein Name	Uniprot Entry Name	Unique peptide number	Cover%	Mascot score	Mw	Biological process
RAB35, member RAS oncogene family	RAB35	4	21.9	299	23025	Protein transport
Paraspeckle protein 1	PSPC1	5	20.5	176	58744	Transcription regulation
Glucocorticoid induced transcript 1	GLCI1	4	16.6	174	58024	
Signal recognition particle 68kDa	SRP68	3	18.6	167	70730	Response to drug
Growth/differentiation factor 7 precursor (GDF-7)	GDF7	4	11.7	165	47891	
Obscurin	OBSCN	6	1.5	161	868484	Differentiation
Zinc finger CCHC domain-containing protein 11	TUT4	5	3.5	149	185166	RNA-mediated gene silencing
PDZ domain containing 4	PDZD4	4	8.6	146	86171	
Dual-specificity tyrosine-(Y)-phosphorylation regulated kinase 2	DYRK2	4	9.8	144	66652	Apoptosis
Surfactant protein D	SFTPD	4	26.9	143	37728	Gaseous exchange
GON-4-like protein	GON4L	4	3.2	141	248620	
Myoferlin	MYOF	4	3.2	140	234709	Endocytic recycling
Myelin expression factor 2	MYEF2	4	20.5	136	64122	Transcription
Trinucleotide repeat containing 6A	TNR6A	4	3.8	136	210297	RNA-mediated gene silencing; translation regulation
Alpha1A-voltage-dependent calcium channel	Q9NS89	4	3.4	132	278848	Cell death
Collagen alpha-1(XXIV) chain	COOA1	4	4.5	132	175496	Fetal development
KCTD2	KCTD2	3	19.6	129	28527	Potassium channel activity
Monarch-1	NAL12	3	6.5	126	120173	Activation of caspase activity
ATP cassette binding transporter 1	ABCA1	5	4.4	120	254302	cAMP-dependent and sulfonylurea-sensitive anion transporter. Key gatekeeper influencing intracellular cholesterol transport.
Hypermethylated in cancer 1	HIC1	3	10.8	120	76508	Transcriptional repressor
VEGF co-regulated chemokine 1	VCC1	3	34.5	120	13819	Angiogenesis and possibly in the development of tumors
ALK tyrosine kinase receptor	ALK	4	5	119	176442	Orphan receptor with a tyrosine-protein kinase activity development and function of the nervous system
Nucleoporin 153kDa	NU153	3	3.7	119	153938	Protein transport
RNA binding protein, autoantigenic (hnRNP-associated with lethal yellow homolog (mouse))	RALY	3	21.5	119	32463	mRNA processing
Rho GTPase activating protein 4	RHG04	3	9.3	118	105026	Stress fiber organization
RNA binding motif protein 47	RBM47	3	10.3	118	64099	RNA binding
A disintegrin and metalloproteinase with thrombospondin motifs 1	ATS1	3	3.7	112	105358	Various inflammatory processes as well as development of cancer cachexia.
Mitogen-activated protein kinase kinase 4	MP2K4	3	15.3	112	44288	JNK cascade
Nebulin	NEBU	5	1.3	111	772927	Cytoplasm; cytoskeleton
Pantothenate kinase 2	PANK2	3	10.9	111	62681	CoA biosynthesis
Filaggrin-2	FILA2	1	1	110	248073	
Vimentin	VIME	3	8.4	109	53652	Intermediate filament
Spatacsin	SPTCS	3	4.2	108	278868	Cell death
Thrombospondin 1	TSP1	3	4.5	108	129383	Cell adhesion

Protein Name	Uniprot Entry Name	Unique peptide number	Cover%	Mascot score	Mw	Biological process
Chromodomain helicase DNA binding protein 5	CHD5	3	2.4	106	223050	Development of the nervous system and the pathogenesis of neural tumors
KCNMA1 protein	KCMA1	2	2	106	137560	Potassium channel
CECR2 protein	CECR2	3	2.8	103	164213	Part of the CERF (CECR2-containing-remodeling factor) complex, which facilitates the perturbation of chromatin structure in an ATP-dependent manner.
Cas-Br-M (murine) ecotropic retroviral transforming sequence	CBL	3	3.3	102	99633	Ubl conjugation pathway
NAV2	NAV2	4	3	102	261724	Neuronal development
Citron Rho-interacting kinase	CTRO	3	1.8	101	231431	Cytokinesis and the development of the central nervous system
DDB1- and CUL4-associated factor 5	DCAF5	4	3	101	103963	Ubl conjugation pathway
Huntingtin	HD	3	1.4	101	347603	Microtubule-mediated transport or vesicle function
Periaxin	PRAX	3	4.2	100	154905	Axon ensheathment
Talin 2	TLN2	4	2.4	99	271613	Cell junction; cell membrane; cytoplasm; cytoskeleton; membrane; synapse
Chromosome 10 open reading frame 104	C5H3H2	2	41.8	98	11667	
Damage-specific DNA binding protein 1	DDB1	1	2.6	98	126968	DNA repair
DNA helicase homolog PIF1	PIF1	3	8.7	98	69799	Cell cycle
Adenylyl cyclase type II	ADCY2	3	4.6	97	123603	Membrane-bound, calmodulin-insensitive adenylyl cyclase
Annexin A1	ANXA1	2	15.2	95	38714	Exocytosis
Brain-specific angiogenesis inhibitor 3	BAI3	4	4.3	95	171518	Might be involved in angiogenesis inhibition and suppression of glioblastoma.
BRCA1-associated RING domain protein1	BARD1	2	3.6	94	86648	Plays a central role in the control of the cell cycle in response to DNA damage.
Caspase 3	CASP3	2	12.7	94	31608	Involved in the activation cascade of caspases responsible for apoptosis execution.
Hepatitis A virus cellular receptor 2	TIMD3	2	12	93	33394	Auto- and alloimmune responses
WW, C2 and coiled-coil domain containing 2	WWC2	2	4	91	133891	
Carbonyl reductase II	DCXR	2	19.7	90	25913	Catalyzes the NADPH-dependent reduction of several pentoses, tetroses, trioses, alpha-dicarbonyl compounds and L-xylulose.
RAB19	RAB19	2	10.1	90	24400	
Rad GTPase	RAD	3	6.5	90	33245	Small GTPase mediated signal transduction
RhoA/RAC/CDC42 exchange factor isoform 3	ARHGP	3	7.1	90	63843	Actin cytoskeleton reorganization
Sjoegren syndrome/scleroderma autoantigen 1	SSA27	2	17	90	21474	Cell cycle; cell division; mitosis
DEAH box protein 57	DHX57	3	1.8	88	155604	RNA helicase
Abnormal spindle-like microcephaly-associated protein homolog	ASPM	4	1	87	409800	Probable role in mitotic spindle regulation and coordination of mitotic processes

Protein Name	Uniprot Entry Name	Unique peptide number	Cover%	Mascot score	Mw	Biological process
Eukaryotic translation initiation factor 3, subunit M	EIF3M	2	8	87	42503	Protein synthesis
Zinc finger protein 185	ZN185	2	4.6	87	73525	Cell junction; cytoplasm; cytoskeleton
Tensin like C1 domain containing phosphatase isoform 1	TENC1	3	4.4	86	152580	Negative regulation of cell proliferation
ZFP36L2 protein	TISD	2	9.3	85	51063	Cell proliferation
Sp4 transcription factor	SP4	2	6.1	84	81985	Transcription regulation
Calpain, small subunit 1	CPNS1	2	26.9	83	28316	Regulatory subunit of the calcium-regulated non-lysosomal thiol-protease which catalyzes limited proteolysis of substrates involved in cytoskeletal remodeling and signal transduction.
Procollagen C-endopeptidase enhancer 2	PCOC2	2	10.6	83	45717	Binds to the C-terminal propeptide of types I and II procollagens
BCL9-like protein	BCL9L	2	2.9	82	157129	Transcriptional regulator that acts as an activator. Promotes beta-catenin transcriptional activity. Plays a role in tumorigenesis. Enhances the neoplastic transforming activity of CTNNB1
Brain-enriched guanylate kinase-associated protein	BEGIN	2	8.3	82	65309	May sustain the structure of the postsynaptic density (PSD).
Neuroligin-2	NLGN2	2	3.8	82	90820	Cell adhesion
vitelline membrane outer layer 1 homolog	VMO1	2	40.4	82	21534	Vitelline membrane formation
SLC45A4 protein	C9JFW9	2	4.3	81	87626	Transmembrane transport
Hyperpolarization activated cyclic nucleotide-gated potassium channel 1	HCN1	1	4.8	80	98796	Ion channel
CDC42-binding protein SCIP1	C42S1	2	54.5	79	8925	Organization of the actin cytoskeleton
Cytochrome P450 monooxygenase	CP20A	2	6.9	79	52432	Flavoprotein
MLLT6 protein	AF17	2	9.8	79	112076	Regulation of transcription, DNA-dependent
Xin actin-binding repeat containing 1	XIRP1	3	1.8	79	198561	Actin binding
RAN binding protein 2 variant	RBP2	2	1.6	78	358199	Protein transport
Stomatin (EPB72)-like 2	STML2	1	4.2	78	38534	
Telomerase reverse transcriptase	TERT	2	5.1	78	126997	DNA strand elongation
Serine/threonine protein kinase	WNK4	2	2.3	77	134739	Cell junction; tight junction
ECHDC2 protein	ECHD2	2	16.8	76	31126	
MTCH1 protein	MTCH1	2	7.6	75	41544	Apoptosis
Septin-2	SEPT2	2	8.3	75	41503	Cell cycle; cell division; mitosis
Tyrosine-protein kinase Fes/Fps	FES	2	4	75	93497	Axon guidance
Chloride channel 1	CLCN1	2	1.9	74	108626	Voltage-gated chloride channel
Collagen alpha-2(VIII) chain	CO8A2	2	7.1	74	67244	Potential role in the maintenance of vessel wall integrity and structure, in particular in artherogenesis
Est1p-like protein A	EST1A	2	2.8	74	160462	Telomere regulation
IFT74 protein	IFT74	2	7.3	74	69239	
RAB26, member RAS oncogene family	RAB26	1	4.3	73	27900	Exocrine secretion
Anaphase-promoting complex subunit 1	APC1	2	1.5	72	216500	Component of the anaphase promoting complex/cyclosome
Poly (ADP-ribose) polymerase 14	PAR14	2	2.5	72	193753	Transcription regulation

Protein Name	Uniprot Entry Name	Unique peptide number	Cover%	Mascot score	Mw	Biological process
Armadillo repeat-containing protein 8	ARMC8	2	4.8	71	75509	
OCIM	MYEOV	2	14.7	71	33556	Overexpressed in tumor cells lines
C2 calcium-dependent domain containing 3	C2CD3	2	1.2	70	260389	
Mitogen-activated protein kinase kinase kinase MLK4	M3KL4	3	15.3	70	113957	Activation of JUN kinase activity
Adenylate cyclase type 1	ADCY1	2	7.6	69	123440	Regulatory processes in the central nervous system
Anaphase-promoting complex subunit 2	ANC2	2	46.6	69	93828	Component of the anaphase promoting complex/cyclosome
Phosphoribosylglycinamide formyltransferase, phosphoribosylglycinamide synthetase, phosphoribosylaminoimidazole synthetase isoform 1 variant	Q59HH3	2	2.8	69	112138	Transferase
TCD	RAE1	2	16.8	69	73476	Sensory transduction; vision
Mitogen-activated protein kinase kinase kinase 10	M3K10	2	4	68	103694	Activation of JUN kinase activity
CHMP1.5	CHM1B	2	11.7	67	22109	Endosomal sorting
Transmembrane protease, serine 6	TMPS6	2	4.5	67	90000	Angiogenesis
Cathepsin O	CATO	2	5.1	66	35958	Proteolytic enzyme possibly involved in normal cellular protein degradation and turnover.
Voltage-dependent calcium channel gamma-8 subunit	CCG8	2	14.6	66	43313	Calcium transport; ion transport; transport
WNK lysine deficient protein kinase 2	WNK2	2	2.8	66	242676	Intracellular protein kinase cascade
Cartilage-derived morphogenetic protein 1	GDF5	1	5.8	65	55411	Could be involved in bone and cartilage formation. Chondrogenic signaling is mediated by the high-affinity receptor BMPR1B
Plasminogen activator inhibitor	PAI2	1	10.4	65	46596	Plasminogen activation
MGAT3	MGAT3	1	5.3	64	61313	Biosynthesis and biological function of glycoprotein oligosaccharides
ZP2 protein	ZP2	2	5	64	82357	Fertilization
Ataxin-7-like protein 1	AT7L1	2	3.5	63	88598	Cell division and chromosome partitioning; actin binding
Chromatin modifying protein 5	CHMP5	1	8.1	61	24571	Vesicle transport
Retrotransposon gag domain containing 4	RGAG4	2	6.7	61	64711	
Tankyrase-related protein	TNKS2	2	3.6	61	126918	Positive regulation of telomere maintenance via telomerase
Vacuolar protein sorting 18	VPS18	2	5.3	61	110186	Protein transport; transport
DIAPH2 protein	DIAP2	2	2	60	125569	Oogenesis; endosome dynamics
Myosin regulatory light chain interacting protein	MYLIP	1	3.1	60	49910	E3 ubiquitin-protein ligase
RNA polymerase II transcription factor TAFII140	TAF3	3	105	8	103582	Transcription regulation

* The bait protein is a mouse MICAL-1 C1 fragment; proteins identified from human HEK293 cells. Mw, molecular weight.

Table 4. MICAL/MICAL-Like binding proteins

MICAL/MICAL-Like	Species	Interacting Protein	(Related) Function	Reference
Mical	Drosophila	plexinA	Axon guidance	Terman et al., 2002
		F-actin	Actin filament and bundle regulation	Hung et al., 2010
MICAL-1	Human	Rab1	Vesicle trafficking	Weide et al., 2003 Fischer et al., 2005
	Human	CasL	Cytoskeleton	Suzuki et al., 2002
		Vimentin	Interfilements	Suzuki et al., 2002
	Mouse	CRMP	Axon guidance	Schmidt et al., 2008
	Mouse	PlexinA1	Axon guidance	Schmidt et al., 2008
	Mouse	NDR1	apoptosis	chapter 4, 5
	Mouse	DOCK7	Axon regulation	chapter 4
	Mouse*	staufen	mRNA-tubulin linker	chapter 4
	Mouse	RanBPM	Axon guidance	Togashi et al., 2006
MICAL-2	Human	Rab1	Vesicle trafficking	Fischer et al., 2005
MICAL-3	Human	Rab1	Vesicle trafficking	Fischer et al., 2005
MICAL-L1	Human	Rab8a and EHD	Endosome recycling	Shrama et al., 2009
MICAL-L2	Mouse	Rab13	Endocytic recycling	Terai et al., 2006
			Epithelial cell scattering	Kanda et al., 2008
			Neurite outgrowth	Sakane et al., 2010
		Rab8	Tight junction	Yamamura et al., 2008
		Actinin-4	Tight junction	Nakatsuji et al., 2008

* Mouse MICAL-1 interacted with human staufen in HEK293 cells.

Acknowledgements

We thank Phebe S.Wulf for help with the biotin-streptavidin based protein purification. This work was supported by the Netherlands Organization for Health Research and Development (ZonMW-VIDI and ZonMW-TOP), the Human Frontier Science Program (HFSP-CDA), and the Genomics Center Utrecht (to R.J.P.). The Fondation Leducq and the British Heart Foundation (to P.H.S and S.J.F.). The European seventh framework program under grant agreement Health-2009-2.1.2-1-242167 (SynSys project, to A.B.S., R.C.v.d.S. and K.W.L.).

Reference

Adelstein RS, Eisenberg E. (1980). Regulation and kinetics of the actin-myosin-ATP interaction. Annu Rev Biochem. 1980;49:921-56.

Ashida, S., M. Furihata, T. Katagiri, K. Tamura, Y. Anazawa, H. Yoshioka, T. Miki, T. Fujioka, T. Shuin, Y. Nakamura, and H. Nakagawa. (2006). Expression of novel molecules, MICAL2-PV (MICAL2 prostate cancer variants), increases with high Gleason score and prostate cancer progression. Clin Cancer Res. 2006 May 1;12(9):2767-73.

Bach I. (2000). The LIM domain: regulation by association. Mech Dev. 2000 Mar 1;91(1-2):5-17.

Beuchle D, Schwarz H, Langegger M, Koch I, Aberle H. (2007). Drosophila MICAL regulates myofilament organization and synaptic structure. Mech Dev. 2007 May;124(5):390-406.

Bron R, Vermeren M, Kokot N, Andrews W, Little GE, Mitchell KJ, Cohen J. (2007). Boundary cap cells constrain spinal motor neuron somal migration at motor exit points by a semaphorin-plexin mechanism. Neural Dev. 2007 Oct 30;2:21.

Burkhard P, Stetefeld J, Strelkov SV. (2001). Coiled coils: a highly versatile protein folding motif. Trends Cell Biol. 2001 Feb;11(2):82-8.

Delva E, Tucker DK, Kowalczyk AP. (2009). The desmosome. Cold Spring Harb Perspect Biol. 2009 Aug;1(2):a002543.

Dennis G Jr, Sherman BT, Hosack DA, Yang J, Gao W, Lane HC, Lempicki RA. (2003). DAVID: Database for Annotation, Visualization, and Integrated Discovery. Genome Biol. 2003;4(5):P3.

Ebnet K, Suzuki A, Horikoshi Y, Hirose T, Meyer Zu, Brickwedde MK. (2001). The cell polarity protein ASIP/PAR-3 directly associates with junctional adhesion molecule (JAM). EMBO J 20:3738–3748.

Fischer J, Weide T, Barnekow A. (2005). The MICAL proteins and rab1: a possible link to the cytoskeleton? Biochem Biophys Res Commun. 2005 Mar 11;328(2):415-23.

Gimona M, Djinovic-Carugo K, Kranewitter WJ, Winder SJ. (2002). Functional plasticity of CH domains.FEBS Lett. 2002 Feb 20;513(1):98-106.

González-Mariscal L, Tapia R, Chamorro D. (2008). Crosstalk of tight junction components with signaling pathways. Biochim Biophys Acta. 2008 Mar;1778(3):729-56.

Hergovich A, Kohler RS, Schmitz D, Vichalkovski A, Cornils H, Hemmings BA. (2009). The MST1 and hMOB1 tumor suppressors control human centrosome duplication by regulating NDR kinase phosphorylation. Curr Biol. 2009 Nov 3;19(20):1692-702.

Hildebrand JD, Schaller MD, Parsons JT. (1993). Identification of sequences required for the efficient localization of the focal adhesion kinase, pp125FAK, to cellular focal adhesions. J. Cell Biol. 123, 993–1005.

Huang DW, Sherman BT, Lempicki RA. (2009). Systematic and integrative analysis of large gene lists using DAVID Bioinformatics Resources. Nature Protoc. 2009;4(1):44-57.

Hung RJ, Yazdani U, Yoon J, Wu H, Yang T, Gupta N, Huang Z, van Berkel WJ, Terman JR. (2000). Mical links semaphorins to F-actin disassembly. Nature. 2010 Feb 11;463(7282):823-7.

Kadrmas JL, Beckerle MC. (2004). The LIM domain: from the cytoskeleton to the nucleus. Nature Reviews Molecular Cell Biology 5:920-931.

Kawasaki Y, Senda T, Ishidate T, Koyama R, Morishita T, Iwayama Y, Higuchi O, Akiyama T. (2000). Asef, a link between the tumor suppressor APC and G-protein signaling. Science. 2000 Aug 18;289(5482):1194-7.

Kay BK, Williamson MP, Sudol M. (2000). The importance of being proline: the interaction of proline-rich motifs in signaling proteins with their cognate domains. FASEB J. 2000 Feb;14(2):231-41.

Kirilly D, Gu Y, Huang Y, Wu Z, Bashirullah A, Low BC, Kolodkin AL, Wang H, Yu F. (2009). A genetic pathway composed of Sox14 and Mical governs severing of dendrites during pruning. Nat Neurosci. 2009 Dec;12(12):1497-505.

Laitinen OH, Hytönen VP, Nordlund HR, Kulomaa MS. (2006). Genetically engineered avidins and streptavidins. Cell Mol Life Sci. 2006 Dec;63(24):2992-3017.

Lansbergen G, Grigoriev I, Mimori-Kiyosue Y, Ohtsuka T, Higa S, Kitajima I, Demmers J, Galjart N, Houtsmuller AB, Grosveld F and Akhmanova A. (2006). CLASPs attach microtubule plus ends to the cell cortex through acomplex with LL5β. Dev Cell 11: 21-32.

Li, K. W., S. Miller, O. Klychnikov, M. Loos, J. Stahl-Zeng, S. Spijker, M. Mayford, and A. B. Smit. (2007). Quantitative proteomics and protein network analysis of hippocampal synapses of CaMKIIalpha mutant mice. J Proteome Res 6:3127-33.

Lin AC, Holt CE. (2008). Function and regulation of local axonal translation. Curr Opin Neurobiol. 2008 Feb;18(1):60-8.

Nadella M, Bianchet MA, Gabelli SB, Barrila J, Amzel LM. (2005). Structure and activity of the axon guidance protein MICAL. Proc Natl Acad Sci U S A. 2005 Nov 15;102(46):16830-5.

Nakatsuji H, Nishimura N, Yamamura R, Kanayama HO, Sasaki T. (2008). Involvement of actinin-4 in the recruitment of JRAB/MICAL-L2 to cell-cell junctions and the formation of functional tight junctions. Mol Cell Biol. 2008 May;28(10):3324-35.

Pasterkamp, R. J., H. N. Dai, J. R. Terman, K. J. Wahlin, B. Kim, B. S. Bregman, P. G. Popovich, and A. L. Kolodkin. (2006). MICAL flavoprotein monooxygenases: expression during neural development and following spinal cord injuries in the rat. Mol Cell Neurosci 31(1):52-69.

Popoff MR, Geny B. (2009). Multifaceted role of Rho, Rac, Cdc42 and Ras in intercellular junctions, lessons from toxins. Biochim Biophys Acta. 2009 Apr;1788(4):797-812.

Ramesh TP, Kim YD, Kwon MS, Jun CD, Kim SW. (2009). Swiprosin-1 Regulates Cytokine Expression of Human Mast Cell Line HMC-1 through Actin Remodeling. Immune Netw. 2009 Dec;9(6):274-84.

Rayala SK, den Hollander P, Manavathi B, Talukder AH, Song C, Peng S, Barnekow A, Kremerskothen J, Kumar R. (2006). Essential role of KIBRA in co-activator function of dynein light chain 1 in mammalian cells. J Biol Chem. 2006 Jul 14;281(28):19092-9.

Schlaepfer DD, Hauck CR, Sieg DJ. (1999). Signaling through focal adhesion kinase. Prog. Biophys. Mol. Biol. 71, 435– 478.

Schmidt EF, Shim SO, Strittmatter SM. (2008). Release of MICAL autoinhibition by semaphorin-plexin signaling promotes interaction with collapsin response mediator protein. J Neurosci. 2008 Feb 27;28(9):2287-97.

Seth A, Sheth P, Elias BC, Rao R.. (2007). Protein phosphatases 2A and 1 interact with occludin and negatively regulate the assembly of tight junctions in the CACO-2 cell monolayer. J Biol Chem. 2007 Apr 13;282(15):11487-98.

Shevchenko, A., M. Wilm, O. Vorm, and M. Mann. (1996). Mass spectrometric sequencing of proteins silver-stained polyacrylamide gels. Anal Chem 68:850-8.

Siebold C, Berrow N, Walter TS, Harlos K, Owens RJ, Stuart DI, Terman JR, Kolodkin AL, Pasterkamp RJ, Jones EY. (2005). High-resolution structure of the catalytic region of MICAL (molecule interacting with CasL), a multidomain flavoenzyme-signaling molecule. Proc Natl Acad Sci U S A. 2005 Nov 15;102(46):16836-41.

Sieg DJ, Hauck CR, Ilic D, Klingbeil CK, Schaefer E, Damsky CH, Schlaepfer DD. (2000). FAK integrates growth-factor and integrin signals to promote cell migration Nature Cell Biology 2, 249 – 256.

Stork O, Zhdanov A, Kudersky A, Yoshikawa T, Obata K, Pape HC. (2004). Neuronal functions of the novel serine/threonine kinase Ndr2. J Biol Chem. 2004 Oct 29;279(44):45773-81.

Sun H, Dai H, Zhang J, Jin X, Xiong S, Xu J, Wu J, Shi Y. (2006). Solution structure of calponin homology domain of Human MICAL-1. J Biomol NMR. 2006 Dec;36(4):295-300.

Suzuki T, Nakamoto T, Ogawa S, Seo S, Matsumura T, Tachibana K, Morimoto C, Hirai H. (2002). MICAL, a novel CasL interacting molecule, associates with vimentin. J Biol Chem. 2002 Apr 26;277(17):14933-41.

Takahashi H, Funakoshi H, Nakamura T. (2003). LIM-kinase as a regulator of actin dynamics in spermatogenesis. Cytogenet Genome Res. 2003;103(3-4):290-8.

Terai T, Nishimura N, Kanda I, Yasui N, Sasaki T. (2006). JRAB/MICAL-L2 is a junctional Rab13-binding protein mediating the endocytic recycling of occludin. Mol Biol Cell. 2006 May;17(5):2465-75.

Terman JR, Mao T, Pasterkamp RJ, Yu HH, Kolodkin AL. (2002). MICALs, a family of conserved flavoprotein oxidoreductases, function in plexin-mediated axonal repulsion. Cell. 2002 Jun 28;109(7):887-900.

Todd AG, Morse R, Shaw DJ, McGinley S, Stebbings H, Young PJ. (2010). SMN, Gemin2 and Gemin3 associate with beta-actin mRNA in the cytoplasm of neuronal cells in vitro. J Mol Biol. 2010 Sep 3;401(5):681-9.

Togashi H, Schmidt EF, Strittmatter SM. (2006). RanBPM contributes to Semaphorin3A signaling through plexin-A receptors. J Neurosci. 2006 May 3;26(18):4961-9.

Vichalkovski A, Gresko E, Cornils H, Hergovich A, Schmitz D, Hemmings BA. (2008). NDR kinase is activated by RASSF1A/MST1 in response to Fas receptor stimulation and promotes apoptosis. Curr Biol. 2008 Dec 9;18(23):1889-95.

Watabe-Uchida M, John KA, Janas JA, Newey SE, Van Aelst L. (2006). The Rac activator DOCK7 regulates neuronal polarity through local phosphorylation of stathmin/Op18. Neuron. 2006 Sep 21;51(6):727-39.

Weide T, Teuber J, Bayer M, Barnekow A. (2003). MICAL-1 isoforms, novel rab1 interacting proteins. Biochem Biophys Res Commun. 2003 Jun 20;306(1):79-86.

Wen Y, Eng CH, Schmoranzer J, Cabrera-Poch N, Morris EJ, Chen M, Wallar BJ, Alberts AS, Gundersen GG. (2004). EB1 and APC bind to mDia to stabilize microtubules downstream of Rho and promote cell migration. Nat Cell Biol. 2004 Sep;6(9):820-30.

Wickham L., Duchaine T., Luo M., Nabi I.R., DesGroseillers L. (1999). Mammalian Staufen is a double-stranded-RNA- and tubulin-binding protein which localizes to the rough endoplasmic reticulum. Mol. Cell. Biol. 19:2220-2230.

Wilm M, Shevchenko A, Houthaeve T, Breit S, Schweigerer L, Fotsis T, Mann M. (1996). Femtomole sequencing of proteins from polyacrylamide gels by nano-electrospray mass spectrometry. *Nature* 379: 466-9.

Yamamura R, Nishimura N, Nakatsuji H, Arase S, Sasaki T. (2008). The interaction of JRAB/MICAL-L2 with Rab8 and Rab13 coordinates the assembly of tight junctions and adherens junctions. Mol Biol Cell. 2008 Mar;19(3):971-83.

Chapter 5

MICAL-1 is a negative regulator of MST-NDR kinase signaling and apoptosis

Yeping Zhou[1], Youri Adolfs[1], W.W.M. Pim Pijnappel[2], Stephen J. Fuller[3], Roel C. Van der Schors[4], Ka Wan Li[4], Peter H. Sugden[3], August B. Smit[4], Alexander Hergovich[5], R. Jeroen Pasterkamp[1]

[1]Department of Neuroscience and Pharmacology, Rudolf Magnus Institute of Neuroscience, University Medical Center Utrecht, Universiteitsweg 100, 3584 CG, Utrecht, The Netherlands
[2]Netherlands Proteomics Center, Department of Physiological Chemistry, University Medical Center Utrecht, Universiteitsweg 100, 3584 CG, Utrecht, The Netherlands
[3] Institute for Cardiovascular and Metabolic Research, School of Biological Sciences, University of Reading, Reading RG6 6BX, UK
[4]Department of Molecular and Cellular Neurobiology, CNCR, Neuroscience Campus Amsterdam, VU University, De Boelelaan 1085, 1081 HV Amsterdam, The Netherlands
[5]UCL Cancer Institute, University College London, 72 Huntley Street, London WC1E 6BT, UK

Mol Cell Biol. 2011 Jul 5.

Abstract
MICALs are atypical multidomain flavoenzymes with diverse cellular functions. The molecular pathways employed by MICAL proteins to exert their cellular effects remain largely uncharacterized. Via an unbiased proteomics approach, we identify MICAL-1 as a binding partner of NDR (nuclear Dbf2-related) kinases. NDR1/2 kinases are known to mediate apoptosis downstream of the mammalian Ste-20-like kinase MST1 and ablation of NDR1 in mice predisposes to cancer as a result of compromised apoptosis. MST1 phosphorylates NDR1/2 kinases at their hydrophobic motif thereby facilitating full NDR kinase activity and function. However, if and how this key phosphorylation event is regulated is unknown. Here we show that MICAL-1 interacts with the hydrophobic motif of NDR1/2 and that overexpression or knockdown of MICAL-1 reduces or augments, respectively, NDR kinase activation and activity. Surprisingly, MICAL-1 is a phosphoprotein but not a NDR or MST1 substrate. Rather, MICAL-1 competes with MST1 for NDR binding and thereby antagonizes MST1-induced NDR activation. In line with this inhibitory effect, overexpression or knockdown of MICAL-1 inhibits or enhances, respectively, NDR-dependent pro-apoptotic signaling induced by extrinsic stimuli. Our findings unveil a previously unknown biological role for MICAL-1 in apoptosis and define a novel negative regulatory mechanism of MST-NDR signaling.

Introduction

Protein kinases are key regulatory enzymes that control important cellular processes such as growth and apoptosis by changing the properties of a substrate through phosphorylation (20). Given the importance of their biological effects, the catalytic activity of protein kinases is stringently controlled and defects in this spatiotemporal regulation can cause major diseases such as diabetes and cancer (20). The mammalian Ste-20-like kinase MST1 is part of evolutionary conserved signal transduction pathways with functions in different cell biological processes. In particular, Hippo signaling (the MST1 fly ortholog) has been studied extensively in *Drosophila*, revealing that Hippo tumor suppressor cascades are crucial in the regulation of cell death and proliferation (45). More recently, mammalian MST1 was established as a tumor suppressor protein controlling cell proliferation and apoptosis (45). However, despite these important functions relatively little is known about the regulation of MST1 or its downstream signaling.

Nuclear-Dbf2-related kinase 1 (NDR1, also known as STK38) and NDR2 (STK38L) can be phosphorylated by MST kinases and mediate apoptotic signaling downstream of MST1 (40). NDR kinases belong to the AGC kinase subfamily and control important cellular processes, such as mitotic exit and apoptosis, in different eukaryotic cells ranging from yeast to neurons (12). Ablation of NDR1 in mice predisposes to the development of T cell lymphoma, presumably as a result of compromised apoptosis (4). The regulation of NDR1/2 kinases by MST kinases and other upstream signaling proteins is best understood in mammalian cells. Binding of MOB1A (Mps-one-binder 1A) to the N-terminal region of NDR1/2 stimulates autophosphorylation on the activation segment and activates NDR kinases (3). The human MOB protein family consists of six distinct members with MOB1 being best studied for its putative tumor suppressive functions through the regulation of NDR/LATS kinases. Additional phosphorylation on the C-terminal hydrophobic motif of NDR1/2 by MST kinases is required for full NDR kinase activation (32). It is evident that these different molecular interactions and activating events need to be tightly controlled as deregulation of members of the MST, NDR and MOB proteins families has been implicated in diseases such as cancer. Intriguingly, another MOB family member, MOB2, competes with MOB1 for NDR1/2 binding at the NDR N-terminal region thereby negatively regulating NDR1/2 kinase activity and related functions in centrosome duplication and apoptosis (16). However, whether similar sophisticated regulatory mechanisms exist to control the activation of NDR1/2 by MST kinases is unknown.

Here we identify the multidomain flavoprotein monooxygenase MICAL-1 (37) as an endogenous binding partner of NDR1/2 kinases. Our findings define a previously unknown biological role for MICAL-1 in apoptosis regulation and show that MICAL-1 negatively controls MST1-NDR apoptotic signaling by competing with MST1 for NDR binding thereby revealing a novel and unique regulatory mechanism of the MST-NDR pathway. This work opens new avenues for the further molecular delineation of MST/NDR functioning in different cell biological processes and in disease.

Materials and methods

Antibodies and reagents

The generation and purification of anti-T444/442-P and anti-S281/282-P antibodies has been described previously (38). Both antibodies were kindly provided by Dr. Brian Hemmings (FMI, Switzerland). It is important to note that the anti-T444-P and anti-S281-P antibodies recognize the phosphorylated forms of both NDR isoforms, NDR1 (T444-P, S281-P) and NDR2 (T442-P, S282-P). A polyclonal rabbit anti-mouse MICAL-1 antibody was generated by immunizing rabbits with an MBP-mMICAL-1 (amino acids 986-1048) fusion protein, which was purified from DH5α cells. The specificity of this antibody was confirmed using western blotting and immunocytochemistry. We used the following commercially available antibodies: anti-Flag (M2; Stratagene), anti-HA (3F10; Roche), anti-NDR1 (N-14; Santa Cruz), STK38 (NDR1) monoclonal antibody (2G8-1F3; Abnova), anti-GST (Cell Signaling), anti-myc (Roche), anti-GFP (Invitrogen), anti-V5 (Invitrogen), anti-α-tubulin (Sigma), anti-actin (Sigma), anti-cleaved caspase-3 (Cell signaling), and anti-PARP Asp241 (BD Biosciences). Okadaic acid (OA) was purchased from Enzo Life Sciences, etoposide from Sigma, tumor necrosis factor-alpha (TNF-alpha) and cycloheximide (CHX) from Sigma.

Construction of plasmids

Mouse MICAL-1 and NDR1 cDNAs were amplified from embryonic whole brain cDNA using standard molecular techniques. To construct a mouse MICAL-1-Flag/HA construct for generating stable L cell lines, mouse MICAL-1 cDNA was subcloned into a pBABE-Flag-HA-puromycin destination vector using the GATEWAY cloning system (Invitrogen). Mouse MICAL-1 cDNA was also subcloned into pRK5-HA and pRK5-myc (N-terminal tags) using SalI and NotI restriction sites, into pEF-His/V5 vector (C-terminal tag) using the GATEWAY cloning system (Invitrogen) and into pEGFP. Truncation mutants of mouse MICAL-1 were cloned via PCR reaction. Individual PCR products were digested with SalI and NotI and cloned into pRK5-HA or pRK5-myc. Mouse MICAL-1 constructs harboring glycine to tryptophan mutations (G3/W3) in the first FAD fingerprint were generated in pRK5-myc and pRK5-HA using the Quickchange site-directed mutagenesis kit (Stratagene). A cDNA encoding the C-terminal 315 amino acids of MICAL-1 was subcloned into the pMAL-P2E vector (BioLabs) between KpnI and HindIII sites for protein expression in *E.Coli*. Mouse NDR1 was subcloned into pFLAG-CMV4 (Sigma) using NotI and BamHI restriction sites. Truncation mutants of mouse NDR1 were cloned via PCR. Individual PCR products were digested with NotI and BamHI and cloned into pFLAG-CMV4. Flag-NDR2, GST-NDR2, NDR1-PIFtide, and HA-MST1 have been described before (8, 11). To generate mouse plexinA4Δecto, a region covering amino acids 1209 to 1891 of the mouse plexinA4 coding sequence was PCR amplified and combined with the plexinA4 signal sequence and a myc tag in the pSG5 vector. All constructs were confirmed by sequence analysis.

To knockdown human *MICAL-1* in cells, SMARTpool technology from Dharmacon was used. A mix of ON-TARGETplus siRNAs directed against the following sequences in human *MICAL-1*: UGGAGAACAUUG-UGUACUA, CCUCAGGCACCAUGAAUAA, GAGUCCACGUCUCCGAUUU, and GUACGAGACCUGU-AUGAUG (Dharmacon) was transiently transfected into cells and efficiently reduced *MICAL-1* levels. An ON-TARGETplus non-targeting siRNA pool from Dharmacon served as a control. To knockdown mouse MICAL-1 in L cells, an siRNA oligo against mouse MICAL-1 (CAGGUGCCAUGACUAAGUAUU (Dharmacon)) was transfected using Oligofectamin and shown to specifically reduce MICAL-1 levels. Non-targeting siRNAs (Dharmacon) were used as controls. To knock down NDR1/2 in L cells, an shRNA vector targeting both NDR1 and NDR2 (38) was transfected using Lipofectamine2000 (Invitrogen).

Cell culture and transfection

L, Phoenix, HEK293, and COS-7 cells were maintained in high glucose Dulbecco's modified Eagle's medium (DMEM; GIBCO) supplemented with 10% FBS (Lonza), penicillin/streptomycin, and L-glutamine (PAA) at 37°C with 5% CO_2. U2OS T-Rex (tetracycline-inducible MST1 knockdown) cells were cultured as described previously (38). To induce tetracycline-controlled transcriptional activation and MST1 knockdown, $5x10^4$ cells were plated in one well of a 6-well plate and supplied with 2 μg/ml tetracycline to the culture medium. For protein analysis, exponentially growing cells were plated at $3.5x10^4$ cells/cm^2 and transfected the next day using Lipofectamine 2000 (Invitrogen) as described by the manufacturer. For COS-7 cell contraction assays or colocalization experiments, $0.5x10^4$ COS-7 cells/cm^2 cells were seeded on glass coverslips and transfected using FuGENE transfection reagent (Roche) according to the manufacturer's instructions. For transfection of MICAL-1 siRNA oligos, exponentially growing HEK293 cells or L cells were seeded at $5x10^4$ per well in a 6-well plate. After overnight culture, cell were washed with Opti-MEM (Invitrogen) and exposed to a mixture of 1 μl oligo (mix) (from a 20 μM stock) and 3 μl Oligofectamine (Invitrogen) in Opti-MEM. Four hours after transfection, medium was replaced by standard culture medium and cells were incubated at 37°C with 5% CO_2 for another 48-72h. For double knock-down experiments with both siRNA oligos (against MICAL-1) and shRNA vector (against NDR1/2), $5x10^4$ L cells were plated in a 6-well plate one day before transfection of MICAL-1 oligo using Oligofectamine. After 24-48h in culture, cells were transfected with shRNA vector by using Lipofectamine 2000 and cultured for another 48h for further treatment.

Generation of stable cell lines

A mouse MICAL-1 cDNA was introduced by GATEWAY cloning into a retroviral destination plasmid derived from pBABE-puro carrying a C-terminal FlagPreScissionHA-tag. L cell clones expressing tagged MICAL-1 were obtained by retroviral transduction and puromycin (Clontech) selection. Positive clonal cell lines were identified by immunoblotting using antibodies directed against HA. After puromycin selection, clonal lines were maintained in 7.5 μg/ml puromycin containing culture medium. L cells with integrated empty pBABE-puro plasmid served as a control.

Pull-down from stable cell lines

Mouse MICAL-1-Flag/HA expressing (D1) and control (C0) L cells were cultured in 500 cm^2 plates (Corning) to 90% confluency. Ten plates from each cell line were harvested by scraping after 2 washes with cold PBS. The cells were centrifuged at 1000 rpm for 15 min at 4°C and lysed by douncing in 3 ml hypotonic lysis buffer containing 10 mM HEPES, pH 8.0, 1.5 mM $MgCl_2$, 10 mM KCl, 0.5 mM PMSF, 0.5 mM DTT and protease inhibitor cocktail (Sigma). After centrifuging at 14,000 rpm for 15 min at 4°C, supernatant was transferred to a clean Falcon tube and an equal volume of 2x salt buffer containing 30 mM HEPES, pH 8.0, 190 mM KCl, 30 mM NaCl, 40% glycerol, 0.4 mM EDTA, 0.5 mM PMSF, 0.5 mM DTT and protease inhibitor cocktail (Sigma) was added. After measuring protein concentration, 100 mg protein from each cell line was added to 100 µl pre-washed M2 affinity resin (Sigma) and incubated at 4°C for 3 hours. Then, the resin was washed 4 times with washing buffer (BC-150) containing 20 mM HEPES, pH 8.0, 150 mM NaCl and 0.5 mM PMSF. Between the third and fourth wash, the sample was washed once in washing buffer (BC-300) containing 20 mM HEPES, pH 8.0, 300 mM NaCl and 0.5 mM PMSF for 10 min. The proteins were eluted with Flag peptide (Sigma) at 16 µg/µl in BC-150 buffer. The eluted proteins were precipitated as described previously (43) and dissolved in 1x NuPAGE LDS Sample buffer (Invitrogen). Finally, proteins were seperated on a NuPAGE Novex 4-12% Bis-Tris gradient gel following the manufacturer's description (Invitrogen). Proteins were stained using the colloidal blue staining kit (Invitrogen) and processed for mass spectrometry. In addition, 1/20 of each sample was loaded on another NuPAGE gel and processed for silver staining. Briefly, the gel was soaked twice in 50% methanol for 15 min and soaked in 5% methanol for 10 min. After 3 rinses in water, the gel was soaked in 10 µM DTT for 20 min, followed by 0.1% AgNO3 for 20 min. Then the gel was washed once in water and twice in developer containing 3% sodium carbonate and 0.0185% formaldehyde. The gel was soaked in developer until protein bands appeared. The reaction was stopped with solid citric acid (about 5% w/v). The gel was washed with water and scanned.

Gel digestion

Separated proteins were in-gel digested according to the method described by Shevchenko et al. (29). Gel lanes corresponding to the different protein samples were sliced into ten bands. Each band was cut into 1 mm cubes, washed with nanopure water, destained (25 mM ammonium bicarbonate, 50% acetonitrile). After three subsequent destaining steps, the bands were dehydrated for 20 min (100% acetonitrile) and dried in a vacuum centrifuge. The pellets were rehydrated in 30 µl trypsin solution (0.02 µg/µL)(Promega) at 4°C for 45 min, followed by addition of 400 µl 50 mM ammonium bicarbonate to cover the gel pieces. After incubating overnight at room temperature peptides were extracted two times in 50% acetonitrile in 0.1% trifluoroacetic acid (TFA). The sample was dried in a vacuum centrifuge prior to LC− MALDI-MS analysis.

NanoLC and MALDI TOF/TOF Analysis.

Samples were analyzed as described previously (22) with minor modification. In brief, peptides were separated on a nanocapillary LC system (LC Packings/Dionex, Sunnyvale, CA) using an analytical capillary C18 column (150 mm x 100 µm ID) at 400 nL/min, using a linear increase in concentration of acetonitrile from 5 to 50% (v/v) in 90 min and to 90% in 10 min. The eluted gradient was mixed with matrix solution (7 mg of re-crystallized α-cyano-hydroxycinnaminic acid in 1 mL 50% (v/v) acetonitrile, 0.1%(v/v) trifluoroacetic acid, 10 mM ammonium dicitrate) and spotted offline to a stainless steel MALDI plate (Applied Biosystems) to form a predefined 16 x 24 array (384 spots) using a ProbotTM system (LC Packings/Dionex). The mass spectrometric analysis was carried out using a MALDI-TOF/TOF instrument (4800 Proteomics Analyzer, Applied Biosystems) with reflector positive ion mode. For MS analysis, 800–3000 m/z mass range was used with 1250 shots per spectrum. A maximum of 20 precursors per spot with minimum signal/noise ratio of 50 were selected for data-dependent MS/MS analysis. An 1-kV collision energy was used for CID, and 2500 acquisitions were accumulated for each MS/MS spectrum. All analyses were performed using default calibration, and the mass accuracy was calibrated to within 100 ppm using calibration standards (Applied Biosystems) before each run.

Cell contraction assay

COS-7 and L cell contraction assays were performed as described previously (28, 36). In brief, COS-7 or L cells were transfected with different expression plasmids, as described above, fixed after 24 h and immunostained with anti-Flag,

anti-HA, anti-myc or anti-eGFP antibodies to identify transfected cells. Immunofluorescence images were captured of randomly selected cells using a CCD camera attached to an Axiovert microscope (Zeiss) and cell area was measured using OpenLab software (Improvision)(17). COS-7 cells with a surface area ≤ 1600 μm^2 were defined as contracted. L cell contraction was quantified as described previously (36).

Apoptosis assay

Wildtype L cells or stable C0, D1 or D2 L cells were seeded at 1 x 10^4 cells/cm^2 in a 24 well plate for 24 hours and treated with either DMSO (0.2%) or etoposide (200 μM) in the cell culture medium for 12 hours. Transiently transfected L cells (overexpressing MICAL-1, MICAL-1 mutants or knock down oligos/vectors) were treated with etoposide after 24h or 48h after transfection. L cells were also induced with TNFα (50 ng/ml) for 6h in the presence of cycloheximide (CHX, 10 μg/ml). For western blotting, cells lysates were prepared in 30 μl lysis buffer (per well of a 24-well plate). For fluorescence microscopy, cells were fixed and incubated with anti-cleaved caspase-3 antibody for 1 hour at room temperature, followed by several washes and incubation in secondary antibody (anti-rabbit Alexa-Fluor 488 staining). Next, cells were washed and incubated with phalloidin-TRITC (Sigma) to visualize cells and cell morphology.

H_2O_2 Detection Assay

The Amplex Red Hydrogen Peroxide/Peroxidase Assay kit (Invitrogen) was used to measure hydrogen peroxide production from the purified enzymatic domain of MICAL-1 and from lysates of transfected HEK293 or L cells as described previously (25, 28). For cell lysate experiments, cells from one well of a 6-well plate were lysed by sonication in 120 μl buffer containing 20 mM HEPES, pH 7.4, 100 mM NaCl, and 1x EDTA-free protease inhibitor mixture (Roche Diagnostics), and lysates were cleared by centrifugation. Reactions were performed in 100 μl consisting of 50 μl of cell lysate, 200 μM NADPH, Amplex Red Reagent (10-acetyl-3,7-dihydroxyphenoxazine), and 0.1 U/ml HRP in reaction buffer. Absorbance at 560 nm was measured using a Wallac Victor 1420 Multilabel counter (PerkinElmer).

In-gel Phosphoprotein Staining

Proteins in a NuPAGE Bis-Tris gradient gel (Invitrogen) were either Coomassie stained or stained with Pro-Q Diamond Phosphoprotein gel stain (Invitrogen) according to the manufacturer's instructions. In brief, the gel was incubated in fix solution (50% methanol and 10% acetic acid) for 30 min followed by a second overnight incubation. The next day the gel was washed 3 times in ultra-pure water, stained in ProQ stain for 90 min in the dark, and destained in a solution containing 20% acetonitrile and 50 mM sodium acetate, pH 4.0. After a brief wash in ultra-pure water, the gel was imaged on a FLA-5000 (Fuji Photo Film Co, Ltd.) using excitation at 532 nm and LPG filter.

Western blotting and Immunoprecipitation

According to standard protocols, cells were collected by centrifuging at 1000 rpm for 10 min at 4°C for 10 min, washed in cold PBS and lysed in lysis buffer containing 20 mM Tris, pH 8.0, 150 mM KCl, 0.1% TritonX100 and protease inhibitor cocktail (Roche). After centrifugation at 14,000 rpm for 10 min at 4°C, the lysate was transferred to a clean eppendorf tube and boiled with sample buffer. For immunoprecipitation, corresponding antibodies were added to each cell lysate and incubated overnight at 4°C. Then pre-washed proteinA or G agarose (Roche) was added to the lysate and incubated for at least 2 h at 4°C. After 4 washes with lysis buffer, proteins were eluted with sample buffer and boiled at 90°C. To analyze proteins from IP samples or cell lysates, we used SDS-PAGE and transfered proteins to nitrocellulose (Hybond-C Extra, Amersham). Chemiluminescence (Supersignal, Thermo Scientific) was detected by CL-XPosure Film (Thermo Scientific) and quantified using ImageJ.

Recombinant protein purification and binding assay

MBP-MICAL-1-C1 (amino acids 734-1048) fusion protein was extracted from DH5α cells and the MICAL-1-C1 fragment was cleaved from the MBP moiety following the instructions of the manufacturer (New England Biolabs). To check the binding of GST-NDR2 to MICAL-1, HA-MICAL-1 (HEK293 expressed full length protein) or MICAL-1-C1 were immobilized on anti-HA- or anti-MICAL-1-coupled proteinG agarose beads, respectively, and mixed with 4 μg GST-NDR2. Antibody-coupled beads were used as negative control to examine the non-specific

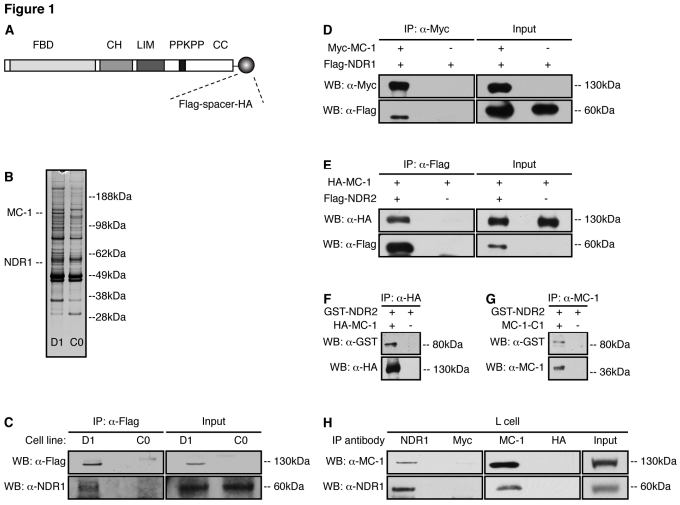

Figure 1. Mass spectrometry identifies NDR kinases as novel MICAL-1 binding partners.
(A) Schematic depicting the domain organization of mouse MICAL-1 fused to C-terminal Flag and HA epitopes linked by a PreScission sequence (MC-1-Flag/HA). FBD, FAD-binding domain; CH, Calponin Homology; PPKPP, CasL-binding; CC, Coiled-coil. (B) Pull-down assays with anti-Flag monoclonal antibody-conjugated agarose beads were performed on lysates from D1 or C0 cells. Bound proteins were eluted with Flag peptide and analyzed by silver staining. Gel positions of MICAL-1 and NDR1 are indicated. (C) Anti-Flag pull-down assays were performed from D1 and C0 cells as shown in (B) and analyzed by western blotting (WB) using the indicated antibodies. (D, E) Lysates from HEK293 cells transfected with epitope-tagged MICAL-1 alone or in combination with Flag-NDR1 (D) or Flag-NDR2 (E) were immunoprecipitated with anti-Myc (D) or anti-Flag (E) antibodies followed by western blotting. (F, G) Recombinant GST-NDR2 and HA-MICAL-1 purified from HEK293 cells (F) or recombinant MICAL-1-C1 purified from bacteria (G) were mixed and subjected to immunoprecipitation with anti-HA (F) or anti-MICAL-1 (G) antibodies followed by western blotting with the indicated antibodies. (H) Immunoprecipitation from untransfected L cell extracts followed by western blotting with the indicated antibodies. Anti-myc and anti-HA antibodies were used as a control for anti-NDR1 and anti-MICAL-1 antibodies, respectively.

binding. After 2h incubation at 4°C, beads were washed 4 times with lysis buffer and boiled in presence of sample buffer. The proteins were then subjected to SDS-PAGE and Western blot analysis.

Kinase assays
NDR kinase peptide assay. Flag-NDR1 was immunoprecipitated from cell lysates expressing Flag-NDR1 alone or in combination with HA-MICAL-1 and assayed for NDR kinase activity in the presence of 1 mM NDR substrate peptide (KKRNRRLSVA), 100 μM γ-^{32}P-ATP (~1000cpm/pmol), and 20 μM ATP in kinase buffer (20 mM Tris, pH7.5, 10 mM $MgCl_2$, 1 mM benzamidine, 4 μM leupeptin, 3 μM microcystin, 3 mM DTT, 1 μM cyclic AMP-dependent protein kinase inhibitor peptide). The reaction mixture was incubated for 60 min at 30°C and stopped by adding 50 mM EDTA, pH 7.5. The supernatant of the mixture was spotted onto squares of P-81 phosphocellulose paper (Whattman) and washed 4 times with 1% orthophosphoric acid followed by an acetone wash. Radioactivity was measured in a liquid scintillation counter.
GST-NDR2 kinase assay using HA-MICAL-1 as a substrate. Full-length rat recombinant NDR2 was cloned into pGEX4-T 3' in frame with GST, expressed in *E. coli* BL21DE3(pLysS) cells with 0.03 mM isopropyl β-D-1-thiogalactopyranoside (IPTG) induction overnight at 25 °C, and purified by glutathione-Sepharose affinity

Table 1

Protein Name	Mascot score	NCBI GI Number	Protein MW (kDa)	Number of unique peptides
MICAL-1	1956	46396473	116,7	264
Septin-9	554	56749655	65,5	12
NDR1	346	56749663	54,1	8
Filamin-B	318	38257404	277,6	8

Table 1. Binding partners of MICAL-1 in stable L cells identified by mass spectrometry.
The table shows proteins identified with a significant Mascot score in pull-down experiments from D1 cell extracts. No peptides were identified for the indicated proteins in a parallel pull-down from C0 control cells.

chromatography. For *in vitro* kinase assays, 3 μg of GST-NDR2 fusion protein was incubated with immunoprecipitated HA-MICAL-1 in the presence of 100 μM γ-^{32}P-ATP (~1000cpm/pmol) and 20 μM ATP in kinase buffer for 30 min at 30 ^{o}C. The reaction was stopped by adding SDS sample buffer and protein phosphorylation was analyzed by SDS-PAGE and subsequent autoradiography.
In vitro phosphorylation with GST-MST1. Recombinant GST-MST1 was obtained from Sigma. To produce immunopurified HA-tagged proteins, COS-7 cells were transfected and processed for immunoprecipitation using anti-HA antibody as described earlier (10). Immunopurified proteins were then washed twice with MST1 kinase buffer (5mM Tris pH 7.5, 2.5mM beta-glycerophosphate, 1mM EGTA, 1mM Na3V04, 4mM MgCl2, 0.1mM DTT), before incubating at 30°C for 30 minutes in 20 μl of reaction buffer [5mM Tris pH 7.5, 100 μM ATP, 2.5mM beta-glycerophosphate, 1mM EGTA, 1mM Na3V04, 4mM MgCl2, 0.1mM DTT, 10 μCi of [γ-^{32}P]ATP (3,000 Ci/mmol; Hartmann Analytic)] in the absence or presence of GST-MST1 (100 ng per reaction). Reactions were stopped by the addition of Laemmli buffer, before proteins were separated by SDS-PAGE. Subsequently, total proteins were visualized by coomassie staining, then gels were dried and phosphorylated proteins were visualized by autoradiography.

Results

Identification of novel MICAL-1 binding partners

MICALs form a recently discovered and unusual family of evolutionary conserved cytoplasmic proteins composed of an enzymatically active flavoenzyme followed by several protein interaction domains or motifs (18). One *MICAL* gene has been identified in *Drosophila* (*Mical*), while humans and mice have three different *MICAL* genes (*MICAL-1*, *-2* and *-3*) (26, 37, 39). Genetic inactivation of *Mical* in fruit flies leads to defects in neural circuit development, myofilament organization, and bristle formation (2, 13, 15, 39). Although *Drosophila* Mical has been implicated in the control of F-actin assembly (13), the molecular pathways employed by MICAL proteins to exert their diverse cellular effects remain largely uncharacterized, especially in vertebrate species. To obtain more insight into the MICAL signaling complex and related functions, we used a retroviral vector system to generate L cell lines that stably express a Flag/HA-tagged version of mouse MICAL-1 (Fig. 1A), the best-characterized vertebrate MICAL to date (37). Mouse L cell fibroblasts were used because of their murine origin, their endogenous MICAL-1 expression and the ability of a constitutively active MICAL-1 construct to induce morphological changes in these cells (Fig. S1A and 1B). This suggests that L cells contain signaling proteins that are crucial for MICAL-1 function. Clonal cell lines were obtained by retroviral transduction followed by puromycin selection, resulting in several clones expressing MICAL-1-Flag/HA at near endogenous levels (Fig. S1C, S1D). One of these lines (D1) was used for large-scale affinity purification of MICAL-1-Flag/HA complexes followed by silver staining, in-gel tryptic digestion, and mass spectrometry analysis. L cells with integrated empty retroviral vector served as a control (C0) (Fig. 1B and S1E). The mass spectrometry analysis identified several proteins that were found in protein complexes from pull-down assays using D1 but not C0 cell extracts. The most significant hits included the GTP-binding cytoskeletal protein septin-9 (42), the serine-threonine kinase NDR1 (12), and the actin-binding protein filamin-B (35) (Table 1).

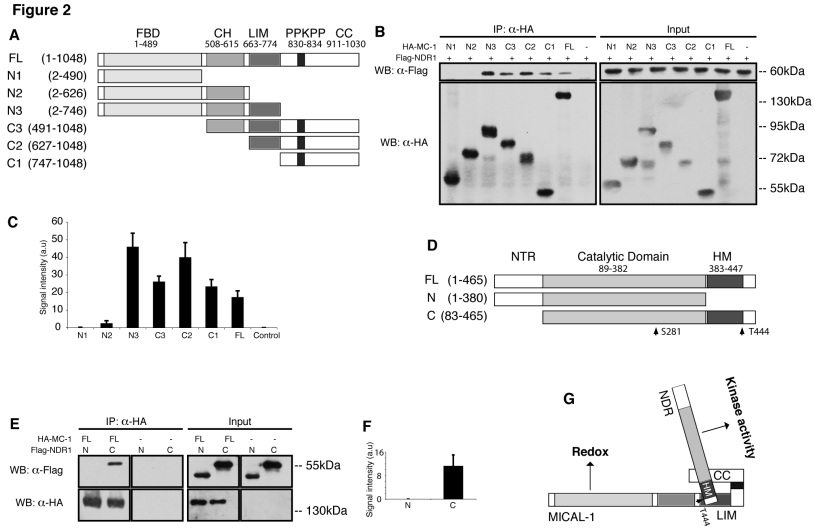

Figure 2. MICAL-1 and NDR1 interact through domains involved in the regulation of their enzymatic activity. (A) Schematic representation of the domain structure of full-length (FL) mouse MICAL-1 and its truncation mutants. Numbers indicate amino acid positions. (B) Lysates of HEK293 cells transfected with Flag-NDR1 and HA-tagged full-length or truncated MICAL-1 were immunoprecipitated with anti-HA antibody and analyzed by western blotting (WB). (C) Microdensitometry of Flag-NDR1 co-immunoprecipitated with HA-MICAL-1 (full-length or truncation mutants) from three independent experiments similar to (B). Data are means ± SD. (D) Schematic depicting NDR1 and its truncation mutants with conserved domains indicated. Position of the Ser281 and Thr444 regulatory phosphorylation sites is shown. HM, hydrophobic motif; NTR, N-terminal regulatory. Numbers indicate amino acid positions. (E) Lysates of HEK293 cells transfected with HA-MICAL-1 and Flag-tagged full-length or truncated NDR1 were immunoprecipitated with anti-HA antibody and analyzed by western blotting. (F) Microdensitometry of Flag-NDR1 co-immunoprecipitated with HA-MICAL-1 from three independent experiments similar to (E). Data are means ± SD. (G) A schematic of the identified interactions between MICAL-1 and NDR1. The LIM and C-terminal domains of MICAL-1 interact with the C-terminal region of NDR1 harboring the hydrophobic motif and the regulatory Thr444 phosphorylation site.

MICAL-1 interacts with NDR1 and NDR2 kinases

Since NDR kinases and MICALs display an intriguing overlap in their reported cellular functions (e.g. neurite growth/patterning and cytoskeletal dynamics (12, 18)), we focused our efforts in this study on understanding the role of MICAL-1/NDR interactions. First, the validity of the NDR1 mass spectrometry result was confirmed by western blotting of independent pull-down samples from C0 and D1 cells with a NDR1 specific antibody. A prominent 55 kDa band was present specifically in the D1 lane following anti-Flag pull-down (Fig. 1C). Immunoprecipitation experiments from HEK293 cells co-expressing myc-MICAL-1 and Flag-NDR1 further confirmed the interaction of MICAL-1 with NDR1 (Fig. 1D). Using several of the available antibodies, we were unsuccessful in staining for endogenous NDR1 or NDR2 in cells (see also (8, 10)). However, fluorescence microscopic analysis of COS-7 cells transfected with epitope-tagged MICAL-1 and NDR1 showed that the distribution of both proteins partially overlapped in the cytoplasm and in specific membrane regions (data not shown).

Two NDR kinases have been identified, NDR1 and NDR2 (12). NDR1 and NDR2 are ~87% identical at the amino acid level and one of the peptides identified in our mass spectrometry analysis was shared

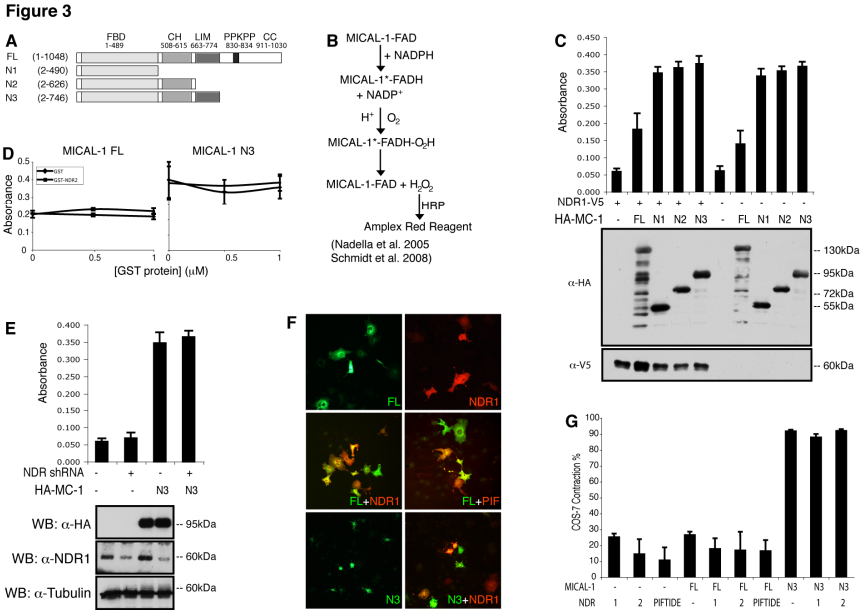

Figure 3. NDR kinases have no effect on MICAL-1 enzymatic or cell contraction activity.
(A) Schematic representation of the domain structure of full-length (FL) mouse MICAL-1 and truncation mutants used for H_2O_2 and COS-7 contraction assays. Numbers indicate amino acid positions. (B) Overview of the enzyme-linked assay used to determine H_2O_2 levels in two different experiments (see C and D). Adapted from (25, 28). (C-E) Cell lysates (C, E; (28)) and purified proteins (D; (25)) were used to study MICAL-1 enzymatic activity in the presence or absence of NDR1/2 kinases. (C, E) Measurement of H_2O_2 production from lysates of HEK293 (C) or L cells (E) transfected with the indicated constructs in the presence of 200 μM NADPH. The lower parts of panels C and E show a representative western blot analysis of lysates used for enzymatic reactions. NDR shRNA targets NDR1 and NDR2. (D) Measurement of H_2O_2 production from purified full-length (FL) and truncated (N3) MICAL-1 proteins in the presence of different concentrations of GST or GST-NDR2. (F) COS-7 cells were transfected with the indicated MICAL-1 constructs alone or in combination with NDR1 (1), NDR2 (2) or NDR1-PIFtide (PIF). Transfected cells were immunostained with anti-GFP (MICAL-1; green) and anti-Flag (NDR1; red) antibodies. (G) Quantification of the cell contraction experiments shown in E (mean ± SEM). Cells with an area ≤1600 μm2 were defined as contracted.

between NDR1 and NDR2 (Fig. S2). It is therefore possible that MICAL-1 also binds to NDR2. To test this idea, HA-MICAL-1 and Flag-NDR2 were co-expressed in HEK293 cells followed by pull-down with anti-Flag antibody. Indeed, HA-MICAL-1 co-precipitated with Flag-NDR2 (Fig. 1E). A similar result was obtained following co-immunoprecipitation of recombinant GST-NDR2 and HA-MICAL-1 protein purified from HEK293 cells (Fig. 1F). To determine whether the interaction between MICAL-1 and NDR1/2 was direct, the C-terminal region of MICAL-1 (C1; Fig. 2A) was purified from bacteria and used in a co-immunoprecipitation experiment with GST-NDR2. The ability of GST-NDR2 to co-precipitate MICAL-1 C1 indicates a direct interaction between NDR2 and the C-terminal region of MICAL-1 (Fig. 1G). Finally, we performed co-immunoprecipitation experiments from naïve L cell lysates using MICAL-1- and NDR-specific antibodies. Importantly, endogenous MICAL-1 co-precipitated with endogenous NDR1 and NDR2, and vice versa, from naïve L cell extracts indicating that in L cells endogenous MICAL-1/NDR1 complexes can be formed (Fig. 1H and data not shown).

Figure 4. MICAL-1 is a phosphoprotein but not a substrate of NDR2.
(A) Lysates from HEK293 cells overexpressing HA-MICAL-1 were subjected to immunoprecipitation with anti-HA antibodies, separated on a gradient gel and stained with Pro-Q phosphoprotein stain or Coomassie stained to visualize all protein. The full-length form of mouse MICAL-1 is phosphorylated. Similar results were obtained with endogenous MICAL-1 protein precipitated from Neuro2A cells or brain lysate (data not shown). (B) HA-MICAL-1, immunoprecipitated from HEK293 cells, was used in an in vitro kinase assay with recombinant GST-NDR2. Right panel, western blotting was used to detect HA-MICAL-1 and GST-NDR2 input. MICAL-1 does not display increased phosphorylation in the presence of GST-NDR2. Vice versa, NDR2 autophosphorylation (indicated by the 80 kDa bands) is unaffected by MICAL-1.

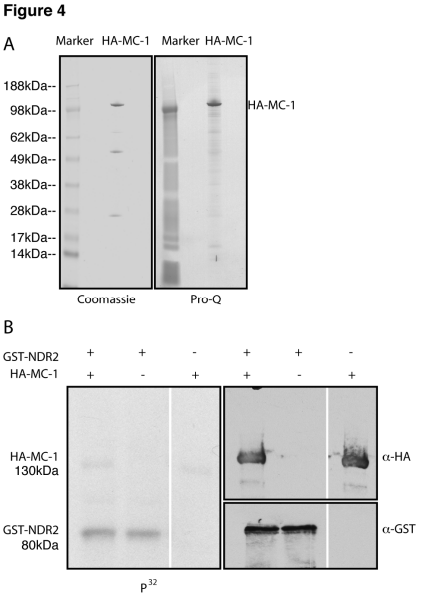

MICAL-1 and NDR1 interact through domains involved in the regulation of their enzymatic activity
Both MICAL-1 and NDR1 are multi-domain proteins. MICAL-1 contains an N-terminal flavoprotein monooxygenase (FM) domain, a calponin homology domain, a LIM domain, proline-rich sequences, and coiled-coil motifs (Fig. 2A). NDR kinases contain an N-terminal regulatory (NTR) domain, a catalytic domain, and a C-terminal hydrophobic motif (HM) (Fig. 2D). To determine the domains required for MICAL-1/NDR1 interactions a series of truncation mutants were generated for MICAL-1 (Fig. 2A) (28) and NDR1 (Fig. 2D) (10) and used in pull-down assays from HEK293 cells co-expressing mutants for MICAL-1 or NDR1 with full-length NDR1 or MICAL-1, respectively. Co-precipitation of endogenous MICAL-1 or NDR1 proteins was not detected in these experimental settings (data not shown). Intriguingly, constructs containing the LIM (N3, C3 and C2) and/or C-terminal domain (C3-C1) of MICAL-1 showed binding to NDR1, indicating that both domains are required for association with NDR1 (Fig. 2B, C). Since intramolecular interactions between the LIM and C-terminal domains of MICAL-1 have been reported to enforce an autoinhibited protein conformation preventing flavoenzyme activity (28), this suggests that NDR1 might bind MICAL-1 in its autoinhibited state. Vice versa, the NDR1 C-terminal region was required for interaction with MICAL-1 (Fig. 2E, F). This is intriguing because the NDR1 C-terminal region harbors the hydrophobic motif surrounding the Thr444 site, whose phosphorylation by MST kinases is required for full NDR1 kinase activity (23, 32, 38). In all, our results reveal an endogenous interaction between MICAL-1 and NDR1. Furthermore, NDR1 associates with two domains of MICAL-1 crucial for regulating its enzymatic activity, while reciprocally MICAL-1 binds a region of NDR1 contributing to the control of NDR kinase activity (Fig. 2G).

MICAL-1 negatively regulates NDR1 kinase activation
To unveil the functional role of MICAL-1/NDR interactions, we first explored the idea that NDR kinases regulate MICAL-1. Thus far, two properties of MICAL-1 have been characterized in detail. First, MICAL-1 is a NADPH-dependent flavoprotein monooxygenase with redox activity (25, 30). Second, C-terminally truncated MICAL-1 proteins (N1-N3; Fig. 2A) induce cell contraction in culture (28). This contraction

Figure 5

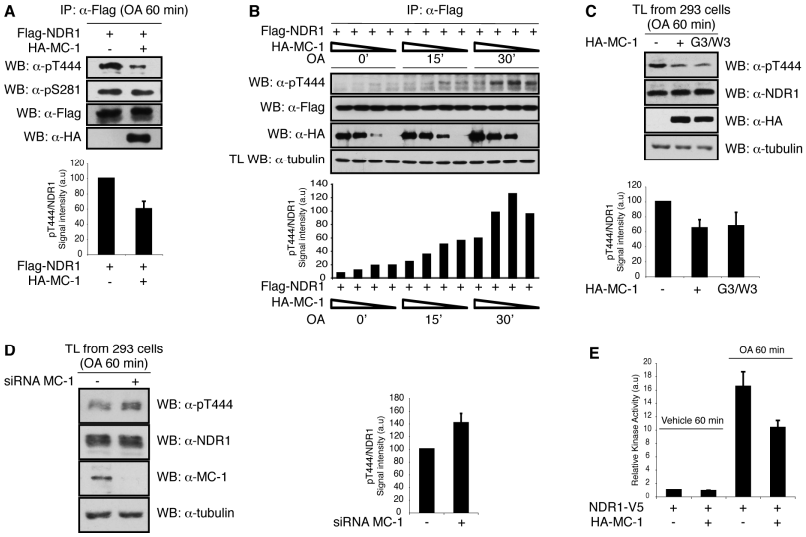

Figure 5. MICAL-1 negatively regulates NDR1 kinase activation and activity.
(A) HEK293 cells were transfected with Flag-NDR1 alone or in combination with HA-MICAL-1, treated with okadaic acid (OA) for 60 min and immunoprecipitated with anti-Flag antibody. Thr444 and Ser281 phosphorylation of precipitated NDR1 was assessed by western blotting (WB) using phospho-specific antibodies. Lower part, microdensitometry from three independent experiments. Data are means ± SD. (B) HEK293 cells were transfected with Flag-NDR1 in the absence or presence of different amounts of HA-MICAL-1 and treated with OA for the indicated periods of time. Lysates were immunoprecipitated with anti-Flag antibodies, analyzed by western blotting and quantified (lower panel). The graph shows microdensitometry of a representative experiment. (C) HEK293 cells were transfected with pRK5 (-), HA-MICAL-1 (+) or HA-MICAL-1 G3/W3 (G3/W3), treated with OA for 60 min and total lysate (TL) was analyzed by western blotting with the indicated antibodies. Lower part, microdensitometry from three independent experiments. Data are means ± SD. (D) HEK293 cells were transfected with a SMARTpool of ON-TARGET siRNAs against MICAL-1 (+) or with a pool of scrambled control siRNAs (-), treated with OA for 60 min, followed by western blotting with the indicated antibodies. Graph on the right shows microdensitometry from three independent experiments. Data are means ± SD. (E) HEK293 cells were transfected with NDR1-V5, alone or in combination with HA-MICAL-1, and treated with vehicle or OA. Immunoprecipitated NDR1-V5 protein was used for NDR peptide kinase assays. Data from a representative experiment with two replicates is shown. Error bars represent SDs.

response is most likely dependent on the FM domain and on redox activity as mutagenesis of essential glycine residues in the MICAL-1 FM domain leads to loss of N1-induced cell contraction (data not shown). Intramolecular interactions between the LIM and C-terminal domains of MICAL-1 can inhibit FM activity (28). Because NDR1 associates with both domains it is tempting to speculate that NDR kinases regulate MICAL-1 activity. To test this hypothesis, an enzyme-linked assay was used to determine the effect of NDR1/2 on MICAL-1 enzymatic activity based on H_2O_2 production (Fig. 3A, B) (25, 28). In line with previous observations, FL MICAL-1 only produced low levels of H_2O_2 whereas constitutively active MICAL-1 N1-N3 truncation mutants showed high enzymatic activity (Fig. 3A-D) (25, 28). In a recent study it was shown that co-transfection of the putative MICAL-1 substrate collapsin response mediator protein-2 (CRMP-2) with MICAL-1 in cells leads to a reduction in MICAL-1 N1-N3 H_2O_2 enzymatic activity. Similarly, recombinant GST-CRMP-2 induced a reduction in MICAL-1 N3 enzymatic activity (28). It was proposed that rather then producing H_2O_2 MICAL-1 may perform redox reactions on CRMP-2 in the presence of this substrate (28). In contrast to these findings, MICAL-1 activity was not inhibited by the co-

Figure 6

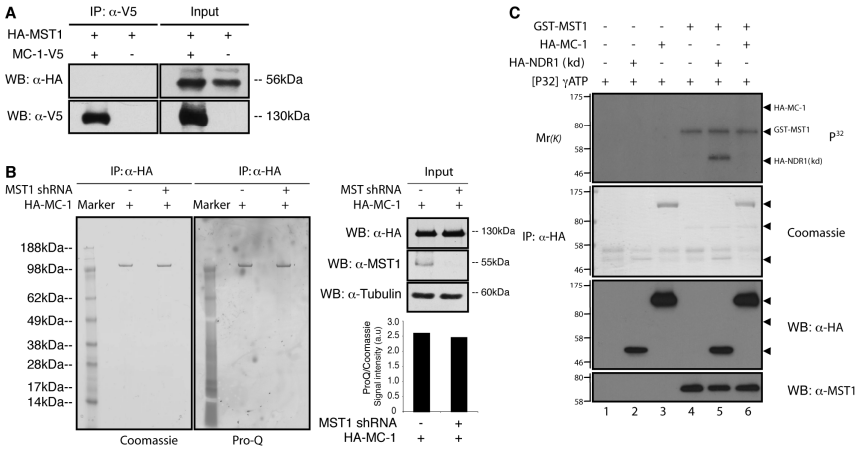

Figure 6. MICAL-1 is not a substrate for MST1 kinase.
(A) Lysates from HEK293 cells transfected with HA-MST1 alone or in combination with MC-1-V5 were immunoprecipitated with anti-V5 antibodies followed by western blotting (WB). (B) Lysates of U2OS T-rex cells were transfected with HA-MC-1 and treated with vehicle (-) or tetracycline (+) to induce MST1 shRNA expression. Lysates were subjected to immunoprecipitation with anti-HA antibodies followed by coomassie or ProQ staining or WB with the indicated antibodies. Graph shows microdensitometry from a representative experiment. (C) Lysates of COS-7 cells transiently expressing empty vector, HA-NDR1 kinase-dead, or HA-MC-1 were subjected to immunoprecipitation with anti-HA antibody. Immunopurified proteins were then processed for kinase assays without or with GST-MST1. Then proteins were separated by SDS-PAGE and visualized either by autoradiography (upper panel) or coomassie staining (upper middle panel). In parallel, samples were analyzed by western blotting using anti-HA and anti-MST1 antibodies. The positions of HA-MC-1, GST-MST1, and HA-NDR1(kd) are indicated by arrowheads.

transfection of NDR1 or by the addition of recombinant NDR2. Furthermore, NDR1/2 did not alter the enzymatic activity of FL MICAL-1 (Fig. 3C, D). In addition, shRNA-mediated knockdown of NDR1/2 in L cells did not affect the enzymatic activity of MICAL-1 N3 (Fig. 3E). Previous work has shown that co-transfection of FL MICAL-1 with CRMP-2 or plexinA1 induces COS-7 cell contraction (28). However, co-expression of NDR1/2 or a constitutively active form of NDR1 (NDR1-PIFTIDE (33)) with FL MICAL-1 did not induce cell contraction nor did NDR1/2 overexpression or knockdown influence contraction triggered by N3 (Fig. 3F, G; data not shown). These experiments argue against a role for NDR1/2 in the control of MICAL-1 enzymatic and contraction activity. We next determined whether MICAL-1 could serve as a substrate for NDR kinases. Although we were able to establish that MICAL-1 is a phosphoprotein (Fig. 4A), GST-NDR2 failed to phosphorylate MICAL-1 in an in vitro kinase assay indicating that MICAL-1 is not a NDR2 substrate (Fig. 4B). Unfortunately, production of GST-NDR1 protein is notoriously difficult and we were unable to obtain sufficient quantities of NDR1 for kinase assays. In summary, our results strongly argue against a direct role for NDR1/2 in regulating MICAL-1 enzymatic activity and, subsequent, cell morphological changes.

Therefore, we next examined whether MICAL-1 may regulate NDR kinases. Multi-site phosphorylation is a general control mechanism of NDR1 and NDR2, which contain two main regulatory phosphorylation sites: Ser281/282 (NDR1/2, the activation segment) and Thr444/442 (the hydrophobic motif) (Fig. 2D). Upon MOB-1A binding to the N-terminal region Ser281/282 is autophosphorylated, whereas Thr444/442 is targeted by upstream MST kinases (12). Treatment of cells with okadaic acid (OA), which preferentially

Figure 7

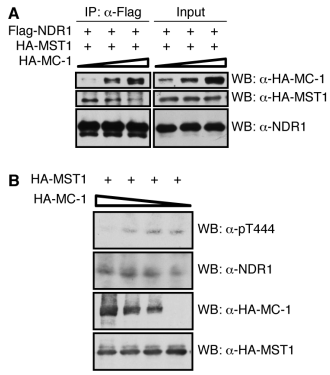

Figure 7. MICAL-1 competes with MST1 for NDR1 binding.
(A) Lysates from HEK293 cells transfected with Flag-NDR1, HA-MST1 or HA-MICAL-1 were mixed as indicated, immunoprecipitated with anti-Flag antibodies and analyzed by western blotting (WB). (B) HEK293 cells were transfected with HA-MST1 in the presence of different amounts of HA-MICAL-1. Lysates were subjected to WB with the indicated antibodies.

inhibits protein phosphatase 2A, results in increased Ser281/282 and Thr444/442 phosphorylation and elevated NDR1/2 kinase activity (3, 32, 38). To study potential effects of MICAL-1 on NDR1/2, we treated HEK293 cells transfected with Flag-NDR1 alone or in combination with HA-MICAL-1 with OA and assessed Ser281 and Thr444 phosphorylation of precipitated Flag-NDR1 protein using phospho-specific antibodies (Fig. 5A). Sixty minutes of OA treatment strongly induced Ser281 and Thr444 phosphorylation (data not shown). MICAL-1 overexpression did not influence OA-induced Ser281 autophosphorylation (Fig. 5A). Consistent with these data we did not find an effect of MICAL-1 on GST-NDR2 autophosphorylation in kinase assays (Fig. 4B). It should be noted, however, that the currently available p-Ser281 antibody is not suitable for work with endogenous NDR kinases (unpublished data). In striking contrast, overexpression of HA-MICAL-1 drastically inhibited phosphorylation of Flag-NDR1 on Thr444 following OA treatment (Fig. 5A). This effect was dose-dependent as higher levels of HA-MICAL-1 were more efficient in lowering OA-induced NDR1 phosphorylation (Fig. 5B). Furthermore, MICAL-1 reduced Thr444 phosphorylation of endogenous NDR1 and NDR2 following OA treatment (Fig. 5C). It has been reported that at certain concentrations H_2O_2 can inhibit Thr444 phosphorylation (8). Since the MICAL-1 FM domain can produce H_2O_2 under specific conditions or potentially facilitate other redox reactions (Fig. 3; (25, 28)) we next asked whether MICAL-1 enzymatic activity mediates the negative effect of MICAL-1 on Thr444 phosphorylation. Site-directed mutagenesis was used to mutate the first FAD fingerprint in the MICAL-1 FM domain. These mutations disrupt FAD binding and block enzymatic activity without affecting the overall structure of the protein (19, 21, 44). MICAL-1 FL G3/W3 could, however, still reduce OA-induced Thr444 phosphorylation suggesting that the inhibitory effect of MICAL-1 on Thr444 phosphorylation is independent of its enzymatic activity (Fig. 5C).

Next, to establish the physiological relevance of the MICAL-1 effect, the level of endogenous MICAL-1 in HEK293 cells was decreased by siRNA. In line with our previous results, knockdown of MICAL-1 resulted in an increased level of Thr444 phosphorylation triggered by OA as compared to control (Fig. 5D). Thus, MICAL-1 is an endogenous negative regulator of NDR1 activation in HEK293 cells. Since phosphorylation of Thr444 is required for full kinase activity we next examined the ability of MICAL-1 to reduce NDR1 kinase activity on NDR substrate peptide (Fig. 5E). NDR1-V5 was expressed in HEK293 cells, alone or in combination with HA-MICAL-1, immunoprecipitated and used in a peptide kinase assay. In line with its negative effect on Thr444 phosphorylation, MICAL-1 robustly inhibited NDR1 kinase activity reducing peptide phosphorylation by about 40%. In conclusion, our results show that MICAL-1 is an endogenous negative regulator of NDR1 activation that inhibits T444 phosphorylation thereby contributing to the control of NDR kinase activity.

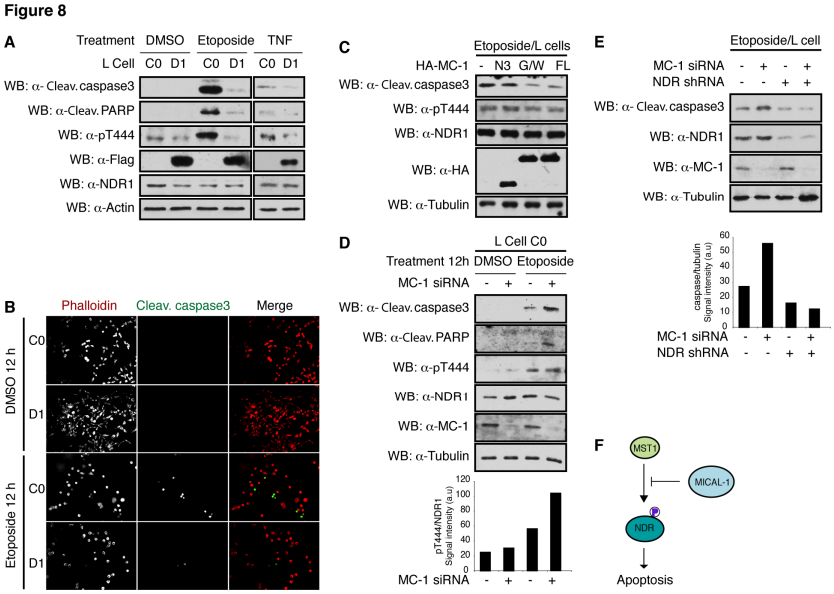

Figure 8. MICAL-1 inhibits NDR-dependent apoptotic signaling.
(A) Stable C0 and D1 L cells were treated with control compound (DMSO or CHX (not shown)), etoposide or TNFα/CHX (4, 40). Lysates were processed for western blotting using the indicated antibodies. (B) Stable C0 and D1 L cells were treated as in (A) and immunostained using phalloidin-TRITC (red), to visualize cell morphology, and anti-cleaved caspase-3 (green) antibody. (C) L cells were transiently transfected with empty vector or constructs for FL MICAL-1, FL MICAL-1 G3/W3 or MICAL-1 N3, treated with etoposide and processed for western blotting using the indicated antibodies. (D) L cells were transfected with non-targeting control siRNA (-) or with siRNA oligos targeting mouse MICAL-1 (+), treated as in (A) and processed for western blotting using the indicated antibodies. Graph shows a quantification of the experiment. (E) L cells were transfected with non-targeting control siRNA or shRNA (-), siRNA oligos targeting mouse MICAL-1 (+), shRNA constructs targeting NDR1/2, or combinations thereof, treated as in (A) and processed for western blotting using the indicated antibodies. Graph shows a quantification of the experiment. (F) Schematic representation of the inhibitory role of MICAL-1 in the MST1-NDR signaling pathway during apoptosis.

MICAL-1 negatively regulates the activation of NDR1 kinase by competing with MST1 for NDR1 binding

Phosphorylation on Thr444/442 of NDR1 and NDR2 can be mediated by MST kinases (32, 40). MST1 can physically associate with the C-terminal hydrophobic motif of NDR1/2 and phosphorylate Thr444/442 upon activation by upstream signals such as RASSF1A. MST1-induced NDR1/2 activation plays a crucial role downstream of RASSF1A in the apoptotic response to death receptor stimulation (40). Therefore, the association of MICAL-1 with the NDR C-terminal region and its ability to reduce Thr444 phosphorylation induced by OA invites the speculation that MICAL-1 regulates NDR kinase activation by interfering with the function of MST kinases. One possible mechanism could be that MICAL-1 associates with MST kinases and thereby controls their function. To test this model, we examined whether MICAL-1 can associate with MST1 following overexpression in cells. Although MST1 bound NDR1 (data not shown; (40)) no interaction between MST1 and MICAL-1 was observed (Fig. 6A). Alternatively, MICAL-1 may serve as a substrate for MST1 competing with NDR kinases for phosphorylation. Therefore, the phosphorylation status of MICAL-1 was determined following shRNA-mediated knockdown of MST1 in cells. Interestingly, MICAL-1 phosphorylation was not affected by MST1 knockdown (Fig. 6B). To further test whether the

regulation of NDR kinases by MICAL-1 involved the phosphorylation of MICAL-1 by MST1 kinase, we analyzed MICAL-1 as a MST1 substrate. This revealed that while NDR1(kd) was strongly phosphorylated by recombinant MST1 (Fig. 6C, lane 5), purified MICAL-1 was not (Fig. 6C, lane 6), although MICAL-1 was present at higher abundance than NDR1. As expected active MST1 also autophosphorylated itself (Fig. 6C, lanes 4-6) and all phosphorylation events were dependent on the presence of active MST1 (Fig. 6C, lanes 1-3). Notably, no effect of MICAL-1 expression on MST1 autophosphorylation was observed. Taken together, these findings suggest that MICAL-1 is not a MST1 substrate, arguing against the possibility that MICAL-1 interferes with phosphorylation of NDR by MST1 through serving as an alternative MST1 substrate.

A third possibility is that MICAL-1 competes with MST kinases for binding on the hydrophobic motif of NDR1. To test this idea, lysates from HEK293 cells expressing Flag-NDR1 and HA-MST1 were mixed with increasing amounts of lysates from HA-MICAL-1-expressing cells followed by anti-Flag immunoprecipitation. Increasing MICAL-1 levels led to a reduction in the amount of MST1 that co-immunoprecipitated with NDR1 despite similar MST1 input levels (Fig. 7A). As reported previously (11, 40), overexpression of MST1 leads to an increase in Thr444 phosphorylation (data not shown). To examine whether overexpression of MICAL-1 not only reduces MST1 binding but also causes a consequent decrease in MST1-induced Thr444 phosphorylation we expressed HA-MST1 in combination with increasing amounts of HA-MICAL-1 and monitored Thr444 phosphorylation of endogenous NDR1/2. Indeed, MICAL-1 decreased MST1-induced Thr444 phosphorylation in a dose-dependent manner (Fig. 7B). In all, these results establish that MICAL-1 interferes with the binding of MST1 to NDR1/2 thereby negatively regulating MST1-induced NDR phosphorylation at the hydrophobic motif.

MICAL-1 interferes with apoptosis signaling

Since our findings indicate that MICAL-1 negatively regulates MST1-NDR signaling, we sought to determine whether MICAL-1 could affect a known biological function of the MST1-NDR pathway (40). The activation of NDR1/2 kinases through phosphorylation by MST1 is necessary for apoptosis signaling in mammalian cells (40). In addition, loss of NDR1/2 kinases can result in resistance to apoptosis (4). Therefore, wild-type L cells or stable C0 and D1 cells were treated for 12 h with vehicle or etoposide, a reagent known to induce apoptosis through NDR kinases (4), harvested and analyzed by immunoblotting (Fig. 8A). Etoposide treatment triggered a robust increase in Thr444/442 phosphorylation in wild-type (not shown) and control (C0) cells concomitant with a strong induction of two apoptotic markers, i.e. cleaved PARP and cleaved caspase-3 (Fig. 8A). Furthermore, many cleaved caspase-3-positive C0 cells were detected following etoposide treatment (Fig. 8B). Intriguingly, etoposide exposure of D1 cells expressing MICAL-1-Flag/HA (see Fig. 1) did not result in enhanced Thr444/442 phosphorylation (Fig. 8A). In line with this prominent inhibition of NDR activation, the signals for cleaved PARP and cleaved caspase-3 were dramatically low in D1 as compared to control C0 cells following etoposide treatment (Fig. 8A) and only few cleaved caspase-3-positive D1 cells were detected (Fig. 8B) suggesting that apoptotic signaling is inhibited in D1 cells. Similar results were obtained in a second, independent MICAL-1-Flag/HA expressing stable line (clone D2; not shown). In addition, the activation of NDR kinases (pThr444) and cleavage of caspase-3 and PARP in response to TNFα/CHX, another pro-apoptotic stimulus known to signal through NDR kinases (40), was reduced in D1 as compared to C0 cells (Fig. 8A). CHX alone did not induce apoptosis or affect pThr444 levels ((40); not shown). Finally, to assess whether the inhibitory effect of MICAL-1 on apoptosis was dependent on its MO domain and redox signaling we transiently transfected the constitutively active MICAL-1 N3 mutant or the FL MICAL-1 G3/W3 mutant into L cells and treated these cells with etoposide. Similar to FL MICAL-1, MICAL-1 G3/W3 reduced the etoposide-induced cleavage of caspase-3 (Fig. 8C). No effect of MICAL-1 N3 was observed. These results support the idea that the inhibitory effect of MICAL-1 on apoptosis is independent of its MO domain.

We also addressed the role of endogenous MICAL-1 in apoptosis regulation by RNAi. Wild-type L cells transfected with non-targeting control siRNAs or siRNAs specifically targeting mouse MICAL-1 were treated for 12 h with vehicle or etoposide, harvested and analyzed by immunoblotting (Fig. 8D). In line with our biochemical and overexpression data, knockdown of MICAL-1 resulted in an increase in the overall amount of Thr444/442 phosphorylated NDR and in increased signals for cleaved PARP and cleaved caspase-3 (Fig. 8D). Although etoposide and TNFα can induce apoptosis through the MST1-NDR pathway it is formally possible that the observed effects of MICAL-1 on apoptosis do not involve modulation of NDR signaling. To address this point, L cells were transiently transfected with siRNAs targeting MICAL-1, shRNA constructs targeting NDR1/2 or combinations thereof, followed by etoposide treatment. Knockdown of MICAL-1 led to increased signals for cleaved caspase-3 while, as shown previously (4), knockdown of NDR1/2 inhibited the cleavage of caspase-3 induced by etoposide (Fig. 8E). Interestingly, following simultaneous knockdown of MICAL-1 and NDR1/2 no induction of caspase-3 cleavage was observed indicating that MICAL-1 and NDR1/2 function in the same pathway. In all, we conclude that MICAL-1 has inhibitory effects on pro-apoptotic signaling through the NDR/MST pathway.

Discussion

Phosphorylation of NDR1/2 kinases by MST1 is required for full NDR kinase activity and for the induction of apoptosis in response to pro-apoptotic stimuli (4, 40). The deregulation of NDR1 and MST kinases predisposes to the development of cancer due to compromised apoptotic responses (4, 31). Despite the critical role of MST-induced NDR phosphorylation in different cell biological processes and in disease, it has remained unknown if or how this key phosphorylation event is regulated. Our findings identify MICAL-1 as a novel endogenous negative regulator of MST1-NDR signaling and apoptosis in mammalian cells (Fig. 8F). MICAL-1 specifically and endogenously interacts with the hydrophobic motif of NDR1/2 (Figure 1, 2), co-localizes with NDR1 in cells, and ectopic expression MICAL-1 reduces NDR kinase activation and activity (Figure 5). Knockdown of endogenous MICAL-1, on the other hand, results in increased NDR kinase phosphorylation (Figure 5). Furthermore, we found that MICAL-1 does not bind MST1 nor serves as a MST1 substrate (Figure 6) but competes with MST1 for NDR binding (Figure 7) and thereby reduces MST1-induced NDR activation (Figure 8). In line with this inhibitory effect, overexpression and knockdown studies show that MICAL-1 negatively affects a known biological function of the MST1-NDR1/2 pathway, namely pro-apoptotic signaling (Figure 8). Together, these results uncover a novel and unique regulatory mechanism of MST-NDR signaling.

Binding of MOB1 to the N-terminal region of NDR1/2 stimulates autophosphorylation and NDR activation (3). Kohler and colleagues recently reported that hMOB2 can act as an inhibitor of hMOB1-NDR signaling by competing with hMOB1 for binding to the N-terminal domain of NDR1/2 (16). Here we describe an unexpected additional level of NDR regulation. By competing with MST1 for binding to the C-terminal hydrophobic motif domain MICAL-1 can regulate NDR1/2 activation (Fig. 8F). Together these studies define a novel level of NDR kinase regulation through competitive inhibitors that directly interfere with the binding of key upstream activating signals such as MOB1 and MST1. How these competitive inhibitors are controlled is unknown. It is possible that previously identified MICAL-1 interactors such as plexin proteins contribute to this regulation. Plexins function as evolutionary conserved type I transmembrane receptors for semaphorin proteins in different cell types and organ systems and mediate diverse cellular processes, including apoptosis(7, 27, 46). For example, semaphorin3A can induce neuron or leukemic cell death through plexinA3 and plexinA1, respectively (1, 24). Intriguingly, MICAL-1 can associate with the cytoplasmic domains of the four class A plexins and semaphorin ligand stimulation enhances this interaction ((28); Y.Z. and R.J.P., unpublished observations). Recruitment of MICAL-1 to plexin upon ligand stimulation may reduce the availability of MICAL-1 for inhibiting MST-induced NDR activation leading to enhanced NDR activity and apoptosis. Alternatively, the regulation of MICAL-1

activity by upstream signaling cues such as protein kinases may be crucial for controlling its inhibitory role in the MST-NDR pathway. This idea gains support from the observation that MICAL-1 is phosphorylated in cells and neural tissues (Figure 4A) suggesting it is a substrate for upstream kinases. Future studies will address these and other possible mechanisms.

It is plausible that the MICAL-1-dependent regulatory mechanism delineated in this study also functions in MST- and/or NDR-dependent cellular processes other than apoptosis. For example, the MST1-NDR pathway was recently implicated in the control of centrosome duplication (11). Furthermore, striking similarities exist between the effects of manipulating MST, MICAL and NDR on neuronal morphology. Knockdown of MST3b or overexpression of constitutively active MICAL-1 in cultured mammalian neurons reduces neurite growth (14, 28), while exogenous NDR2 expression enhances neurite growth (34). Loss of *Tricornered* (NDR) or *Hippo* (MST) in *Drosophila* and of *SAX-1* (NDR) in *C. elegans* leads to altered dendritic arborization and tiling defects (i.e. ectopic overlap between individual dendritic trees) (5, 6, 9). Loss of *Drosophila Mical* also results in enlarged dendritic fields due to deficits in dendritic pruning (15). These observations together with our own findings support a model in which MST, MICAL and NDR are components of a common molecular pathway that controls the formation and remodeling of the initial imprecise neuronal network into functional neuronal connections.

In the present study, no effect of NDR1/2 on MICAL-1 enzymatic activity or cell contraction was detected but it is possible that NDR1/2 influences other proposed MICAL effects such as on Rab-mediated vesicle transport (41) or myofilament organization (2). It is also interesting to note that knockdown of MST3b leads to a reduction in CRMP-1, a putative substrate for the MICAL-1 flavoprotein monooxygenase domain (14, 28). Thus, MICAL-1 may not only negatively regulate MST kinases, but MSTs might also influence MICAL-1 function by controlling its substrate levels.

Taken together, this study reveals a previously unknown biological role for MICAL-1 in apoptosis and defines a novel negative regulatory mechanism of MST-NDR signaling. Future experiments are needed to decipher the precise role of MICAL-1 in the activation of NDR kinases by extrinsic and intrinsic apoptotic stimuli. Further elucidation of the role of MICAL-1 in MST/NDR signaling can be expected to open new avenues for the molecular delineation of MST/NDR functioning in different cell biological processes and for understanding how deregulation of this pathway contributes to disease.

Acknowledgements

We thank Dianne van den Heuvel for providing the plexinA4Δecto construct and Jeroen den Hertog and Peter Burbach for comments on the manuscript. Anti-T442/444-P and anti-S281/282-P antibodies were kindly provided by Dr. Brian Hemmings (FMI, Switzerland). This work was supported by the Netherlands Organization for Health Research and Development (ZonMW-VIDI and ZonMW-TOP), the Human Frontier Science Program (HFSP-CDA), and the Genomics Center Utrecht (to R.J.P.). The Fondation Leducq and the British Heart Foundation (to P.H.S and S.J.F.). The European seventh framework program under grant agreement Health-2009-2.1.2-1-242167 (SynSys project, to A.B.S., R.C.v.d.S. and K.W.L.). A.H. is supported by a Wellcome Trust Career Development Research Fellowship.

References

1. **Ben-Zvi, A., O. Manor, M. Schachner, A. Yaron, M. Tessier-Lavigne, and O. Behar.** 2008. The Semaphorin receptor PlexinA3 mediates neuronal apoptosis during dorsal root ganglia development. J Neurosci **28:**12427-32.

2. **Beuchle, D., H. Schwarz, M. Langegger, I. Koch, and H. Aberle.** 2007. Drosophila MICAL regulates myofilament organization and synaptic structure. Mech Dev **124:**390-406.

3. **Bichsel, S. J., R. Tamaskovic, M. R. Stegert, and B. A. Hemmings.** 2004. Mechanism of activation of NDR (nuclear Dbf2-related) protein kinase by the hMOB1 protein. J Biol Chem **279:**35228-35.

4. **Cornils, H., M. R. Stegert, A. Hergovich, D. Hynx, D. Schmitz, S. Dirnhofer, and B. A. Hemmings.** Ablation of the kinase NDR1 predisposes mice to the development of T cell lymphoma. Sci Signal **3:**ra47.

5. **Emoto, K., Y. He, B. Ye, W. B. Grueber, P. N. Adler, L. Y. Jan, and Y. N. Jan.** 2004. Control of dendritic branching and tiling by the Tricornered-kinase/Furry signaling pathway in Drosophila sensory neurons. Cell **119:**245-56.

6. **Emoto, K., J. Z. Parrish, L. Y. Jan, and Y. N. Jan.** 2006. The tumour suppressor Hippo acts with the NDR kinases in dendritic tiling and maintenance. Nature **443:**210-3.
7. **Franco, M., and L. Tamagnone.** 2008. Tyrosine phosphorylation in semaphorin signalling: shifting into overdrive. EMBO Rep **9:**865-71.
8. **Fuller, S. J., S. Pikkarainen, L. Tham el, T. E. Cullingford, J. D. Molkentin, H. Cornils, A. Hergovich, B. A. Hemmings, A. Clerk, and P. H. Sugden.** 2008. Nuclear Dbf2-related protein kinases (NDRs) in isolated cardiac myocytes and the myocardium: activation by cellular stresses and by phosphoprotein serine-/threonine-phosphatase inhibitors. Cell Signal **20:**1564-77.
9. **Gallegos, M. E., and C. I. Bargmann.** 2004. Mechanosensory neurite termination and tiling depend on SAX-2 and the SAX-1 kinase. Neuron **44:**239-49.
10. **Hergovich, A., S. J. Bichsel, and B. A. Hemmings.** 2005. Human NDR kinases are rapidly activated by MOB proteins through recruitment to the plasma membrane and phosphorylation. Mol Cell Biol **25:**8259-72.
11. **Hergovich, A., R. S. Kohler, D. Schmitz, A. Vichalkovski, H. Cornils, and B. A. Hemmings.** 2009. The MST1 and hMOB1 tumor suppressors control human centrosome duplication by regulating NDR kinase phosphorylation. Curr Biol **19:**1692-702.
12. **Hergovich, A., M. R. Stegert, D. Schmitz, and B. A. Hemmings.** 2006. NDR kinases regulate essential cell processes from yeast to humans. Nat Rev Mol Cell Biol **7:**253-64.
13. **Hung, R. J., U. Yazdani, J. Yoon, H. Wu, T. Yang, N. Gupta, Z. Huang, W. J. van Berkel, and J. R. Terman.** Mical links semaphorins to F-actin disassembly. Nature **463:**823-7.
14. **Irwin, N., Y. M. Li, J. E. O'Toole, and L. I. Benowitz.** 2006. Mst3b, a purine-sensitive Ste20-like protein kinase, regulates axon outgrowth. Proc Natl Acad Sci U S A **103:**18320-5.
15. **Kirilly, D., Y. Gu, Y. Huang, Z. Wu, A. Bashirullah, B. C. Low, A. L. Kolodkin, H. Wang, and F. Yu.** 2009. A genetic pathway composed of Sox14 and Mical governs severing of dendrites during pruning. Nat Neurosci **12:**1497-505.
16. **Kohler, R. S., D. Schmitz, H. Cornils, B. A. Hemmings, and A. Hergovich.** Differential NDR/LATS Interactions with the Human MOB Family Reveal a Negative Role for hMOB2 in the Regulation of Human NDR Kinases. Mol Cell Biol.
17. **Kolk, S. M., R. A. Gunput, T. S. Tran, D. M. van den Heuvel, A. A. Prasad, A. J. Hellemons, Y. Adolfs, D. D. Ginty, A. L. Kolodkin, J. P. Burbach, M. P. Smidt, and R. J. Pasterkamp.** 2009. Semaphorin 3F is a bifunctional guidance cue for dopaminergic axons and controls their fasciculation, channeling, rostral growth, and intracortical targeting. J Neurosci **29:**12542-57.
18. **Kolk, S. M., and R. J. Pasterkamp.** 2007. MICAL flavoprotein monooxygenases: structure, function and role in semaphorin signaling. Adv Exp Med Biol **600:**38-51.
19. **Kubo, A., S. Itoh, K. Itoh, and T. Kamataki.** 1997. Determination of FAD-binding domain in flavin-containing monooxygenase 1 (FMO1). Arch Biochem Biophys **345:**271-7.
20. **Lahiry, P., A. Torkamani, N. J. Schork, and R. A. Hegele.** Kinase mutations in human disease: interpreting genotype-phenotype relationships. Nat Rev Genet **11:**60-74.
21. **Lawton, M. P., and R. M. Philpot.** 1993. Functional characterization of flavin-containing monooxygenase 1B1 expressed in Saccharomyces cerevisiae and Escherichia coli and analysis of proposed FAD- and membrane-binding domains. J Biol Chem **268:**5728-34.
22. **Li, K. W., S. Miller, O. Klychnikov, M. Loos, J. Stahl-Zeng, S. Spijker, M. Mayford, and A. B. Smit.** 2007. Quantitative proteomics and protein network analysis of hippocampal synapses of CaMKIIalpha mutant mice. J Proteome Res **6:**3127-33.
23. **Millward, T. A., D. Hess, and B. A. Hemmings.** 1999. Ndr protein kinase is regulated by phosphorylation on two conserved sequence motifs. J Biol Chem **274:**33847-50.
24. **Moretti, S., A. Procopio, R. Lazzarini, M. R. Rippo, R. Testa, M. Marra, L. Tamagnone, and A. Catalano.** 2008. Semaphorin3A signaling controls Fas (CD95)-mediated apoptosis by promoting Fas translocation into lipid rafts. Blood **111:**2290-9.
25. **Nadella, M., M. A. Bianchet, S. B. Gabelli, J. Barrila, and L. M. Amzel.** 2005. Structure and activity of the axon guidance protein MICAL. Proc Natl Acad Sci U S A **102:**16830-5.
26. **Pasterkamp, R. J., H. N. Dai, J. R. Terman, K. J. Wahlin, B. Kim, B. S. Bregman, P. G. Popovich, and A. L. Kolodkin.** 2006. MICAL flavoprotein monooxygenases: expression during neural development and following spinal cord injuries in the rat. Mol Cell Neurosci **31:**52-69.
27. **Pasterkamp, R. J., and R. J. Giger.** 2009. Semaphorin function in neural plasticity and disease. Curr Opin Neurobiol **19:**263-74.
28. **Schmidt, E. F., S. O. Shim, and S. M. Strittmatter.** 2008. Release of MICAL autoinhibition by semaphorin-plexin signaling promotes interaction with collapsin response mediator protein. J Neurosci **28:**2287-97.
29. **Shevchenko, A., M. Wilm, O. Vorm, and M. Mann.** 1996. Mass spectrometric sequencing of proteins silver-stained polyacrylamide gels. Anal Chem **68:**850-8.
30. **Siebold, C., N. Berrow, T. S. Walter, K. Harlos, R. J. Owens, D. I. Stuart, J. R. Terman, A. L. Kolodkin, R. J. Pasterkamp, and E. Y. Jones.** 2005. High-resolution structure of the catalytic region of MICAL (molecule interacting with CasL), a multidomain flavoenzyme-signaling molecule. Proc Natl Acad Sci U S A **102:**16836-41.

31. **Song, H., K. K. Mak, L. Topol, K. Yun, J. Hu, L. Garrett, Y. Chen, O. Park, J. Chang, R. M. Simpson, C. Y. Wang, B. Gao, J. Jiang, and Y. Yang.** Mammalian Mst1 and Mst2 kinases play essential roles in organ size control and tumor suppression. Proc Natl Acad Sci U S A **107:**1431-6.
32. **Stegert, M. R., A. Hergovich, R. Tamaskovic, S. J. Bichsel, and B. A. Hemmings.** 2005. Regulation of NDR protein kinase by hydrophobic motif phosphorylation mediated by the mammalian Ste20-like kinase MST3. Mol Cell Biol **25:**11019-29.
33. **Stegert, M. R., R. Tamaskovic, S. J. Bichsel, A. Hergovich, and B. A. Hemmings.** 2004. Regulation of NDR2 protein kinase by multi-site phosphorylation and the S100B calcium-binding protein. J Biol Chem **279:**23806-12.
34. **Stork, O., A. Zhdanov, A. Kudersky, T. Yoshikawa, K. Obata, and H. C. Pape.** 2004. Neuronal functions of the novel serine/threonine kinase Ndr2. J Biol Chem **279:**45773-81.
35. **Stossel, T. P.** Filamins and the potential of complexity. Cell Cycle **9**.
36. **Suto, F., K. Ito, M. Uemura, M. Shimizu, Y. Shinkawa, M. Sanbo, T. Shinoda, M. Tsuboi, S. Takashima, T. Yagi, and H. Fujisawa.** 2005. Plexin-a4 mediates axon-repulsive activities of both secreted and transmembrane semaphorins and plays roles in nerve fiber guidance. J Neurosci **25:**3628-37.
37. **Suzuki, T., T. Nakamoto, S. Ogawa, S. Seo, T. Matsumura, K. Tachibana, C. Morimoto, and H. Hirai.** 2002. MICAL, a novel CasL interacting molecule, associates with vimentin. J Biol Chem **277:**14933-41.
38. **Tamaskovic, R., S. J. Bichsel, H. Rogniaux, M. R. Stegert, and B. A. Hemmings.** 2003. Mechanism of Ca2+-mediated regulation of NDR protein kinase through autophosphorylation and phosphorylation by an upstream kinase. J Biol Chem **278:**6710-8.
39. **Terman, J. R., T. Mao, R. J. Pasterkamp, H. H. Yu, and A. L. Kolodkin.** 2002. MICALs, a family of conserved flavoprotein oxidoreductases, function in plexin-mediated axonal repulsion. Cell **109:**887-900.
40. **Vichalkovski, A., E. Gresko, H. Cornils, A. Hergovich, D. Schmitz, and B. A. Hemmings.** 2008. NDR kinase is activated by RASSF1A/MST1 in response to Fas receptor stimulation and promotes apoptosis. Curr Biol **18:**1889-95.
41. **Weide, T., J. Teuber, M. Bayer, and A. Barnekow.** 2003. MICAL-1 isoforms, novel rab1 interacting proteins. Biochem Biophys Res Commun **306:**79-86.
42. **Weirich, C. S., J. P. Erzberger, and Y. Barral.** 2008. The septin family of GTPases: architecture and dynamics. Nat Rev Mol Cell Biol **9:**478-89.
43. **Wessel, D., and U. I. Flugge.** 1984. A method for the quantitative recovery of protein in dilute solution in the presence of detergents and lipids. Anal Biochem **138:**141-3.
44. **Wierenga, R. K., P. Terpstra, and W. G. Hol.** 1986. Prediction of the occurrence of the ADP-binding beta alpha beta-fold in proteins, using an amino acid sequence fingerprint. J Mol Biol **187:**101-7.
45. **Zhao, B., L. Li, Q. Lei, and K. L. Guan.** The Hippo-YAP pathway in organ size control and tumorigenesis: an updated version. Genes Dev **24:**862-74.
46. **Zhou, Y., R. A. Gunput, and R. J. Pasterkamp.** 2008. Semaphorin signaling: progress made and promises ahead. Trends Biochem Sci **33:**161-70.

Supplemental Figures

Supplemental Figure 1. Generation of stable mouse L cell lines expressing MICAL-1-Flag/HA.

(A) L cell fibroblast lysates were processed for western blotting (WB) with a polyclonal anti-mouse MICAL-1 (MC-1) antibody. Adult mouse brain lysates were used as a positive control for MICAL-1 expression. L cells endogenously expressed MICAL-1. (B) Expression of a MICAL-1 protein lacking its C-terminal region (N3) but not full-length MICAL-1 induces COS-7 cell contraction (28). To establish whether MICAL-1 N3 can also induce contraction in murine cell lines, mouse L cells were transiently transfected with cDNAs for GFP, full-length mouse myc-tagged MICAL-1 (MC-1 FL), C-terminally truncated myc-tagged mouse MICAL-1 (MC-1 N3), or Flag-tagged mouse plexinA4 lacking its extracellular domain (PlexA4Δecto). PlexinA4Δecto has been reported to induce L cell contraction and was used as a positive control. MICAL-1 constructs were co-transfected with GFP to allow identification of transfected cells. Cells transfected with plexinA4Δecto were immunostained using anti-Flag antibodies. Graph on the right shows a quantification of contraction responses of transfected cells (in % of total). Data including standard deviations from three independent experiments are displayed. MICAL-1 N3 induced L cell contraction indicating that these cells contain signaling pathways crucial for MICAL-1 function.

(C) A pBABE-based retroviral vector system was used to generate stable L cell lines expressing the MICAL-1-Flag/HA fusion protein depicted in Fig. 1A. Several different stable clones were identified by western blotting with anti-HA antibodies. L cells with integrated empty retroviral vector served as a control (C0). PC, polyclonal. (D) Lysates from D1 or C0 cells were analyzed by WB with polyclonal anti-mouse MICAL-1 antibody. (E) Pull-down assays with anti-Flag monoclonal antibody-conjugated agarose beads were performed with lysates from MICAL-1-Flag/HA (D1) or control (C0) cells. Proteins bound to beads were eluted with Flag peptide and precipitates were analyzed by western blotting using anti-HA antibody. Input corresponds to 10 % of the extract used to obtain the lanes marked "elution".

Supplemental Figure 1

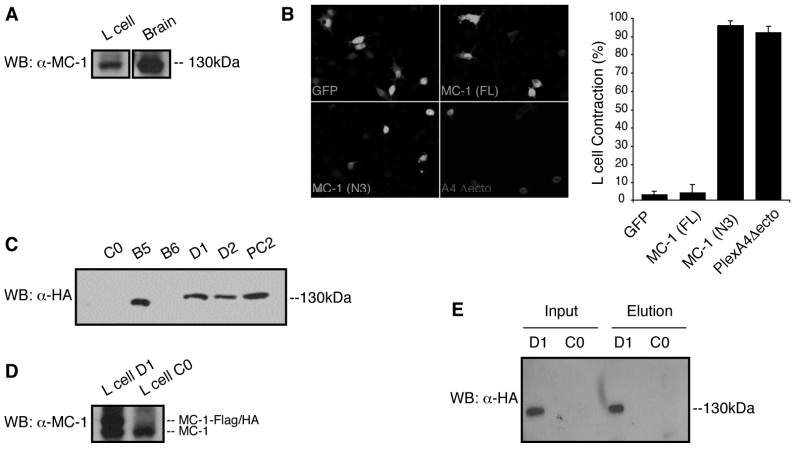

Supplemental Figure 2. Peptide coverage NDR1 and NDR2.

Amino acid sequence alignment of mouse NDR1 and mouse NDR2. Peptides identified in the mass spectrometry analysis are indicated (in blue (NDR1) and red (NDR2). Note that one of the identified peptides can be found in both the NDR1 and NDR2 amino acid sequence (KETEFLRL).

Supplemental Figure 2

```
      1         10        20        30        40        50
mNDR1 MAMT-GSTPCSSMSNHTKERVTMTKVTLENFYSNLIAQHEEREMRQKKLEKVMEEEGLKD
      MAMT G+T    MSNHT+ERVT+ K+TLENFYSNLI QHEERE RQKKLE  MEEEGL D
mNDR2 MAMTAGATTTFPMSNHTRERVTVAKLTLENFYSNLILQHEERETRQKKLEVAMEEEGLAD
      60        70        80        90        100       110
mNDR1 EEKRLRRSAHARKETEFLRLKRTRLGLEDFESLKVIGRGAFGEVRLVQKKDTGHVYAMKI
      EEK+LRRS HARKETEFLRLKRTRLGL+DFESLKVIGRGAFGEVRLVQKKDTGH+YAMKI
mNDR2 EEKKLRRSQHARKETEFLRLKRTRLGLDDFESLKVIGRGAFGEVRLVQKKDTGHIYAMKI
      120       130       140       150       160       170
mNDR1 LRKADMLEKEQVGHIRAERDILVEADSLWVVKMFYSFQDKLNLYLIMEFLPGGDMMTLLM
      LRKADMLEKEQV HIRAERDILVEAD  WVVKMFYSFQDK NLYLIMEFLPGGDMMTLLM
mNDR2 LRKADMLEKEQVAHIRAERDILVEADGAWVVKMFYSFQDKRNLYLIMEFLPGGDMMTLLM
      180       190       200       210       220       230
mNDR1 KKDTLTEEETQFYIAETVLAIDSIHQLGFIHRDIKPDNLLLDSKGHVKLSDFGLCTGLKK
      KKDTLTEEETQFYI+ETVLAID+IHQLGFIHRD+KPDNLLLD+KGHVKLSDFGLCTGLKK
mNDR2 KKDTLTEEETQFYISETVLAIDAIHQLGFIHRDVKPDNLLLDAKGHVKLSDFGLCTGLKK
      240       250       260       270       280       290
mNDR1 AHRTEFYRNLNHSLPSDFTFQNMNSKRKAETWKRNRRQLAFSTVGTPDYIAPEVFMQTGY
      AHRTEFYRNL H+ PSDF+FQNMNSKRKAETWK+NRRQLA+STVGTPDYIAPEVFMQTGY
mNDR2 AHRTEFYRNLTHNPPSDFSFQNMNSKRKAETWKKNRRQLAYSTVGTPDYIAPEVFMQTGY
      300       310       320       330       340       350
mNDR1 NKLCDWWSLGVIMYEMLIGYPPFCSETPQETYKKVMNWKETLTFPPEVPVSEKAKGLILR
      NKLCDWWSLGVIMYEMLIG+PPFCSETPQETY+KVM+WKETL FPPEVPVSEKAK LILR
mNDR2 NKLCDWWSLGVIMYEMLIGFPPFCSETPQETYRKVMSWKETLAFPPEVPVSEKAKDLILR
      360       370       380       390       400       410
mNDR1 FCCEWEHRIGAPGVEEIKNNLFFEGVDWEHIRERPAAISIEIKSIDDTSNFDEFPESDIL
      FC + E+RIG  GVEEIK + FFEGVDW HIRERPAAI IEI+SIDDTSNFD+FPESDIL
mNDR2 FCTDSENRIGNGGVEEIKGHPFFEGVDWGHIRERPAAIPIEIRSIDDTSNFDDFPESDIL
      420       430       440       450       460
mNDR1 KPTVTTSSHPETDYKNKDWVFINYTYKRFEGLTARGAIPSYMKAAK
      +P   T+   E DYK+KDWVF+NYTYKRFEGLT RG+IP+YMKA K
mNDR2 QPVPNTT---EPDYKSKDWVFLNYTYKRFEGLTQRGSIPTYMKAGK
```

Chapter 6

NDR1 binds MICAL-1 and activated plexinA1 but is not regulated during neuronal Sema3A signaling

Yeping Zhou, Rou-Afza F. Gunput,
M. Liset Rietman, Anita J.C.G.M. Hellemons, R. Jeroen Pasterkamp

Abstract
Class 3 semaphorins (Sema3s) are regulators of tissue morphogenesis and homeostasis through their effects on cell growth, survival, migration and proliferation. During axon guidance in the developing nervous system, Sema3s transduce their signals via a receptor complex composed of neuropilins and plexinAs to modulate the cytoskeleton and induce growth cone steering. A recently identified protein family, MICALs, has been implicated in Sema3 signal transduction. Increasing evidence suggests that vertebrate MICAL-1 mediates Sema3A and 3F signaling by binding plexinAs and the actin cytoskeleton. In a search for MICAL-1 interacting proteins, the serine-threonine kinases NDR1 and NDR2 were identified. Interestingly, MICAL-1 can regulate NDR activity and NDRs have been implicated in the control of neurite growth and the actin cytoskeleton. Here, we show that *NDR1* and *MICAL-1* show highly similar patterns of expression in the embryonic mouse brain and interact with activated plexinA1. This suggests that a tripartite NDR1/MICAL-1/plexinA1 complex may function in Sema3 signaling. However, Sema3A treatment of neurons did not change the activation state or expression of NDR kinases. Thus, NDR (in)activation may not be involved in Sema3 signaling. Although these preliminary experiments provide a framework for studying the cooperation of NDRs and MICALs in semaphorin/plexin signaling, further functional studies are needed to establish the role of NDRs in semaphorin signaling.

Introduction

The proper functioning of our nervous system relies on the interconnection of billions of neurons. These connections form during embryonic development when neurons send out axons to their targets. The control of axon navigation is called axon guidance, a process during which axons are attracted or repelled by environmental molecules (guidance cues) into a specific direction. Axon guidance cues are detected by receptors on the surface of the growth cone at the leading tip of the axon. Interactions between guidance cues and receptors (in)activate intracellular signaling molecules, and consequently, alter cytoskeletal structures thereby dictating growth cone steering (Tessier-Lavigne and Goodman, 1996).

Class 3 semaphorins (Sema3s) are well-known guidance cues during neuronal development (Kolodkin et al., 1993; Derijck et al., 2010). Their role in repulsive axon guidance has been studied in most detail, although Sema3s are known to also act as axon attractants. In most cases, neuropilins and class A plexins (plexinAs) work together to function as Sema3 receptor complexes on the growth cone (Takahashi et al., 1999; Derijck et al., 2010; chapter 2). Neuropilins are highly conserved single-pass transmembrane proteins specific to vertebrates and serve as ligand-binding modules for Sema3s (Schwarz and Ruhrberg, 2010). PlexinAs are also transmembrane proteins with highly conserved cytoplasmic domains (Winberg et al., 1998; Nakamura et al., 2000). In the Sema3 receptor complex, plexinAs serve as signal transducing receptor components, regulating intracellular molecules that induce cytoskeleton remodeling, and as a result, growth cone morphology. Interestingly, the interaction between Sema3, neuropilin and plexinA not only mediates guidance in neuronal systems, but can also control the morphology of non-neuronal cells. For example, after coexpression of neuropilin and plexinA1 in COS-7 cells, cells undergo contraction when Sema3s are applied (Takahashi and Strittmatter, 2001).

The signal transduction pathways downstream of Sema3 receptor complexes remain poorly chacterized. In *Drosophila,* Mical is required for semaphorin/plexinA-controlled motor axon pathfinding. Mical physically interacts with both plexinA and actin filaments and can induce actin depolymerization through its monooxygenase domain presumably following sema-1a/plexinA interactions (Terman et al., 2002; Hung et al., 2010). Also in mammalian cells, plexinAs may transduce Sema3 signals via MICAL proteins (Terman et al., 2002; Pasterkamp et al., 2006; Schmidt et al., 2008). When MICAL-1 redox function is blocked by specific monooxygenase inhibitors, axons lose their repulsive response to Sema3A or Sema3F (Terman et al., 2002; Pasterkamp et al., 2006). Furthermore, knockdown of MICAL-1 or MICAL-3 reduces growth cone collapse induced by Sema3A (Morinaka et al., 2010).

In a search for MICAL-1 interacting proteins, NDR kinases were identified (chapter 4, 5). NDR1 and 2 (NDR1/2) belong to a family of highly conserved serine-threonine kinases, the NDR (Nuclear Dbf2-related Kinase) family, which has been classified as a subgroup of the AGC (protein kinase A (PKA) /PKG /PKC-like) kinase family (Hergovich and Hemmings, 2009). NDR1 and 2 (NDR1/2) can be activated by MST kinases through phosphorylation of a threonine residue (T444 and T442 for NDR1/2, respectively). This phosphorylation is required for full kinase activity of NDR (Tamaskovic et al., 2003; Hergovich et al., 2006). In our previous studies, we demonstrated a regulatory role for MICAL-1 on NDR1 kinase activity. MICAL-1 competes with MST1 for binding to the regulatory region of NDR1 and thereby prevents T444/442 phosphorylation (chapter 5). NDR kinases have been demonstrated to function in neuronal regulation in different species. Studies in *C. elegans* and *Drosophila* show that the NDR homologs, SAX-1 and Trc, respectively, are essential for the control of dendritic tiling (Zallen et al., 2000; Gallegos and Bargmann, 2004; Emoto et al., 2006). Interestingly, *Drosophila* Mical also regulates dendritic structure (Kirilly et al., 2009). In vertebrates, NDR2 mediates neurite outgrowth (Stork et al., 2004), a process MICAL proteins have been implicated in as well (Schmidt et al., 2008). These results hint at a functional relationship between MICALs and NDRs in the nervous system. For example, MICALs and NDRs may cooperate in semaphorin/plexin signaling.

Therefore we investigated the potential role of NDR1 in Sema3A/plexinA1/MICAL-1-induced axon guidance and cell morphology regulation. We show that *MICAL-1* and *NDR1* expression in the embryonic brain significantly overlap and that NDR1, similar to MICAL-1 (Schmidt et al., 2008), interacts with a constitutively active mutant of plexinA1. However, no evidence for the (in)activation of NDR1 following Sema3A exposure to neurons was observed. Although our results indicate the existence of a tripartite complex containing NDR1, MICAL-1 and plexinA1, further functional studies are needed to establish the functional significance of this complex.

Material and methods

Antibodies and reagents

The generation and purification of the anti-T444/442-P antibody have been described previously (Tamaskovic et al., 2003) and the antibody was kindly provided by Dr. Brian Hemmings (FMI, Switzerland). It is important to note that the anti-T444-P antibody recognizes the phosphorylated forms of both NDRs, NDR1 (T444-P) and NDR2 (T442-P). The generation and characterization of a polyclonal rabbit anti-mouse MICAL-1 antibody is described in detail in the Results section of this chapter. We used the following commercially available antibodies: anti-FLAG (M2; Stratagene), anti-HA (3F10; Roche), anti-NDR1 (N-14; Santa Cruz), STK38 (NDR1) monoclonal antibody (2G8-1F3; Abnova), anti-myc (Roche), anti-V5 (Invitrogen), anti-tubulin (Sigma), anti-actin (Sigma) and anti-VSV (Sigma).

Construction of Plasmids

Mouse *MICAL-1* and *NDR1* cDNAs were amplified from embryonic whole brain cDNA using standard molecular biology techniques. The *MICAL-1* cDNA was subcloned into pRK5-HA and pRK5-myc (N-terminal tags) using *SalI* and *NotI* restriction sites, into the pEF-His/V5 vector (C-terminal tag) using the GATEWAY cloning system (Invitrogen), and into the pEGFP-C1 vector (Clontech). Truncation mutants of mouse *MICAL-1* were cloned via PCR reaction. Mouse *NDR1* was subcloned into pFLAG-CMV4 (Sigma) between *NotI* and *BamHI* restriction sites and into pRFP-C1 vector between *HindIII* and *BamHI* sites. Mouse plexinA1 and plexinA1Δect were a kind gift from Dr. Stephen Strittmatter (Yale, USA) (Takahashi and Strittmatter, 2001). All constructs were confirmed by sequence analysis.

Cell culture

HEK293 and COS-7 cells were maintained in high glucose Dulbecco's modified Eagle's medium (DMEM; GIBCO) supplemented with 10% FBS (Lonza), penicillin/ streptomycin, and L-glutamine (PAA) at 37°C with 5% CO_2. For protein analysis, exponentially growing cells were plated at 3.5×10^4 cells/cm^2 and transfected the next day using Lipofectamine 2000 (Invitrogen) as described by the manufacturer. For COS-7 cell contraction assays or colocalization experiments, 0.5×10^4 COS-7 cells/cm^2 cells were seeded on glass coverslips and transfected using FuGENE transfection reagent (Roche) according to the manufacturer's instructions. Cells were incubated at 37°C with 5% CO_2 for another 48-72 hrs.

Dissociated DRG culture

After removing the dorsal root ganglion (DRG) from E14.5 embryos on ice, DRGs were kept in L15 medium containing 5% FCS on ice. DRGs were then transferred to 10 ml DMEM/F12 medium for 5 min at 4°C and centrifuged at 1000 rpm for 5 min. The medium was removed, followed by trypsin treatment (0.25% trypsin in DMEM/F12) for 15 min at 37°C. Then, 5 ml medium was carefully aspirated by pipetting without disturbing the pellet. To inactivate the trypsin, 5 ml DMEM/F12 with 20% FCS was added. After centrifugation and removal of the supernatant, cells were resuspended in 10 ml DMEM/F12 containing 10% FCS and 20 μg/ml DNaseI, and then dissociated by trituration using a fire polished Pasteur pipette. The suspension was filtered through a mesh (cell strainer 70 μm Nylon) and centrifuged at 1000 rpm for 5 min. DRG neurons were cultured in Opti-MEM (Invitrogen) containing 25% F12, 0.5% FCS, 1× glutamine, 0.04 M Glucose, 1× penicillin/ streptomycin and 20 ng/ml NGF at a density of 0.5×10^4 cells/cm^2 on poly-D-Lysine coated plates at 37 °C with 5% CO_2 for 1-2 days.

Semaphorin3A treatment
The culture medium was removed from the cells and medium containing 5 nM Sema3A-Fc (R&D systems) was applied. Fc fragment (5 nM, R&D systems) was used as negative control. The treatment was stopped by placing the plates on ice followed by immediate removal of the medium and application of lysis buffer containing 20 mM Tris-HCl, pH 8.0, 150 mM KCl, 1% TritonX-100 and complete protease inhibitors (Roche). Proteins in the lysates were analyzed by SDS-PAGE and Western blotting.

Co-Immunoprecipitation and Western blotting
According to standard protocols, transfected HEK293 cells were re-suspended and collected by centrifugation at 1000 rpm for 10 min at 4°C, washed in cold PBS and lysed in lysis buffer containing 20 mM Tris, pH 8.0, 150 mM KCl, 0.1% TritonX-100 and protease inhibitor cocktail (Roche). After centrifugation at 14,000 rpm for 10 min at 4°C, lysates were transferred to a clean eppendorf tube. For Western blotting, protein lysates were mixed with sample buffer and boiled at 90°C for 5-10 min. For immunoprecipitation, antibodies were added to each cell lysate and incubated overnight at 4°C. Then pre-washed proteinA or G agarose (Roche) was added to the lysates and incubated for at least 2 hrs at 4°C. After 4 washes with lysis buffer, proteins were eluted with sample buffer and boiled at 90°C. To analyze proteins from IP samples or cell lysates, we used SDS-PAGE and transferred proteins to nitrocellulose (Hybond-C Extra, Amersham). Chemiluminescence (Supersignal, Thermo Scientific) was detected by CL-XPosure Film (Thermo Scientific). Band intensities were analyzed by using ImageJ software.

In situ hybridization
Nonradioactive *in situ* hybridization was performed using alkali-hydrolysed digoxigenin (DIG)-labeled cRNA probes transcribed from mouse *MICAL-1* (entire coding region, Pasterkamp et al., 2006) and mouse *NDR1* (a 303 bp fragment corresponding to nucleotides 271–574 of the coding region). *In situ* hybridization was performed as described previously (Pasterkamp et al., 1998). Briefly, cryostat sections of 20 μm were cut at -20°C, thaw-mounted on Superfrost plus slides (Fisher Scientific, Den Bosch, The Netherlands), and post-fixed with 4% PFA in PBS for 10 min at room temperature (RT). To enhance tissue penetration and decrease aspecific background staining, sections were acetylated with 0.25% acetic anhydride in 0.1 M triethanolamine for 10 min, all at RT. Subsequently, sections were prehybridized for 2 hrs at RT in hybridization buffer (50% formamide, 5 × Denhardt's solution, 2 × SSC, 250 μg/ml bakers yeast tRNA, and 500 μg/ml sheared and heat-denatured herring sperm DNA). Hybridization was performed for 15 hrs at 68°C, using 400 ng/ml denatured DIG-labeled cRNA probe diluted in hybridization buffer. After hybridization, sections were washed briefly in 2 × SSC followed by 2 hrs in 0.2 × SSC, all at 68°C, and adjusted to RT in 0.2 × SSC for 5 min. DIG-labeled RNA hybrids were detected with an anti-DIG Fab fragment conjugated to alkaline phosphatase (Boehringer Mannheim) diluted 1:3000 in TBS, pH 7.4, overnight at 4°C. Binding of alkaline-phosphatase-labeled antibody was visualized by incubating the sections in detection buffer (100 mM Tris, pH 9.5, 100 mM NaCl, and 5 mM $MgCl_2$) containing 240 μg/ml levamisole and color reagents nitro-bluetetrazolium chloride/5-bromo-4-chloro-3-indolylphosphate (NBT/BCIP, Roche) for 14 hrs at RT. Sections hybridized with sense probes exhibited no specific hybridization signal.

Results

MICAL-1 binds to plexinAs.
In *Drosophila*, Mical mediates repulsive sema-1a/plexinA signaling during motor axon pathfinding (Terman et al., 2002). In vertebrates, MICAL-1 physically interacts with plexinA1 and contributes to Sema3A/ plexinA1-induced changes in cell morphology (Schmidt et al., 2008). Four plexinAs (A1-A4) exist in vertebrates, sharing highly conserved intracellular domains and exerting overlapping or individual functions in Sema3 signaling (Tamagnone et al., 1999; chapter 2). To determine whether MICAL-1 is a downstream effector for different plexinAs, we examined the interaction of the four plexinAs with MICAL-1.

HEK293 cells were cotransfected with epitope-tagged plexinA1-4 and MICAL-1 and the interaction of these proteins was examined by co-immunoprecipitation (co-IP) (Fig. 1). The previously described interaction of plexinA1 and MICAL-1 was confirmed by showing that FLAG-plexinA1 co-precipitated with myc-MICAL-1 after anti-myc IP (Fig. 1A). Similarly, myc-MICAL-1 precipitated with VSV-tagged plexinA2 and A3 following anti-VSV IP (Fig. 1B, C). Finally, MICAL-1-V5 co-IPed with myc-plexinA4 following

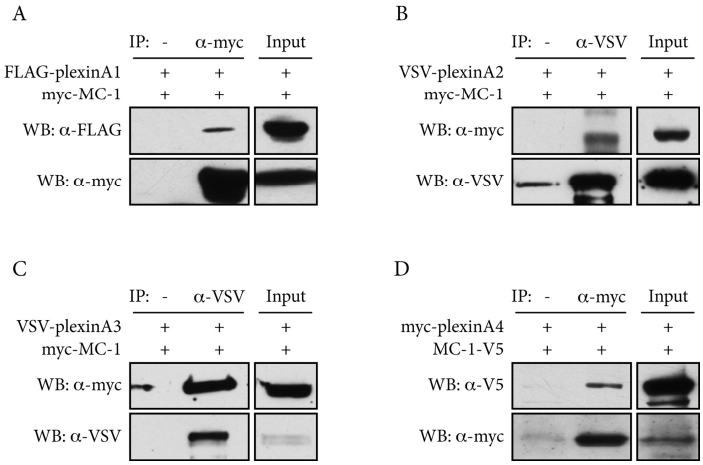

Figure 1. MICAL-1 interacts with plexinAs.

(A) Lysate from HEK293 cells transfected with FLAG-plexinA1 and myc-MICAL-1 were subjected to immunoprecipitation with anti-myc antibody followed by Western blotting with anti-FLAG and anti-myc antibodies.

(B-D) A similar approach as described in (A) was applied to lysates expressing VSV-plexinA2 and myc-MICAL-1 (B), VSV-plexinA3 and myc-MICAL-1 (C), and myc-plexinA4 and MICAL-1-V5 (D) followed by immunoprecipitation with anti-VSV for plexinA2 and A3 or anti-myc for plexinA4. The bands detected in negative controls in (B-D) are due to overflow from adjacent lanes or aspecific binding of the antibody. MC-1, MICAL-1.

anti-myc IP (Fig. 1D). These results show that all plexinAs can bind MICAL-1 following overexpression and indicate that MICAL-1 may be involved in the signaling cascades triggered by all plexinAs.

Mouse MICAL-1 antibodies specifically detect MICAL-1.

In order to further investigate the MICAL-1-plexinA interaction at the endogenous protein level, we generated rabbit anti-mouse MICAL-1 polyclonal antibodies.

In line with a study by Suzuki et al. (2002), in which anti-human MICAL-1 antibodies against the C-terminus of MICAL-1 were generated, we used the corresponding mouse MICAL-1 C-terminal region for antibody production. The last 63 amino acids of mouse MICAL-1 (MC-1-CT) were flanked by the maltose-binding protein (MBP) and a signal sequence directing pre-MBP-fusion proteins to the periplasm of *E. coli*. By using the cold osmotic shock method, MBP-MC-1-CT was extracted from the periplasm (Fig. 2A).

The proteins were separated in an 11% SDS-PAGE gel and the band corresponding to MBP-MC-1-CT was collected and mixed with Freund's adjuvant (Sigma, USA), complete and incomplete for initial immunization and three boosts, respectively. Two rabbits, numbered 6117 and 6118 were immunized and sera were collected before and after immunization (Fig. 2A).

The antibodies were purified from the sera using a biotin-streptavidin based purification system. As shown in Fig. 2B, a MICAL-1-C1 construct containing the C-terminal residues 901-1048 was tagged with eGFP and a biotinylation peptide, which can be biotinylated by the biotin ligase BirA. Biotinylated MICAL-1-C1 was bound to streptavidin coupled magnetic Dyna-beads (Invitrogen). These beads were then used to immobilize anti-MC-1 antibodies from the immune sera. After several washing steps to remove non-specific

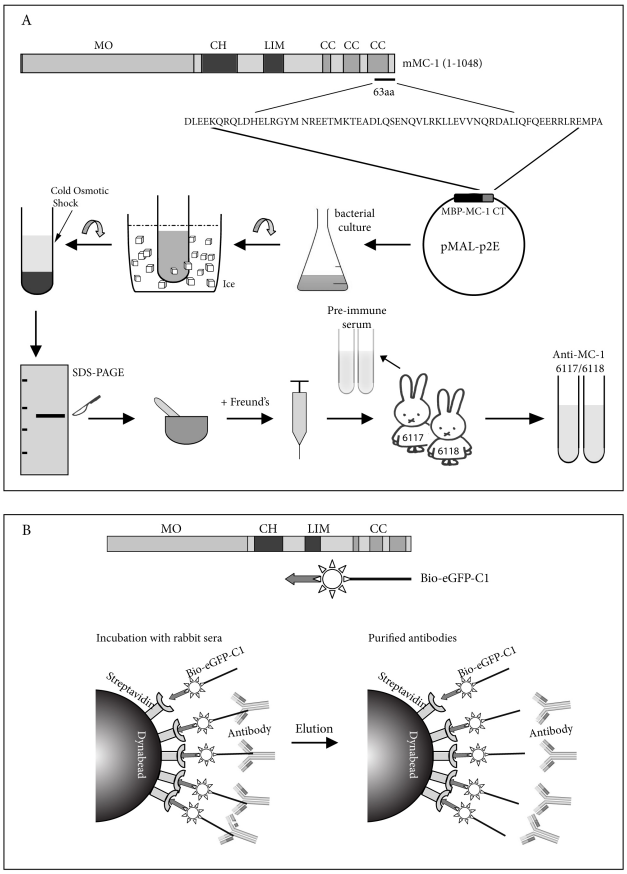

Figure 2. Generation of rabbit anti-mouse MICAL-1 antibodies.

(A) The C-terminal 63 amino acids of mouse MICAL-1 were cloned into a pMAL-P2E vector and expressed in bacteria. Cold osmotic shock was used to collect protein and the fusion protein was purified using SDS-PAGE. The MBP-MC-1-CT band was excised from gel and mixed with Freund's adjuvant and used to immunize two rabbits (6117 and 6118).

(B) A streptavidin-biotin based purification system was used to collect anti-mouse MICAL-1 antibodies from the immune sera; bio-eGFP-MC-1-C1 was immobilized to streptavidin beads and incubated with the rabbit sera. Non-specific proteins were removed by washing and purified antibodies were eluted with glycine. MO, monooxygenase domain; CH, Calponin Homology domain; LIM, LIM domain; CC, coiled-coil motif.

proteins, purified antibodies were eluted from the purification system by a low pH Glycine solution (Fig. 2B).

The purified antibodies (6117 and 6118) were evaluated using Western blotting and IP. As shown in Fig. 3A, overexpressed mouse MICAL-1-V5 in HEK293 cells could be detected by both 6117 and 6118 antibodies. However, the pre-immune serum of 6117 (6117-) weakly detected protein(s) with size comparable to MICAL-1. This band can represent overexpressed MICAL-1 or protein(s) of identical size. Nevertheless, this potential non-specific detection was only observed following overexpression of MICAL-1. The pre-immune serum of 6118 (6118-) did not show aspecific bands. Furthermore, 6118 appeared to detect endogenous human MICAL-1 in non-transfected HEK293 cells as shown in Fig. 3A (arrow). The 6117 antibody only detected a fraction of the endogenous MICAL-1 protein (Fig. 3A). The 6118 antibody specifically recognized endogenous mouse MICAL-1 in brain lysates of wild-type but not MICAL-1 knock out tissue (Fig. 3B, C) (R.F.G. and R.J.P., unpublished). These results show that the 6118 antibody recognizes the MICAL-1 protein under endogenous and exogenous situations, while the 6117 antibody is most suitable for detecting exogenous MICAL-1.

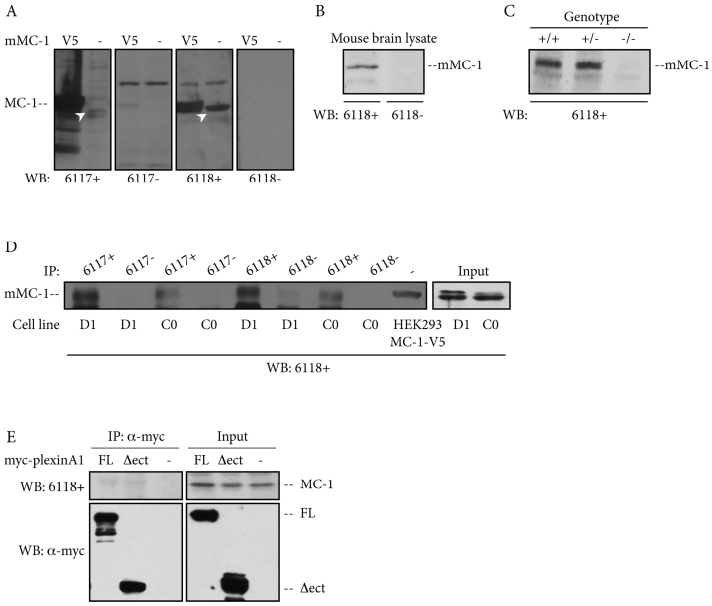

Figure 3. Characterization of rabbit anti-mouse MICAL-1 antibodies.

(A) Lysates from non-transfected HEK293 cells or cells transfected with MICAL-1-V5 were analyzed by Western blotting with rabbit anti-MICAL-1 antibodies. Both 6117 and 6118 antibodies detected overexpressed and endogenous (arrows) MICAL-1 (MC-1). The pre-immune serum of 6117 (6117-) detects aspecific bands, while the 6118- serum does not show aspecific binding.

(B-C) The 6118 antibody, but not the corresponding pre-immune serum, detects endogenous MICAL-1 from adult mouse brain lysate. (C) No signals are detected in lysates from *MICAL-1* knockout embryos when using the 6118 antibody (R.F.G. and R.J.P., unpublished observations).

(D) Lysates from stable L cells expressing MICAL-FLAG-HA (D1) or vector (C0) were immunoprecipitated with MICAL-1 antibodies or pre-immune sera and analyzed with 6118 antibody. Both 6117 and 6118 antibodies are able to pull down MICAL-1. Lysates from HEK293 cells overexpressing MICAL-1-V5 were used as a control.

(E) Lysates from L cells overexpressing myc-plexinA1 or myc-plexinA1Δect were immunoprecipitated with anti-myc antibody followed by Western blotting with anti-myc and anti-MICAL-1 6118 antibodies.

To examine the ability of the 6117 and 6118 antibodies to IP MICAL-1, we performed immunoprecipitation experiments using two stable cell lines, D1 and C0. D1 is a manipulated L cell line which stably expresses MICAL-1-FLAG-HA fusion protein, while C0 is a control cell line, which expresses endogenous MICAL-1 only (see chapter 4 and 5). As shown in Fig. 3D, both antibodies were able to pull down MICAL-1 from the D1 and C0 cell lines. In comparision, more protein was IPed from D1 cells because of the additional exogenous expression of MICAL-1. Together, these data show that both antibodies can detect MICAL in its native (IP) and denatured form (Western blotting).

PlexinA1 binds endogenous MICAL-1

The co-IP experiments in Fig. 1 show that overexpressed MICAL-1 and plexinA1 interact. To show that endogenous MICAL-1 can associate with plexinA1 in its normal or activated state, we performed co-IPs

Figure 4. NDR1 specifically interacts with plexinA1Δect.
Lysates of HEK293 cells expressing myc-plexinA1 (FL) or myc-plexinA1Δect (Δect) alone or in combination with FLAG-NDR1 were subjected to immunoprecipitation with anti-FLAG antibody followed by Western blotting using the indicated antibodies.

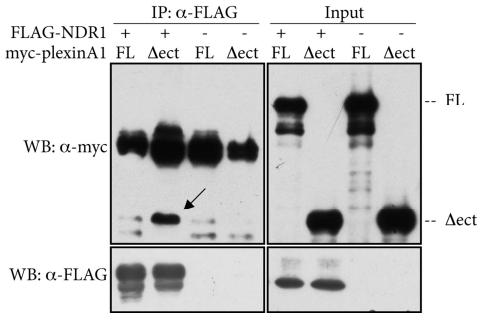

using overexpressed plexinA1 and plexinA1Δect proteins. PlexinA1Δect lacks the extracellular domain, resulting in a constitutively active form of plexinA1 (Takahashi and Strittmatter, 2001). It has been shown that overexpressed plexinA1Δect induces growth cone and cell contraction, identical to Sema3/neuropilin/plexinA1 induced cell morphology changes (Takahashi and Strittmatter, 2001). Myc-tagged plexinA1 or plexinA1Δect were transfected in L cells and immunoprecipitated using anti-myc antibody. After separation of the protein complexes on SDS-PAGE, endogenous MICAL-1 was detected with the 6118 antibody. As shown in Fig. 3E, MICAL-1 associates with both full length plexinA1 and plexinA1Δect. Schmidt et al., (2008) have previously reported that the plexinA1Δect binds MICAL-1 more efficiently as compared to full length plexinA1 when the proteins are overexpressed in HEK293 cells. However, our data did not reveal a difference between the binding of MICAL-1 to plexinA1 and plexinA1Δect. This may be due to the much lower levels of endogenous MICAL-1 detected in our study as compared to the robust co-IP when using overexpressed proteins only. This result confirms the interaction of plexinA1 and MICAL-1 at the semi-endogenous level. In further studies, anti-plexinA1 and anti-MICAL-1 antibodies will be used to examine the interaction of these proteins at the endogenous protein level.

NDR1 binds to plexinA1Δect but not full length plexinA1.
In a previous study, we found that NDR1 kinase interacts with MICAL-1 and is regulated by MICAL-1 (chapter 4, 5). We therefore asked whether NDR1 is also able to form a complex with plexinA1. To investigate the interaction between NDR1 and plexinA1, full length plexinA1 and constitutively active plexinA1Δect (myc-tagged) were cotransfected with FLAG-NDR1 in HEK293 cells and subjected to co-IP. FLAG-NDR1 was precipitated from cell lysates using anti-FLAG antibody followed by Western blotting using anti-myc antibody to detect plexinA1. Interestingly, plexinA1Δect but not full length plexinA1 co-IPed with myc-MICAL-1 (Fig. 4, arrow). Considering the interaction of MICAL-1 with both plexinA1Δect and NDR1, these data suggest that plexinA1, MICAL-1 and NDR1 may form a complex when plexinA1 is activated.

The expression of MICAL-1 and NDR1 partially overlaps in the brain.
MICAL-1 has been suggested to function in developing brain for example during axon growth and guidance (Pasterkamp et al., 2006). NDR kinases also have implicated in neuronal functions in different species, e.g. in the control of dendritic tiling and neurite outgrowth (Zallen et al., 2000; Emoto et al., 2006; Stork et al., 2004). To examine whether MICAL-1 and NDR1 may function together during brain development, we examined the expression of these two proteins by *in situ* hybridization. Non-radioactive *in situ* hybridization on consecutive sagittal cryosections of embryonic day (E) 16.5 mouse embryos was performed. *MICAL-1* and *NDR1* were broadly expressed in the nervous system (Fig. 5A-C). We focused on the olfactory bulb, cortex, hippocampus, cerebellum, dosal root ganglion (DRG) and olfactory epithelium, which have been

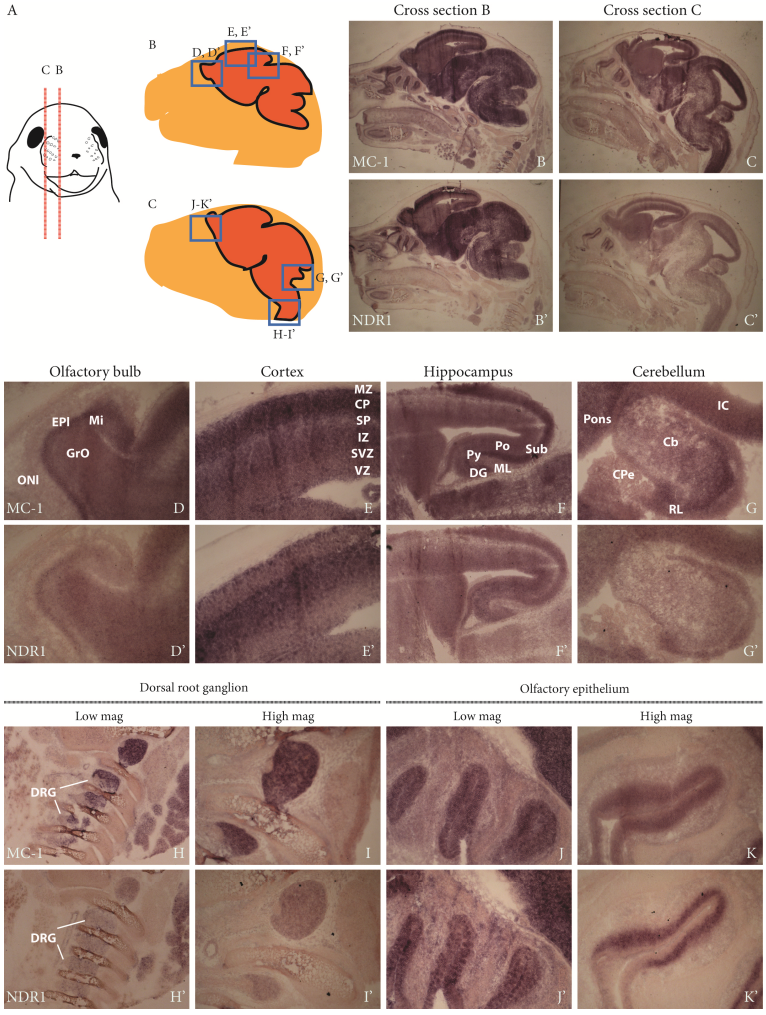

Figure 5. *MICAL-1* and *NDR1* expression in the embryonic nervous system.

(A) A schematic representation of a mouse embryo (E16.5) indicating the positions of the two sagittal sections shown in (B) and (C). Boxes indicate the regions shown at a higher magnification in (D-K').

(B-C, B'-C') Non-radioactive *in situ* hybridization was performed on consecutive sagittal sections for *MICAL-1*(B-C) and *NDR1*(B'-C').

(D-K, D'-K') The expression of *MICAL-1* and *NDR1* in the olfactory bulb (D, D'), cortex (E, E'), hippocampus (F, F'), cerebellum (G, G'), dorsal root ganglion (H, H', I, I') and olfactory epithelium (J, J', K, K'). EPI, external plexiform layer; GrO, granule cell layer of the olfactory bulb; Onl, olfactory nerve layer; Mi, mitral cell layer; MZ, marginal zone; CP, cortical plate; SP, sub plate; IZ, intermediate zone; VZ, ventricular zone; SVZ, sub ventricular zone; DG, dentate gyrus; Po, polymorph layer; Py, pyramidal cell layer; sub, subiculum; ML, molecular layer; IC, inferior colliculus; CPe, choroid plexus epithelium; RL, cerebellar rhombic lip (RL).

studied previously in the context of *MICAL* expression (Pasterkamp et al., 2006). In the olfactory bulb, *MICAL-1* and *NDR1* showed a similar distribution. Both genes were highly expressed in the external plexiform layer (EPI) and granule cell layer of the olfactory bulb (GrO) and only weakly in olfactory nerve layer (Onl). In the mitral cell layer (Mi), *NDR1* expression was lower than *MICAL-1* (Fig. 5D, D'). In the cortex, *MICAL-1* was strongly expressed in the marginal zone (MZ) and cortical plate (CP), while *NDR1* was also expressed in the MZ, but not in the CP. In the subplate (SP), strong expression of *NDR1* was detected, however, *MICAL-1* was absent from this structure (Fig. 5E, E'). From intermediate zone (IZ) to ventricular zone (VZ), the expression of both *MICAL-1* and *NDR1* showed a decreasing gradient (Fig. 5E, E'). In the hippocampus, both *MICAL-1* and *NDR1* were expressed in the dentate gyrus (DG), polymorph layer (Po), pyramical cell layer (Py), and subiculum (sub). The expression was strong for both probes and completely overlapping. However, the expression of *MICAL-1* in the Py was higher than in the Po, while this difference in expression was not found for *NDR-1*. Expression in the molecular layer (ML) was weak for both *MICAL-1* and *NDR1* (Fig. 5F, F'). In the cerebellum, *MICAL-1* was highly expressed in the pons, inferior colliculus (IC), and cerebellar rhombic lip (RL). An expression gradient was found in the cerebellar plate (Cb) and RL. In the choroid plexus epithelium (CPe), *MICAL-1* was also expressed in a gradient with highest expression towards the medulla. *NDR1* showed a similar expression pattern as *MICAL-1* (Fig. 5G, G'). In the dorsal root ganglion (DRG), *MICAL-1* was more strongly expressed as compared to *NDR1*. However, the overall distribution patterns of these two genes was similar in the DRGs (Fig. 5H-I, H'-I'). In the olfactory epithelium, *MICAL-1* and *NDR1* showed similar expression levels and distribution patterns (Fig. 5J-K, J'-K'). The *MICAL-1* expression patterns reported here were consistent with previous observations (Pasterkamp et al., 2006). Overall, the overlapping expression patterns of *MICAL-1* and *NDR1* in the developing brain suggest a functional relationship between NDR1 and MICAL-1 during nervous system development.

Overexpression of NDR1 does not change the effect of MICAL-1 or plexinA1Δect on cell morphology

To further understand the functional interaction between NDR1 and MICAL-1 in the brain, we sought to determine whether NDR1 is involved in Sema3A-mediated signaling, in which both MICAL-1 and activated plexinA1 play important roles (Schmidt et al., 2008; chapter 2). To achieve this goal we utilized the COS-7 contraction assay, a cell morphology assay widely used for studying semaphorin/plexin induced cell contraction (Takahashi and Strittmatter, 2001). PlexinA1Δect or MICAL-1-N3 are both constitutively active forms of the full length proteins and induce cell contraction after overexpression in COS-7 cells (Takahashi and Strittmatter, 2001; Schmidt et al., 2008; chapter 3, 5). Co-expression of full length MICAL-1 and plexinA1 also induces cell contraction, while none of these proteins alters cell morphology alone (Schmidt et al., 2008; Fig. 6B). We asked whether NDR1 expression can influence changes in cell morphology induced by plexinA1 and MICAL-1. Full length MICAL-1 or plexinA1 or their constitutively active mutants were transfected into COS-7 cells with or without NDR1 (tagged with Red Fluorescent Protein (RFP)) and visualized by a combination of immunostaining or RFP fluorescence, respectively. As shown in Fig. 6, when NDR1 was overexpressed together with full length MICAL-1 or plexinA1, no contraction responses were detected. Furthermore, NDR1 did not influence the effects of constitutively active MICAL-1 or plexinA1 (Fig. 6). Therefore, overexpression or knockdown (data not shown) of NDR1 neither activates full length plexinA1 or MICAL-1 for cell morphology regulation nor impairs the constitutively active effects of these proteins.

Sema3A signaling does not activate NDR1

NDR1 can be activated via phosphorylation of the T444 residue in its C-terminal hydrophobic motif (Stegert et al., 2005). The activation of NDRs has been shown to regulate centrosome dupilication and apoptosis in cells (Hergovich et al., 2009; Vichalkovski et al., 2008). Overexpressed NDR1 does not influence cell morphology but it is possible that NDRs need to be activated to function in cell morphology

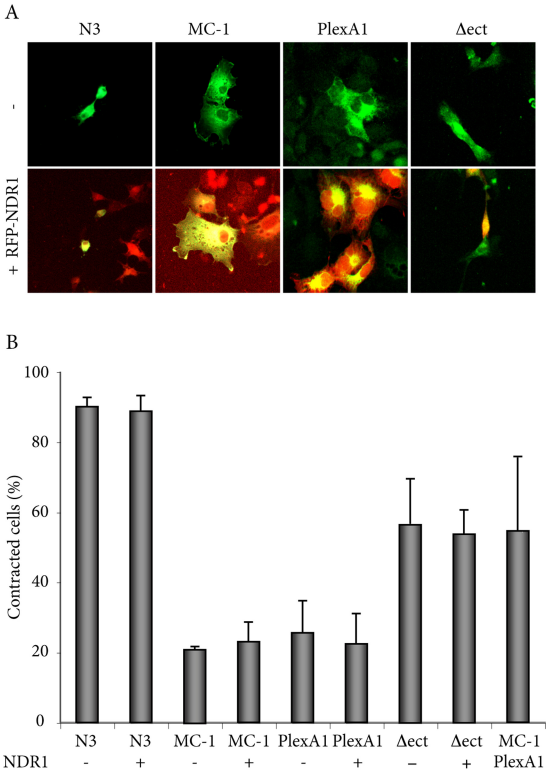

Figure 6. NDR1 does not modulate changes in cell morphology induced by activated MICAL-1 or plexinA1.

(A) COS-7 cells were transfected with combinations of the indicated cDNAs. MICAL-1 or plexinA1 were detected by immunocytochemistry (green), while NDR1 was detected by RFP fluorescence (red).

(B) Measurement of the percentage of contracted cells (cells with an area less than 1600 μm²). Means ± SEM from 3 independent experiments are presented. N3, MICAL-1-N3; MC-1, MICAL-1; PlexA1, plexinA1; Δect, plexinA1Δect.

changes as is suggested by their specific interaction with activated plexinA1 (Fig. 6) (chapter 5). To investigate the activation of NDR1 in semaphorin signaling in neurons, NDR phosphorylation was assessed following exposure to Sema3A.

We first examined NDR1/2 phosphorylation after overexpression of constitutively active MICAL-1 (MICAL-1-N3) or plexinA1 (plexinA1Δect) (Fig. 7A). HEK293 cells were transfected with control vector, HA-MICAL-1-N3 or myc-plexinA1Δect and cell lysates were analyzed using anti-T444-P antibody, which recognizes phosphorylated NDR1 and 2 at T444 and T442 residues, respectively (Bichsel et al., 2004). As shown in Fig. 7A, overexpression of MICAL-1-N3 or plexinA1Δect induced a small reduction in endogenous NDR1/2 phosphorylation at T444/442 indicating that the phosphorylation state of T444/442 may be regulated during MICAL-1 or plexinA1 activation.

To further check whether NDR can be influenced by Sema3A stimulation, we performed direct treatment of DRG neurons, in which both *NDR1* and *MICAL-1* are highly expressed (Fig. 5H, H'). E14.5 DRG neurons were plated in a 24-well plate one day before treatment with Sema3A-Fc or Fc (Fig. 7B). Phosphorylation of NDR1/2 was assessed by Western blotting using the anti-T444-p and anti-NDR1 antibodies. The phosphorylation level of NDR kinases did not show a consistent change after Sema3A-Fc treatment. In addition, we examined the endogenous expression of both MICAL-1 and NDR1 by using anti-MICAL-1 (6118) and anti-NDR1 antibodies. As shown in Fig. 7C, the expression of MICAL-1 and

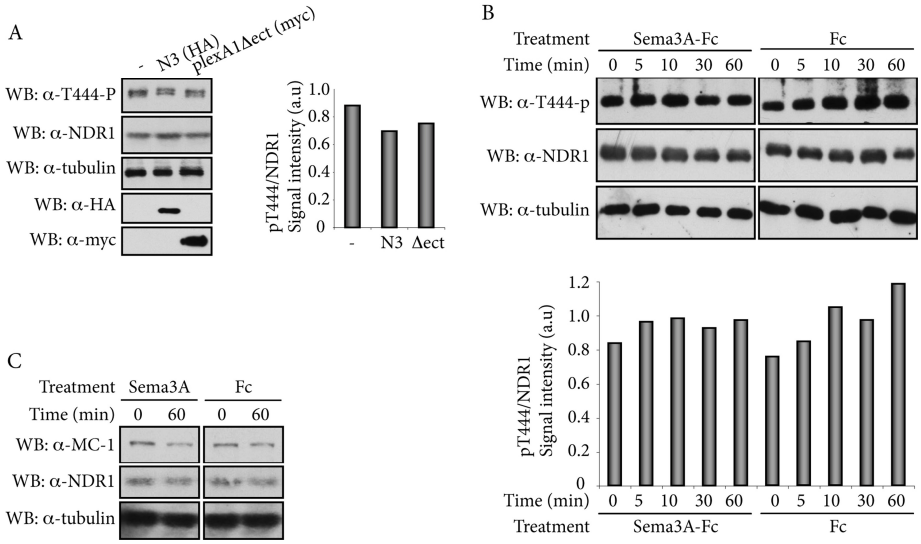

Figure 7. Sema3A treatment does not affect NDR1 activation or MICAL-1/NDR1 expression.

(A) HEK293 cells were tranfected with MICAL-1-N3, plexinA1Δect or control vector (-). Lysates were analyzed using anti-T444-P, anti-NDR1 or anti-tubulin antibodies. Quantification of band intensities indicates ratio of T444 phosphorylation to total NDR1, a.u. arbitrary unit.

(B) DRG neurons were treated with Sema3A-Fc or Fc for 0, 10, 30 or 60 min. Cell lysates were analyzed using anti-T444-P, anti-NDR1 or anti-tubulin antibodies. Quantification of band intensities indicates ratio of T444 phosphorylation to total NDR1 after Sema3A treatment.

(C) DRG neurons were treated with 5 nM Sema3A-Fc or 5 nM Fc for 60 min and the corresponding lysates were analyzed using anti-MICAL-1 (6118), anti-NDR1 or anti-tubulin antibodies.

NDR1 was unchanged after Sema3A treatment. Overall, these data suggest that Sema3A does not (in)activate NDR kinases in neurons.

Discussion

The present study shows the interaction of mouse MICAL-1 with all plexinAs and unveils a protein complex containing MICAL-1, NDR1 and activated plexinA1. In addition, *NDR1* and *MICAL-1* are reported to be expressed in similar patterns in developing mouse brain suggesting common functions. However, NDR expression and phosphorylation were not affected by Sema3A treatment of culture neurons. Thus, although NDR1, MICAL-1 and plexinA1 may function together the functional relevance of NDR kinases during semaphorin/plexin signaling remains to be established.

Sema3A, plexinAs and MICAL function together to mediate repulsive axon guidance and cell contraction (Takahashi and Strittmatter, 2001; Terman et al., 2002; Schmidt et al., 2008; chapter 2). Receptor complexes composed of neuropilins and plexinAs bind Sema3A and transduce Sema3A signals into cytoplasm and are thought to activate MICAL-1 (Schmidt et al., 2008; Morinaka et al., 2011). Activated MICAL-1 may then induce depolymerization of the actin cytoskeleton leading to morphological changes (Hung et al., 2010). Interestingly, similar to MICALs, NDR2 is able to bind actin and has been suggested to

mediate neurite outgrowth through the regulation of actin dynamics (Stork et al., 2004). Furthermore, in *Drosophila*, both NDR and Mical influence dendritic morphology, most likely by controlling the actin cytoskeleton (Emoto et al., 2006; Kirilly et al., 2009). Based on their related functional roles, physical interaction and similar neuronal distribution of MICAL-1 and NDR1, it is tempting to speculate that these proteins cooperate during aspects of neural development.

Our preliminary data in non-neuronal cells do not support a functional collaboration between NDR1 and plexinA1 or MICAL-1 in cell morphology changes. In addition, our data suggest that Sema3A does not activate NDR kinases during growth cone collapse. However, it is important to point out that although NDR activation is not part of the signaling response to Sema3A exposure, NDR kinases could still play an important role in Sema3A-induced growth cone collapse or axon repulsion, e.g. by interacting with the cytoskeleton or through the regulation of other proteins independent of their kinas activity. Further functional studies are needed to examine whether knockdown of NDR kinases can affect Sema3A-induced growth cone collapse. In addition, since plexinA1 is the principal receptor for Sema6D (Toyofuku et al., 2004; Yoshida et al., 2006), it will be important to test neuronal NDR activation in response to Sema6D and other semaphorins. It is intriguing that NDR1 was found to interact with the constitutively active form of plexinA1 but not with the full length form, suggesting that NDR1 may be recruited to plexinA1 following ligand binding. A similar model has been proposed for MICAL-1 and plexinA1 (Schmidt et al., 2008).

Class 3 and 6 semaphorins are very pleiotropic and regulate cellular processes as diverse as cell proliferation, survival, and apoptosis (Gaur et al., 2009; Gagliardini and Fankhauser, 1999; Guttmann-Raviv et al., 2007). NDR kinases have also been implicated in the control of these processes and a functional link between NDRs and MICAL-1 has been shown for apoptosis regulation (chapter 5). Since semaphorins and plexins are known to control apoptosis, it is tempting to speculate that semaphorins, plexins, MICALs and NDRs cooperate during apoptosis regulation.

The vertebrate nervous system undergoes massive cell death during development, with a loss of approximately half of the neurons (Oppenheim, 1991). Semaphorin family members such as Sema3A and 3F can induce death of neurons (Gagliardini and fankhauser, 1999; Guttmann-Raviv et al., 2007; Ben-Zvi et al., 2008). The receptors that mediate these apoptotic signals remain largely uncharacterized. However, plexinA3 was shown to be required for Sema3A-induced neuronal cell death (Bagnard et al., 2001; Ben-Zvi et al., 2008). Interestingly, in the immune system, Sema3A facilitates Fas-mediated apoptosis and a receptor complex composed of neuropilin-1 and plexinA1 may mediate this effect (Moretti et al., 2008). Fas is a "death receptor" from the tumor necrosis factor (TNF) receptor superfamily and Fas receptor stimulation leads to the activation of NDR1/2 by inducing MST1-dependent phosphorylation at the hydrophobic motif (Vichalkovski et al., 2008). NDR1/2 is essential for Fas-induced apoptosis as shown by the observation that NDR knockdown reduces cell death whereas overexpression of NDR1 potentiates apoptosis (Vichalkovski et al., 2008). We have previously demonstrated that MICAL-1 inhibits NDR1 activation during apoptosis. This inhibition is due to the competition of MICAL-1 with MST1 for NDR binding. Reduced MST1 binding results in decreased phosphorylation and activation of NDR1 (chapter 5). Together these results support a model in which Sema3s regulate apoptosis through plexinAs by regulating MICAL-1/NDR interactions. Future experiments will undoubtedly focus on these and other functions of the MICAL/NDR pathway.

Semaphorins are crucial regulators of morphogenesis and homeostasis in various tissues. Unraveling the signal tranduction pathways that mediate semaphorin functions in different tissues and organ systems will help us to understand how these structures are formed, maintained and in some instances changed as a result of disease. Although the results presented in this study do not provide functional support for a role for NDR kinases in semaphorin signaling, further studies are needed to establish the functional significance of the interaction between NDR kinases and plexinAs. Based on our findings and on the published functions of MICALs and NDRs we propose that plexinAs, MICALs and NDRs cooperate in various biological processes in and outside the nervous system.

Acknowledgements
We thank Dr. Brian Hemmings (FMI, Swizerland) for providing us with antibodies and Dr. Stephen Strittmatter (Yale, USA) for cDNA constructs. This work was supported by grants from the Netherlands Organization for Scientific Research, the Human Frontier Science Program Organization and the Utrecht Genomics Center (to R.J.P.).

Reference

Bagnard D, Vaillant C, Khuth ST, Dufay N, Lohrum M, Puschel AW, Belin MF, Bolz J, Thomasset N. (2001). Semaphorin 3A-vascular endothelial growth factor-165 balance mediates migration and apoptosis of neural progenitor cells by the recruitment of shared receptor. J Neurosci. 2001 May 15;21(10):3332-41.

Ben-Zvi A, Manor O, Schachner M, Yaron A, Tessier-Lavigne M, Behar O. (2008). The Semaphorin Receptor PlexinA3 Mediates Neuronal Apoptosis during Dorsal Root Ganglia Development. J Neuroscience, 2008 Nov 19; 28(47):12427-12432

Bichsel SJ, Tamaskovic R, Stegert MR, Hemmings BA. (2004). Mechanism of activation of NDR (nuclear Dbf2-related) protein kinase by the hMOB1 protein. J Biol Chem. 2004 Aug 20;279(34):35228-35.

Derijck AA, Van Erp S, Pasterkamp RJ. (2010). Semaphorin signaling: molecular switches at the midline. Trends Cell Biol. 2010 Sep;20(9):568-76.

Emoto K, Parrish JZ, Jan LY, Jan YN. (2006). The tumour suppressor Hippo acts with the NDR kinases in dendritic tiling and maintenance. Nature. 2006 Sep 14;443(7108):210-3.

Gagliardini V, Fankhauser C. (1999). Semaphorin III can induce death in sensory neurons. Mol Cell Neurosci 14:301–316.

Gallegos ME, Bargmann CI. (2004). Mechanosensory neurite termination and tiling depend on SAX-2 and the SAX-1 kinase. Neuron. 2004 Oct 14;44(2):239-49

Gaur P, Bielenberg DR, Samuel S, Bose D, Zhou Y, Gray MJ, Dallas NA, Fan F, Xia L, Lu J, Ellis LM. (2009). Role of class 3 semaphorins and their receptors in tumor growth and angiogenesis. Clin Cancer Res. 2009 Nov 15;15(22):6763-70.

Guttmann-Raviv N, Shraga-Heled N, Varshavsky A, Guimaraes-Sternberg C, Kessler O, Neufeld G. (2007). Semaphorin-3A and semaphorin-3F work together to repel endothelial cells and to inhibit their survival by induction of apoptosis. J Biol Chem 282:26294–26305.

Hergovich A, Hemmings BA. (2009). Mammalian NDR/LATS protein kinases in hippo tumor suppressor signaling. Biofactors. 2009 Jul-Aug;35(4):338-45.

Hergovich A, Kohler RS, Schmitz D, Vichalkovski A, Cornils H, Hemmings BA. (2009). The MST1 and hMOB1 tumor suppressors control human centrosome duplication by regulating NDR kinase phosphorylation. Curr Biol. 2009 Nov 3;19(20):1692-702.

Hergovich A, Lamla S, Nigg EA, Hemmings BA. (2007). Centrosome-associated NDR kinase regulates centrosome duplication. Mol Cell. 2007 Feb 23;25(4):625-34.

Hergovich A, Stegert MR, Schmitz D, Hemmings BA. (2006). NDR kinases regulate essential cell processes from yeast to humans. Nat Rev Mol Cell Biol. 2006 Apr;7(4):253-64.

Hung RJ, Yazdani U, Yoon J, Wu H, Yang T, Gupta N, Huang Z, van Berkel WJ, Terman JR. (2010). Mical links semaphorins to F-actin disassembly. Nature. 2010 Feb 11;463(7282):823-7.

Kirilly D, Gu Y, Huang Y, Wu Z, Bashirullah A, Low BC, Kolodkin AL, Wang H, Yu F. (2009). A genetic pathway composed of Sox14 and Mical governs severing of dendrites during pruning. Nat Neurosci. 2009 Dec;12(12):1497-505.

Kolodkin, A.L., Matthes, D.J. and Goodman, C.S. (1993). The semaphorin genes encode a family of transmembrane and secreted growth cone guidance molecules. Cell 75, 1389–1399.

Moretti S, Procopio A, Lazzarini R, Rippo MR, Testa R, Marra M, Tamagnone L, Catalano A. (2008). Semaphorin3A signaling controls Fas (CD95)-mediated apoptosis by promoting Fas translocation into lipid rafts. Blood. 2008 Feb 15;111(4):2290-9.

Nakamura F, Kalb RG, Strittmatter SM. (2000). Molecular basis of semaphorin-mediated axon guidance. J Neurobiol. 2000 Aug;44(2):219-29.

Oppenheim RW. (2008). Cell death during development of the nervous system. Annu Rev Neurosci. 1991;14:453-501.J Neurosci. Nov. 19, 2008, 28(47):12427-12432

Pasterkamp RJ, Dai HN, Terman JR, Wahlin KJ, Kim B, Bregman BS, Popovich PG, Kolodkin AL. (2006). MICAL flavoprotein monooxygenases: expression during neural development and following spinal cord injuries in the rat. Mol Cell Neurosci. 2006 Jan;31(1):52-69.

Pasterkamp RJ, De Winter F, Holtmaat AJ, Verhaagen J. (1998). Evidence for a role of the chemorepellent semaphorin III and its receptor neuropilin-1 in the regeneration of primary olfactory axons. J Neurosci. 1998 Dec 1;18(23):9962-76.

Schmidt EF, Shim SO, Strittmatter SM. (2008). Release of MICAL autoinhibition by semaphorin-plexin signaling promotes interaction with collapsin response mediator protein. J Neurosci. 2008 Feb 27;28(9):2287-97.

Schwarz Q, Ruhrberg C. (2010). Neuropilin, you gotta let me know: should I stay or should I go? Cell Adh Migr. 2010 Jan-Mar;4(1):61-6.

Stegert MR, Hergovich A, Tamaskovic R, Bichsel SJ, Hemmings BA. (2005). Regulation of NDR protein kinase by hydrophobic motif phosphorylation mediated by the mammalian Ste20-like kinase MST3. Mol Cell Biol. 2005 Dec;25(24):11019-29.

Stork O, Zhdanov A, Kudersky A, Yoshikawa T, Obata K, Pape HC. (2004). Neuronal functions of the novel serine/threonine kinase Ndr2. J Biol Chem. 2004 Oct 29;279(44):45773-81.

Suzuki T, Nakamoto T, Ogawa S, Seo S, Matsumura T, Tachibana K, Morimoto C, Hirai H. (2002). MICAL, a novel CasL interacting molecule, associates with vimentin. J Biol Chem. 2002 Apr 26;277(17):14933-41.

Takahashi T, Strittmatter SM. (2001). Plexina1 autoinhibition by the plexin sema domain. Neuron. 2001 Feb;29(2):429-39.

Takahashi, T., Fournier, A., Nakamura, F., Wang, L.H., Murakami, Y., Kalb, R.G. (1999). Plexin-neuropilin-1 complexes form functional semaphorin-3A receptors. Cell 99, 59–69.

Tamagnone, L., Artigiani, S., Chen, H., He, Z., Ming, G.I., Song, H. (1999). Plexins are a large family of receptors for transmembrane, secreted, and GPI-anchored semaphorins in vertebrates. Cell 99, 71–80.

Tamaskovic R, Bichsel SJ, Rogniaux H, Stegert MR, Hemmings BA. (2003). Mechanism of Ca2+-mediated regulation of NDR protein kinase through autophosphorylation and phosphorylation by an upstream kinase. J Biol Chem. 2003 Feb 28;278(9):6710-8.

Taylor RC, Cullen SP, Martin SJ. (2008). Apoptosis: controlled demolition at the cellular level.Nat Rev Mol Cell Biol. 2008 Mar;9(3):231-41.

Terman JR, Mao T, Pasterkamp RJ, Yu HH, Kolodkin AL. (2002). MICALs, a family of conserved flavoprotein oxidoreductases, function in plexin-mediated axonal repulsion. Cell. 2002 Jun 28;109(7):887-900.

Tessier-Lavigne M, Goodman CS. (1996). The molecular biology of axon guidance. Science. 1996 Nov 15;274(5290):1123-33.

Toyofuku T, Zhang H, Kumanogoh A, Takegahara N, Suto F, Kamei J, Aoki K, Yabuki M, Hori M, Fujisawa H, Kikutani H. (2004). Dual roles of Sema6D in cardiac morphogenesis through region-specific association of its receptor, Plexin-A1, with off-track and vascular endothelial growth factor receptor type 2. Genes Dev. 2004 Feb 15;18(4):435-47.

Vichalkovski A, Gresko E, Cornils H, Hergovich A, Schmitz D, Hemmings BA. (2008). NDR kinase is activated by RASSF1A/MST1 in response to Fas receptor stimulation and promotes apoptosis. Curr Biol. 2008 Dec 9;18(23):1889-95.

Winberg, M.L., Noordermeer, J.N., Tamagnone, L., Comoglio, P.M., Spriggs, M.K., Tessier-Lavigne, M. (1998). Plexin A is a neuronal semaphorin receptor that controls axon guidance. Cell 95, 903–916.

Yoshida Y, Han B, Mendelsohn M, Jessell TM. (2006). PlexinA1 signaling directs the segregation of proprioceptive sensory axons in the developing spinal cord. Neuron. 2006 Dec 7;52(5):775-88.

Zallen JA, Peckol EL, Tobin DM, Bargmann CI. (2000). Neuronal cell shape and neurite initiation are regulated by the Ndr kinase SAX-1, a member of the Orb6/COT-1/warts serine/threonine kinase family. Mol Biol Cell. 2000 Sep;11(9):3177-90.

Chapter 7

General discussion

Since their original identification in 2002, MICAL proteins have been implicated in various cell biological and disease processes including axon guidance, tight junction formation, spinal cord injury and cancer (for details see chapter 1). As signaling proteins, MICALs are unusual as they contain a monooxygenase (MO) domain in addition to several protein-protein interacting modules, including a Calponin Homology (CH) domain, a LIM domain and coiled-coil motifs (CC) (Suzuki et al., 2002; Terman et al., 2002; Weide et al., 2003; Pasterkamp et al., 2006). This thesis aimed at further characterizing vertebrate MICALs at the molecular and functional level, using MICAL-1 as a prototype family member.

In the studies outlined in chapters 3 to 7, several novel molecular properties of MICAL-1 were reported. For example, it was demonstrated that MICAL-1 can form dimers or oligomers most likely through the CH domain (chapter 3). This self-association may regulate MICAL-1 activity or function in the association with binding partners. In addition, we found that MICAL-1 is a phospho-protein, both in cell lines and in brain tissue *in vivo*. Serine 777 was identified as one of the phosphorylation sites in mouse MICAL-1. This finding indicates that MICALs may be regulated by protein kinases. In experiments on the potential monooxygenase activity of MICAL-1, we demonstrated that the constitutively active MO domain (i.e. C-terminally truncated MICAL-1) catalyzes the synthesis of hydrogen peroxide (H_2O_2) in presence of NADPH (chapter 3; Schmidt et al., 2008). In mammalian cells, the constitutively active MO domain induced cell contraction but this effect did not depend on H_2O_2. This result supports the idea that the effects of MICAL-1 on cell morphology are mediated by direct redox modification of potential substrates such as CRMP and F-actin.

To further characterize the signaling pathways in which MICALs participate, we screened MICAL-1 binding proteins using pull down approaches followed by mass spectrometry (chapter 4). The various putative MICAL-1 interactors identified implicate roles for MICAL-1 in diverse cellular processes such as cytoskeletal remodeling, tight junction formation, apoptosis, transcriptional and translational regulation. Among the candidate interactors identified, NDR kinases were studied in more detail (chapter 5). NDR kinases (NDR1/2) did not influence enzymatic activity of MICAL-1, however, MICAL-1 negatively regulated NDR1/2 phosphorylation and therefore activity. This new mechanism of negative NDR kinase regulation was depended on the competitive binding of MICAL-1 to the C-terminal part NDR1/2 which is also targeted by MST1 kinase. MST1 normally activates NDR1/2 by phosphorylating Threonine 444/442 (in NDR1/2). MICAL-1 prevents MST1 binding and thereby negatively regulates the pro-apoptotic effects mediated by the MST1-NDR pathway.

Finally, we observed overlapping expression patterns for MICAL-1 and NDR1 in developing brain and provided data to suggest that MICAL-1, NDR1 and activated plexinA1 exist in a tripartite protein complex (chapter 6). However, so far preliminary analyses did not provide support for a role for NDR kinases in mediating signaling with MICAL-1 downstream of plexinA receptors and their semaphorin ligands in neurons. Further studies are needed to examine the role of NDR kinases in semaphorin/plexinA signaling.

Cell signaling pathways are often composed of extracellular signaling molecules, cell surface receptors, intracellular signal transduction proteins and targets such as the cytoskeleton. All these components function together to translate extracellular signals into changes in cell morphology and behavior. MICAL family members are signaling proteins that receive information from cell surface receptor(s) or other intracellular protein(s) and transfer this information to downstream effectors or targets to induce cellular changes (Fig. 1). The combination of protein-protein interaction domains and motifs present in MICALs suggest a role as a scaffold protein involved in the assembly of larger protein complexes. In the following sections, we first discuss the molecular properties of MICAL proteins, followed by activators and effectors of MICALs in view of their biological functions.

Molecular properties of MICALs

The MICAL MO domain

Since the original identification of MICALs, a lot effort has been put in characterizing the MICAL MO domain. Although this domain (~500 aa) bears little sequence similarity to other flavoprotein monooxygenases (Terman et al., 2002), all the available structural and enzymatic data support the idea that MICALs are true flavoprotein monooxygenases (e.g. the presence of a flavin (FAD) co-factor in the crystal structure, conserved FAD fingerprints, their tertiary structure and their ability to mediate NADPH-dependent reactions) (Terman et al., 2002; Nadella et al., 2005; Siebold et al., 2005; Schmidt et al., 2008; Hung et al., 2010). In chapter 3, we found that constitutively active MICAL-1 mutants can produce hydrogen peroxide (H_2O_2), which is in line with previous observations (Nadella et al., 2005; Schmidt et al., 2008). It has been proposed that MICALs may produce H_2O_2 in the absence of substrates but may mediate redox modification of protein substrates if present (Nadella et al., 2005; Siebold et al., 2005; Schmidt et al., 2008; Joosten and van Berkel, 2007). As discussed in one of the following sections, both F-actin and CRMP-1 are considered potential substrates for the MICAL-1 MO domain. However, it remains unclear whether these proteins are true MICAL-1 substrates and, if so, whether their regulation involves H_2O_2 or not. In our pull down experiment using the MICAL-1 MO domain (chapter 4), proteins were identified with functions in transcription/translation regulation, energy transduction, membrane organization, protein transport, apoptosis and cytoskeletal regulation. Although the binding of these proteins to MICAL-1 remains to be confirmed, they may represent potential substrates of the MICAL MO domain.

The MICAL C-terminal domains

The C-terminal part of MICAL proteins contains the CH domain, LIM domain, coiled-coil motifs and variable linker regions (Terman et al., 2002; Pasterkamp et al., 2006). This combination of domains in conjunction with a MO domain is not found in other currently known proteins (Terman et al., 2002; Joosten and van Berkel, 2007). These domains do not only interact with other proteins but they are also required for regulating the enzymatic activity of MICAL proteins and have been suggested to present substrate(s) to the MO domain (Terman et al., 2002; Schmidt et al., 2008; Hung et al., 2010). The coiled-coil containing region forms intramolecular interactions, presumably by binding to a region around the LIM domain, to inhibit the activity of the MO domain (Schmidt et al., 2008). The CH domain mediates dimer (or oligomer) formation of MICAL-1 (chapter 3). This is intriguing as protein dimerization (or oligomerization) is a common regulatory mechanism in enzymes known to modulate enzyme activity or accession of the substrate (Marianayagam et al., 2004). Therefore, it will be interesting to determine whether the dimerization or oligomerization of MICAL-1 is important for controlling monooxygenase activity.

Several proteins have been identified that bind to the C-terminal region of MICAL-1 (Schmidt et al., 2008; Suzuki et al., 2002; Terman et al., 2002; Weide et al., 2003). Given the fact that the MICAL-1 C-terminal region enforces an autoinhibitory conformation of the protein, these interactors may be involved in activating MICAL-1. For example, neurite growth inhibition by Sema3A has been suggested to involve activation of MICAL-1 by plexinA1, which binds the MICAL-1 C-terminal region (Schmidt et al., 2008). But experimental evidence to support such an activation is still lacking. Other than autoregulatory functions, the C-terminal part of MICAL exerts signaling roles independent of the MO domain in apoptosis. The most C-terminal part of MICAL-1, together with the LIM domain region, can interact with NDR kinases thereby negatively regulating kinase activity (chapter 5). However, despite the interaction of NDR kinases with MICAL domains involved in the autoinhibitory regulation of the MO domain, manipulating NDR levels did not affect MICAL-1 enzymatic activity or contraction responses. (chapter 5).

MICAL-1, a phospho-protein

A novel and interesting feature of MICALs described in this thesis is that MICAL-1 is phospho-protein. We applied several different methods to confirm the phosphorylation status of MICAL-1 and identified one

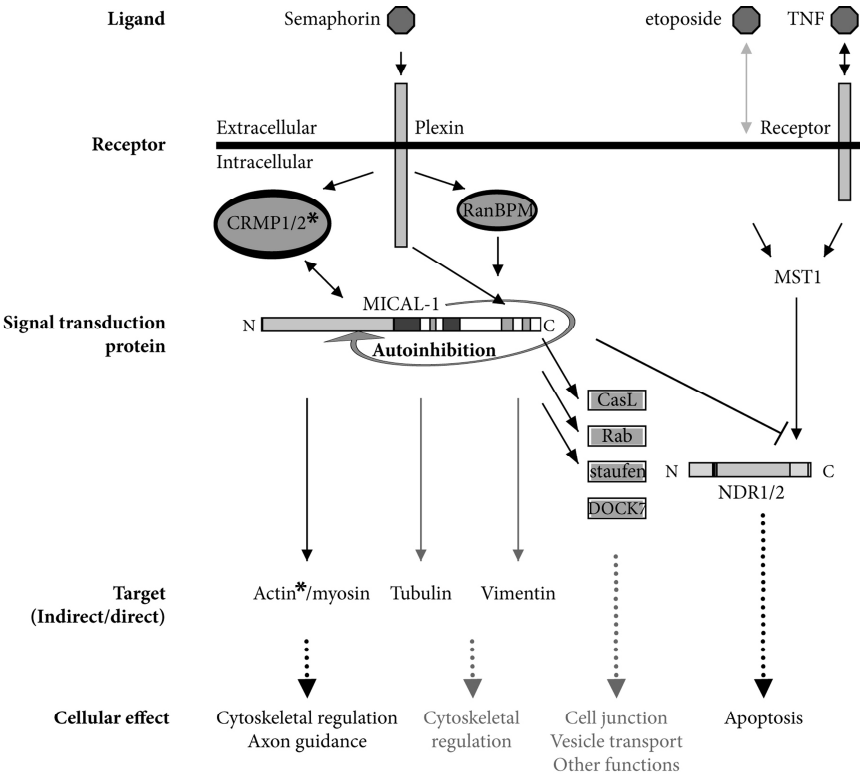

Figure 1. Activators, effectors and targets of MICAL-1.

Models of MICAL-1 signaling cascades. The extracellular protein semaphorin binds and activates plexinA receptors, thereby activating an intracellular signaling complex that contains the signaling proteins MICAL-1, CRMP-1 and/or RanBPM. This ultimately leads to changes in the cytoskeleton and thereby axon guidance. MICAL-1 is an autoinhibited protein and activation of MICAL-1 monooxygenase activity leads to the disassembly of actin filaments or other cytoskeletal components. Besides cytoskeletal regulation, MICAL-1 has an anti-apoptotic function independent of its monooxygenase domain. Etoposide and tumor necrosis factor alpha (TNF) induce activation of MST1 kinase, which phosphorylates and activates NDR1/2 kinases to induce apoptosis. MICAL-1 binds NDR kinases and inhibits MST1-induced phosphorylation by competing with MST1 for NDR binding. Other MICAL binding signaling proteins such as CasL and Rabs provide links to cellular processes such as cell junction formation and vesicle transport. N, N-terminus; C, C-terminus. Black or gray arrows indicate known or expected interactions and functions, respectively. Stars (*) indicate potential MICAL substrates.

specific phosphorylation site, serine 777 (S777) in mouse MICAL-1 (chapter 3). However, this phosphorylation site is neither conserved among family members nor required for any of the currently known cellular functions of MICAL-1. Furthermore, the S777A MICAL-1 mutantation did not show an effect on the subcellular distribution, autoinhibition or the binding of MICAL-1 to known interactors (i.e. plexinA1, CRMP1 and NDR1). According to several (prediction) programs, (e.g. DISPHOS 1.3 and PHOSIDA) MICAL proteins may contain several different potential phosphorylation sites, most of them serine or threonine residues (data not shown). In line with this observation, our own data indicate that MICAL-1 contains at least one more phosphorylation site in addition to S777. Future studies are needed to

unveil the full complement of phosphorylation sites in MICAL-1 and other MICAL proteins, the function of these phosphorylation events and the upstream kinases involved. Our own work excludes NDR1/2 and MST1 as kinases that phosphorylate MICAL-1, but places MICAL-1 in the MAPK pathway inviting the speculation that MICALs might be phosphorylated by MAPKs.

Modulation of MICAL activity

Activation of MICALs by semaphorin-plexin signaling

PlexinA receptors have been suggested to activate MICALs upon semaphorin ligand binding. In *Drosophila*, Mical can bind the plexinA cytoplasmic domain and loss-of-function flies for *Mical*, *plexinA* or *sema-1a* show similar motor axon phenotypes indicating a role of Mical in the Sema1a-plexinA signaling pathway (Terman et al., 2002). *In vivo* mutagenesis experiments of the Mical MO domain indicate a role for the MO domain in sema-1a/plexinA signaling (Terman et al., 2002). Since plexinA binds the C-terminal region of Mical, it is unlikely that mutations in the MO region affect plexinA binding. However, this remains to be tested. Rather it has been proposed that Sema-1a binding to plexinA leads to activation of the Mical MO domain which then controls the cytoskeleton to induce axon repulsion. In COS-7 cells, semaphorin 3A (Sema3A) induces contraction when its receptors neuropilin1 and plexinA1 are both expressed (Takahashi and Strittmatter, 2001). Interestingly, MICAL-1 interacts with plexinA1, and other plexinAs (chapter 6), and co-expression of MICAL-1 and plexinA1 directly induces COS-7 cell contraction, implicating MICAL-1 in the Sema3A/plexinA1 signaling pathway (Schmidt et al., 2008). This is supported by the ability of the C-terminal region of MICAL-1 (which binds plexinAs) to act as a dominant negative mutant, preventing Sema3A induced neurite growth inhibition (Schmidt et al., 2008). Finally, cultured DRG axons are repelled by Sema3A and this effect can be blocked by EGCG (epigallocatechin gallate), known to inhibit monooxygenases most likely through inhibition of the MO domain of MICAL proteins (Terman et al., 2002; Pasterkamp et al., 2006). Together these observations support a model in which binding of semaphorins to their plexinA receptors triggers the activation of the MICAL MO domain leading to cell morphological changes such as axon repulsion or cell contraction. How plexinAs might activate MICALs remains unclear. The interaction of plexinAs with the C-terminal region of MICALs may induce a conformational change that releases the autoinhibited conformation of MICAL thereby stimulating MO activity. Alternatively, the activation of MICALs may consist of the recruitment of this protein to specific locations in the cell. In light of this hypothesis it is interesting to note that, after Sema3A stimulation, more MICAL-1 is recruited to plexinA1 (Schmidt et al., 2008). Finally, plexinAs may activate other proteins which then affect MICALs.

Other potential modulators of MICAL activity

An increasing number of proteins is known to bind the C-terminal region of MICALs (e.g. plexinAs, Rabs, NDR1/2). Since this region of MICALs is involved in mediating an autoinhibitory conformation it is tempting to speculate that proteins binding the MICAL C-terminus or LIM domain region, which interacts with the C-terminus, may help to activate the protein. In this thesis we tested one interesting candidate, NDR1, which binds both the LIM domain and the most C-terminal region of MICAL-1. However, neither NDR1 nor NDR2 appeared to be involved in the (in)activation of MICAL-1 with respect to enzymatic or contraction activity (chapter 5). In the future, known and novel (chapter 4) MICAL-1 interactors should be tested in enzymatic and contraction assays to unveil whether they can act as activators or inhibitors of the MICAL proteins.

MICAL substrates and downstream effectors

Potential substrate: F-actin

An intriguing feature of Mical is its ability to bind actin and disassemble actin bundles through direct oxidation *in vitro* (Hung et al., 2010). Oxidation of actin is known to lead to disassembly of actin filaments,

reduced ability of actin to interact with actin-crosslinking proteins and a decrease in the ability of actin monomer to form polymers (Dalle-Donne et al., 2001a,b; Mizani et al., 1997; Terman et al., 2002). These results and the extensive cell morphological effects mediated by MICAL proteins in cells and *in vivo* supports the idea that actin also serves as a substrate for the MO domain and is a target for MICAL proteins during cell morphological changes. Although MICAL-1 truncation mutants can produce H_2O_2, several experiments described in chapter 3 argue against the idea that MICAL-1 utilizes H_2O_2 to induce cell contraction. Therefore, regulation of the cytoskeleton by MICAL-1 is most likely also due to direct redox modification of actin or other cytoskeletal components by the MO domain.

In addition to actin, MICAL-1 physically interacts with other cytoskeletal proteins, i.e. vimentin and tubulin (Suzuki et al., 2002; Fischer et al., 2005). Interestingly, vimentin can be oxidized by H_2O_2 (Rogers et al., 1991), raising the possibility that MICAL may induce vimentin oxidation. Tubulin can be oxidized as well and its oxidation abolishes polymerization activity (Landino et al., 2004). The effects of Mical during bristle formation in *Drosophila* are likely to be dependent on modification of actin as this is the major constituent of the bristle (Hung et al., 2010). However, in other cells MICALs may target different components of the cytoskeleton and therefore it will be interesting to determine whether redox regulation of other cytoskeletal proteins occurs under the influence of MICAL proteins.

Potential substrate: CRMP-1

CRMP-1 is another potential substrate of the MICAL-1 MO domain (Schmidt et al., 2008). It has been reported that in the absence of their proper substrate, some monooxygenases can produce H_2O_2. Addition of substrate blocks H_2O_2 production and redox modification of the substrate occurs instead. Therefore, H_2O_2 production can be used as a measure of enzymatic activity and a reduction in H_2O_2 levels following binding of a protein to the enzyme may indicate that this protein is a substrate. The first hint that CRMP-1 may be a MICAL-1 substrate came from an experiment showing that addition of CRMP-1 to recombinant MICAL-1 protein inhibits H_2O_2 production by the MICAL-1 MO domain (Schmidt et al., 2008). A very recent and elegant paper indicated further that H_2O_2 produced by MICAL-1 following activation by Sema3A in neurons may oxidize CRMP-2 and thereby enable homodimerization. This CRMP-2 homodimer is then phosphorylated by upstream kinases leading to growth cone collapse (Morinaka et al., 2011). In this study, the authors found that H_2O_2 and Sema3A treatment induce CRMP-2 dimerization, a process triggered by CRMP-2 oxidation at Cysteine 504 site. This oxidation-induced dimerization requires MICAL proteins as knock down of MICAL-1 and 3 in neurons abolished CRMP-2 dimerization. The most probable mechanism by which CRMP-2 is oxidized is through redox reactions mediated by activated MICALs. In line with this idea, endogenous H_2O_2 levels increased after Sema3A stimulation (Morinaka et al., 2011). However, direct evidence that MICALs modify CRMPs is still lacking. Co-expression of CRMPs with different MICAL-1 mutants followed by mass spectrometry may help to directly assess MICAL-mediated redox modifications of CRMPs. Interestingly, whereas actin has been proposed to be a direct target of the MO domain, CRMPs may be modulated by the intermediate H_2O_2. Further experimental evidence is needed to firmly establish the precise mechanism by which MICALs modify their substrates.

Downstream effector: NDR kinases

In chapter 4 and 5, we identified NDR kinases as novel interactors of MICAL-1. Interestingly, our studies show that the regulation of NDR kinases by MICAL-1 is markedly distinct from the MICAL-mediated regulation of actin and CRMPs.

NDR1/2 can be phosphorylated by MST1 on Threonine 444/442 and this phosphorylation is required for full NDR kinase activity (Stegert et al., 2005). Overexpression and knockdown of MICAL-1 inhibits or enhances NDR activation, respectively. MICAL-1 binds to the C-terminal region of NDR, which is also the binding region for MST1, the kinase responsible for phosphorylating T444/442. MICAL-1 does not bind MST1 but competes with MST1 for NDR binding and thereby reduces MST1-induced NDR activation

(chapter 5). This inhibition of MST1-NDR signaling plays a role in pro-apoptotic signaling as manipulation of MICAL-1 levels affects apoptosis induced through the MST1/NDR complex. Together, these observations define a novel negative regulatory mechanism in MST-NDR signaling and a new role for MICAL-1 in apoptosis. The ability of MICAL-1 to inhibit NDR kinases is independent of its MO domain, which is in contrast to most physiological functions reported for this protein so far.

MICAL-1 and NDR1 colocalize in the embryonic mouse brain and both proteins are able to bind constitutively active plexinA1 (chapter 6). This potential protein complex, MICAL-1, NDR1 and activated plexinA1, may function together during neuronal development, for example in axon guidance or apoptosis. Our results do not directly support a role for NDR kinases in growth cone collapse (chapter 6), although our merely biochemical data should be expanded with functional approaches to conclusively establish a role for NDRs in plexin-mediated axon guidance. The MICAL-1/NDR/plexinA protein complex may also be involved in mediating apoptotic signaling in the nervous system. Sema3A, Sema3F and plexinA3 have been reported to function in cell death (Gagliardini and fankhauser, 1999; Guttmann-Raviv et al., 2007; Bagnard et al., 2001; Ben-Zvi et al., 2008). Interestingly, in the immune system Sema3A facilitates TNF-mediated apoptosis, a process that requires NDR activation (Moretti et al., 2008; Vichalkovski et al., 2008). Since MICAL-1 can bind plexinA3 and MICAL-1 and NDR1/2 cooperate in apoptosis (Schmidt et al., 2008; chapter 6), it seems possibly that Sema3A, Sema3F or other semaphorins induce apoptotic signaling via MICALs and NDRs.

Other Binding partners of MICALs

Rab GTPases

Several Rab GTPases have been found to interact with MICAL or MICAL-like proteins (Weide et al., 2003; Fischer et al., 2005; Terai et al., 2006; Yamamura et al., 2008). They bind MICALs or MICAL-like proteins via their coiled-coil containing region (Weide et al., 2003; Fischer et al., 2005; Yamamura et al., 2008). The interaction has been confirmed by several methods, including Y2H, GST-pull down and co-IP (Weide et al., 2003; Fischer et al., 2005; Yamamura et al., 2008). Interestingly, in our screening for MICAL-1 interacting proteins, several Rab GTPases were identified when using the C-terminal region of MICAL-1 as a bait, including Rab1a, 1b, 8a, 8b, 13, 15 and 35 (chapter 4). Rab1 has previously been reported to interact with MICAL-1, while Rab8 and 13 interact with MICAL-L2 protein (Weide et al., 2003; Fischer et al., 2005; Terai et al., 2006; Yamamura et al., 2008). Protein complexes containing MICAL-L2 and Rabs are required for tight junction formation and endocytosis (Terai et al., 2006; Yamamura et al., 2008; Kanda et al., 2008; Sakane et al., 2010). However, how these proteins work together is still obscure. Most likely, MICAL-L2 functions as a protein scaffold that recruits Rabs to subcellular structures where Rabs exert their functions (Yamamura et al., 2008; Kanda et al., 2008). Since MICAL-Ls and MICALs share a similar domain organization (except for the MO domain which is lacking in MICAL-Ls), MICAL proteins are likely to have a similar role in Rab mediated signaling. Indeed, among the Rabs identified in the protein-protein interaction screens (chapter 4), several Rabs were identified with functions in tight junction formation, a process which is regulated by MICAL-Ls (chapter 4). Future experiments are needed to examine whether and how MICALs and Rabs function together.

Other MICAL binding proteins

Besides proteins that have been confirmed as (potential) activators, effectors and targets of MICALs, several additional binding partners of MICAL have been confirmed using biochemical approaches, i.e. CasL, RanBPM, DOCK7 and staufen (Suzuki et al., 2002; Togashi et al., 2006; chapter 4). Intriguingly, all these proteins, including MICALs, are known to function in the regulation of the cytoskeleton. CasL is a member of the p130 Cas protein family, involved in integrin-induced signaling and cytoskeletal regulation (Suzuki et al., 2002). Integrins mediate cell spreading by activating the small GTPase Rac and other downstream signaling cues (Price et al., 1998). DOCK7 is a guanine nucleotide exchange factor (GEF) for Rac and is an

important regulator of microtubule dynamics in axon outgrowth (Pinheiro and Gertler, 2006; Watabe-Uchida et al., 2006). Finally, MICAL-1 and RanBPM have been reported to mediate axon growth (Schmidt et al., 2008; Togashi et al., 2006). It is therefore tempting to speculate that these different proteins function together and perhaps use MICALs as a signaling platform. Furthermore, staufen binds both microtubules and mRNA, and is important for mRNA transport to neurites (Köhrmann et al., 1999). Dendritic mRNA transport is required for local translation, a strategy for local protein synthesis that regulates neurite growth and guidance. Since MICALs bind staufen and microtubules, it is possible that MICALs facilitate mRNA transport into neurites and thereby regulate cytoskeletal dynamics.

In chapter 4, numerous potential MICAL-1-interacting proteins were identified with various functions unrelated to the cytoskeletal regulation, e.g. transcription-translation regulation, biosynthesis, energy transduction, membrane organization and protein transport (chapter 4). This finding strongly suggests that MICALs play a more general function as has been shown so far and are likely to influence a wide array of cellular processes.

Final words

Overall, in this thesis, we characterized the MICAL-1 protein, identified novel MICAL-1 interacting proteins and unraveled an interesting new function for MICAL-1 in apoptosis. First, the dimerization and phosphorylation of MICAL-1 may represent regulatory mechanisms to control protein activity or protein-protein interactions. Second, the identification of MICAL-1 interacting proteins provides new directions for further research on the role of MICAL proteins in different signaling pathways. Third, the ability of MICAL-1 to function as a competitive inhibitor of the MST1-NDR pathway provides insight into a novel regulatory mechanism involving MICAL proteins, which should be studied in other cellular processes in the future. Further research on MICALs and their interactors will lead to a better understanding of neuronal development and of pathological conditions characterized by changes in MICAL expression and/or function such as cancer progression or neuronal injury (Pasterkamp et al., 2006; Ashida et al., 2006).

Reference

Ashida S, Furihata M, Katagiri T, Tamura K, Anazawa Y, Yoshioka H, Miki T, Fujioka T, Shuin T, Nakamura Y, Nakagawa H. (2006). Expression of novel molecules, MICAL2-PV (MICAL2 prostate cancer variants), increases with high Gleason score and prostate cancer progression. Clin Cancer Res. 2006 May 1;12(9):2767-73.

Bagnard D, Vaillant C, Khuth ST, Dufay N, Lohrum M, Puschel AW, Belin MF, Bolz J, Thomasset N. (2001). Semaphorin 3A-vascular endothelial growth factor-165 balance mediates migration and apoptosis of neural progenitor cells by the recruitment of shared receptor. J Neurosci. 2001 May 15;21(10):3332-41.

Ben-Zvi A, Manor O, Schachner M, Yaron A, Tessier-Lavigne M, Behar O. (2008). The Semaphorin Receptor PlexinA3 Mediates Neuronal Apoptosis during Dorsal Root Ganglia Development. J Neuroscience, 2008 Nov 19; 28(47):12427-12432

Beuchle D, Schwarz H, Langegger M, Koch I, Aberle H. (2007). Drosophila MICAL regulates myofilament organization and synaptic structure. Mech Dev. 2007 May;124(5):390-406.

Dalle-Donne I, R. Rossi, A. Milzani, P. Di Simplicio and R. Colombo. (2001a). The actin cytoskeleton response to oxidants: from small heat shock protein phosphorylation to changes in the redox state of actin itself, Free Radic. Biol. Med. 31 2001, pp. 1624–1632.

Dalle-Donne I, R. Rossi, D. Giustarini, N. Gagliano, L. Lusini, A. Milzani, P. Di Simplicio and R. Colombo. (2001b). Actin carbonylation: from a simple marker of protein oxidation to relevant signs of severe functional impairment, Free Radic. Biol. Med. 31 2001, pp. 1075–1083.

Fischer J, Weide T, Barnekow A. (2005). The MICAL proteins and rab1: a possible link to the cytoskeleton? Biochem Biophys Res Commun. 2005 Mar 11;328(2):415-23.

Fukata Y, Itoh TJ, Kimura T, Ménager C, Nishimura T, Shiromizu T, Watanabe H, Inagaki N, Iwamatsu A, Hotani H, Kaibuchi K. (2002). CRMP-2 binds to tubulin heterodimers to promote microtubule assembly. Nat Cell Biol. 2002 Aug;4(8):583-91.

Gagliardini V, Fankhauser C. (1999). Semaphorin III can induce death in sensory neurons. Mol Cell Neurosci 14:301–316.

Guttmann-Raviv N, Shraga-Heled N, Varshavsky A, Guimaraes-Sternberg C, Kessler O, Neufeld G. (2007). Semaphorin-3A and semaphorin-3F work together to repel endothelial cells and to inhibit their survival by induction of apoptosis. J Biol Chem 282:26294–26305.

Hergovich A, Hemmings BA. (2009). Mammalian NDR/LATS protein kinases in hippo tumor suppressor signaling. Biofactors. 2009 Jul-Aug;35(4):338-45.

Hung RJ, Yazdani U, Yoon J, Wu H, Yang T, Gupta N, Huang Z, van Berkel WJ, Terman JR. (2010). Mical links semaphorins to F-actin disassembly. Nature. 2010 Feb 11;463(7282):823-7.

Joosten V, van Berkel WJ. (2007). Flavoenzymes. Curr Opin Chem Biol. 2007 Apr;11(2):195-202.

Kanda I, Nishimura N, Nakatsuji H, Yamamura R, Nakanishi H, Sasaki T. (2008). Involvement of Rab13 and JRAB/MICAL-L2 in epithelial cell scattering. Oncogene. 2008 Mar 13;27(12):1687-95.

Kirilly D, Gu Y, Huang Y, Wu Z, Bashirullah A, Low BC, Kolodkin AL, Wang H, Yu F. (2009). A genetic pathway composed of Sox14 and Mical governs severing of dendrites during pruning. Nat Neurosci. 2009 Dec;12(12):1497-505.

Köhrmann M, Luo M, Kaether C, DesGroseillers L, Dotti CG, Kiebler MA. (1999). Microtubule-dependent recruitment of Staufen-green fluorescent protein into large RNA-containing granules and subsequent dendritic transport in living hippocampal neurons. Mol Biol Cell. 1999 Sep;10(9):2945-53.

Landino LM, Moynihan KL, Todd JV, Kennett KL. (2004). Modulation of the redox state of tubulin by the glutathione/glutaredoxin reductase system. Biochem Biophys Res Commun. 2004 Feb 6;314(2):555-60.

Marianayagam NJ, Sunde M, Matthews JM. (2004). The power of two: protein dimerization in biology. Trends Biochem Sci. 2004 Nov;29(11):618-25.

Milzani A, I. Dalle-Donne and R. Colombo. (1997). Prolonged oxidative stress on actin, Arch. Biochem. Biophys. 339, 1997, pp. 267–274.

Moretti S, Procopio A, Lazzarini R, Rippo MR, Testa R, Marra M, Tamagnone L, Catalano A. (2008). Semaphorin3A signaling controls Fas (CD95)-mediated apoptosis by promoting Fas translocation into lipid rafts. Blood. 2008 Feb 15;111(4):2290-9.

Morinaka A, Yamada M, Itofusa R, Funato Y, Yoshimura Y, Nakamura F, Yoshimura T, Kaibuchi K, Goshima Y, Hoshino M, Kamiguchi H, Miki H. (2011). Thioredoxin Mediates Oxidation-Dependent Phosphorylation of CRMP2 and Growth Cone Collapse. Sci Signal. 2011 Apr 26;4(170):ra26.

Nadella M, Bianchet MA, Gabelli SB, Barrila J, Amzel LM. (2005). Structure and activity of the axon guidance protein MICAL. Proc Natl Acad Sci U S A. 2005 Nov 15;102(46):16830-5.

Pasterkamp RJ, Dai HN, Terman JR, Wahlin KJ, Kim B, Bregman BS, Popovich PG, Kolodkin AL. (2006). MICAL flavoprotein monooxygenases: expression during neural development and following spinal cord injuries in the rat. Mol Cell Neurosci. 2006 Jan;31(1):52-69.

Price LS, Leng J, Schwartz MA, Bokoch GM. (1998). Activation of Rac and Cdc42 by integrins mediates cell spreading. Mol Biol Cell. 1998 Jul;9(7):1863-71.

Rogers KR, Morris CJ, Blake DR. (1991). Oxidation of thiol in the vimentin cytoskeleton. Biochem J. 1991 May 1;275 (Pt 3):789-91.

Sakane A, Honda K, Sasaki T. (2010). Rab13 regulates neurite outgrowth in PC12 cells through its effector protein, JRAB/MICAL-L2. Mol Cell Biol. 2010 Feb;30(4):1077-87.

Schmidt EF, Shim SO, Strittmatter SM. (2008). Release of MICAL autoinhibition by semaphorin-plexin signaling promotes interaction with collapsin response mediator protein. J Neurosci. 2008 Feb 27;28(9):2287-97.

Schmidt EF, Strittmatter SM. (2007). The CRMP family of proteins and their role in Sema3A signaling. Adv Exp Med Biol. 2007;600:1-11.

Sharma M, Giridharan SS, Rahajeng J, Caplan S, Naslavsky N. (2010). MICAL-L1: An unusual Rab effector that links EHD1 to tubular recycling endosomes. Commun Integr Biol. 2010 Mar;3(2):181-3.

Siebold C, Berrow N, Walter TS, Harlos K, Owens RJ, Stuart DI, Terman JR, Kolodkin AL, Pasterkamp RJ, Jones EY. (2005). High-resolution structure of the catalytic region of MICAL (molecule interacting with CasL), a multidomain flavoenzyme-signaling molecule. Proc Natl Acad Sci U S A. 2005 Nov 15;102(46):16836-41.

Stegert MR, Hergovich A, Tamaskovic R, Bichsel SJ, Hemmings BA. (2005). Regulation of NDR protein kinase by hydrophobic motif phosphorylation mediated by the mammalian Ste20-like kinase MST3. Mol Cell Biol. 2005 Dec;25(24):11019-29.

Suzuki T, Nakamoto T, Ogawa S, Seo S, Matsumura T, Tachibana K, Morimoto C, Hirai H. (2002). MICAL, a novel CasL interacting molecule, associates with vimentin. J Biol Chem. 2002 Apr 26;277(17):14933-41.

Takahashi T, Strittmatter SM. (2001). Plexina1 autoinhibition by the plexin sema domain. Neuron. 2001 Feb;29(2):429-39.

Terai T, Nishimura N, Kanda I, Yasui N, Sasaki T. (2006). JRAB/MICAL-L2 is a junctional Rab13-binding protein mediating the endocytic recycling of occludin. Mol Biol Cell. 2006 May;17(5):2465-75.

Terman JR, Mao T, Pasterkamp RJ, Yu HH, Kolodkin AL. (2002). MICALs, a family of conserved flavoprotein oxidoreductases, function in plexin-mediated axonal repulsion. Cell. 2002 Jun 28;109(7):887-900.

Togashi H, Schmidt EF, Strittmatter SM. (2006). RanBPM Contributes to Semaphorin3A Signaling through plexin-A Receptors. J Neurosci. 2006 May 3; 26(18): 4961–4969.

Vanderhaeghen P, Cheng HJ. Guidance molecules in axon pruning and cell death. Cold Spring Harb Perspect Biol. 2010 Jun 1;2(6):a001859.

Vichalkovski A, Gresko E, Cornils H, Hergovich A, Schmitz D, Hemmings BA. (2008). NDR kinase is activated by RASSF1A/MST1 in response to Fas receptor stimulation and promotes apoptosis. Curr Biol. 2008 Dec 9;18(23):1889-95.

Watabe-Uchida M, John KA, Janas JA, Newey SE, Van Aelst L. (2006). The Rac activator DOCK7 regulates neuronal polarity through local phosphorylation of stathmin/Op18. Neuron. 2006 Sep 21;51(6):727-39.

Weide T, Teuber J, Bayer M, Barnekow A. (2003). MICAL-1 isoforms, novel rab1 interacting proteins. Biochem Biophys Res Commun. 2003 Jun 20;306(1):79-86.

Yamamura R, Nishimura N, Nakatsuji H, Arase S, Sasaki T. (2008). The interaction of JRAB/MICAL-L2 with Rab8 and Rab13 coordinates the assembly of tight junctions and adherens junctions. Mol Biol Cell. 2008 Mar;19(3):971-83.

Nederlandse samenvatting

De vertaling van extracellulaire signalen in een cellulaire reactie zoals bijvoorbeeld de uigroei van zenuwvezels of de migratie van cellen is afhankelijk van de activatie van een cascade van interacterende eiwtten. Extracellulaire eiwitten binden receptoreiwitten op het oppervlakte van de cel die vervolgens intracellulaire eiwtten binden en activeren met als uiteindelijke uitkomst veranderingen in bijvoorbeeld het cytoskelet of in genexpressie. De eiwitten die het onderwerp van onderzoek zijn in dit proefschrift, MICALs, vormen een nieuwe familie van intracellulaire eiwitten die een brug vormen tussen receptoreiwitten en andere eiwtten in de cel, bijvoorbeeld eiwitten zoals actine die het cytoskelet van de cel vormen. MICALs functioneren in diverse cellulaire processen in verschillende diersoorten, bijvoorbeeld in de mens en de muis maar ook in de fruitvlieg, een veelvuldig gebruikt genetisch onderzoeksmodel. Het doel van dit proefschrift was om MICAL-1, het meest bekende lid van de MICAL eiwitfamilie in zoogdieren, verder te karakteriseren. De verschillende hoofdstukken beschrijven studies naar de activiteit en functie van een enzym dat deel uit maakt van het MICAL eiwit, een zogenaamde flavin-afhankelijke monooxygenase, naar nieuwe interacterende eiwitten voor MICAL-1, en naar nieuwe cellulaire functies.

Sinds hun ontdekking in 2002 hebben experimenten een rol voor MICAL eiwitten vastgesteld in cellulaire processen zoals axon guidance en de vorming van celcontacten (tight junctions), maar ook in ziekten zoals kanker en ruggenmergletsel. Deze functies en ook andere karakteristieken van MICAL eiwitten worden samengevat in Hoofdstuk 1. MICAL eiwitten zijn bijvoorbeeld opgebouwd uit een unieke verzameling van eiwitdomeinen en motieven en hebben naast een FM domein, een calponin homology (CH) domein, een LIM domein, and coiled-coil (CC) motieven. Studies waarin de kristalstruktuur van het MICAL FM domein is bepaald laten zien dat het FM enzymatisch actief is en waarschijnlijk in staat is andere eiwitten te modificeren en daarmee te (in)activeren.

In Hoofdstuk 3 wordt inderdaad aangetoond dat MICALs de morfologie van cellen kunnen reguleren via hun FM domein. Een actief MICAL-1 eiwit, waarbij het meest C-terminale deel van het eiwit is verwijderd, produceert waterstof peroxide (H_2O_2) via het FM domein in de aanwezigheid van NADPH en induceert de contractie van cellen. Deze contractierespons is niet afhankelijk van H_2O_2 zoals is aangetoond in andere studies voor andere eiwitten. Het is dus waarschijnlijk dat MICALs geen H_2O_2 gebruiken om veranderingen in het cytoskelet van cellen aan te brengen, maar juist eiwitten van het cytoskelet direct binden en modificeren. Verder worden er nog twee andere interessante moleculaire eigenschappen van het MICAL-1 eiwit ontdekt. De eerste is dat MICAL-1 zichzelf kan binden en dimeren of oligomeren kan vormen via het CH domein. Deze binding is waarschijnlijk belangrijk voor de activiteit van het eiwit of voor de interactie met andere eiwitten. De tweede bevinding is dat MICAL-1 wordt gefosforyleerd en dus gereguleerd kan worden door zogenaamde eiwitkinases. Fosforylering is een manier om de activiteit van eiwitten te reguleren.

Omdat MICAL-1 een groot eiwit is met verschillende eiwitdomeinen en motieven is het waarschijnlijk dat een groot aantal andere eiwitten MICAL-1 kunnen binden en reguleren. Hoofdstuk 4 beschrijft technieken om MICAL-1 eiwitcomplexen uit cellen te zuiveren en vervolgens de eiwitten die MICAL-1 binden in deze complexen te identificeren. De eiwitten die in deze experimenten worden gevonden impliceren MICAL-1 in cellulaire processen waarin reeds een rol voor MICAL eiwtten was aangetoond maar ook in onbekende processen zoals apoptose, transcriptie en translatie. Verdere functionele experimenten zijn nodig om de precieze rol van MICAL-1 in deze processen te onderzoeken. In het laatste deel van dit hoofdstuk wordt voor een aantal nieuwe interactoren door middel van biochemische methoden bevestigd dat ze MICAL-1 kunnen binden. Het betreft NDR1, DOCK7 en staufen.

De interactie van MICAL-1 en NDR1 wordt verder onderzocht in Hoofdstuk 5 en Hoofdstuk 6. NDRs zijn eiwitkinases die andere eiwitten kunnen fosforyleren en een rol spelen in de deling en apoptose van cellen. Hoewel in Hoofdstuk 5 wordt beschreven dat MICAL-1 een fosfoeiwit is, wordt ook

aangetoond dat NDR kinases niet in staat zijn MICAL-1 te fosforyleren. Verder lijken NDR kinases niet betrokken te zijn bij de regulatie van MICAL-1, bijvoorbeeld tijdens celcontractie. Echter MICAL-1 blijkt wel in staat NDR kinases te reguleren. MICAL-1 bindt het meest C-terminale deel van NDR kinases. Dit deel van NDR kinases wordt normal gefosforyleerd door een andere eiwitkinase, MST1. Deze fosforylering is belangrijk voor de activatie van NDR kinases en hun rol in celdeling en apoptose. De binding van MICAL-1 aan NDR kinases voorkomt de fosforylering door MST1 en daarmee de activatie van NDR kinases en het resulterende stimulerende effect op apoptose. MICAL-1 is dus in staat door het remmen van de activatie van NDR kinases apoptose te inhiberen. Dit hoofdstuk beschrijft daarmee een nieuwe cellulaire functie voor MICAL-1.

In voorgaande studies is aangetoond dat MICALs een rol spelen in de ontwikkeling van zenuwbanen. Gedurende de embryonale ontwikkeling worden zenuwvezels onder invloed van extracellulaire eiwitten een specifieke richting opgestuurd zodat ze uiteindelijk aankomen bij de cel waarmee ze een verbinding moeten gaan maken. Deze extracellulaire eiwitten binden aan receptoreiwitten op het oppervlakte van de zenuwvezel die vervolgens eiwitten in de cel (in)activeren om de zenuwvezel te kunnen sturen. MICALs binden aan zulke receptoreiwitten, plexins, en vormen een brug naar het cytoskelet. Veranderingen in het cytoskelet zorgen er uiteindelijk voor dat de zenuwvezel in een bepaalde richting kan groeien. De functies van plexins en de intracellulaire eiwitten die door plexins worden gereguleerd worden beschreven in Hoofdstuk 2. Omdat NDR kinases ook de groei van zenuwvezels kunnen regeluren wordt in Hoofdstuk 6 onderzocht of NDR kinases en MICAL-1 samenwerken in het sturen van zenuwvezels, zoals ze ook samenwerken in het reguleren van apoptose. MICAL-1 en NDR1 blijken op dezelfde plaatsen in de embryonale hersenen voor te komen en ook beide aan plexins te kunnen binden. Echter biochemische studies tonen vooralsnog geen rol aan voor de activatie van NDR kinases in de intracellulaire eiwitcascades die worden gebruikt door plexins. Verdere functionele experimenten zijn nodig om te onderzoeken of NDR kinases een rol spelen in het sturen van zenuwvezels door plexins en hun liganden.

In Hoofdstuk 7, worden de resultaten van dit proefschrift bediscussieerd en worden suggesties voor toekomstig onderzoek gegeven. De resultaten die in dit proefschrift worden beschreven leiden tot een betere karakterisering van MICAL-1, en van MICAL eiwitten in het algemeen, en vormen een beginpunt voor verdere studies naar de rol van deze eiwitten in nieuwe cellulaire processen die hier worden geidentificeerd maar ook in geval van ziekten zoals kanker en verlammig na ruggenmergletsel.

List of publications

Zhou Y, Gunput RA, Pasterkamp RJ. Semaphorin signaling: progress made and promises ahead. Trends Biochem Sci. 2008 Apr;33(4):161-70. Review.

Zhou Y, Adolfs Y, Pijnappel WW, Fuller SJ, Van der Schors RC, Li KW, Sugden PH, Smit AB, Hergovich A, Pasterkamp RJ. MICAL-1 is a Negative Regulator of MST-NDR Kinase Signaling and Apoptosis. Mol Cell Biol. Mol Cell Biol. 2011 Sep;31(17):3603-15. Epub 2011 Jul 5

Zhou Y, Gunput RF, Adolfs Y, Pasterkamp RJ. MICALs in control of the cytoskeleton, exocytosis, and cell death. Cell Mol Life Sci. 2011 Aug 6. [Epub ahead of print] Review.

Maarten J. A. Moes, **Yeping Zhou** and Johannes Boonstra. Co-localization of the PDGF β-receptor and actin during PDGF stimulation in mouse fibroblasts. (submitted).

Ewout JN Groen, Katsumi Fumoto, JooYeon Engelen-Lee, Dianne MA van den Heuvel, **Yeping Zhou**, Max Koppers, Anna M Blokhuis, Jeroen AA Demmers, Janine Kirby, Pamela J Shaw, Wim GM Spliet, Jan H Veldink, Leonard H van den Berg, and R Jeroen Pasterkamp. FUS mutations induce a cytoplasmic redistribution of SMN1 and change in snRNA expression: a link between ALS and SMA. (submitted).

Curriculum Vitae

Yeping Zhou was born on the 7th of November 1977 in China. After receiving her BSc in Biology at Fudan University (Shanghai, China) in 2000, she worked in The9 limited (company) as a web-editor. In September 2003, she started her Master study in Utrecht University in the Netherlands. For this study two traineeships were performed. The first was performed in Department of Biochemistry and Cell Biology, investigating actin dynamics in living cells. The second was in Department of Physiological Chemistry, Centre for Biomedical Genetics, UMC Utrecht, where she studied protein regulation and localization. From February 2006, she has worked in the Rudolf Magnus Institute of Neuroscience in UMC Utrecht for her doctorate research investigating the signaling transduction mechanism of MICAL proteins in the nervous system. The research described in this book was carried out under the supervision of Dr. R. J. Pasterkamp.

Acknowledgements

I would like to acknowledge everyone who provided direct or indirect help during my study and express my sincere gratitude for their contribution.

First of all, I would like to thank Dr. Jeroen Pasterkamp, Prof. Peter Burbach and Prof. Leonard van den Berg. Jeroen, thank you for your patient supervision and knowledge. Your help, guidance, support, constructive criticisms and corrections helped me to improve my quality of research and develop as a researcher. As I said before, I highly appreciate all your help. Peter, thank you for your kind encouragement. A lot times, your questions during work discussions helped me to re-examine my project. Leonard, thank you for your kind support and providing me an opportunity to participate in your research. Without your help, I would not be able to complete graduation procedure so smoothly. Thank you very much.

Then, my dear roommates, Asheeta and Rahul, I am thankful to have both of you as my roommates. You make our room a nice and cozy place. I like all our discussions about life and science. Asheeta, my information source, I hope you a fruitful career and life in the coming future. Rahul, you are so nice and kind, I hope you a lot success.

Rou-Afza, my MICAL friend, I appreciate all our discussions and chat in the past several years. I hope you enjoy your life and research in your new project.

Dianne, Youri, Anita, my first colleagues in Pasterkamp lab. Thank you so much for all the support.

All the members in the Pasterkamp lab, Susan, Eljo, Ewoud, Ewout, Koushik, Bart, Francesca, Max and Amila, thank you all for the nice discussions about the work.

Marina, Leo, Henk, Lars, Keith, thank you for all your help from DNA to protein. Your work makes the labs organized.

Ria, Joke, Vicki and Sandra, thank you for helping me now and then with my "paper work" and all kinds of "Identity"-related problems.

To my dear landlord, Leo, thank you for your hospitality and kindness in these many years. My dear neighbour, Abao and Shouli, I hope you a happy life together with your little angel, Ranran.

To my dear Chinese friends and my family.

非常感恩，能有一个机会书面感谢大家。

钟牧师和师母，谢谢你们这么多年的牧养。你们在真理上的教导与实践都成为我有形无形的帮助。

小羊牧场的弟兄姐妹们，你们是我一直以来的帮助和安慰。在大家中间得到接纳，包容与关爱，你们见证我的成长，我们也一路一起成长！

牧场元老级的 Martin 和 Sharon，你们的关心和劝导给了我很多帮助，可能当时不觉得，但是回想起来，有很多益处。

Gary&Nicole en Mia; 徐俊&心萍；庆一&刘洋；玲玲&Philip；Layla&Erik；也许可以把张麒&Phuong 也放在这组里。大家在生活里见证主，你们的生活也成了美好的见证。

还有小朋友们，煦阳，小硕，悦华，娜娜，思思，韫婕，Alex，殷尊，杨帆，文俊，睿杰。大家真是很可爱，要加油成长啊。

亚迪，小祁，这么多年一起走过来，祝福你们！

晓莉，期待你回来！

再特别感谢一下玲玲和小范范，谢谢你们来给我当 Paranimfen，辛苦了。

远在中国的家人，爸爸妈妈，谢谢你们一路的支持。你们是我走到今天的动力。你们让家成为美好的地方，你们的付出也是女儿报答不完的。姐姐和姐夫，因为有你们在，我才能绕半个地球来生活。谢谢你们。